Year : 2011

Experience-dependent plasticity in the mouse barrel cortex

Johnston-Wenger Nathalie

UNIL | Université de Lausanne
Faculté de biologie et de médecine

Département de Biologie Cellulaire et de Morphologie

EXPERIENCE-DEPENDENT PLASTICITY IN THE MOUSE BARREL CORTEX

Thèse de doctorat en Neurosciences

présentée à la

Faculté de Biologie et de Médecine
de l'Université de Lausanne

par

Nathalie JOHNSTON-WENGER

Biologiste diplômée de l'Université de Lausanne, Suisse

Jury

Prof. Jean-Pierre Hornung, Président du jury
Prof. Egbert Welker, Directeur de thèse
Prof. Dominique Muller, Expert
Dr. Gilles Bonvento, Expert
Dr. Isabelle Décosterd, Experte

Lausanne 2010

Programme doctoral interuniversitaire en Neurosciences des Universités de Lausanne et Genève

UNIL | Université de Lausanne

UNIVERSITÉ DE GENÈVE

UNIL | Université de Lausanne

Programme doctoral interuniversitaire en Neurosciences des Universités de Lausanne et Genève

UNIVERSITÉ DE GENÈVE

Imprimatur

Vu le rapport présenté par le jury d'examen, composé de

Président	Monsieur	Prof.	Jean-Pierre **Hornung**
Directeur de thèse	Monsieur	Prof.	Egbert **Welker**
Co-directeur de thèse			
Experts	Monsieur	Prof.	Dominique **Muller**
	Madame	Dr	Isabelle **Decosterd**
	Monsieur	Dr	Gilles **Bonvento**

le Conseil de Faculté autorise l'impression de la thèse de

Madame Nathalie Johnston-Wenger

Biologiste diplômée de l'Université de Lausanne

intitulée

EXPERIENCE-DEPENDENT PLASTICITY IN THE MOUSE BARREL CORTEX

Lausanne, le 23 avril 2010

pour Le Doyen
de la Faculté de Biologie et de Médecine

Prof. Jean-Pierre Hornung

Résumé

La capacité des neurones à modifier leur connectivité en fonction d'une nouvelle expérience, appelée la plasticité neuronale dépendante de l'expérience, est une caractéristique fondamentale du système nerveux qui nous permet de nous adapter aux nouvelles situations. Dans le but de comprendre comment une expérience sensorielle façonne notre cerveau et laisse des traces dans le circuit neuronal, nous avons étudié les aspects temporels, moléculaires et ultrastructuraux de la plasticité dans un modèle expérimental bien définis : «the whisker-to-barrel pathway» des rongeurs. Ces animaux utilisent les vibrisses de leur museau, appelées communément «moustaches», pour explorer leur environnement. L'information sensorielle collectée par ces organes tactiles est ensuite relayée vers l'aire sensorielle primaire du cortex cérébral. Dans cette partie du cortex, les corps cellulaires de la couche IV sont organisés en anneaux délimitant des structures appelées tonneaux. Chaque tonneau reçoit l'information d'une seule vibrisse et la distribution des tonneaux dans le cortex correspond exactement à la distribution des vibrisses sur le museau des rongeurs. Cette particularité cyto-architecturale nous permet de sélectionner très précisément la partie corticale dévolue au traitement de l'information sensorielle provenant d'une seule vibrisse et d'y étudier les changements corticaux occasionnés par une modification de l'expérience sensorielle. Il a été montré que vingt-quatre heures de stimulation continue et passive d'une des vibrisses, pendant que l'animal adulte peut se comporter librement, induit des changements synaptiques et physiologiques dans cette partie du cortex somatosensoriel. Ces changements sont en partie maintenus 4 jours après la cessation de la stimulation (Knott et al., 2002; Quairiaux et al., 2007). Ici, en sélectionnant très précisément cette partie du cerveau chez la souris et en utilisant les techniques de la microscopie électronique et des puces à ADN, nous avons étudié l'évolution temporelle des changements synaptiques et moléculaires induits dans la couche IV du cortex somatosensoriel primaire au cours de 24 heures de stimulation des vibrisses. Nous montrons qu'au niveau de l'ultra-structure, des changements rapides du circuit neuronal se mettent en place et ceci en 2 phases. Dès 6 heures de stimulation, des synapses excitatrices sont insérées au niveau du tronc dendritique. Ces synapses sont transitoires et disparaissent entre 18 et 24 heures de stimulation. Pendant ce laps de temps, des synapses inhibitrices s'insèrent sur les épines dendritiques. Il a été montré auparavant que ces synapses-là sont maintenues après la cessation de la stimulation (Knott et al., 2002). Au niveau de l'expression des gènes, nous montrons que la stimulation des vibrisses orchestre un vaste programme transcriptionnel sur une période de 24 heures de stimulation. En effet, 261 gènes apparaissent différentiellement activés par la stimulation et ceci de manière très régulée dans le temps. Dans les premières heures de stimulation des gènes codant pour des facteurs de transcription et des protéines liées aux synapses excitatrices sont activés. Ces phases de transcription sont suivies, après 15 heures de stimulation, par une régulation négative de l'expression d'une grande quantité de gènes. Parmi les gènes qui sont négativement régulés à ce moment se trouvent des gènes

codant pour des molécules d'adhésion et pour des facteurs connus pour inhiber la croissance cellulaire. Etant observée juste avant l'insertion des synapses inhibitrices sur les épines, cette régulation négative de l'expression des gènes est perçue comme un événement essentiel à leur formation. Finalement, la régulation de l'expression des gènes a aussi été étudiée lorsque les animaux ont été exposés à une deuxième période de stimulation, ceci 4 jours après 24 heures de stimulation. A la suite de cette deuxième période de stimulation, nous montrons que l'expression des gènes diffère considérablement de l'expression des gènes induite par la première période de stimulation. En conclusion, ces résultats montrent que le circuit neuronal est rapidement modifié lors d'une nouvelle expérience sensorielle et cela par des phases successives de changements au niveau moléculaires et aussi au niveau ultra-structurel avec la formation de nouvelles connections synaptiques. Ces changements engendrent en 24 heures la formation de traces mnésiques dans le circuit cortical qui modifient la réponse neuronale à une deuxième expérience sensorielle similaire à la première.

Abstract

Experience-dependent plasticity, or the capacity of the neurons to modify their connectivity in function of altered experience, is a fundamental process that enables the brain to continuously adapt to new conditions. In order to understand how sensory experience leads to the formation of long-lasting changes within the neuronal network, we have studied the temporal, molecular and structural aspects of plasticity within a single experimental paradigm: the whisker-to-barrel pathway of rodents. In these animals, whiskers are used to actively explore their nearby environment. The sensory information collected by these tactile organs is then relayed to the primary sensory cortex. In layer IV of this cortical area, the cell bodies are organized into clusters delineating structure called barrels. Each barrel treats the sensory information coming from one whisker and the distribution of the barrels are precisely organized to map the organization of the whiskers on the rodents' snout. This particular cytoarchitectural organization enables one to precisely select the cortical area devoted to one particular whisker and study the cortical changes induced by a change in the sensory periphery. Twenty-four hours of continuous whisker stimulation has already been shown to induce synaptic and physiological changes in layer IV of the adult somatosensory cortex and part of these changes were shown to remain 4 days after the end of the stimulation period (Knott et al., 2002; Quairiaux et al., 2007). Here, using serial section electron microscopy and microarray technologies, we studied the structural and molecular changes induced in layer IV of the somatosensory cortex across the first 24 hours of continuous whisker stimulation. We show that at the ultrastructural level, modification of the circuitry in the neuropil occurs rapidly and in two phases, with first a significant, temporary increase in excitatory synapses on dendritic shafts that is already present after 6 hours of stimulation. This phase is followed by a significant increase of the occurrence of inhibitory synapses on spines that takes place after 24 hours. At the transcriptional level, we show that whisker stimulation orchestrates a vast transcriptional program across 24 hours with 261 genes being significantly altered in their expression, and that this transcriptional program is tightly regulated over time. Quickly after the onset of the stimulation, genes coding for transcription factors as well as for proteins related to the excitatory synapses are found regulated. These transcriptional phases are followed after 15 hours of stimulation by the down-regulation of many genes among which are adhesion molecules and myelin associated growth inhibitors. Being observed in the last time-point investigated before the appearance of long-lasting inhibitory synapses on spines, the down-regulation of these genes is perceived as a prerequisite for their insertion. Finally, the transcriptional response to a second exposure of whisker stimulation 4 days later was investigated and was shown to differ considerably from the response in naïve mice. Altogether, our findings show that the mature cortical network is rapidly modified by a new sensory experience and this, through successive phases of molecular and structural modifications. These changes lead within 24 hours to the formation of long-lasting traces in the cortex which alter the neuronal response to subsequent similar sensory experience.

Contents

List of Abbreviations

µm	micro-meter
A/m	amper per meter of conductor
ADCYAP1	adenylate cyclase activating polypeptide 1
adj p value	p value adjusted for false discovery rate using Benjamini Hochberg method
AMPA	α-amino-3-hydroxyl-5-methyl-4-isoxazole-propionate
ARC	activity-regulated cytoskeleton-associated protein
BDNF	brain derived neurotrophic factor
CACNG2	calcium channel, voltage-dependent, gamma subunit 2
CaMK II	calcium-calmodulin kinase II
cAMP	cyclic adenosine monophosphate
cDNA	complementary deoxyribonucleic acid
CNS	central nervous system
CRE	cAMP response element
CREB	cyclic-AMP response element binding protein
CREM	cAMP responsive element modulator
CTRL	control animals
DEPC	diethyl pyrocarbonate
DNA	deoxyribonucleic acid
DOT1L	DOT1-like, histone H3 methyltransferase (S. cerevisiae)
EGR1, 2, 3	early growth response 1, 2, 3...
EM	electron microscopy
EST	expressed sequence tags
EtOH	ethanol
GABA	γ-aminobutyric acid
GABAa	GABA receptor type A
GAD	glutamic acid decarboxylase
GFP	green fluorescent protein
GO	gene ontology
GRASP	GRP1 (general receptor for phosphoinositides 1)-associated scaffold protein
GRIK1	glutamate receptor, ionotropic, kainate 1
Hz	hertz
i.p.	intra-peritoneal
ICER	inducible cAMP early repressor
IER5	immediate early response 5
IterPlier	iterative probe logarithmic intensity error
LTD	long-term depression
LTP	long-term potentiation
MAG	myelin-associated glycoportein
MAPK	mitogen-activated protein kinase
MME	membrane metallo-endopeptidase
mRNA	messenger ribonucleic acid
ms	millisecond
MSK1	mitogen- and stress-activated kinase 1

Mylk3	myosin light chain kinase 3
ηm	nano-meter
NMDA	N-methyl-D-aspartate
NonStim	samples from barrels that were not stimulated but adjacent to stimulated ones (but at least one arc apart)
NPAS4	neuronal PAS domain protein 4
NPTX2	neuronal pentraxin II
PACAP	pituitary adenylate cyclase-activating peptide
PCSK1	proprotein convertase subtilisin/kexin type 1
PKA	protein kinase A
PKC	protein kinase C
Plier	probe logarithmic intensity error
PO	posterior thalamic nucleus
poly(A) tail	multiple adenosine monophosphates added to the end of an RNA molecule
PrV	principalis trigeminal subnucleus
RefSeq	NCBI reference sequence
REST	RE1 silencing transcription factor
Restim6h	group of mice that had their whiskers stimulated for 24 hours, then were returned to their home cage for 4 days and then had their whiskers stimulated for 6 hours
RIN	RNA integrity number
RNA	ribonucleic acid
RTN4	reticulon 4
SCN7A	sodium channel, voltage-gated, type VII, alpha
SpVc	caudalis trigeminal subnucleus
SpVi	interpolaris trigeminal subnucleus
SpVo	oralis trigeminal subnucleus
Stim	samples from barrels whose corresponding whiskers were stimulated
TNNC1	troponin C type 1 (slow)
Tukey HSD	Tukey honestly significant difference
VB	ventrobasal thalamic nucleus

List of Figures and Tables

List of Appendix

Acknowledgement

I would like here to thank wholeheartedly all the people who have been present during the elaboration of this thesis. Their support, their faith in this project and in me, their knowledge, technical assistance, wisdom, encouragements and all the good moments that we have shared have helped me to overcome the moments of doubts and difficulties and to complete this work.

My deepest gratitude and respect to Professor Egbert Welker who welcomed me in his group and handed me these beautiful projects. With great wisdom and sensibility, he watched each step made at the distance required for the experiments to be performed but somehow, being always there to guide me when I most needed it. Without his support, strength and sense of precision, I could not have been able to perform and complete this work.

Thank you to Graham Knott, Christel Genoud, Caroline Musetti and Véronique Mamin for watching my first steps in the lab and for sharing their knowledge on electron microscopy as well as for sharing the frustrations and joys that are inherent to this beautiful technique. Also thank you to Charles Quairiaux for his help on my first experiments on dissected barrel columns and for sharing his enthusiasm about the microarray project.

Thank you also to Sonia Naegele-Tollardo for her great technical assistance in the microarray experiment and this, always with great care and dedication. Thank you to have overcome the moments of doubts and difficulties and made it possible. Thanks also to David Rodriguez Sobreiro for his technical assistance on a preliminary set of microarrays that gave us the certitude that microarray on laser microdissected barrels, despite being difficult and demanding, was actually feasible.

My gratitude to Professor Markus Ruegg who agreed to hand me the microarray project . A very special thanks to Filippo Oliveri for his technical assistance in pooling all the barrels and for doing the hybridization, showing always great enthusiasm for the project.

My gratitude to Rudolf Kraftsik for discussion and help on statistical analyses, always with great patience, kindness and commitment, for sharing his passion for science and for his capacity to materialize the most abstract ideas.

Thank you to Antonio Mucciolo who has always been there with great kindness to fix any problem that I would face at the electron microscope so that I could work in the best conditions possible. Thank you to Franco Arizzoni, who first introduced me to the electron microscope.

My gratitude to Gregory Lefebvre for all the fruitful discussions and to have pushed me into the world of microarray data analysis.

To Fabien Pichon, Margo Rumerio, Jyoti Chuckowree, Carolyn Sacco, Iratxe Ciriza, Michel Kielar, Christine Savary, Aouatef Abazza and Ines Khadimallah a big THANK YOU for your daily support, your kindness and smiles and for your precious friendship and, for the last ones to have joined the group, for having brought with you a new wind of freshness and new strengths. You have all given life to the work at the bench or at the computer in many ways and made it a

place where it actually felt good to be. Thank you.

All my gratitude and love to my family. They have always been there for me, giving me a place where I could rest and feel loved no matter the circumstances. A special thank you to Ryan for always encouraging me and making me see beyond what was most visible. Without him, this thesis would simply never have been accomplished. Thank you to Sophie who has always been present with me on this path giving me the support that I needed and who has somehow felt in her heart each step that was being made.

Thank you to everybody else: through discussion, a kind word or a smile, you have made a difference.

Introduction

As humans, we all have the potential to feel, remember, think, create and act. This is made possible by our nervous system as it enables us to perceive the world sensed by the sensory organs, to process the information and to generate a response. It is through its plasticity, or its ability to change in response to experience, that changes in perception and learning occur; giving us the potential to always evolve and adapt to an ever changing world. That the brain remains capable to change its connections in function of experiences, a phenomena called experience-dependent plasticity, was first suggested to underlie learning and behavioral changes by Ramon y Cajal when he wrote that "the acquisition of new skills requires many years of mental and physical practice. In order to fully understand this complex phenomenon it becomes necessary to admit, in addition to the reinforcement of pre-established organic pathways, the formation of new pathways through ramification and progressive growth of the dendritic arborization and the nervous terminals." (Ramon y Cajal, 1904). Although Cajal laid down more than a century ago the principles of plasticity as the underlying mechanism for learning and memory, it was only after the development of more sophisticated neurophysiologic methods and of the electron microscopy that neuroscientists could start to test his hypothesis.

Since Cajal, electrophysiological recordings confirmed that altering the neuronal activity has a functional impact on pre-established connections between two neurons as they may be reinforced or weakened (Bliss and Lomo, 1973; Douglas and Goddard, 1975; Markram et al., 1997). At the structural level, the development of the electron microscope revealed that connections between neurons (named synapses; see below) may be gained or lost in response to change in sensory experience or neuronal activity (Chang and Greenough, 1982; Greenough et al., 1985; Trommald et al., 1996). Most recently advancements in imaging technology have revealed that the brain

and its interneuronal connectivity are much more dynamic than ever conceived. Indeed, studies combining the electron microscope with the two-photon laser-scanning microscope revealed that small protuberances from the neurons called spines as well as their associated synapses appear and disappear over time *in vivo* in the adult mice (Trachtenberg et al., 2002; Holtmaat et al., 2005; Knott et al., 2006). This constitutive turn-over of spines may be altered by change in sensory experience (Trachtenberg et al., 2002). Also, the same combination of techniques revealed *in vitro* that spines less than a few hours old may already present a synaptic contact (Zito et al., 2009). Finally, recent advancements in biotechnologies such as genetic manipulation and microarray screens have revealed that the functional and structural aspects of plasticity are paralleled by changes in gene expression and by various molecular mechanisms (for review see Tropea et al., 2009). These modifications at the cellular level have important functional consequences. They influence for example the way sensory information is represented within the brain. This is best illustrated in studies addressing the topographic representations of sensory modalities (named "maps") at the level of the neocortex. Many studies have shown that the organization of the cortical maps is shaped by sensory experience and may be altered throughout life (Van der Loos and Woolsey, 1973; Merzenich et al., 1983; Recanzone et al., 1992). Most of them have been based on cases of lesions that deprive the cortex from its normal input but it occurs also after intensive training (for review see Buonomano and Merzenich, 1998; Pascual-Leone et al., 2005). As the organization of sensory maps in the neocortex reflects the connectivity between cortical neurons, map plasticity is the most striking evidence that the brain remains capable to change its connections in function of alteration in experiences.

Plasticity of the neuronal circuitry is now widely accepted as being the underlying mechanism to sustain learning and memory. It is also now known to involve the molecular, functional and structural level of brain cells and many models have been used by scientists to investigate the underlying mechanisms; one of them, the whisker-to-barrel pathway of rodents, has been of particular value. First, whiskers on the rodents' snout are parts of highly mobile sensory organs that are easily distinguishable and accessible and therefore can be very simply manipulated to alter sensory experience. Second, in layer IV of the neocortex, neurons that respond to the activation of the same whisker are gathered into clusters called barrels which are visible on common histological preparation (Woolsey and Van der Loos H., 1970). This feature of the whisker-to-barrel pathway enables one to easily manipulate the sensory organ at the sensory periphery and to study the potential changes that are being induced at the cortical level in the corresponding brain area. Finally, mice are one of the most studied animal models in biomedical research and, as they may easily be genetically modified, have proven to be of a particular value to investigate function of specific genes and molecules. In addition, the sequence of their whole genome has been known since 2002 (Waterston et al., 2002). For all the above reasons,

the whisker-to-barrel pathway has already been extensively investigated and has considerably contributed to develop the idea that sensory experiences shape the brain and have further shade light on the underlying cellular mechanisms (for review see Feldman and Brecht, 2005). The present study joins this field of research and focuses on how, within 24 hours of passive whisker stimulation, the neuronal network of the neocortex modifies its connectivity, and how this form of neuronal plasticity is paralleled by changes in gene expression. However, before presenting my observations, I will introduce in the following sections a few basic notions on the nervous system and especially the organization and plasticity of the sensory system with special emphasis on the whisker-to-barrel pathway in rodents.

I. The neocortex

The neocortex is part of the central nervous system (CNS) and is involved in functions such as sensory perception, generation of motor commands, and higher cognitive skills such as language, conscious thoughts and reasoning. It is the most superficial part of the cerebral hemispheres and in human it is the most prominent part of the brain occupying 80% of its volume (Passingham R, 1982). It is made of neurons, endothelial cells and three types of glial cells: the astrocytes, the oligodendrocytes and the microglia.

I.1. Synaptic connections

In 1904, Ramon y Cajal revealed for the first time, thanks to the staining technique developed by Camillo Golgi, that the neocortex, and the nervous system in general, was made up of individual cells, the neurons, that send out long filaments called neurites (Ramon y Cajal, 1904; Golgi, 1873). The neurites are of two types: axons and dendrites. Dendrites are compartments involved in receiving the signals from other neurons while axons are involved in the transmission and contact other cells at highly specialized contact points called synapses. Synapses are specialized areas between two neurons where the neuronal signal which is of electrical nature is transformed into a chemical signal that is directionally passed from the presynaptic to the postsynaptic neuron (Figure 1). In the postsynaptic cell, the chemical signal is converted into an electrical one. The presynaptic compartment, also called synaptic bouton, contains neurotransmitters enclosed in synaptic vesicles. When the electrical signal arrives in the synaptic bouton, it opens voltage-dependent calcium channels. This induces a transient increase in the intracellular calcium level and triggers the fusion of the synaptic vesicles with the plasma membrane at a specialized membranous area called the active zone. In this way, the neurotransmitters are released in the synaptic cleft (Figure 1). The postsynaptic membrane that is immediately opposite to the active zone contains receptors for the neurotransmitters.

When bound to their ligand, the receptors become activated and enable the entrance of specific ions in the postsynaptic compartment. The entrance of these ions modifies the potential of the plasma membrane regenerating the electrical signal in the postsynaptic cell (Figure 1). In addition to the neuronal elements, synapses are also often surrounded by astrocytic processes which isolate the synapse, provide metabolic support and play an important role in removing neurotransmitters from the synaptic cleft (Magistretti and Pellerin, 1999). Astrocytes may also release, in a calcium-dependent manner, neurotransmitters (which are called in this case gliotransmitters) such as glutamate and hence have the potential to be active partners in the neuronal signaling (Jourdain et al., 2007). The type of neurotransmitters that is expressed in a cell defines two major classes of neurons in the neocortex: the excitatory neurons and the inhibitory neurons. Excitatory neurons release glutamate as their neurotransmitter. Glutamate released in the synaptic cleft binds to its receptors on the postsynaptic membrane, the AMPA (α-amino-3-hydroxyl-5-methyl-4-isoxazole-propionate) receptors, the NMDA (N-methyl-D-aspartate) receptors or the kainate receptors, which are sodium or calcium channels which depolarize the postsynaptic compartment. The inhibitory neurons release gamma-amino butyric acid (GABA) which bind to GABA receptors and open chloride ion channels, which most

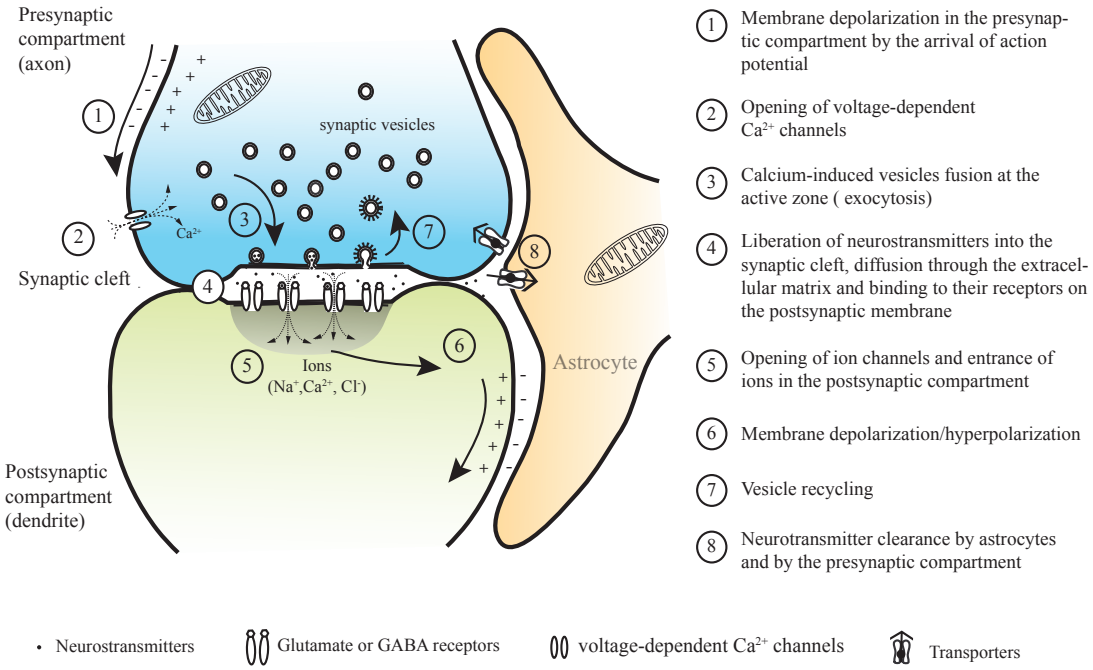

Figure 1. Signal transmission at the chemical synapse. Description of the series of events (1 to 6) that take place at the synapse and lead to the transmission of the electrical signal from the axon of the presynaptic cell to the dendrite of the postsynaptic cell. After the activation of the synapse, the vesicles are recycled (7) and the neurotransmitters cleared from the synaptic cleft by transporters (8).

commonly hyperpolarize the postsynaptic compartment. In the neocortex, 80% of the neurons are excitatory, the rest inhibitory (Gabbott and Somogyi, 1986).

As the smallest integrative unit of the nervous system, synapses were for the first time visualized in the 50's, thanks to the development of the electron microscope (EM; Palay, 1956). To sustain its structural and functional characteristics, a synapse requires a variety of molecules, from ion channels, receptors, scaffolding proteins to the molecular machinery necessary for vesicles release. Hence synapses are rich molecular units, a feature that is recognizable at the electron microscope as the opposing parts of the membranes are electron-dense. Inexorably, synapses are recognized on an electron micrograph by the presence of a cluster of vesicles in the presynaptic compartment and two apposed electron-dense membranes separated by a synaptic cleft (Figure 2). Additionally, it appeared that the molecular composition of the synapse affects their

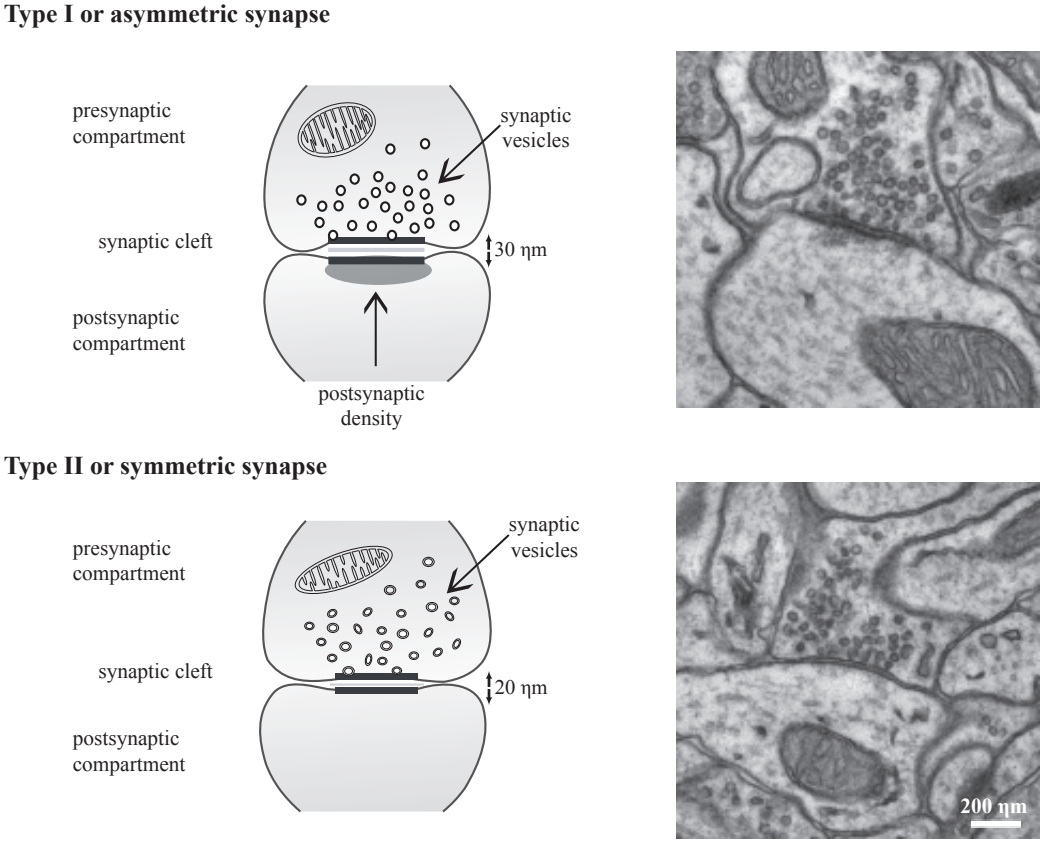

Figure 2. Synapses at the ultrastructural level are recognized by the presence of a cluster of vesicles in the presynaptic compartment and two apposed thickened membranes. When the synapse is cut transversally, a clear synaptic cleft is observed. In addition, two classes of synapses can be distinguished at the ultrastructural level. As defined by Gray (1959) Type I or asymmetric synapses are characterized by round, homogeneous vesicles, a thick postsynaptic density and a synaptic cleft of around 30 ηm. These synapses are excitatory. Type II or symmetric synapses have heterogeneous vesicles and a thin postsynaptic density. Their synaptic cleft is of around 20 ηm. These synapses are inhibitory. The examples shown to the right are both electron micrographs of a synapse made directly on a dendritic shaft. Scale bar pertains to both electron micrographs.

morphology and two major types of synapses were recognized (Gray, 1959a). In the neocortex the majority of synapses have round and clear vesicles and a thick postsynaptic density. It gives them an asymmetric appearance. These synapses were named “type I” or “asymmetric” synapses (Figure 2). In the other type of synapses, the vesicles are flattened or heterogeneous in shape, the synaptic cleft is narrow and no particular density in the postsynaptic compartment can be noticed. They were named “type II” or “symmetric” synapse (Figure 2). In the neocortex, 84% of the synapses are asymmetric and 16% are symmetric (Beaulieu and Colonnier, 1985). Asymmetric synapses are generally excitatory and symmetric ones are usually inhibitory (Peters A et al., 1991; De Felipe et al., 1997; Knott et al., 2002; Douglas R. et al., 2004). However, the association between morphology and function does not hold for each brain region and may be influenced by histological processing of the tissue.

The presynaptic elements of the synapses, called synaptic boutons, can be of two sorts: en passant boutons, which are swellings along the axonal branch, or terminaux boutons which are swellings at the tip of small axonal protrusions (McGuire et al., 1984; Anderson and Martin, 2001; De Paola et al., 2006). On dendrites, synapses may target directly the dendritic shaft or small dendritic protrusions called spines (Figure 3; Gray, 1959b). In the neocortex, spines are present on dendrites from excitatory neurons but scarce or absent on dendrites of inhibitory neurons. The inhibitory neurons are therefore often referred as the “aspiny” or “smooth” neurons while the excitatory neurons are often called the “spiny” neurons. Spines are the main target of excitatory neurons in the neocortex as about 79% of all excitatory synapses are made onto them, while the vast majority of the remaining ones contact the dendritic shafts (Beaulieu and Colonnier, 1985; for a review on spine see Bourne and Harris, 2008).

I.2. Dendritic spines

Generally, the spine is characterized by a thin neck that branches from the dendritic shaft and that presents a bulbous ending called the head (Figure 3). The neck length and diameter as well as the head size of the spines may vary and have functional implication. Indeed, the size of the spine is correlated to the size of the associated postsynaptic density, to the number of receptors and to the number of vesicles in the presynaptic axonal bouton (Harris and Stevens, 1989). In addition, the neck, depending on its length and especially its diameter, restricts passive diffusion and provides electrical and biochemical isolation of the synapse from the parent dendrite (Koch and Zador, 1993; Bloodgood and Sabatini, 2005; Grunditz et al., 2008). Hence, in spines, due to their neck resistance and compared to similar synapses on dendritic shaft, the depolarization of the membrane is larger and localized, the intracellular calcium concentration raises to a much higher level and the second messenger molecules are confined to the site of their activation (Muller and Connor, 1991).

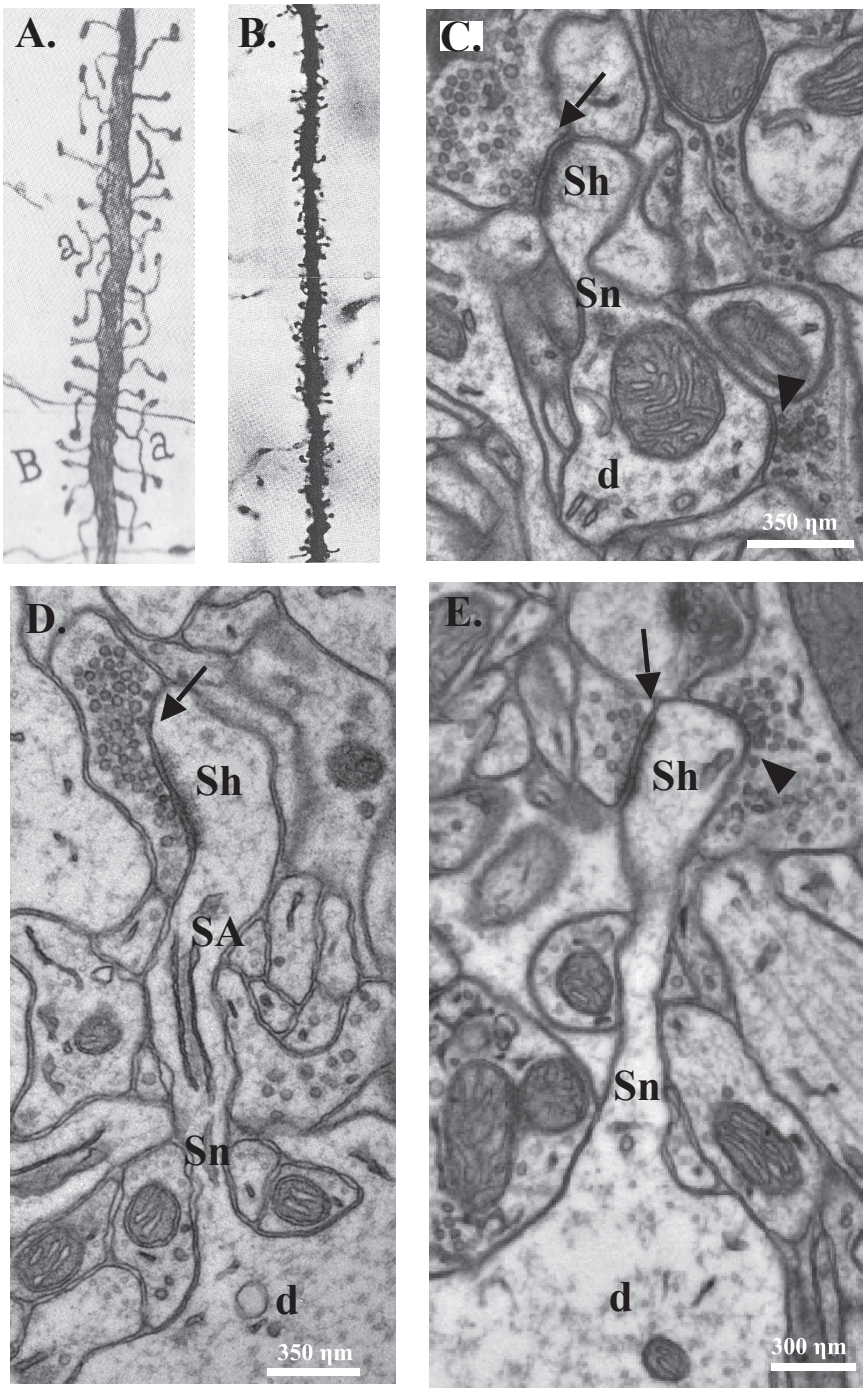

Figure 3. Dendritic spines in light (A, B) and electron microscopy (C,D,E). A. Drawing by Ramon y Cajal depicting a dendritic segment from the human cerebral cortex and the various spines that are protruding from the dendrite that were stained using Golgi's method. Cajal was the first one to describe these dendritic protrusions. B. Photomicrograph from Valverde (1971) of a dendritic segment stained using Golgi's method and its spines from a mouse re-exposed to light after dark rearing. C.D.E. Electron-micrographs showing the characteristics of spines at the ultrastructural level. Spines have a neck (Sn) emanating from the dendritic shaft (d) and a spine head (Sh). A spine apparatus is often present (SA). Spines make an excitatory synapse (arrow) usually at the level of their head. The double-innervated spines, in addition to their excitatory synapse also make synapse with an inhibitory bouton (arrow-head). The majority of the synapses in the cerebral cortex are made on spines, however, they may also be made directly on the dendritic shaft. For example, in C, an inhibitory bouton forms a synapse (arrow head) on the dendritic shaft.

Several morphological categories of spines have been described (Bourne and Harris, 2008). Among them, the "mushroom spines" are characterized by a large head and a thin neck, the "thin spines" by a small head and a narrow neck and the "stubby or sessile spines" present an equal head and neck diameter and an overall length that equals its width. In addition, "branched spines" or also named "double/multiple-headed spines" are spines whose neck branches into two or several spines. All of these are considered mature spines and present an excitatory synapse located usually on the head. About 10-20 % of them have a spine apparatus (Gray, 1959a; Peters A et al., 1991) made of stacks of smooth endoplasmic reticulum (Figure 3D) (Spacek and Harris, 1997). It is believed to be the site of internal calcium storage and of protein synthesis and also to play a role in the insertion and the recycling of plasma membrane. Another category of spines is made by the filopodia-like protrusions that are often long and very thin with a pointy ending instead of bulbous. They are considered immature as they are often transient, very motile and especially numerous during development (Harris et al., 1992; Lendvai et al., 2000; Petrak et al., 2005). They may have either no synapse at all or one or several along their length. Finally another category of spines have been shown by electron microscopy studies which are spines that synapse with both an excitatory and an inhibitory bouton (Figure 3E). These are named the double-innervated spines and make up about 10% of the spine population in the neocortex (Jones and Powell, 1969b). Although the functional significance of the inhibitory synapses on the spine cannot be directly tested, it is believed to have a strategic significance as it may, very specifically and powerfully, veto the electrical current generated by the active excitatory synapse, this of course depending on the relative timing of activation of both synapses (Rall, 1970; Diamond et al., 1970). Inhibitory synapses on double-innervated spine has also been suggested to have the capacity to amplify the activity of the associated excitatory synapse by a phenomenon of post-inhibitory rebound depolarization (Knott et al., 2002; Quairiaux et al., 2007).

I.3. Cortical network

In the neocortex, one cubic millimeter contains 2.78 x 10^8 synaptic contacts, 50'000 neurons and 3 km of axons (Douglas et al., 2004). However, to process information and mediate behavior, a variety of neuronal cell types exists and those cells are not randomly distributed but are precisely organized and interconnected throughout the cortex to form functional circuits (for review see Douglas R. et al., 2004).

In addition to the common excitatory/inhibitory division, two major classes of neurons can be distinguished. They are the projection neurons and the interneurons. The projections neurons have axons which may span long distance and connect to other parts of the nervous system while the axons of the interneurons are mainly confined to the cortical area in which their cell

bodies are located and are involved in the local processing of information. According to this criterion, the excitatory neurons in the neocortex may be divided into two classes: the pyramidal cells being projection neurons and the spiny stellate cells being interneurons. The pyramidal cells are the major excitatory cell type in the neocortex as they represent 70% of the neurons. As projection neurons, they are the major output neurons of the neocortex with their long axons connecting to different cortical areas or subcortical structures like the thalamus. Despite this characteristic, they also present rich intracortical collateral axons and therefore take part in shaping the local circuitry. The pyramidal cell is recognizable by its apical dendrite, which, in most of the cases, emerges from the cell body in the direction of the surface of the cortex. In contrast to the pyramidal cells, the spiny stellate cells have their axons confined to the same cortical area; as they participate solely to the local circuitry, they are part of the interneurons. In comparison to the pyramidal cell, they have a lower spine density while more synapses are made directly on their dendritic branches. They are the major recipients of the thalamic inputs (Benshalom and White, 1986). Concerning the inhibitory neurons, they are in general considered to be interneurons and may be subdivided in a variety of classes based on their axonal arbors, the synaptic connections that they make and their immunoreactivity to calcium binding proteins as well as to neuropeptides (Demeulemeester et al., 1991; Cauli et al., 1997; Markram et al., 2004; Gupta et al., 2000; and for review see Markram et al. 2004).

In the neocortex, the different neuronal cell types are arranged in distinctive layers and give the neocortex a laminar organization. In general, 6 layers can be distinguished, each one containing a characteristic distribution of neuronal cell types and connections with other cortical and subcortical regions. Layers were numbered from surface towards the underlying white matter. In general, the cell bodies from the pyramidal cells are found mainly in layers II, III, V and VI while the spiny stellate cells are found at the highest concentration in layer IV. Inhibitory interneurons are found throughout all layers, but the various types may be differentially distributed (for review see Markram et al., 2004).

The relative thickness of the 6 cortical layers and the cellular distribution vary throughout the neocortex. This characteristic is evident in standard histological preparation. At the beginning of the 20th century, it enabled Brodmann to divide the neocortex into various cytoarchitectonic areas (Brodmann, 1909). It only later appeared that each area defined by Brodmann gathered neurons devoted to process a very specific type of information. For example, neurons of Brodmann's area 4 are selective to motor processing and define the primary motor cortex, the one from area 17 are devoted to visual processing and form the primary visual cortex while neurons from area 3, 1 and 2 form the somatosensory cortex. However, the segregation of the information is even finer than that. Indeed the neocortex is further subdivided into radially oriented columns that are

devoted to process specific information.

Cortical columns were first brought to light by Mountcastle in 1957 when he recorded the firing pattern of cortical cells in cats after stimulation of the sensory organs on the skin (Mountcastle, 1957). In his study, he showed that cells which lie in a narrow cortical column are part of a functional unit as they respond to the activation of the same class of receptors at the periphery which are also located on the same skin area; hence in this case, cells from the same cortical column share the same set of sensory receptors. In the context of sensory physiology, the set of sensory receptors that influence the activity of a neuron makes up the receptive field of this neuron. Hence, as neurons from the same cortical column are most responsive to the same set of receptors, they have a common receptive field. Since the work of Mountcastle, cortical columns have been recognized as being the basic anatomical and functional units of the neocortex (Szentagothai, 1978). Cortical columns are made of neurons that have a common receptive field and are part of a specific cortical network. Another important feature of the cortical columns is that the projections that they receive or send are organized in such a way that cortical columns that are functionally most related are located the closest to one another. However, the spatial organization of the projections is even more precise than that. Indeed, neurons from adjacent cortical columns have receptive fields that are slightly different, but still overlapping. This principle gives rise to the map organization of the neocortex. This is particularly striking for primary sensory cortices and gives rise in the cortex to the so called topographic maps. For example in the somatosensory cortex, the projections are spatially organized so that adjacent areas on the skin are mapped by neurons from adjacent columns; a pattern called somatotopy.

The somatotopic organization of the cortex is most evident in the whisker sensory system of the rodents where a spatial distribution of the neurons responsive to whisker stimulation makes the cortical columns visible in common histological preparations. For this reason, this system is widely used by neuroscientists to understand the basic properties of a cortical column and of the generation of the receptive field.

II. The whisker sensory system of rodents

Mystacial whiskers are tactile sensory organs which rodents use to investigate their nearby environment just as humans may use their hands to feel their close-by surroundings or explore an object. Indeed, rodents actively move their whiskers back and forth at a frequency of 5 to 15 Hz to locate objects in their surroundings and extract information about their size, shape and texture; this active behavior, called “whisking”, is coordinated with their body and head movement and is of a particular use when their vision is prevented (for review see Diamond et

al., 2008). On the snout of rodents, the large mystacial whiskers are arranged in horizontal rows and cross-row arcs forming the whiskerpad. The 5 rows are labeled from A to E; rows A and B contain generally 4 whiskers, while rows C, D and E contain between 8 and 10 (see Figure 4A). Between the caudal extremity of the rows, 4 whiskers are found and named straddlers. In addition to this mystacial whiskerpad, smaller whiskers, called the rostral whiskers, are found in proximity to the snout. In the mouse, the pattern of the whiskers distribution is particularly constant; however some variations may be observed as some whiskers may be supernumerary or lacking (Van der Loos H. et al., 1984).

From the whiskers, tactile information is conveyed in a one-to-one somatotopic manner into clusters of neurons in layer IV of the primary somatosensory cortex. This particular part of the somatosensory cortex was described and first proposed to be related to the whiskers by Thomas Woolsey and Hendrik Van der Loos in 1970. They called it the barrel cortex as neurons in layer IV are clustered into barrel-like three dimensional structures (Woolsey and Van der Loos, 1970). The wall of the barrel consists of a high density of cells which surround the hollow made principally of a dense network of axon terminals, dendrites and glial cell processes which is called neuropil and where most synapses are found. In the mouse, barrels are about 100 μm by 200 μm across and contain around 2000 cells (Pasternak and Woolsey, 1975). They are separated from one another by the presence of a cell-poor region called the septum. The spatial distribution of the barrels reproduces the organization of the whiskers on the animal's snout; a feature evident in sections through layer IV cut tangentially to the brain surface (Figure 4). Indeed, the barrel field is formed by 5 rows of 4 to 10 barrels as are the mystacial whiskers on the rodents' snout (Figure 4B) (Woolsey and Van der Loos H., 1970). In addition, when a whisker is naturally lacking or manually removed from birth, the corresponding barrel is consistently absent (Van der Loos H. and Woolsey, 1973; Van der Loos H. et al., 1984).

The one-to-one relationship between a barrel and its whisker was first confirmed at the functional level by Carol Welker in 1976 (Welker, 1976). Subsequent electrophysiological studies confirmed that neurons from a barrel respond maximally and at shorter latency to the deflection of its anatomically corresponding whisker called the principal whisker and that neurons located above and below a barrel also respond preferentially to the deflection of its principal whisker (Simons, 1978; Armstrong-James and Fox, 1987; Welker et al., 1993; Moore and Nelson, 1998) In addition to the principal whisker, cells of a barrel column also respond to the surrounding whiskers; this set of whiskers makes up the surround receptive field of the barrel. However, the dominance of the single principal whisker over the surrounding ones on the response of a cortical column confirms the idea that each barrel is part of a multi-neuronal entity which spans the entire cortical depth and confirms that barrels are the anatomical representation in layer IV

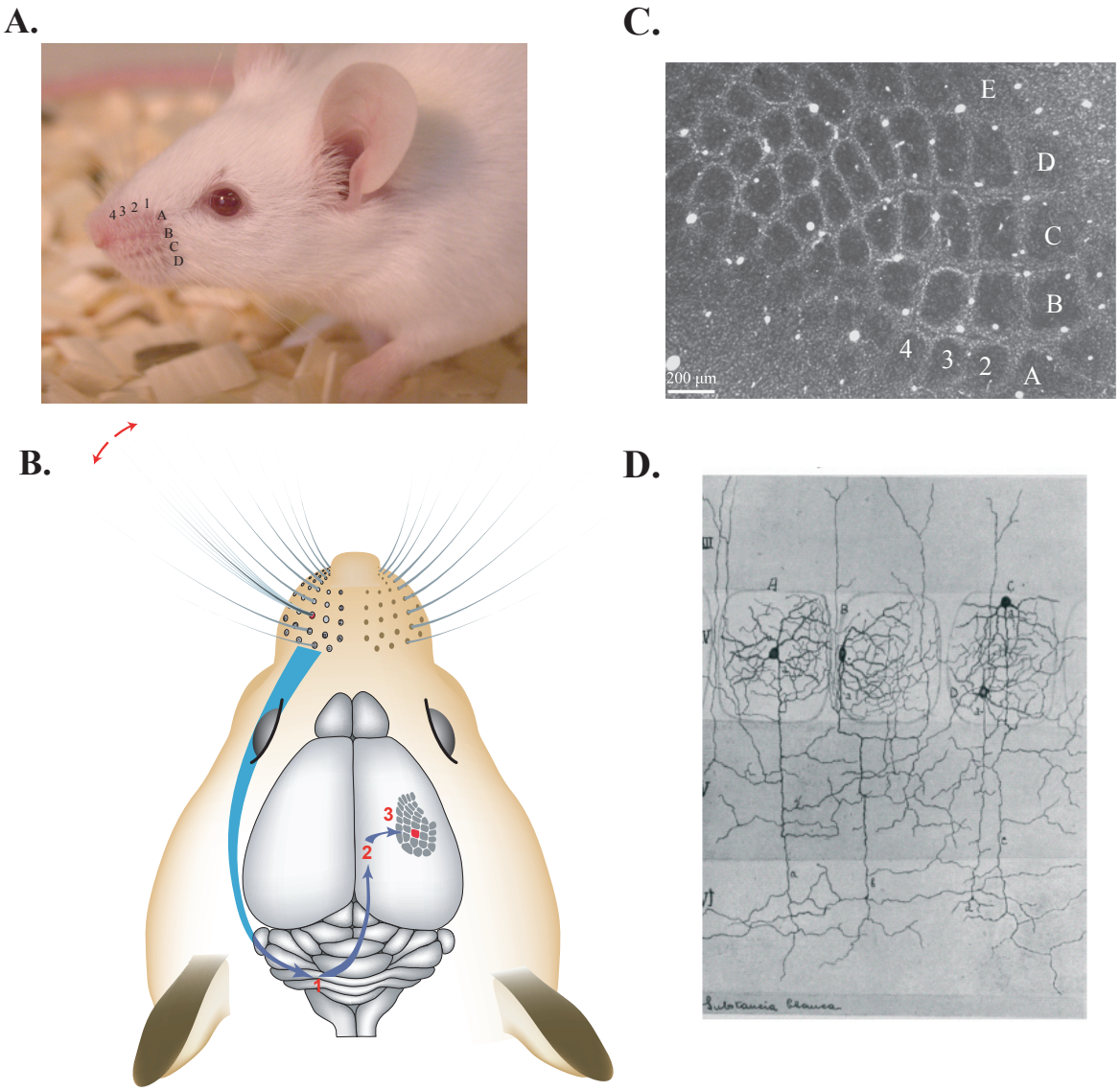

Figure 4. The whisker sensory system in the mouse. A. Whiskers are distinct sensory organs found on the snout of rodents and organized in 5 horizontal rows labeled A-E. Within each row, whiskers are identified by numbers. By whisking, mice use their sensory organs to extract information about their surroundings. B. Illustration of the whisker-to-barrel pathway, where sensory information from one whisker is projected to the contralateral cortex via two relays, one in the trigeminal nucleus in the brain stem (1) and one in the ventrobasal and posterior nuclei of the thalamus (2). Axons from the thalamus project to the somatosensory cortex (3) where they terminate principally in cortical layer IV within the corresponding barrel (illustration from Graham Knott, with permission). C. Osmium-fixed tangential section cut parallel to the pia through layer IV of the somatosensory cortex reveals the barrelfield where the organization of the barrels map exactly the whiskers follicles on the mouse snout. D. Drawing from Lorente de No (Fairent et al., 1992) showing spiny stellate cells in layer IV with their dendrites restricted to their corresponding barrel. This cytoarchitectural organization gives rise to the barrels. Also notice that these cells project fine axons within the boundaries of the cortical column.

of the functional cortical columns. The pathway that convey the sensory information from the whiskers to the cortical columns in the primary somatosensory cortex is called "the whisker-to-barrel pathway" and is made up by two subcortical relays, one in the brainstem and one in the thalamus (Figure 4B).

II.1. The whisker-to-barrel pathway

Whiskers are made up by a hair shaft whose base is enclosed in a follicle-sinus complex (Rice et al., 1986). The complex is highly innervated by several types of mechanosensory neurons which are sensitive to deflections of the vibrissae. Depending on the species and its location on the whiskerpad, a whisker is innervated by 60 to 200 fibers (Lee and Woolsey, 1975; Rice et al., 1986). Axons from one row of follicles are grouped into one row nerve which all merge together to compose the infraorbital nerve. The sensory neurons of the infraorbital nerve have their cell bodies in the trigeminal ganglia and terminate in the trigeminal nucleus located in the brainstem. The trigeminal nucleus is divided into 4 spinal trigeminal subnuclei called principalis (PrV), oralis (SpVo), interpolaris (SpVi) and caudalis (SpVc). All 4 subnuclei have a complete representation of the whiskers but an anatomical representation, called barrellette, is found only in PrV, SpVi and SpVc. There, the distribution of the barrellettes maps the whiskerpad (Belford and Killackey, 1979; Ma, 1991). PrV and SpVi are the main trigeminal nuclei to send projections to the contralateral somatosensory thalamus and more precisely into the ventrobasal nucleus (VB) and the posterior nucleus (PO). PrV sends projections mainly to VB while SpVi sends projections principally to PO (Chiaia et al., 1991; Veinante et al., 2000).

In the ventrobasal nucleus of the thalamus (VB), an anatomical topographical representation of the whiskers is visible and named barreloids (Van der Loos H., 1976). In VB, cells in one barreloid respond maximally to the deflection of the corresponding whisker. In PO, no anatomical representation of the whiskers is visible and cells respond equally to the deflection of several whiskers (Diamond et al., 1992).

Cells from the two thalamic nuclei, VB and PO, send their axons to the barrel cortex, the primary somatosensory cortex that is devoted to the whiskers. Thalamocortical axons from VB make most of their synapses in layer IV within the barrels and are also found in layer III and at the border of layer V and VI (Killackey, 1973; White, 1978; Frost and Caviness Jr., 1980; White et al., 1985; Bernardo and Woolsey, 1987). The projections from VB to the barrel cortex are known as the lemniscal pathway. They form the main thalamocortical projections received by the barrel cortex. They innervate the barrel cortex in a highly organized manner: the terminals from an individual barreloid cluster principally within the cortical column of the corresponding barrels; thus imposing the somatotopy at the cortical level. The thalamocortical projections

from PO terminate mainly in layer V and I and also in the septa-related region in layer IV and II/III (Koralek et al., 1988). They form the paralemniscal pathway. Thalamocortical inputs to the barrel cortex from VB have a small receptive field and short response latencies; the lemniscal pathway is therefore well adapted to carry the spatio-temporal characteristic of the stimulus. In contrast, thalamocortical inputs from PO have a large receptive field and long response latencies and are more suited to carry information about the overall movement of the whiskers (Brecht, 2007). As the paralemniscal pathway is mainly restricted to the septa region, information processing within a barrel column is principally devoted to the lemniscal pathway; although these two pathways converge in layer V where neurons integrate the information and relay it to various subcortical areas.

II.2. The barrel column

II.2a. Layer IV

Layer IV is the main recipient of the thalamic input and thus considered to be the entrance of sensory information to cortical processing. It is for this reason of great importance. In layer IV, three main cell types are found: the inhibitory interneurons and the two excitatory cell types, the spiny stellate cells and the star pyramidal cells. While the cell bodies of these cells are found throughout the barrel, they are mostly compacted in a ring forming the wall of the barrels. Their dendritic arborization is mostly confined to their respective barrel as first described and beautifully drawn by Raphael Lorente de No in 1922 (Figure 4D) (Fairént et al., 1992). Only 15% of them span two or more barrels (Woolsey et al., 1975). Layer IV also contains dendrites from cells that have their cell bodies located in layer III, V and VI (Gottlieb and Keller, 1997; Zhang and Deschenes, 1997). Using voltage-sensitive dye on brain slice in which inhibition mediated by $GABA_A$ receptors was blocked, it was shown that excitation spreads well beyond the barrel column in layers II/III and V, but remains confined within the barrel boundaries in layer IV (Petersen and Sakmann, 2001). This reveals that in layer IV, it is principally the confinement of the axonal and dendritic arbors within the barrel in which the cell bodies are located that gives the barrel its functional independence from the neighboring barrel columns. In contrast, for the other layers, the spread of the signal into neighboring columns is mainly controlled by the inhibitory neurons; a process referred as lateral inhibition and well known for its role in fine tuning the cortical columns.

Although layer IV is the main recipient of thalamic projections, thalamocortical terminals make only 18% of the synapses present in this layer, the rest being of an intracortical origin (Benshalom and White, 1986a). Excitatory neurons are the main targets of the thalamocortical axons as more than 80% of the thalamocortical terminals make synapses on spines (Benshalom and White, 1986; Keller and White, 1987; White et al., 2004). The spiny stellate cells are the

most contacted ones with 10 to 23% of their synapses being thalamocortical (Benshalom and White, 1986). The inhibitory neurons make up 9% of the cells in the barrelfield (Micheva and Beaulieu, 1995b). In layer IV, all of the inhibitory neurons receive thalamocortical input corresponding to about 8% of all the thalamocortical connections made in this layer (Keller and White, 1987; Staiger et al., 1996). Although both excitatory and inhibitory neurons receive thalamocortical synapses on their dendrites, inhibitory neurons also receive this type of synapses directly on their soma (Keller and White, 1987; Benshalom and White, 1986). Proportionally, 92% of thalamocortical synapses are made on spines and less than 1% on the dendritic shaft of excitatory cells, 7% on dendritic shafts of inhibitory cells and less than 1% on the soma of inhibitory cells (Staiger et al., 1996). In addition to the thalamocortical input, layer IV also receives projections from layer VI cells (Zhang and Deschenes, 1997; Pichon et al., 2008).

As the activation of thalamocortical synapses on excitatory layer IV neurons elicits small postsynaptic potentials, a large number of these synapses have to be activated synchronously for the postsynaptic neuron to be sufficiently depolarized and fire an action potential (Bruno and Sakmann, 2006). With this characteristic, neurons filter the coherent signal from the background and thus select the signal coming from the principal whisker from the rest and in particular from the surrounding whiskers. In addition, thalamocortical axons contact not only excitatory neurons but also the inhibitory ones. In the inhibitory neurons, the response to the activation of thalamocortical axons is faster and stronger than in the excitatory neurons (Cruikshank et al., 2007). Hence as demonstrated by Welker et al. (1993), the activation of the cortical column is initially inhibitory in nature. Once activated, the inhibitory cells make synapses locally on excitatory neurons that also receive direct thalamocortical synapses. This means that the excitation of the excitatory neurons by the thalamocortical axons is followed by their inhibition 1 to 2 ms later. This di-synaptic circuit serves to restrict the activity of the excitatory neurons to a short time-window; a feature necessary to represent precisely the temporal characteristic of a stimulus. All these studies highlight the role of inhibition in layer IV and reveal common principles of sensory processing that take place in this layer; indeed the activity of inhibitory and excitatory neurons are precisely tuned and this temporal relationship between inhibition and excitation shapes the cortical response and is relevant to code for different aspects of a stimulus (Wilent and Contreras, 2005 and for review see Miller et al., 2001).

II.2b. Cellular network

Layer IV cells have their axons restricted to the cortical column and pass the signal vertically to the layers above (the supragranular layers) and below (the infragranular layers) and mainly to layer II/III. There, the cells spread the signal horizontally to several barrel columns (Feldmeyer et al., 2006). In addition to their horizontal axons, layer II/III cells also project to layer V and

I and to the white matter (Gottlieb and Keller, 1997; Feldmeyer et al., 2006). Hence layer II/III is the layer where the signals from several whiskers converge to be integrated and passed on to other cortical or subcortical areas. Layer V neurons have their dendrites in layer I, II/III and IV (Gottlieb and Keller, 1997). They project their axons to the opposite hemisphere and to subcortical areas and have collaterals that terminate in all layers of the barrel cortex except layer I. Layer VI cells receive projections from the thalamus and cortical areas such as the secondary somatosensory cortex and the primary motor cortex and project mainly to contralateral and ipsilateral neocortex and to the thalamus. They also send axons within the barrel cortex that terminate in layers II/III, IV and V. Although their axons may spread horizontally over several barrels, they always make at least twice as many synapses in their own barrel column than in the surrounding barrel columns (Pichon et al., 2008).

II.2c. Flow of activation in the cortical column

The neuronal connections determine the spreading of the signal within the barrel column as well as its mode of activation. This was revealed by recording the neuronal response to whisker deflection in each cortical layer in mice or in rats. First, a subclass of neurons of layer IV and II/III, the fast neurons, respond within 15 ms and are the first ones to be activated followed by the "slow" neurons of these layers and by neurons of layer I, V and VI which become active after 15 ms (Welker et al., 1993). Hence the spread of the signal is delayed as it is passed on vertically and horizontally and this mainly due to interposition of additional synapses. Furthermore, for neurons in all layers, it holds that stimulation of the principal whisker elicits the greatest response with the shortest response latency. However, differences between the layers have been noticed. Indeed neurons from layer IV respond almost exclusively to deflection of their principal whisker while neurons from the supragranular layers and the infragranular layers respond to deflection of several surrounding whiskers (Armstrong-James and Fox, 1987; Welker et al., 1993). Altogether, the greatest response is found in the fast neurons of layers IV. By stimulating in rats several whiskers at various time-intervals and by recording the neuronal response to the deflection, studies showed that the neuronal response to the deflection of a whisker is reduced or increased if it is preceded by the stimulation of an adjacent whisker, but that the suppression or facilitation of the signal depends on the time interval between the two stimuli and on the relative position of the two whiskers (Simons, 1985; Shimegi et al., 1999). These characteristics reveal that the convergence of information of several whiskers occurs at the cortical level, and mainly in the extragranular layers, and is well suited to integrate the temporal and spatial characteristics of a stimulus.

III. Experience-dependent plasticity

The activation of the cortical column by a specific and restricted set of receptors at the periphery, the flow of information within the column as well as the topological organization of the columns into maps are common properties to all sensory modality and are determined by the neuronal connections. As mentioned in the first paragraphs of the introduction, past sensory history shapes cortical activity and in particular sensory experience drives the map organization of the neocortex. The effects of an altered sensory experience on cortical activity and map organization have been studied in case of deprivation caused by injury of a sensory organ or as the result of a new sensory stimulus.

One main animal model of experience-dependent plasticity is the primary visual cortex where deprivation may be induced by dark-rearing, eye-lid suture or by binocular or monocular enucleation (for review see Hofer et al., 2006b; Spolidoro et al., 2009). The primary visual cortex is composed of ocular dominance columns, where neurons from the same cortical column respond the best to the right or the left eye. When deprivation from light is induced in one eye, neurons shift their preference for the eye that remained open (Wiesel and Hubel, 1963). This shift in ocular dominance is associated with degraded visual acuity after reopening of the eye (Muir and Mitchell, 1973). Early studies revealed that this plasticity was only inducible during a certain period during development (Hubel and Wiesel, 1970) and contributed to the idea that plasticity is lost or considerably reduced in the mature brain. However, electrophysiological recordings made in the somatosensory cortex of monkeys revealed that in the cortex, the orderly topographic map representation of the skin is continuously under the influence of the sensory activity even in adults (for review see Merzenich and Jenkins, 1993). In adult monkeys, digit amputation immediately enlarges the surround receptive fields in some part of the deprived cortical area as neurons in this region become active to the surrounding skin area. After several weeks, all the area that was dedicated to the amputated digit reorganized itself and becomes activated by stimulation of the sub-adjacent skin area and by stimulation of the adjacent fingers (Merzenich et al., 1984). Furthermore, when the skin of two digits are surgically fused to one another, the skin along the suture line becomes activated simultaneously by a stimulus and instead of having a clear segregation of information in the cortex, cortical neurons representing the skin along the suture line become as responsive to stimulation of one finger as to stimulation of the other (Allard et al., 1991). In this case, the segregation of information into two separate cortical columns is lost. Cortical representation is also affected when one part of the skin is over-stimulated. In this case, this particular part of the skin is overrepresented in the cortex and the receptive field enlarged. Similarly, in humans, tasks that involve nearly simultaneous stimulation of fingers such as the one performed by professional musicians result in loss of independent digit control, a condition called focal dystonia, and is due to mal-adaptive cortical

reorganization as the cortical representation of the fingers into segregated entities is disturbed in the somatosensory cortex as well as in the motor cortex (Byl et al., 1996; Bara-Jimenez et al., 1998). In contrast, when monkeys are over-stimulated with a stimulus that moves across the skin, the cortical representation of the portion of the skin that is stimulated is enlarged but the receptive fields are smaller (Jenkins et al., 1990). Similar sensory stimulation in humans results in enhanced perceptual skills. Another example of such experience-dependent plasticity in humans is given in case of visual deprivation. TIhe visual primary cortex deprived from its primary sensory input becomes responsive to and integrates tactile and auditory stimulus and this occurs already 5 days after deprivation (reviewed in Pascual-Leone et al., 2005). For example, Braille reading in blind persons involves the primary visual cortex.

Basic principles rise from the few experiments mentioned above. First, although the cortex might be most plastic during development, the cortex undergoes plastic changes throughout life. Second, plasticity allows the expansion of the cortical representation of the most active part of the sensory periphery. Last, the receptors that receive coherent and synchronous stimuli are represented as one entity while the periphery that receives incoherent and asynchronous stimulation is segregated into several, independent entities so to sub-serve coherent input. Hence the level of neuronal activity, the coherence between sensory signals coming from the periphery and the timing of the sensory stimulation are important factors in shaping the cortical circuitry. Moreover, it is evident that such plasticity determines the perceptual and motor abilities of the individual and sustain performance such as the one exemplified by the radiologists and professional musicians and that it also sustains recovery or the acquisition of compensatory skills after loss of function at the periphery or in the central nervous system (reviewed in Pascual-Leone et al., 2005). Unfortunately, it may also lead to mal-adaptive conditions such as focal dystonia and phantom syndrome.

In an attempt to search for the synaptic mechanisms involved in the forms of experience-dependent plasticity summarized above, neuroscientists have studied plasticity by artificially altering neuronal activity and by recording the neuronal response in the postsynaptic cells. They have found that burst of high frequency (tetanic) stimulation of afferent pathways synapsing on a neuron potentiates in the postsynaptic neuron the response to stimulation of the presynaptic neuron, a phenomena called long-term potentiation (LTP) (Bliss and Lomo, 1970; Bliss and Lomo, 1973; Artola and Singer, 1987; Bindman et al., 1988). Conversely, stimulation at low frequency decreases the neuronal response and is called long-term depression (LTD) (Barrionuevo et al., 1980; Feldman et al., 1998). Hence following LTP-inducing protocols, the connection between two neurons is potentiated while it is decreased following protocols inducing LTD. Synaptic transmission might also be altered by varying the spike timing in both the

presynaptic and postsynaptic neurons, a phenomena known as spike-timing dependent plasticity (Markram et al., 1997). In general, if the presynaptic neurons fire before the postsynaptic one, the synaptic transmission is increased; while it is decreased, if the postsynaptic neuron fires before the activation of the presynaptic element. Hence coincidence of activity between two neurons regulates their connectivity. These changes in synaptic transmission are sustained by alteration of its molecular constituents and initiated by the activity-dependent activation of specific receptors at the plasma membrane that will initiate a series of molecular events in the cells.

III.1. Molecular plasticity and signaling pathways

Activity-dependent modification of synaptic transmission is sustained by changes at the molecular level, through a cascade of interactions in the cells, called signaling pathways. Signaling pathways are first generated by the activation of receptors on the outer surface of the cell membrane by molecules that are released in the extracellular space. These molecules can be neurotransmitters, growth factors or neuro-modulators which, once released, bind to their specific receptors that convert the signal into molecular activity in the cytoplasm and in the nucleus to modulate gene transcription and other molecular events that finally lead to modified synaptic function and/or structural adaptations.

Current knowledge on the molecular pathways involved in synaptic plasticity is mainly based on studies using LTP. The studies demonstrated that the main and primary signal to initiate signaling cascades in the post-synaptic cell is the calcium ion. Calcium ions enter the cytoplasm through various ways, the main one being the activation of NMDA receptor complex. NMDA receptors are bound by glutamate, the main excitatory neurotransmitter in the brain, but this binding alone is not sufficient to open the ion-channels, as they are blocked by magnesium ions that are present in the channels and are making them inactive. The only way for the magnesium ions to be released from the channels is by a strong depolarization of the plasma membrane. The depolarization is obtained by the entry of sodium following a strong activation of neighboring AMPA receptors. Hence, NMDA receptors need the occurrence simultaneously of glutamate release by its presynaptic partner and depolarization of its membrane to be activated and act as a coincidence detector. Once this criterion is met, the channels are opened and the concentration of calcium ions rises in the postsynaptic cytoplasm. This combined activity is one of the basic mechanisms involved in the generation of LTP, and hence of the various modifications of the synapse observed in response to alteration in the neuronal activity (see for review Lisman, 2003). However there are other ways through which the cytoplasmic calcium concentration can rise: through the opening of voltage-gated calcium channels at the plasma membrane or by the ligand-mediated opening of channels located at the plasma membrane or on internal stores such

as the spine apparatus.

In the cytoplasm, there are various Ca^{2+} sensors, the main one being the calcium-calmodulin kinase II (CaMKII). CaMKII is a kinase that is activated and auto-phosphorylated by protocols inducing LTP (Fukunaga, 1993; Otmakhov et al., 2004) and it is required to induce functional changes of the synapses mediated by the activation of NMDA receptors (Otmakhov et al., 1997; Giese et al., 1998). Other studies demonstrated that CaMKII is required for map plasticity following whisker trimming in adolescent and adult mice (Glazewski et al., 1996; Glazewski et al., 2000) as well as for plasticity in the visual cortex (Taha et al., 2002). Another calcium sensor involved in LTP is the calcium-calmodulin activated adenylate cyclase which increases the level of cAMP (Chetkovich and Sweatt, 1993). The cAMP level can also be increased by the activation of receptors coupled to G-protein, such as the metabotropic receptors to glutamate. The cAMP, in turn, activates the cAMP-dependent protein kinase called PKA (Mayr and Montminy, 2001). Other Ca^{2+} sensors are the protein kinase C (PKC) or the nitric oxide synthase.

Through phosphorylation, kinases alter synaptic strength by acting on a series of molecular processes (see Figure 5). For example, kinases act directly on the receptors for glutamate or GABA increasing their efficacy or control their insertion at the synapse (for review see Song and Huganir, 2002; Luscher and Keller, 2004). In the presynaptic terminal, activation of kinases also regulates the exocytotic machinery and hence the probability of neurotransmitter release. In addition to these local and short lasting modifications of the molecules present at the synapse, longer lasting modifications of the neuronal function are required to generate altered synaptic function. The more persistent modifications depend on de novo protein synthesis and altered gene expression that is mediated by the activity of the kinases (Huang, 1998).

Gene expression is a highly regulated and multi-molecular event that leads to the de novo synthesis of a functional gene product, generally proteins, and was shown to be essential in the formation of long-lasting memories (Igaz et al., 2002). Gene expression starts with transcription, a step during which the sequence in deoxyribonucleic acids (DNA) of a gene serves to the transcription of a complementary strand made of ribonucleic acids (RNA), the RNA transcript. The RNA transcript then undergoes steps of splicing and polyadenylation. During splicing, certain parts of a RNA sequence called introns (sequence of a gene that are not translated into proteins) are removed while during polyadenylation, a multiple adenosine phosphates (polyA) tail is added to the end of the RNA. The mature RNA transcript is then translocated from the nucleus to the cytoplasm to be translated into a protein (a phase called translation). Transcription is initiated when transcription factors and a RNA polymerase recognize and bind to DNA domains within the promoter site of a gene. The activity and/or the expression of many transcription factors

are regulated by neuronal activity and it is the interplay between transcription activators and repressors present at the promoter site, their post-translational states (such as phosphorylation) as well as the configuration of the DNA (open chromatin or condensed) that determines whether a gene will be transcribed or not and the rate at which it will be transcribed (for review see Alberini, 2009). Gene transcription was shown to be necessary in memory formation and to occur in at least two phases: one at the time of training and the other 3 to 6 hours later. This was revealed by injecting an inhibitor of the polymerase II in the hippocampus before and after a step down inhibitory avoidance task and by measuring the step down latencies 24 hours later (Igaz et al., 2002).

One known transcription factor regulated by neuronal activity is the cAMP-responsive element binding protein (CREB). CREB activity has already been shown to be important for map plasticity in the somatosensory cortex of rodents as plasticity is impaired in mutant mice (Glazewski et al., 1999) and cAMP response element (CRE)-mediated gene transcription occurs in layer IV following altered sensory experience (Barth et al., 2000). CREB activity initiates the expression of CRE-mediated genes, which code for synaptic molecules or molecules associated with plasticity, among which Brain Derived Neurotrophic Factor (BDNF). BDNF is a secreted growth factor known to regulate axonal and dendritic growth as well as synaptogenesis. Short or long exposure to BDNF has different effects on the cortical circuit. Short exposure enhances excitability in the circuit while lasting exposure stabilize the activity of the network by balancing the excitatory inputs on the pyramidal cells and the ones on the inhibitory interneurons (Turrigiano and Nelson, 2000).

Recently microarray technology has been developed. DNA microarrays are two-dimensional arrays of spots (features) on a glass or a silicon chip. Each spot contains known oligonucleotide sequences (probes) designed to hybridize with specific nucleic sequences within the transcribed genome. Microarrays are hybridized with RNAs that were extracted from biological samples, fragmented and fluorescently labeled. After series of washing steps, the intensity of fluorescence for each probe is measured; giving the relative abundance of the sequence of RNA targeted by a particular probe within the sample. Intensity signals from all the probes designed to recognize various part of the same RNA transcript are then summarized into a gene signal. Value of a gene signal gives the relative abundance in the sample for the RNA transcript(s) encoded by that gene. The hundred thousands or even millions of features that microarrays contain enable the simultaneous screening of thousands of RNA transcripts and measure their relative abundance. Thus, this method enables to assess simultaneously the level of expression of thousands of genes (i.e. practically the entire genome). The first studies applying this technology in the domain of cortical plasticity in sensory systems revealed that plasticity is sustained by the regulation of

hundreds of genes that are composed of growth factors, transcription factors, calcium binding proteins, receptors as well as components of the extracellular matrix (Lachance and Chaudhuri, 2004; Tropea et al., 2006; Oh et al., 2007; Lyckman et al., 2008; Harris et al., 2008; and for review see Tropea et al., 2009). In these studies, regulation of gene expression was assessed in response to sensory deprivation. It appears that the molecular changes at the synapses and gene expression regulation do not only modify synaptic strength but also sustain structural modifications.

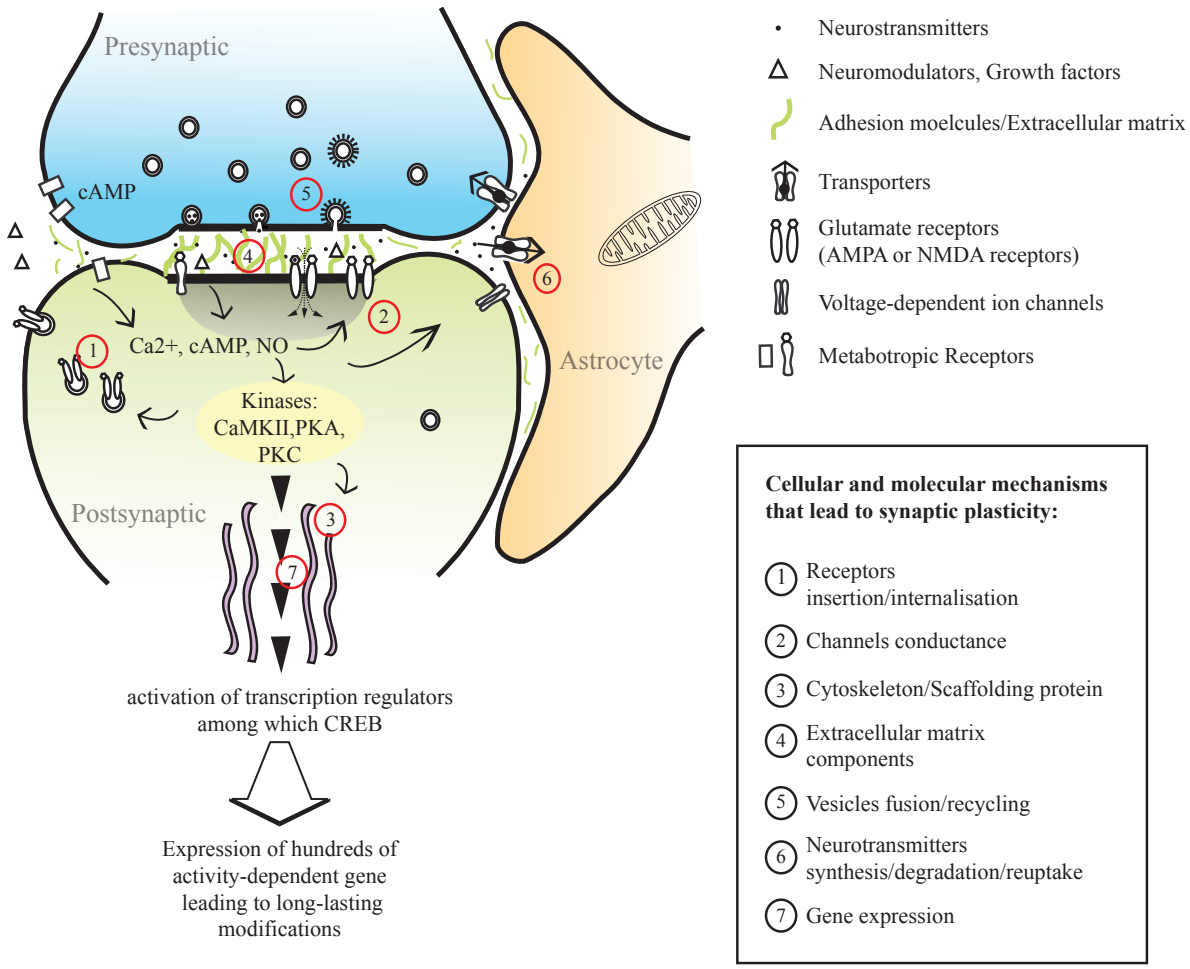

Figure 5. Short and long-term modifications that are taking place at the synapse in response to an increased neuronal activity. The activation of receptors at the plasma membrane lead to an increase in intracellular level of calcium (Ca2+) or other second messengers (cAMP, NO) which is followed by the activation of protein kinases and a series of signalling cascades. These changes lead to the modification of various cellular and molecular processes at the synapse mediating synaptic plasticity.

III.2. Ultrastructural aspects of neuronal plasticity

The effect of neuronal activity on structural changes have been studied using protocols inducing LTP or LTD. Electron microscopy analysis after LTP-inducing protocol performed on anesthetized rats showed that the density of synapses on dendritic shafts is increased within 45 min while various properties of the spines such as neck width and length of the postsynaptic density become less variable (Lee et al., 1980). In this study, no distinction was made between excitatory or inhibitory synapses. Similar results were found after LTP-inducing protocol in hippocampal slices, in which the number of synapses on dendritic shafts is increased (Chang and Greenough, 1984). This effect is induced as early as 10 min after the stimulation and is still present 8 hours after. These two studies were performed on the neuropil subjected to LTP and contrast with EM-analyses limited to branches of dendrites of identified neurons from which electrophysiological recordings were made during the period of LTP-induction. Indeed, electron microscopy reconstruction of dendrites from granular cells of the dentate molecular layer of the hippocampus show that these cells present an increased number of spines and especially of double-headed spines after LTP (Trommald et al., 1996). Also two-photon imaging of dendritic branches from hippocampal neurons in CA1 show that spines are formed after LTP and this no earlier than 30 min after LTP induction (Engert and Bonhoeffer, 1999). As a complement to alterations at the level of spines, subsequent studies demonstrated structural plasticity of axons (for review see Gogolla et al., 2007). In particular, repeated confocal imaging on hippocampal slices showed that axonal protrusions, or “terminal boutons”, as well as varicosities of the axonal shaft, called “en passant boutons” are formed within 10 min in response to LTP-inducing protocol (Nikonenko et al., 2003). At this time, only half of the filopodia-like structures are in close contact with postsynaptic elements as revealed by subsequent electron microscopy analysis and in only 18% of the cases is a postsynaptic density visible in the target. Twenty and thirty minutes later, morphologically mature synaptic contacts are made in 90% of the cases. In addition, filopodia-like axonal protrusions initially make synaptic contact with dendritic shafts but 30 min after LTP induction, they synapse with spines (Nikonenko et al., 2003). This study reveals that structural remodeling with insertion of synaptic contacts may occur rather quickly and this within half an hour.

In addition to these studies which focus on the excitatory neurons, plasticity of the inhibitory interneurons has also been analyzed. Co-labeling of excitatory and inhibitory synapses and electrophysiological recordings performed on cultured hippocampal neurons show that excitatory and inhibitory synapses on dendritic branches are precisely and evenly distributed along the dendritic branches to maintain a 4:1 ratio across the dendritic surface and balance the neuronal output (Liu, 2004). Furthermore, this functional balance between inhibition and excitation is actively regulated (Kilman et al., 2002; Liu, 2004). In particular, when neuronal

activity is blocked, the number of GABA receptors clustered at synapses decreases leading to a significant reduction in the number of inhibitory synapses but maintaining the overall synaptic density constant (Kilman et al., 2002).

LTP and LTD are artificially generated and although it can be elicited in some brain area at every age, stimulation of thalamocortical axons elicits LTP or LTD in layer IV of the somatosensory neocortex only upon P7 in thalamocortical slice preparation from rat pups (Crair and Malenka, 1995; Feldman et al., 1998). However, despite the fact that LTP and LTD can no longer be induced in layer IV of the adult somatosensory cortex, response of layer IV cortical neurons can still be altered following a novel sensory activity initiated in adult animals (Diamond et al., 1993; Armstrong-James et al., 1994; Wallace and Fox, 1999; Rema et al., 2006; Quairiaux et al., 2007). Hence, although LTP and LTD mechanisms are possibly involved in the experience-dependent plasticity they cannot be considered to explain all the alterations of response properties induced by the altered neuronal activity. It is therefore of great importance to study whether structural modifications also occur *in vivo* following sensory alteration in the adult cerebral cortex.

In the visual system of adult animals, novel sensory experience was shown to induce structural modification. In adult rats that had explored an enriched environment for 30 days, neurons show an increase in the number and the length of dendrites (Uylings et al., 1978). Electron microscopy analysis showed that the ratio of synapses per neuron is increased and that the synaptic contact zone is larger after 30 days of exploring a complex environment (Sirevaag and Greenough, 1985; Turner and Greenough, 1985). Also 4 months old rats that have explored an enriched environment for 60 days have a higher density of axonal boutons which synapse with both a dendritic spine and a dendritic shaft (Jones et al., 1997). Also, the density of dendritic spines is altered in animals raised in different housing conditions (Globus et al., 1973; Connor and Diamond, 1982).

III.3. Dynamic of structural plasticity *in vivo*

Spines have been extensively studied in the context of plasticity as they can be visualized by optical imaging and about 80% of the synapses in the cortex are made on these dendritic protrusions and thus are the major recipient of excitatory synapses in the neocortex (Beaulieu and Colonnier, 1985). In addition, their morphology is often affected in neurological disorders; a strong indication of their importance in cortical function (Fiala et al., 2002). Recently, the dynamic of spine motility has been studied in the most superficial layers of the cortex by performing time-lapse two photons microscopy on living animals with neurons expressing green fluorescent protein (GFP) (Chen et al., 2000; Lendvai et al., 2000; Trachtenberg et al., 2002; Grutzendler et al., 2002). By imaging the spines every 10 min for 90 min, Lendvai and colleagues

showed that spines change their length and shape within minutes and some population appear and disappear over tens of minutes (Lendvai et al., 2000). The motility is highest in young animals when cortical receptive fields are most plastic (Lendvai et al., 2000; Grutzendler et al., 2002). Also a similar study performed in adult animals shows that three classes of spines can be distinguished: 17% are transient with a lifetime less than a day, 23% are semi-stable, with a lifetime of 2 to 3 days and 60% of them are stable persisting for more than 8 days. Among the stable ones, only 15% of them disappear within the following 30 days (Trachtenberg et al., 2002). With age, the pool of stable spines increases gradually from 35% at P16-25 to 73% at P175-222 (Holtmaat et al., 2005). It is important to note that spines disappearing between imaging session are replaced by new ones, maintaining the spine density constant (Lendvai et al., 2000; Trachtenberg et al., 2002). Although in another study, it is reported that spine density decreases with age through a differential rate of spine elimination and spine formation (Zuo et al., 2005).

Although spines are continuously formed and eliminated throughout life, the turn-over of the spines are considerably altered when neuronal activity is modified. Indeed, when modifying the normal sensory activity in the adult mice by trimming the whiskers in a chessboard pattern, the pool of transient spines imaged in the living animal increases 2 to 4 days after the onset of the deprivation while the pool of stable spines decreases (Trachtenberg et al., 2002). Hence, in this case, the overall spine density is not affected by changes in sensory input whereas electrophysiological recordings had demonstrated that this deprivation paradigm induces alterations in receptive field properties. In contrast, Zuo and colleagues showed that the spine elimination that they observed to occur naturally with age is slowed down by trimming all whiskers resulting in a higher density of spines as compared to control animals (Zuo et al., 2005).

Reconstructions from serial section electron microscopy of previously imaged dendritic branches *in vivo* with the two photons electron microscope clearly demonstrate that spine formation and retraction is paralleled by excitatory synapse insertion and elimination (Trachtenberg et al., 2002; Holtmaat et al., 2005; Knott et al., 2006). Synapses insertion may occur rapidly after spine formation as spines less than 2.5 hours old are already contacted by excitatory synapses as reported from study on spines formed in response to two-photons glutamate uncaging in hippocampal slice (Zito et al., 2009) or, in an equivalent slice preparation, may require more than 15 hours to be inserted on the newly formed spine (Nagerl et al., 2007). However, in this case, spines were formed in response to tetanic stimulation and not to the uncaging of glutamate. This may explain the longer time interval between spine formation and synapse insertion. How quickly spine formation is followed by synapse insertion *in vivo* is still unknown and currently

the focus of intensive research. As a first attempt, Knott and colleagues showed that spines that were reconstructed shortly after they had appeared (less than 4 days old) often lack synapses, while spines that are 4 days old or older always had one (Knott et al., 2006).

Structural plasticity of the axonal branches of excitatory cells and their boutons has also been observed by time-lapse two photons microscopy in the superficial layers of the adult mice primary somatosensory cortex or the primary visual cortex of the adult Macaque monkeys (De Paola et al., 2006; Stettler et al., 2006). The two studies reveal that axons are dynamic structures even in adults; while at a large scale the axonal branching pattern remains stable, small branches and some of the axonal synaptic boutons appear and disappear. In the somatosensory cortex, some branches could grow or retract over a distance of up to 150 μm in 4 days. Also a subset of en passant boutons and of terminaux boutons appear and disappear over time of days but keeping the bouton density constant (De Paola et al., 2006). In addition, axons from different types of neurons exhibit different axonal branches and boutons pattern and differ by their plasticity. Pyramidal cells from layer VI exhibit the most proportion of terminaux boutons which appear and disappear frequently; overall only 30% of their boutons survived more than 1.5 months (De Paola et al., 2006). In contrast, boutons from cells from POm are highly stable, with the vast majority that survive for 9 months (De Paola et al., 2006). It was also noticed that terminaux boutons are more dynamic than the ones en passant (De Paola et al., 2006). Sensory activity was however not altered in these experiments and it is therefore not known how axonal dynamics *in vivo* is affected by altered sensory experience. It appears that new spines tend to establish synaptic contact with already existing boutons forming multi-synaptic boutons after chessboard whisker trimming or whisker stimulation (Knott et al., 2006; Genoud et al., 2006a). Similarly in the visual cortex, it is the multi-synaptic boutons that are increased in adults after the exploration of an enriched environment for 60 days (Jones et al., 1997). However, formation of new single-synaptic boutons cannot be ruled out.

III.4. Experience-dependent plasticity in the Whisker-to-barrel pathway

In the whisker sensory system of rodents, experience-dependent plasticity is most often studied by clipping or trimming the whiskers in a variety of different patterns or by removing a certain number of whisker-follicles. Altering sensory experience by peripheral deprivation is the most extensively used paradigm to study experience-dependent plasticity in this sensory pathway.

III.4a. Peripheral deprivation in the sensory system of rodents

The barrel field in rodents appears within their first week of life. First thalamocortical projections invade the cortex in a somatotopic manner within the first day of life while barrels appear on postnatal day 4 (P4) (Erzurumlu and Jhaveri, 1990; Senft and Woolsey, 1991; Agmon et al.,

1993). When a whisker is naturally lacking or when supernumerary follicles occur, the cortical representation of the whiskerpad is similarly altered: the corresponding barrel is absent or an extra one is present (Van der Loos et al., 1984; Welker and Van der Loos, 1986). Also, when whiskers are injured shortly after birth, the corresponding barrels are absent (Van der Loos and Woolsey, 1973). This effect is only observed when lesions are performed before postnatal day 4 (P4) in mouse, but up to P6 lesions reduce the barrel size (Woolsey and Wann, 1976; Jeanmonod et al., 1981). Hence, the cytoarchitectural organization of the barrels requires an intact periphery to form and past this critical period, lesions do not any longer induce alteration of the barrelfield pattern.

In contrast to lesion-induced alteration of the sensory signal, if one starts at birth to pluck all the whiskers but one, in rats, the general barrel pattern is not altered although in a few cases the spared-barrels appear slightly enlarged (Fox, 1992). When started at P2, the modification of the barrel size is no longer observed. However, despite the absence of any morphological modifications of the barrel pattern, the neuronal response of layer IV neurons recorded between P30 and P90 is altered in animals from which all whiskers were removed early during their development and up to 4-7 days before the recordings (Fox, 1992). This experiment showed further that the induced alteration of the neuronal response depends on the age of the animal at which peripheral deprivation is initiated and also depends on the location of the recorded neuron within the different cortical layers. When initiated at birth, 37% of the neurons from the deprived barrels in layer IV respond preferentially to the spared whisker than to their anatomically related re-grown whiskers. However, the capacity of layer IV neurons to shift their response towards the spared whisker decreases rapidly with age as only 12% and 14% of the cells in this layer present a shift in their response towards the spared whisker when the removal of the whiskers is initiated respectively at P4 and P7 and their response is recorded in adult (Fox, 1992). This shift in response is due to an increase in the response magnitude to stimulation of the spared whisker and not to a decrease in the response to the principal re-grown whisker. Neurons in layer II/III also shift their response towards the spared whisker where more than 50% of the cells are dominated by the spared whisker after peripheral deprivation while less than 5% of the cells respond preferentially to an adjacent whisker in a control animal (Fox, 1992). This alteration of the response shows only a slight decrease when peripheral deprivation was initiated at P7 instead of P0. Also in contrast to layer IV neurons, this shift in layer II/III is due both to a decrease in the response magnitude to the principal re-grown whisker as well as to an increase in the response magnitude to the spared whisker (Fox, 1992). Hence in layer II/III, the usual vertical input inside the cortical column is depressed and the horizontal intracortical connections are potentiated. In layer IV, it is only the intracortical connections that are altered and plasticity in this layer decreases rapidly with development.

Another study, using the same peripheral deprivation paradigm, shows that layer II/III remains plastic beyond the first postnatal week as deprivation initiated at P28 also elicits changes of the neuronal response 7, 20 or 60 days later (Glazewski and Fox, 1996). In this study, removing the whisker at P28 and recording the response at various time intervals in layer II/III reveals that the potentiation of the response to the spared whisker and the suppression of the response to the principal deprived whisker have distinct time-course of induction. After 7 days of peripheral deprivation, the response to the spared whisker is at the control level after 7 days and becomes potentiated only after 20 days and continues to increase by 60 days, while the response to the deprived principal whisker is already suppressed after 7 days and is at its lowest level after 20 days (Glazewski and Fox, 1996). Hence, in this study, suppression of the vertical input appears to be the first component of the plastic changes initiated by the altered sensory experience. Again, in this study where deprivation started at P28, layer IV neurons show no clear sign of plasticity, confirming the idea of a critical period in the first postnatal week for neurons in this layer, at least with this experimental paradigm. However, when studied by 2-deoxyglucose method as a marker of neuronal metabolic activity, clipping all but one whisker during adulthood leads to an increase in the size of the corresponding barrel which becomes significant after 7 days (Levin and Dunn-Meynell, 1991). Hence although the receptive field may not be significantly altered in layer IV, more subtle changes are still occurring in this layer.

Additional studies reveal that receptive field plasticity depends on the level and the pattern of sensory activity and that these are important factors especially for layer IV plasticity. By trimming all the whiskers except two, thus keeping the activity of the two whiskers correlated ("paired"), Diamond and colleagues showed that the receptive fields of layer IV neurons retain their plasticity in adult rats. Indeed, the cortical response to the adjacent paired-whiskers becomes potentiated while the response to the adjacent cut-whiskers is depressed and this already 3 days after the onset of the sensory alteration (Diamond et al., 1993). These changes are already present after 24 hours in layer II/III neurons (Diamond et al., 1994). The importance of the level of sensory experience on plasticity is further exemplified by an experiment where the rats were able to explore an enriched environment after whisker trimming. In these conditions and using the same experimental paradigm just described, 15 hours is sufficient to induce plasticity in adult rats in both layer IV and layer II/III neurons (Rema et al., 2006). Hence receptive field plasticity can be accelerated by increasing the level of sensory experience. It is to note that in these experiments, 15 hours appears to be the shortest time at which plastic changes can be evaluated as the animals have to be anesthetized for whisker trimming and once again before electrophysiological recordings.

Three basic principles emerge from these experimental studies:

1. The main one is that following an altered sensory experience, the receptive fields of the cortical neurons, and thus the cortical sensory maps, are altered. This experience-dependent plasticity is age-dependent: some type of plasticity can be induced in young animals but can no longer be elicited in adults.
2. Cortical plasticity is layer-dependent. Indeed, layer II/III retains its capacity for plasticity throughout adulthood while layer IV becomes far less plastic as the animals mature.
3. Cortical changes induced by the altered sensory experience as well as the time necessary to elicit those changes depend on the level of sensory activity.

III.4b. Peripheral stimulation in the whisker-to-barrel pathway of rodents

As the level of sensory activity determines the capacity of the cortical circuitry to adapt to altered sensory experience, it is important to study experience-dependent plasticity in case of increased sensory activity instead of deprivation. This is achieved by exposing the animal to an enriched environment or by passively stimulating one or several whiskers.

Rats placed in a naturalistic habitat which promotes innate sensory-motor behavior such as subterranean tunneling, foraging and three-dimensional navigations as well as social interactions have their sensory activity elevated compared to animals that are kept in standard laboratory cage. By intrinsic signal optical imaging and single unit recording, it was shown that after exposing adults rats (3 months old) to such an environment for 4 to 6 weeks the receptive field size and the whisker-evoked peak amplitude decreases in layer II/III (Polley et al., 2004). There, responses to the principal whisker as well as to the adjacent whiskers are both decreased but not equally so that the response is shifted towards the principal whisker resulting in the sharpening of the receptive field. Hence, exposition to an enriched environment induces functional refinement of the cortical sensory maps.

To specifically study the mechanisms of map refinement induced by an increased sensory activity, the activity of a subset of whiskers may be passively elevated and the modifications induced in the corresponding cortical barrel columns directly compared to the adjacent ones. Passive whisker stimulation is achieved by gluing a piece of metal on the selected whiskers and placing the mice in the Lausanne whisker stimulator (Melzer et al., 1985). There, the animal can freely move while being exposed to magnetic field bursts that passively stimulate the whiskers at normal whisking frequency. Deoxyglucose study showed that by doing so for 45 min, the corresponding barrel columns are activated (Melzer et al., 1985). After such stimulation of a subset of whiskers for 1, 2 or 4 days, animals that are left to explore a new environment for

45 min show a reduction in 2-deoxyglucose uptake in the barrel columns corresponding to the passively stimulated whiskers indicating that adaptation has occurred to reduce the level of cortical activity (Welker et al., 1992). In agreement, extracellular recordings showed that the spontaneous activity is decreased and the neuronal response to the stimulated whisker is depressed in the corresponding barrel, in layer IV as well as in layer II/III and this after 24 hours of such chronic passive stimulation (Quairiaux et al., 2007). However, barrel neurons still respond preferentially to their principal whisker with a diminished response to stimulation of neighboring in-row (Quairiaux et al., 2007). In addition, the response to the deflection of the stimulated whisker is reduced in the adjacent barrels, but only in layer II/III suggesting that the surround receptive field of the adjacent barrel columns is also reduced. Post-stimulus epoch analysis reveals that the modifications of the response to the stimulated whisker are more likely to occur at the cortical level and are not generated at the subcortical relays as it is decreased in the period 12-25 ms after deflection of the whisker (Quairiaux et al., 2007). Interestingly, four days after the end of the stimulation, the response magnitude is not decreased anymore but is significantly increased. This increase is mainly observed in the 50-100 ms post-stimulus period.

The functional modifications summarized in the previous paragraphs are paralleled by changes of cortical circuitry and seem to involve especially the inhibitory innervations. This is exemplified by the fact that the density of axonal boutons that are immuno-reactive for glutamic acid decarboxylase (GAD), the enzyme that catalyzes the synthesis of the inhibitory neurotransmitter GABA, is decreased or increased following respectively whisker ablation and whisker stimulation (Welker et al., 1989b; Welker et al., 1989a). Similarly GAD immuno-reactivity is also increased after whisker stimulation paired with an aversive stimulus (Siucinska and Kossut, 2006). Furthermore, the increase in the corresponding barrel columns in the level of GAD immuno-reactivity following 4 days of chronic whisker stimulation lasts 2 days after the end of the stimulation and returns to normal level after 5 (Welker et al., 1989a). Using serial section electron microscopy, Knott and colleagues showed that the density of synapses is increased in the stimulated barrel after 24 hours of stimulation (2002). Especially the number of inhibitory synapses on spine is increased by 4 fold and the overall ratio between inhibitory and excitatory synapses is shifted towards higher inhibition (from 0.22 to 0.35). Interestingly, the inhibitory synapses on spines remain present 4 days after the end of the stimulation while the ratio returns to normal level (Knott et al., 2002). In adult rats which were sensory deprived from birth, the number of inhibitory synapses on spines is found to be decreased (Micheva and Beaulieu, 1995a), suggesting that this specific type of synaptic connections play an important role in shaping the neuronal response in function of sensory activity. In addition, the fact that inhibitory synapses on spines appear with increased sensory activity and are retained several

days after the end of stimulation suggests that they could be part of long-lasting structural modifications leaving a lasting trace of the period of altered sensory input. This could be interpreted as a form of adaptation of the cortical circuit and it has parallels with memory formation. It is to note that this specific class of spines can only been distinguished from the rest of the spine population in electron microscopy studies and that in the cerebral cortex in general they make up 10% of the spine population (Jones and Powell, 1969).

Concerning the molecules that could sustain the functional and morphological changes triggered by the increased sensory activity, BDNF is up-regulated in the corresponding barrel column of adult mice after 6 hours of whisker stimulation (Rocamora et al., 1996) and is required for the synaptogenesis that is associated with 24 hours of this altered sensory experience (Genoud et al., 2004). Also the protein level for two astrocytic glutamate transporters is up-regulated following 24 hours of whisker stimulation and could be implicated in reducing neuronal excitability (Genoud et al., 2006b).

The up-regulation of BDNF mRNA level suggests that gene expression is implicated and necessary for experience-dependent plasticity in adult animals which is associated with structural and functional modifications of the neurons, however, apart from BDNF, few other genes are known to be, in this way, regulated by the increased sensory activity and in adults. Further it is so far unknown how quickly the structural modifications occur after the onset of sensory stimulation. Combined, these two aspects gave raise to the following question: “at which time scale do structural modifications take place in the living animals following sensory stimulation and what are the genes that are underlying these changes?” The study presented here is an attempt to answer this question.

Aim of this study

This study aims to elucidate the time-course of structural modifications that are associated with an increased sensory activity in adult animals and explore the network of genes that are differentially expressed in parallel to these structural changes. Ultrastructural analysis was performed on images obtained from serial section electron micrographs and synaptic density was determined in the corresponding barrel after 6, 12, 18 and 24 hours of whisker stimulation, hence giving a glimpse on the time-course of the structural modifications. In parallel, gene expression patterns after 3, 6, 9, 15 and 24 hours of whiskers stimulation was determined on microdissected barrels using high density microarray technology. We further asked whether a prior experience, which leaves long-lasting structural traces, modifies 4 days later the gene expression levels when the stimulus is given for a second stimulation period. We focused on layer IV of the somatosensory cortex, the cortical layer that is the primary recipient of the thalamic projections and the first one to be activated by a sensory stimulus. It is therefore the first stage in the processing of the sensory signal at the cortical level and it is known to be the less plastic of all the cortical layers in adult animals. The overall aim of this study is to broaden our understanding of the dynamism of the structural and molecular changes that are taking place in a mature cortex in response to an increased sensory activity and to start exploring the physiological implications of such changes.

Experimental Part

The experimental part presents the result of this study and is divided into two parts: one for the ultrastructural analysis and one for the microarray analysis. For each part, the presentation of the results is preceded by the material and the methods used and followed by a short discussion. A general discussion of the results constitutes the third part of this thesis.

I. Ultrastructural analysis

I.1 Material and Methods

Passive whisker stimulation

The ultrastructural analysis was performed on 20 female mice of the NOR strain derived from the ICR stock (Van der Loos et al., 1986). The mice were between 6 and 7 weeks old. Sixteen of them were submitted to a period of chronic stimulation of their left C2-whisker while the other whiskers were kept untouched. Mice were anesthetized with Nembutal (Sodium pentobarbital, 60 mg/kg, i.p.) and a piece of ferrous metal of 1.5 mm was glued on the chosen whiskers of their left whiskerpad approximately 3 mm away from the skin surface. All the other whiskers were kept intact. After full recovery from the anesthesia, mice were placed for a period of 6 hours (6h, n=4), 12 hours (12h, n=4), 18 hours (18h, n=4) or 24 hours (24h, n=4) in the Lausanne whisker stimulator (Melzer et al., 1985), a cylindrical cage surrounded by an electromagnetic coil which delivers magnetic field bursts at 9 Hz (Burst duration: 40 ms; intensity: $7x10^3$ A/m, frequency during burst: 50 Hz). Mice had access to food and water and could move freely. Only the whiskers that had kept their metal throughout the whole stimulation period were considered to be stimulated. Mice were raised in 12 hours day/night cycle and the experiment was planned so that all periods of stimulation ended between 2 to 3 hours after light exposure. Immediately after the stimulation period, the mice were anesthetized and processed for electron microscopy. Four non-stimulated adult mice were used as control (Ctrl).

Fixation and embedding

Mice were anesthetized with Nembutal (60 mg/kg, i.p.) and perfused intracardially with an initial rinsing solution (phosphate buffer saline 0.01M, 0.9% NaCl, pH 7.4) for 5 seconds followed by 300 ml of fixative (4% Paraformaldehyde, 2.5% Glutaraldehyde in 0.1M phosphate buffer at pH 7.4). Brains were removed one hour later. Vibratome sections were cut at 60 μm tangentially to the surface of the barrel cortex contralateral to the stimulated whisker. The sections were rinsed in cacodylate buffer (0.1M, pH 7.4) and postfixed 40 min in 1.5 % potassium ferrocyanide in osmium tetroxide (1% in cacodylate buffer 0.1M, pH 7.4) followed by 40 min in osmium tetroxide (1% in cacodylate buffer 0.1M, pH 7.4) and by 40 min in uranyl acetate (1% in water). Sections were dehydrated in alcohol and in propylene oxide and embedded in Durcapan ACM resin (Fluka, Neu-Ulm, Germany) between silicon-coated glass slides. The resin was then hardened at 65° for 24 hours. Barrels were identified in the resin embedded section and a trapezoidal block encompassing the C2 barrel was trimmed (Figure 6). Semithin sections of 1 μm thick were cut and Nissl stained to ensure that the block was made within the depth of

the barrel hollow (Figure 6). Series of 100-200 thin sections were cut at 50 ηm (ultracut UCT; Leica, Germany) and collected on pioloform carbon-coated, single-slot gold-coated copper grids (Figure 6). Sections were washed in bi-distilled water and contrasted with lead citrate.

Acquisition of stacks of serial sections and analysis of synaptic density

Sections were observed in a Phillips CM10 electron microscope and serial images (Figure 6) were taken in the neuropil of the C2 barrel at 10500x using a digital camera at a resolution of 2004 x 1336 pixels except for one stack that was taken at a resolution of 4008 x 2672 pixels (Morada camera coupled to the iTEM software, Olympus Soft Imaging Solutions, Münster, Germany). Images were aligned using Adobe Photoshop CS version 8.0 (Adobe Systems Incorporated, San Jose, CA, USA). The stack of images were then visualized in Neurolucida software (version 6.02, Microbrightfield, Williston, VT, USA) where a counting square (ranging between 42 and 57 μm^2) was placed over an area of neuropil devoid of cell body, blood vessel and large myelinated axons. The sampled volume of each stack was calculated by multiplying the surface area of the counting square by the number of sections (between 89 and 140) and their thickness. The thickness of the sections was calculated by measuring the diameter and the number of sections that span a mitochondrion cut in its horizontal. The average for at least 20 mitochondria per stack was used to determine the thickness as previously described (Kirov et al. 1999); the thickness being the average of each mitochondrial diameter divided by the number of sections that it occupies. In average, the calculated section thickness was of 0.046 ± 0.03 ηm. Synapses, which were recognized by the presence of two apposed, thickened membranes spanning at least 3 sections and by the presence of at least 3 vesicles in the presynaptic element, were identified in the delineated volume and counted. Synapses touching the top or the left sides of the counting square were eliminated while the one touching the right or the bottom ones were included. Similarly the synapses seen in the first image of the stack were excluded while synapses seen in the last image of the stack were included and all synapses fully within the borders of the volume were included (Sterio, 1984). Synaptic densities were calculated by dividing the number of synapses counted in the sampled volume divided by its volume in μm^3 calculated as mentioned above. The synapses were classified according to their pre- and postsynaptic elements. The presynaptic elements were identified as inhibitory or excitatory buttons depending on the symmetrical or asymmetrical feature of the synapse. The postsynaptic elements were identified as spine or dendritic shaft. Spine and dendritic shafts were distinguished by their size, characteristic profiles and the presence of mitochondria and microtubules.

The statistical analysis was made with SAS statistical package (SAS Institute Inc., Cary, NC, USA.). The normal distribution of variables was tested for normality (Shapiro-Wilk and Cramer-von Mises tests). As some variables showed significant deviation from normality, ranking

transformation was used. Homogeneity of variance was tested with Levene's test. When variance was homogeneous, significant difference among groups was tested with ANOVA followed by Dunnett's t tests for multiple means comparisons of all stimulation periods against the control. When variance was not homogeneous significant difference among groups was tested using Welch's ANOVA followed by a Satterthwaite's test – a t-test for unequal variance- to reveal significant difference between groups with a p value for significance set at 0.0125 to correct for multiple comparison. To test overall effect of whisker stimulation multivariate analysis (Wilks' Lambda) was performed on the following four variables: densities of excitatory synapses on shaft, inhibitory synapses on shaft, excitatory synapses on spine and inhibitory synapses on spine.

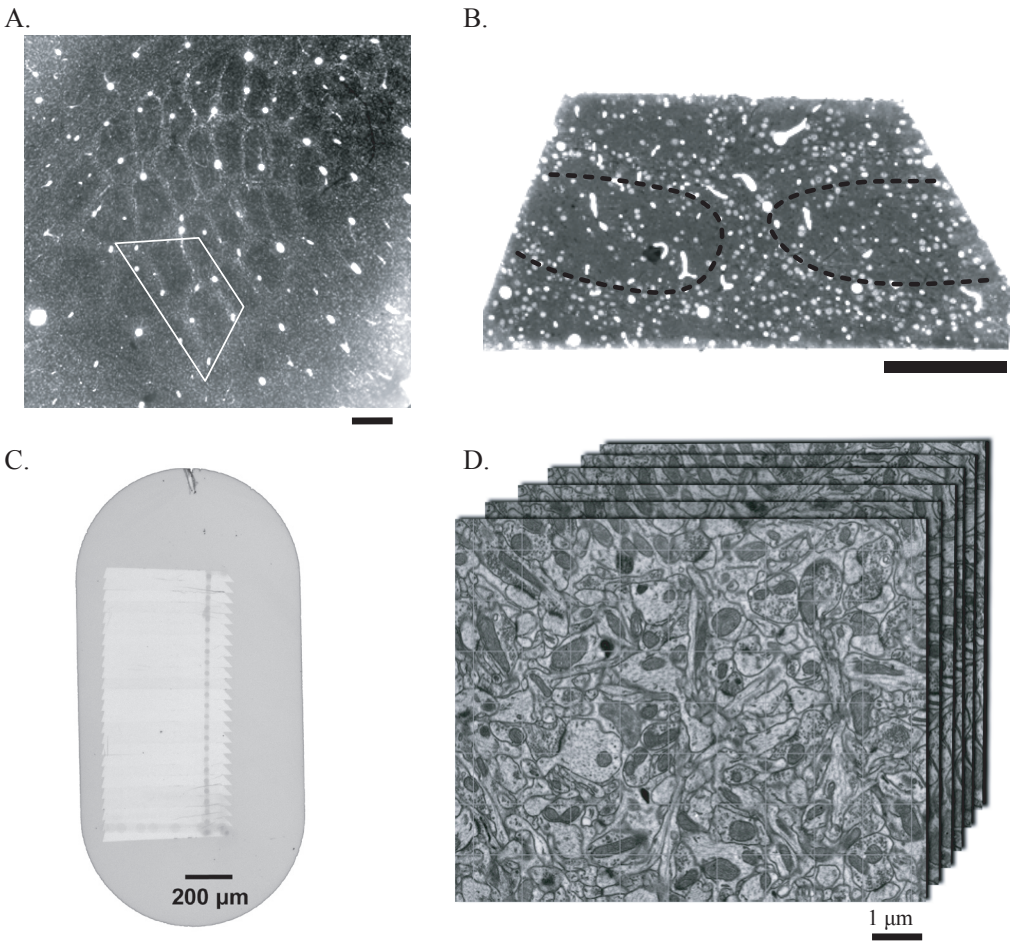

Figure 6. Identification, orientation and sampling of the neuropil within barrel hollow. In A, tangential sections through the barrel cortex cut at 60 microns through the barrel cortex, stained with osmium and embedded in resin. From this, a trapezium encompassing the barrel B2 and C2 is cut (white trapezium). Scale bar: 200 µm. B. a semithin section 1 µm thick from the block is cut and Nissl stained, showing the cytoarchitecture that delineates the barrels. This section serves as a guide to cut the final block within the C2 and B2 barrels. Scale bar 200 µm. In C, example of serial sections cut in ribbons and collected on a pioloform carbon-coated single-slot grid. Each serial section is imaged at the same location giving a series of electron micrographs within the neuropil as shown in D. From this stack of images, synapses are identified within the volume of neuropil and counted using an unbiased stereological method.

I.2. Results of the ultrastructural analysis

Ultrastructural analysis was performed on 5 groups of animals: one in which all whiskers were left unstimulated, considered as control group, and 4 in which the left C2 whiskers were stimulated for 6, 12, 18 or 24 hours. Series between 89 and 140 of serial section electron micrographs were taken within the neuropil of the right C2 barrel and synapses were counted in volumes of neuropil ranging between 199 and 265 μm^3. Summary of the number of mice per group and total volume analyzed per group are given in Table 1. Analysis showed no significant differences between the groups concerning the total synaptic density, density of all excitatory synapses and density of all inhibitory synapses ($p \geq 0.1$, ANOVA, Table 1). However, closer look at the excitatory and inhibitory synapses and their postsynaptic target show significant differences among groups for density of inhibitory synapses on spines and excitatory synapses on dendritic shafts ($p = 0.02$, MANOVA, Table 1).

Inhibitory synapses

Of all the synapses in the brain, only 10 to 20 % are inhibitory. Despite their relative small preponderance, the inhibitory synapses are however essential for the proper functioning of the nervous system. Here, we find that in the control neuropil, the inhibitory synapses form 16 ± 2 % of all the synapses with a mean density of 0.24 ± 0.03 synapses per μm^3. Among them, one third is made with dendritic spines and the others target dendritic shafts. The analysis shows

Table 1. Results of the synaptic densities measured in the neuropil of control and stimulated C2 barrels.

	Control	6h	12h	18h	24h
Total volume analyzed	901μm^3	952 μm^3	940 μm^3	886 μm^3	885 μm^3
(number of animals)	(4)	(4)	(4)	(4)	(4)
Density of all synapses per μm^3	1.54 ± 0.05	1.65 ± 0.16	1.67 ± 0.14	1.55 ± 0.09	1.45 ± 0.16
Density of inhibitory synapses per μm^3					
On spines and shafts	0.24 ± 0.03	0.29 ± 0.02	0.29 ± 0.05	0.27 ± 0.06	0.32 ± 0.02
Only on spines	0.08 ± 0.01	0.11 ± 0.03	0.08 ± 0.01	0.09 ± 0.01	0.12 ± 0.01*
Only on shafts	0.16 ± 0.02	0.18 ± 0.03	0.21 ± 0.05	0.18 ± 0.06	0.20 ± 0.02
Ratio of inhibitory synapses on shafts versus on spines	1.99 ± 0.08	1.88 ± 0.80	2.54 ± 0.50	2.04 ± 0.68	1.62 ± 0.23▪
Density of excitatory synapses per μm^3					
On spines and shafts	1.30 ± 0.05	1.36 ± 0.14	1.38 ± 0.14	1.28 ± 0.10	1.13 ± 0.16
Only on spines	1.25 ± 0.07	1.24 ± 0.13	1.22 ± 0.06	1.14 ± 0.12	1.07 ± 0.15
Only on shafts	0.05 ± 0.03	0.12 ± 0.03••	0.16 ± 0.11	0.14 ± 0.06••	0.07 ± 0.02
Ratio of excitatory synapses on shafts versus on spines	0.04 ± 0.02	0.10 ± 0.02••	0.13 ± 0.09	0.13 ± 0.06	0.06 ± 0.02
Ratio of inhibitory versus excitatory synapses	0.19 ± 0.03	0.21 ± 0.01	0.21 ± 0.05	0.21 ± 0.05	0.29 ± 0.05*

Total number of animals and total volumes of neuropil sampled from the right C2 barrels and mean values ± SD of the synaptic densities calculated for the 5 group of animals: no treatment (control), 6 hours of whisker stimulation (6h), 12 hours of stimulation (12h), 18 hours of stimulation (18h) and 24 hours of stimulation (24h). Level of significance * $p < 0.05$ (Dunnett's test), ▪ $p < 0.02$ and •• $p < 0.01$ (Satterthwaite's t-test). Satterthwaite's t-test was used when variances and means were significantly different between groups.

that these two types of inhibitory synapses are differentially regulated by sensory stimulation. Concerning the inhibitory synapses on dendritic shafts, no significant differences among the groups can be observed ($p=0.23$, ANOVA). However, the density of inhibitory synapses on spines differs significantly among the 5 groups analyzed ($p=0.03$, ANOVA, Figure 7A). Subsequent comparison between the different stimulation periods and the control showed that the density of inhibitory synapses on spines is significantly increased after 24 hours of stimulation and this by 1.5 fold. After 6 hours of stimulation, the mean and the standard deviation appear to be slightly higher than for the control but the differences are not important enough to pass statistical significance. Changes in the ratio of inhibitory synapses on shaft versus on spines can reflect the dynamic modification of the inhibitory innervations. The ratio of inhibitory synapses on shaft versus on spines varies with sensory stimulation as the 5 groups differs in their mean and their variability ($p < 0.01$, Levene's Test, $p=0.02$, Welch's Test, Table 1). After 24 hours of sensory stimulation, this ratio shows a tendency to be decreased by 0.83 fold and is at the limit of significance ($p=0.018$, Satterthwaite's Test with $p \leq 0.012$ set as the limit of significance for multiple comparison). Altogether, these results show that the inhibitory innervations undergo structural rewiring which becomes significant more than 18 hours after the onset of the increased sensory stimulation and concerns the inhibitory synapses on spines.

Excitatory synapses

Excitatory synapses are the most frequent synaptic contacts in the cerebral cortex and are formed in the majority of the cases on dendritic spines. In the control neuropil, they constitute 81 ± 3 % of all synaptic contacts with a mean density of 1.25 ± 0.07 synapses per μm^3. Surprisingly, sensory stimulation does not significantly alter this population of synapses, as the mean density of excitatory synapses on spines is not significantly different among the 5 groups of animals ($p=0.24$, ANOVA). Excitatory synaptic contacts can also occur on dendritic shafts (Figure 7C) but at a much lower frequency. In the control neuropil, they constitute only 4 ± 2 % of all the excitatory synapses with a mean density of 0.05 ± 0.03 synapses per μm^3. The variance and the mean density of excitatory synapses on dendritic shafts are significantly affected by sensory stimulation ($p = 0.01$ Levene's Test, $p=0.01$ Welch's Test, Figure 7B). Subsequent comparison between the periods of stimulation and the control group showed that the mean density is significantly increased after 6 and 18 hours of whisker stimulation ($p <0.01$, Satterthwaite's Test). There are respectively 2.4 fold and 2.7 fold more synapses on the dendritic shafts after 6 hours and 18 hours of whisker stimulation compared to the control animals. After 12 hours, the inter-individual variation is increased as reflected by a standard deviation 4 fold bigger than in the control group. Considering the ratio of excitatory synapses on shafts versus on spines, the groups differ significantly in their variance and their mean ($p=0.02$ Levene's Test, $p=0.02$ Welch's Test, Table 1). This ratio is significantly increased by 2.3 fold after 6 hours

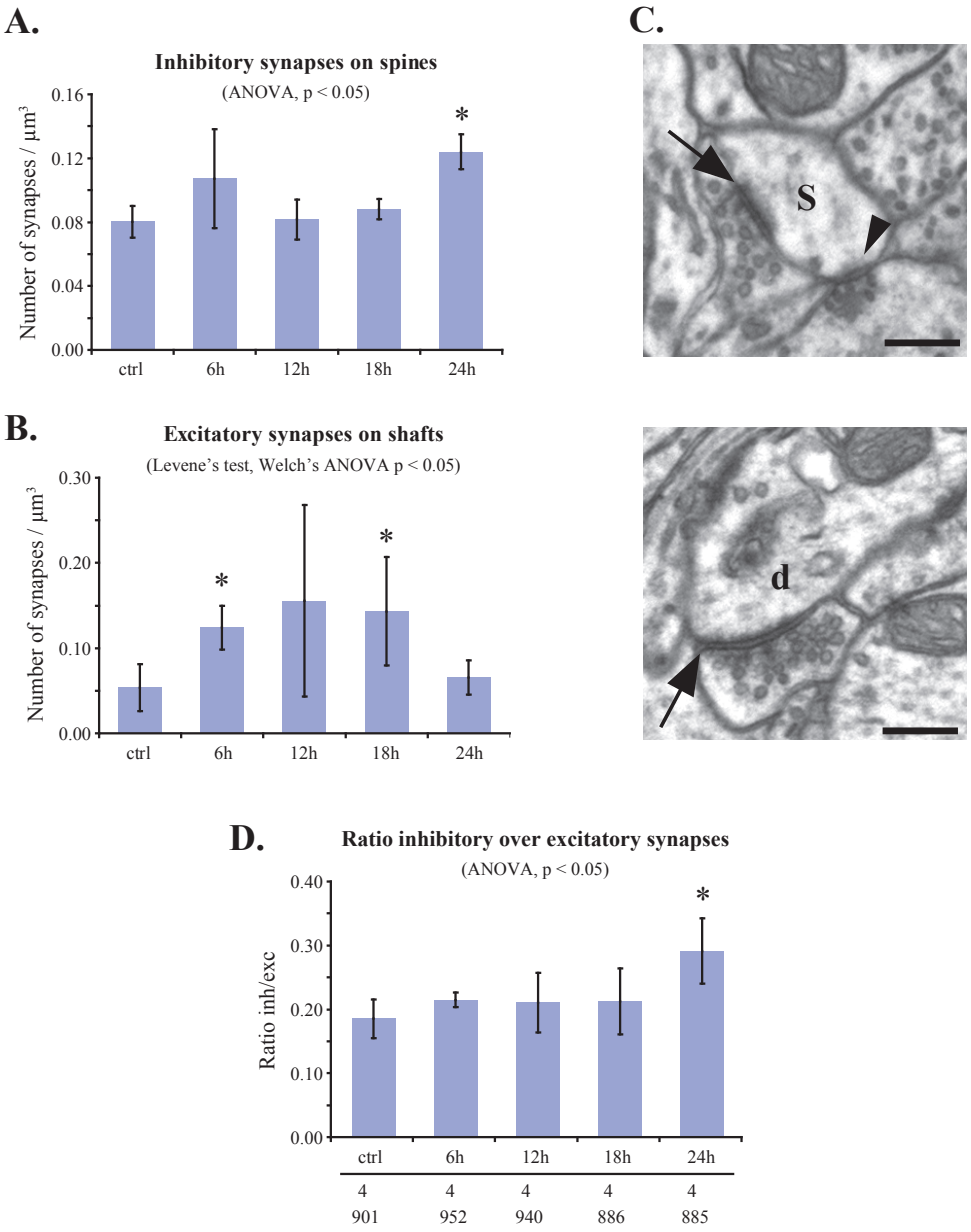

Figure 7. Temporal profile of synaptic densities across 24 hours of whisker stimulation. Graphics showing the mean and standard deviation for the density of inhibitory synapses on spines (A) and excitatory synapses on shafts (B) from neuropil within the right C2 barrel hollow from naïve animals (ctrl) and animals that had their left C2 whisker stimulated for 6h, 12h, 18h or 24h. For the density of excitatory synapses on shaft, Levene's test of homogeneity of variance shows significant difference between groups so Welch's ANOVA was used to test significant differences between all means followed by the Satterthwaite t-test with adjusted p value for multiple comparisons. C. EM images from the neuropil analyzed showing on top, a double-innervated spine (S) that contains one inhibitory (arrowhead) and one excitatory synapse (arrow). Insertion of inhibitory synapses on spines occurs following 24 hours of whisker stimulation. Below, an excitatory synapse (arrow) on a dendritic shaft (d). Its occurrence is increased after 6 and 18 hours of stimulation. Scale bar = 250 ηm. D. Graphic of the ratio between inhibitory synapses and excitatory synapses showing a significant shift towards inhibition after 24 hours of stimulation relative to control ($p < 0.05$ Dunnett's t-test). Below the bar: identification of the groups, the number of mice used and the total volume of neuropil analyzed in cubic microns for each group. These values pertain to the three graphics. Asterisks indicate statistically significant increase in the corresponding group relative to control values ($p < 0.05$, Dunnett's Test or $p<0.012$ Satterhwaite t-test)

of whisker stimulation ($p < 0.01$ Satterthwaite's t-test). These results demonstrate that the excitatory innervations are altered as quickly as 6 hours after the onset of the increased sensory activity, the earliest time-point analyzed, with an increase in the density of excitatory synapses on dendritic shafts. These modifications are transient, as the density of excitatory synapses on shafts returns to control value after 24 hours of whisker stimulation. The dynamic modification of the excitatory circuitry might be further underlined by the increase in the inter-individual variation in the density of excitatory synapses on shaft observed after 12 and 18 hours of stimulation.

Ratio between inhibitory and excitatory synapses

Specific changes were observed in the excitatory and inhibitory innervations, but how do they relate to one another? In terms of the change in the ratio between inhibitory and excitatory synapses in the neuropil considering all synapses (whether on spines or on dendritic shafts), the increased neuronal activity induces no significant changes after 6, 12 or 18 hours of stimulation, while after 24 hours, a 1.57 fold shift towards more inhibition has taken place ($p = 0.04$, ANOVA, Dunnett's test, Figure 7D). This indicates that up to 18 hours of stimulation, for each inhibitory synapse there are about 5 excitatory synapses (5.00 ± 0.85, mean for the 3 groups: control, 6h, 12h and 18h) but after 24 hours of stimulation, for each inhibitory synapses there are 3.5 excitatory synapses (3.51 ± 0.59). This change in the ratio between inhibitory and excitatory synapses after 24 hours of stimulation is due to a significant 1.8 fold increase in the ratio of inhibition and excitation on the spines ($p= 0.02$, ANOVA, Dunnett's Test). Levene's test and Welch's test show that the variances and the means are statistically different between groups for the ratio between inhibition and excitation for synapses on dendritic shafts ($p <0.01$ Levene's Test, $p< 0.03$,Welch's Tests). However, no difference can be highlighted statistically for any comparisons between the control and the different periods of stimulation using Satterthwaite's t-test and a p value threshold set at 0.012 to correct for multiple comparisons ($p > 0.03$, Satterthwaite's t-test).

Qualitative observations

On a qualitative point of view, when spines could be entirely followed within the stacks, it was observed that inhibitory synapses found on spines contacted spines that also had an excitatory synapse, called doubled innervated spines as previously reported (Figure 7C). However, in the stacks analyzed, there were uncommon cases of spines that could be observed in their totality and had clearly and unambiguously no sign at all of an excitatory synapse on it. A three-dimensional reconstruction illustrates one of them (Figure 8A). These spines, although very rare, have been seen in stacks from both control and stimulated neuropil but not in each one of them. Also observed in both stimulated and control neuropils were excitatory synapses

on dendritic shafts in the close vicinity of synapse-less filopodia-like protrusions (Figure 8B). A specific analysis focusing on spines would be required to precisely and accurately quantify these observations and was beyond the scope of this study.

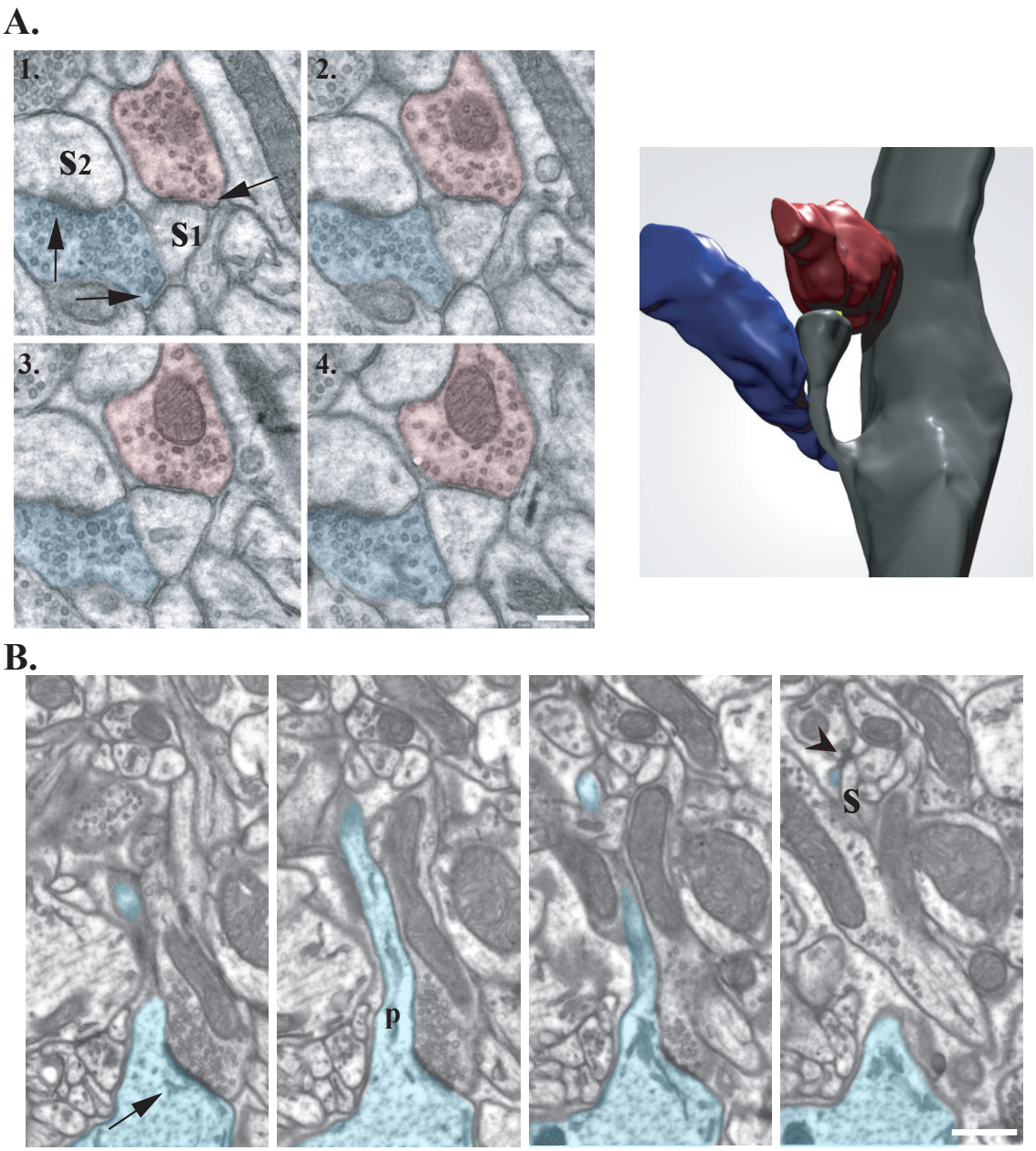

Figure 8. Structures observed in the analyzed neuropils. A. Series of four consecutive EM images showing a spine (S1) that was found in the analyzed stack and which is solely innervated by an inhibitory axon (in red). An excitatory axon (in blue) is apposed to it without forming a synapse with it but forms a synapse on the neighboring spine (S2). Synapses are indicated with an arrow. A. three dimensional reconstruction of the spine and its dendrite and the axons shows the excitatory and inhibitory axons along the spine; only the inhibitory axon forms a synapse on it. Scale bar = 250 nm. B. Series of 8 consecutive EM images (only each second image is shown here) showing a dendritic protrusion (p) with an excitatory synapse at its base (arrow). The protrusion itself is not innervated by a synapse but its tip finishes closes to a synapse made between an excitatory bouton and another spine (arrowhead). Scale bar = 500 nm.

I.3 Discussion of the ultrastructural analysis

Twenty-four hours of an increased sensory experience by whisker stimulation induces physiological and structural changes in the somatosensory cortex of adult animals (Quairiaux et al., 2007; Knott et al., 2002). Adding to these observations, here we show that the first signs of structural modifications occur as early as 6 hours after the onset of the stimulation (the first time-point analyzed) while a shift in the balance between inhibition and excitation through the addition of inhibitory synapses on spine requires more than 18 hours to take place.

Experience-dependent modifications at the molecular level had already been shown to occur in the somatosensory cortex within a few hours after an altered sensory activity (Rocamora et al., 1996; Gierdalski et al., 2001). However, to our knowledge, this is the first demonstration that a novel sensory experience induces the formation of new synapses as early as 6 hours after the onset of the stimulus and this in an adult animal and in cortical layer IV known for being less plastic than other cortical layers (Diamond et al., 1994; Glazewski and Fox, 1996). This finding highlights the importance of an increased level of activity and of a new sensory experience to induce plasticity in adult animal as opposed to sensory deprivation. Indeed as revealed by electrophysiological recordings, 15 hours of altered sensory activity by whisker clipping does not induce any changes of the receptive fields except when the animals are exposed to an enriched environment (Rema et al., 2006).

That 24 hours of whisker stimulation increase the density of inhibitory synapses on spines was already shown by Knott et al. (2002) and is being confirmed here. However our findings differ with some of the findings reported in their study. Indeed, in addition to the inhibitory synapses on spines, Knott and colleagues showed an overall increase in the synaptic density following whisker stimulation affecting both the excitatory and the inhibitory innervations. These overall modifications of the circuitry were not observed here. In addition, the mean synaptic densities were considerably lower in their study. This was the case for all synaptic densities analyzed, except for the density of excitatory synapses on shaft which is remarkably stable between the two studies (see Appendix 1 -page 119- for comparison with published EM studies in the somatosensory cortex). Many reasons could be accounted for the observed discrepancies. Although the same strain of mice was used, the animals in our study were slightly younger (6-7 weeks old versus 8 weeks old) and were housed differently (presence of objects in the cage). Both of these factors, age and environment, have an effect on synaptic densities in adult rodents (Diamond et al., 1964; Mollgaard et al., 1971; Diamond et al., 1975). In addition, in our study, the presence of an identifiable synaptic cleft was not one of the criteria for synapses identification in contrast to Knott's analysis; this criterion was discarded here as the visualization of a synaptic cleft on the micrographs greatly depends on the plane of sectioning relative to the

plane of the synapse. Finally, the two studies differed in the magnifications at which the sections were viewed (7-8x10^3 in Knott et al. versus 10.5 x10^3 here) and in the acquisition of the images, which both affect the resolution and thus the identifications of the synapses. It is not possible to point out which one(s) of these parameters is/are responsible for the differences between the two studies. However, it is remarkable to note that despite the differences, the percentage of inhibitory synapses in the control neuropil as well as the shift in the balance between inhibition and excitation after 24 hours are almost identical between the two studies.

Plasticity of the excitatory synapses on dendritic shafts

The early and transient modification of the neuronal wiring occurs through an increase of excitatory synapses on dendritic shafts. The dynamic nature of the modifications is further expressed by a significant increase of inter-individual variations within groups that is evident in the first 18 hours of whisker stimulation. That the activity-dependent structural reorganization of the neuronal circuitry occurs through rapid addition of synapses on dendritic shaft was observed *in vitro* and *in vivo* after long-term potentiation (Lee et al., 1980; Chang and Greenough, 1984; Nikonenko et al., 2003). By using a protocol that induces LTP in hippocampal slices (6 trains at 100 Hz for 1 s or 200 Hz for 0.5 s), synapses are formed on dendritic shafts within 10 minutes and remain present for at least 8 hours (Chang and Greenough, 1984) while when LTP was induced in anesthetized animals they were shown to appear within 45 minutes (Lee et al., 1980). It is to note that in our study, 6 hours was the first time-point analyzed and no attempt was made to reveal the earliest time-point at which structural changes take place; however these studies on LTP suggest that the changes seen here may occur at a much faster rate.

The density of excitatory synapses on shaft per cubic microns found in our control neuropil is remarkably similar to the values that were previously reported in the literature for layer IV of the mature somatosensory cortex of rats and NOR mice, the same strain of mice than used in our study (see Appendix 1, page 119; Micheva and Beaulieu, 1995b; Knott et al., 2002). However, it is worthy to note that there are strain differences as these values do differ from the one obtained in the somatosensory cortex of C57 mice (see Appendix 1). This specific population of synaptic contact is significantly increased by whisker stimulation reaching a value of 0.12 synapses per cubic microns. This represents a relatively small proportion of the total synaptic population, as numerically it means that the excitatory synapses that are added by 6 hours of whisker stimulation represent only 4% of the total number of synapses present at that time. However, thalamic inputs make up only 18% of the total population of synapses in layer IV (Benshalom and White, 1986) and only 7% of them contact inhibitory neurons thus representing the 1.27 percent of the total synaptic population (Staiger et al., 1996) although these two populations of synaptic contacts drive and shape the activity of the cortical column. In addition, evidences suggest that shaft

synapses are more powerful than spine synapses in generating evoked response potentials in the cells. Indeed, the size of the postsynaptic densities and the number of AMPA receptors present at the synapse, two variables related to one another and ultimately to the synaptic efficacy, are larger at shaft synapses than at spine synapses (Nusser et al., 1998; Rusakov et al., 1998). Thus, the addition of these synapses within the cortical network, although of small number, could have a strong impact on cortical processing.

The numerical as well as the physiological importance of the additional excitatory synapses on dendritic shaft would depend whether these synapses are added on excitatory or inhibitory cells. Indeed, in the cortex the majority of the excitatory synapses that contact dendritic shafts are found on the inhibitory neurons (Douglas R. et al., 2004). In the cerebral cortex, target of the excitatory terminals may be identified as excitatory or inhibitory depending on the spine density of their dendrites (Kawaguchi et al., 2006). However spine density varies between cell types and with the distance from the soma (Larkman, 1991) and inhibitory neurons do also bare spines even though at a much lower density than excitatory cells (Feldman and Peters, 1978; Kawaguchi, 1993; Kawaguchi et al., 2006). In the hippocampus, high frequency stimulation induces the formation of shaft synapses in CA1 (Lee et al., 1980; Chang and Greenough, 1984). Using morphological criteria as such as the presence of spines or the diameter of the dendrites, it was suggested that these shaft synapses were made either on inhibitory neurons solely (Lee et al., 1980) or on both cell types (Chang and Greenough, 1984). Although noteworthy in these studies, no differentiation between symmetric and asymmetric synapses was made. In our cases, excitatory shaft synapses were seen both on dendrites that had spines as well as on the ones that were apparently devoid of any, suggesting that both cell types could be the target of these additional synapses. However, specific analysis would be required to examine segment of dendrites and preferentially of immuno-labeled cells to know whether the activity-dependent formation of excitatory shaft synapses is selective to a specific neuronal cell type.

Two-photon uncaging of glutamate on dendritic segment of pyramidal cell in slice combined with electrophysiological recordings showed that signals sum up linearly in the soma (100 % of expected arithmetic sum) when two spines on the same dendritic branch are activated, but sum sublinearly (70 % of expected arithmetic sum) when two shaft synapses or a spine and a shaft synapse from the same branch are activated (Araya et al., 2006). According to this study, and in accordance with the computational model of Rall (1970) shaft synapses have shunting effects on excitatory inputs while spine neck can electrically isolate the excitatory inputs. Hence, depending on the timing of the activation, the end result of the increased number of excitatory synapses on dendritic shafts induced by increased sensory activity might be to temporally lower the level of neuronal activity until the insertion of inhibitory synapses. However, with

their higher efficiency, their shunting effect and their targets that could be either excitatory or inhibitory neurons, it is difficult to predict how cortical processing is affected by the structural changes and electrophysiological recordings would be required to address this point.

Plasticity of dendritic spines

Time-lapse two-photon microscopy performed in supragranular layers of adult mice revealed that, although total spine density is not affected by altered sensory experience, spine turnover is increased (Trachtenberg et al., 2002; Holtmaat et al., 2005). Activity-dependent changes in spine turn-over are related to the differential stabilization of spines and an indication of circuitry rewiring: spines that are activated are stabilized and the ones that are not activated are destabilized and replaced by new ones (De Roo et al, 2008). Our study was not focused directly on spines and no significant changes in the density of excitatory synapses on spines could be highlighted. However changes in density of excitatory synapses on spines may be difficult to reveal in our analysis as the mean density and the within groups variability in contrast to the small number of animals used here gives a small statistical power to reveal changes of relatively small magnitude, if any. To obtain this statistical power would require doubling the number of animals, assuming that the variability within groups remain the same. In addition, the criteria that were set for identification of a synapse limit our analysis to mature synapses and small or immature synaptic contacts that were encountered in the stacks, and in most cases on dendritic protrusions, were not considered here, though they could be sign of pruning or of on going spinogenesis and synaptogenesis (Nagerl et al., 2007) and thus indicators of circuitry reorganization. Indeed, in addition to their physiological role, several evidences link shaft synapse on excitatory neurons to spine synapse. First, the proportion of excitatory synapses on shaft versus on spine is high during development and decreases with age and lead to the model of spine synapses emerging from shaft synapses (Fiala et al., 1998; Harris, 1999; Bourne and Harris, 2007). Furthermore, a study on hippocampal slices shows that LTP induces transient excitatory synapses on shaft which are replaced 10 minutes later by an increase of excitatory synapses on spines (Nikonenko et al., 2003). Moreover, other studies on cell cultures suggest that spines that disappear leave an excitatory synapse on the dendritic shaft, where new spines may form (Marrs et al., 2001; Hasbani et al., 2001; Ovtscharoff Jr. et al., 2008). Hence, transient synapses seen on shafts may represent hot spots on the dendrite where pruning of spines or the appearance of new ones occurs. Noteworthy, in the neuropils analyzed, the observation of shaft synapses at the base of dendritic protrusions, often devoid of any synapse (as in the example presented in Figure 8B), supports this hypothesis. Thus, the transient insertion of excitatory synapses on dendritic shafts following whisker stimulation may be sign of changes in spine turnover. Study focusing on spines and in which spines may be divided into various morphological classes such as mushroom-like, stubby, filopodia-like and multiple headed-

spines (Harris KM et al., 1989) may reveal changes in spine-turnover as spine morphology has been related to their dynamics (Holtmaat et al., 2005; Zuo et al., 2005; Knott et al., 2006; Bourne and Harris, 2007).

Interestingly, a study combining electron microscopy with time lapse two-photon imaging showed that although newly formed spines from pyramidal neurons in hippocampal slices may form rapidly in response to theta-burst stimulation, 15 to 19 hours is required for a new spine to acquire what is considered at the electron microscopy level a mature synaptic contact (Nagerl et al., 2007). This time interval of 15 to 19 hours matches the time at which Knott and colleagues show that the density of double-innervated spines is increased in the stimulated neuropil (Knott et al., 2002). The increased number of inhibitory synapses on spines found in our study after 24 hours of whisker stimulation and which are most often seen on spines that also are innervated by an excitatory synapse support Knott's finding. Remarkably, the number of excitatory synapses on the shaft has returned to control level at a time when inhibitory synapses on spines are added.

Plasticity of the inhibitory synapses on spines

Similarly to excitatory synapses on shaft, inhibitory synapses on spines would have shunting effect on the potentials elicited by the excitatory synapse on the spine but it would be much more localized (Rall, 1970; Dehay et al., 1991). In addition, GABA released in the synaptic cleft may spill–over and activates $GABA_B$ receptors located in the neighboring presynaptic excitatory terminal depressing neuronal transmission (Isaacson et al., 1993). Also due to their postsynaptic rebound, it was suggested that inhibitory synapses on spine may also enhance the synaptic activity at the spine if the excitatory synapse is activated during the time-window imposed by the postsynaptic rebound (Quairiaux et al., 2007). According to these considerations, inhibitory synapses on spines may potentiate or inhibit the synaptic activity at the spine and thus stabilize or destabilize the excitatory synapse at the spine depending on their correlated activity. Interestingly, Zuo et al showed that 3-5% of adult spines are formed and eliminated over two weeks (Zuo et al., 2005). Remarkably, in the analyzed neuropil, inhibitory synapses on spines represent 6% of all synapses on spines in the control animals and 10 % after 24 hours of whisker stimulation. Thus, inhibitory synapses on spine, in addition to strictly reducing or gating neuronal activity, may play a role in circuitry rewiring through spine destabilization and stabilization depending on the timing of the activity between the excitatory and the inhibitory synapse. The rare occurrence in both control and stimulated animals of spine solely innervated by an inhibitory synapse (as in Figure 8a) may be the outcome of such destabilization while their maintenance 4 days after whisker stimulation (Knott et al., 2002) may be the outcome of such stabilization.

It is interesting to note that the first neuronal cell type to react to the increased neuronal activity is the excitatory cell type which is followed by plasticity of the inhibitory neurons. Such delay in the plasticity of the inhibitory neurons compared to the excitatory was already reported by electrophysiological recordings made in the visual system during the critical period. Indeed, it was shown that excitatory neurons shift their ocular dominance to the open eye within 2 days of monocular deprivation while 4 days are necessary for inhibitory neurons to shift their ocular dominance to the open eye (Froemke et al., 2007; Gandhi et al., 2008). These differences between the excitatory and inhibitory neurons could be attributed to the spines that characterize the excitatory neurons. Spines are special compartments where synaptic activity, in contrast to synapses on shafts, may quickly and easily raise the intracellular calcium level, through the activation of NMDA receptors or voltage-gated calcium channels (Grunditz et al., 2008). The entrance of calcium channel would then activate molecular cascade leading to synaptic plasticity. Among the molecular events that would be activated and underlie the modification of the circuitry is the regulation of gene expression itself. Identification of the genes that are regulated in their expression following whisker stimulation constitutes the second part of this thesis.

Altogether, this experiment shows that the cortical circuitry undergoes, at the structural level, rapid and transient changes in response to the altered sensory activity and the changes lead to a shift in the balance between inhibition and excitation that comes about after 24 hours of chronic whisker stimulation. Electrophysiological recordings and analysis of spine dynamics would now be required to further understand how these two events are connected.

II. Microarray analysis

II.1 Material and Method

The gene chip analysis was performed on male C57 Bl/6J mice (Janvier, Saint-Ile le Genest, France). Mice were anesthetized with Nembutal (Sodium pentobarbital, 60 mg/kg, i.p.) and a piece of ferrous metal of 1.5 mm was glued on a set of whiskers (see below) on the left whiskerpad approximately 3 mm away from the skin surface. All other whiskers were kept intact and their presence on the whiskerpad verified. Particular attention was paid to the presence or absence of the B4 follicle which was noticed to be missing in ¾ of the cases. After full recovery from the anesthesia, mice were placed for a period of 3, 6, 9, 15 or 24 hours in the Lausanne whisker stimulator (Melzer et al., 1985), a cylindrical cage surrounded by an electromagnetic coil which delivers magnetic field bursts at 9 Hz (Burst duration: 40 ms; intensity: $7x10^3$ A/m, frequency during burst: 50 Hz). Mice had access to food and water and could move freely. All were between 6 and 7.5 weeks old at the time of stimulation. The experiment was planned so that the stimulation period ended for all mice always at the same moment in the day/night cycle. The experimental design used for this experiment is shown in Figure 9.

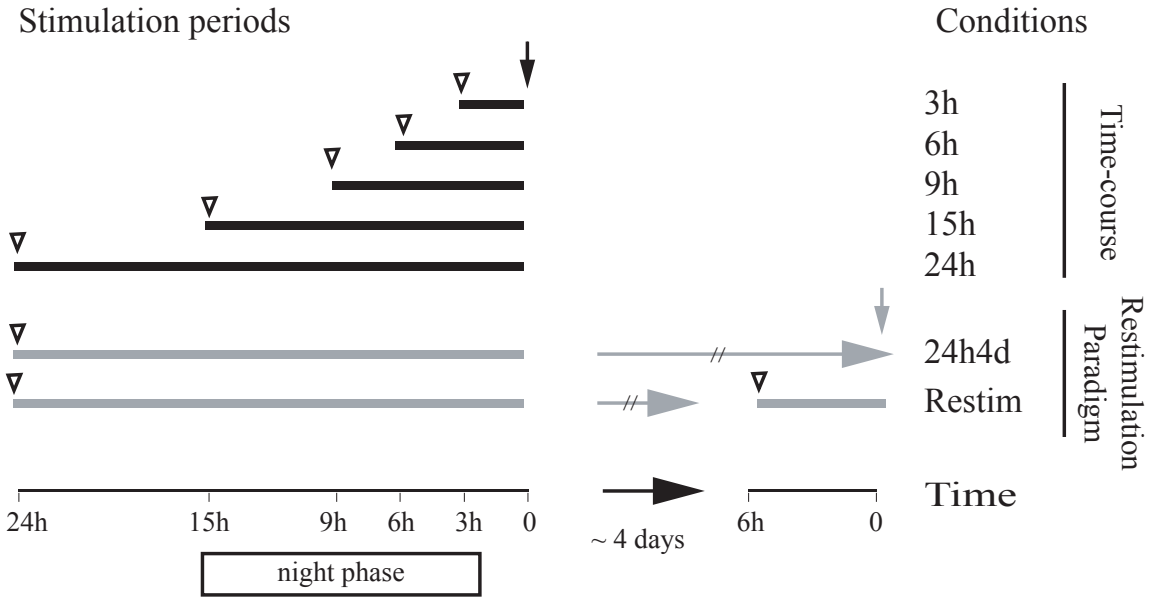

Figure 9. Experimental design used for whisker stimulation. All animals were sacrificed at the same moment in their day/night cycle between 2 and 3 hours after the night phase, which corresponds to the active phase for nocturnal animals as used in this study. Open arrowheads point to the onset of the stimulation period; solid down-pointing arrow, to its end.

The mice had their left B1, B2, C1, C2, D1, D2 whiskers stimulated for 3h (n=22), 6h (n=22), 9h (n=20), 15h (n=23) or 24h (n=14). In addition, 35 mice had their B1, B2, C1, C2, D1, D2 whiskers stimulated for 24h then returned to their home cage for 4 days (24h4d, n=17). For these 35 mice, just after the stimulation period and before being replaced in their home cage, the ferrous metals were gently removed from the whiskers with a cotton bud dipped in acetone while the animals were under anesthesia (2.5% isoflurane) (Abott, Baar, Switzerland). This procedure was performed using a dissection microscope. At the end of the "rest" period, whiskers that had been previously stimulated for 24 hours were submitted to a second period of stimulation for 6 hours (Restim6h, n=18). For this group of mice, whiskers were considered stimulated only when they had kept their metals throughout the two stimulation periods.

In all the procedures that follow, great care was taken to work in RNase-free environment.

Tissue preparation and laser microdissection

Right after whisker stimulation, mice were anesthetized with Nembutal (60 mg/kg, i.p.), decapitated and their brain removed. The hemispheres were separated and orientated for tangential sectioning over the barrelfield, frozen in dried-ice and kept at -73°C until sectioning. This whole procedure was done as quickly as possible to maintain the integrity of the RNA and did not exceed 8 min per brain. Cryostat sections were cut serially at 20 µm tangentially to the barrel cortex contralateral to the stimulated whiskers and collected on Polyethylene naphthalate (PEN) membrane-covered glass slides (MembraneSlide 1.0 PEN, Carl Zeiss MicroImaging GmbH, Bernried, Germany). For each hemisphere, sections not including the barrels in layer IV were added on supplementary slides for testing the quality of the RNA. Tissue was then fixed by immersing the slides in ice-cold 70% EtOH/DEPC-water for 10 min, quickly rinsed in DEPC-water and stained for 10 min in 1% O-Toluidine blue/DEPC-water. Sections were then rinsed quickly in DEPC-water and differentiated 3 min in 70% EtOH/DEPC and dehydrated 1 min in 100% EtOH. Sections were dried 10 min on a heating plate set at 37°C and the barrelfield was imaged with an AxioCam digital camera attached to the microscope Axioplan 2 imaging system and with the digital image processing software AxioVision (Carl Zeiss MicroImaging GmbH, Bernried, Germany). Immediately after imaging, sections were stored at -73°C until further use.

Assessment of RNA integrity

Slides containing sections that did not include the barrels in layer IV but which were processed with the others up to storage at -73°C were dried on a heating plate set at 37°C for 10 min and samples cut out of the sections with a razor blade. The RNA was extracted using RNeasy mini kit from Qiagen. Genomic DNA contamination was eliminated by on column DNase digestion using the RNase-Free DNase Set from Qiagen. Integrity of the RNA was determined by using

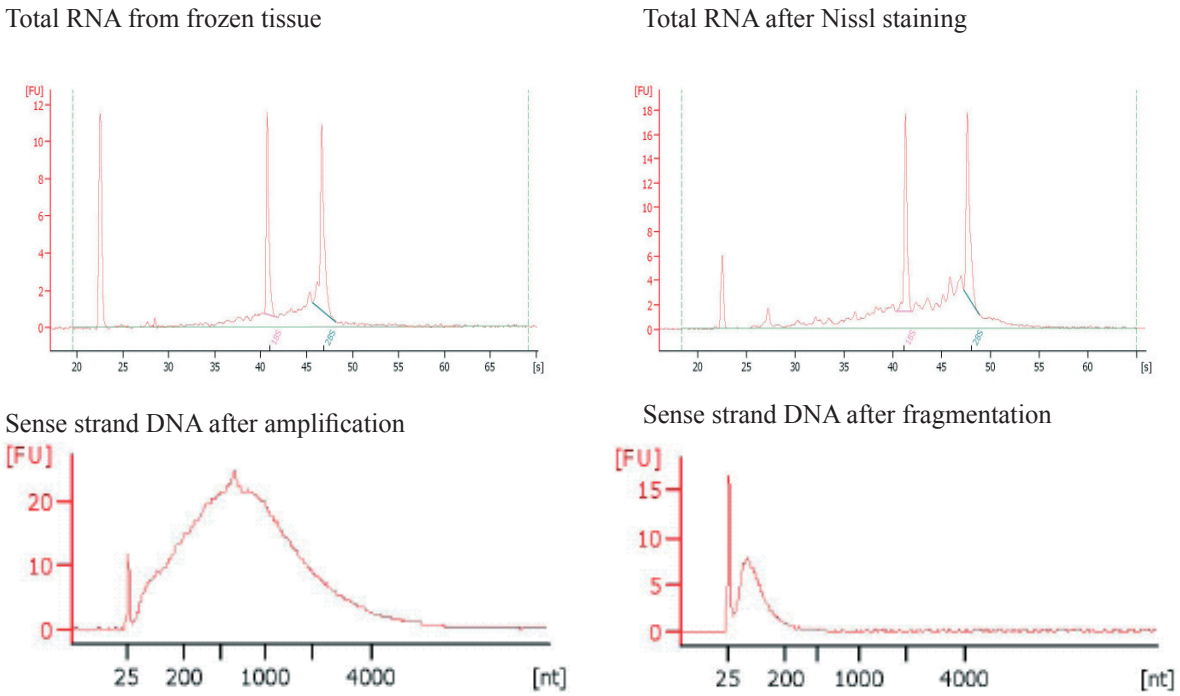

Figure 10. Typical electrophoresis profile of total RNAs and sense strand DNAs from materials used in the current experiment. Integrity of initial RNA was determined by the RNA integrity number (RIN) which is based on the entire electrophoresis profile. RIN numbers for the electrophoretic traces in the 2 examples at the top, was 8.5 before any histological preparation and 7.3 after Nissl staining and visualization of the barrelfield at the microscope. Electrophoresis profiles for sense strand DNA attest the amplification of large and small transcripts and their fragmentation into fragments of approximately 35 to 200 nucleotides (nt). [FU]=fluorescence

an Agilent Bioanalyzer 2100 and Pico or Nano 6000 LabChip (Agilent technology, Palo Alto, USA). The RNA Integrity Number (RIN) was used to assess RNA quality. RIN is an algorithm to assign integrity values from 0 (low integrity) to 10 (high integrity) to RNA measurements based on the entire electrophoretic trace of the RNA sample (Schroeder et al., 2006). The RIN of the samples used in this study ranged between 7.6 and 6.8 (Figure 10).

Barrel identification and laser microdissection

Each stack of images spanning the barrel field of the contralateral hemisphere to the stimulated whiskers were aligned using Adobe Photoshop CS version 8.0 (Adobe Systems Incorporated, San Jose, CA, USA), enabling the visualization of the whole barrelfield and the exact identification of the barrels present in each section. After removing the sections from -73°C and drying the sections for 10 min on the heating plate, the stimulated barrels were laser microdissected using the PALM Laser MicroBeam system (PALM, Bernried, Germany), mounted on Zeiss Axiovert 200 (Carl Zeiss MicroImaging GmbH, Bernried, Germany) and catapulted into the caps of microcentrifuge tube (Figure 11). Also from the same sections, non-stimulated barrels which

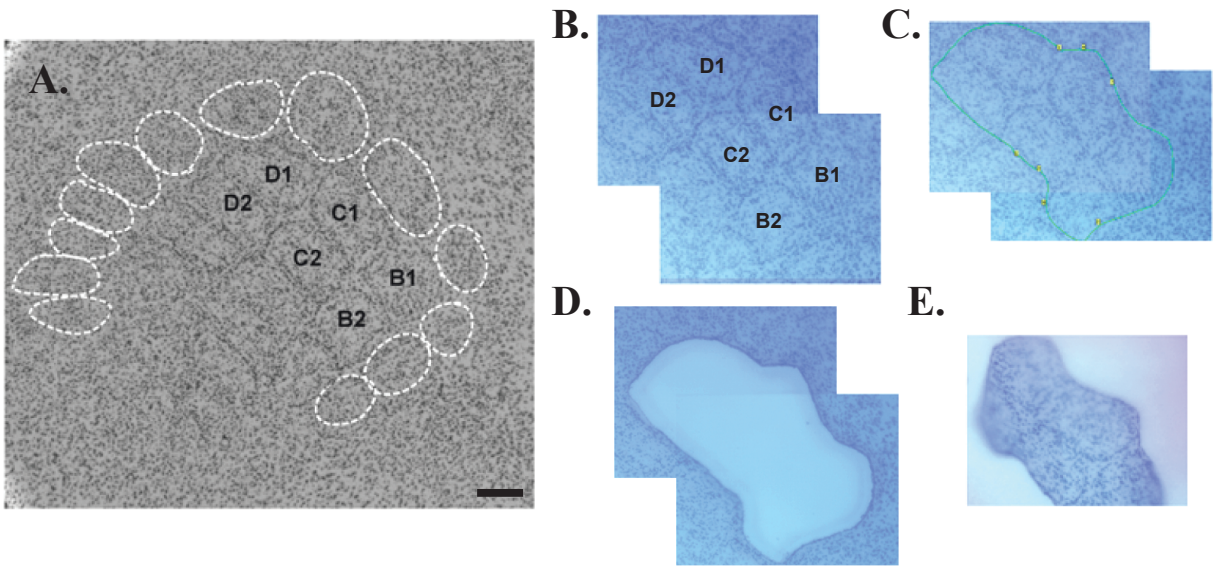

Figure 11. Laser microdissection of stimulated barrels. A. Image showing stimulated barrels (B1, B2, C1, C2, D1 and D2) in a 20 µm Nissl stained section complemented by the outlines of barrels identified in neighboring sections (white dashed lines). B. Image showing the same section just prior to laser microdissection. C. Image of section with an outline around the stimulated barrels which determines the position of the laser. D. Image after the catapulting of the laser-dissected barrels. E. Image showing the dissected barrels in the cap of the eppendorf tube. Scale bar = 200 µm.

served as controls were taken. Non-stimulated barrels are barrels that receive normal sensory input from whiskers located on the same whisker pad as the chronically stimulated ones, but at least one arc away. Once collected, tissue was suspended in the extraction buffer from the Pico Pure RNA isolation Kit (Arcturus, Mountain View, Ca, USA), immediately frozen in Nitrogen and kept at -73°C until extraction of the RNA. Attention was paid so that the whole laser microdissection procedure did not exceed 15 min per slide, ensuring that all tissue sampled would be kept under the microscope for a limited amount of time and thus preserving the integrity of the RNA.

Once all the samples were collected, they were thawed out on ice. Dissected barrels were pooled in 6 sets per stimulation period, 3 for the stimulated barrels and 3 for the non-stimulated ones. Each set gathered 121 to 191 dissected barrels distributed over 15 to 29 eppendorfs and belonging to between 4 and 8 mice. Their total RNA was extracted with the Arcturus PicoPure RNA Isolation Kit according to the manufacturer's protocol (Arcturus, Mountain View, Ca, USA).

Target synthesis and chip hybridization

Two cycles of linear amplification of the RNA was performed by *in vitro* transcription. To amplify the RNA along its entire length, transcription was initiated both at the 3' end and randomly throughout the whole transcriptome. Amplification was performed using the Ribo-

SPIA™ Technology developed by NuGEN (San Carlos, USA).

Extracted RNA was reverse-transcribed and amplified with the WT-Ovation Pico RNA amplification system from NuGEN (San Carlos, USA). From the single-stranded antisense cDNA obtained, sense strand DNA was generated with the WT-Ovation Exon Module, then fragmented and biotin-labeled using the FL-Ovation cDNA Biotin Module V2 (NuGEN Technologies). Fragmentation is a combined chemical and enzymatic process that yields single-stranded sense DNA products in the 50-100 base range while labeling is done via enzymatic attachment of a biotin-labeled nucleotide to the 3-hydroxyl end of the fragmented cDNA. The quality of the amplification and fragmentation was verified on Bioanalyzer electropherogram using Agilent Bioanalyzer 2100 and Nano 6000 LabChip (Agilent technology, Palo Alto, USA) (see Figure 10).

To determine RNA and DNA concentrations, a Nano-drop (ND-1000 Spectrophotometer, Thermo scientific, USA) was used. Starting material of total RNA extracted from the pooled barrels was 35 ng. From each first strand synthesis, on average 10.6 µg (± 1.98 SD) of cDNA was obtained. The second strand of synthesis yielded on average 7 µg of cDNA and from those, 5 µg was used for fragmentation and labeling. All synthesis reactions were carried out in 0.2 ml tubes (pre-amplification) and 0.5 ml tubes (post-amplification) using a thermocycler (Biometra TProfessional, Biometra, Gottingen, Germany) to ensure the highest possible degree of temperature control.

The hybridization cocktail (200 µl) containing fragmented biotin-labeled sense strand DNA at a final concentration of 25 ng/µl was transferred into Affymetrix GeneChip Mouse Exon 1.0 ST Array (Affymetrix, Santa Clara, CA, USA) and incubated at 45°C on a rotator in a hybridization oven 640 (Affymetrix) for 17 h at 60 rpm. The arrays were washed and stained on a Fluidics Station 450 (Affymetrix) by using the Hybridization Wash and Stain Kit (Affymetrix) and the Fluidics Procedure FS450_0001. The GeneChips were processed with an Affymetrix GeneChip® Scanner 3000 7G. DAT image files of the microarrays were generated using Affymetrix GeneChip Command Console (AGCC, version 0.0.0.676).

Microarray data analysis

Forty-two chips were hybridized, six chips per stimulation periods (3, 6h, 9h, 15h, 24h, 24h4d and restim6h) corresponding to 3 biologically and technically independent replicates for the stimulated barrels and 3 biologically and technically independent replicates for the adjacent non-stimulated barrels. Two separate analyses of the chips were performed; one for the time-course experiment where chips from the 3h, 6h, 9h, 15h and 24h conditions were processed

together and one for the restimulation paradigm where chips from 6h and 24h conditions were processed with the chips of 24h4d and Restim6h. Also to note is that, altough being processed with the others, the data sets from the 24h4d group of animals has for the moment not been fully investigated and for this reason will not be presented in the results.

Quality control of microarray data was assessed with Expression Console 1.1 software from Affymetrix (Affymetrix, Santa Clara, USA) and the Quality Control module in Genespring GX 10.0 (Agilent technology, Palo Alto, USA). Quality assessment metrics based on the probe level data prior and after the application of the summarization algorithm show that all the arrays were of good quality (see Figure 12 for example). A correlation analysis across RNA arrays which gives the correlation coefficient for each pair of arrays showed that the data from all arrays were highly correlated; the minimal correlation coefficient being of 0.91.

Analysis from Affymetrix GeneChip MoEx-1_0-st-v1 was performed with Genespring GX 10.0. Probe Logarithmic Intensity Error (Plier) estimation and IterativePlier (IterPlier) were used as the summarization algorithms to perform background correction, quantile normalization and probe summarization. In addition, Genespring adds a constant, 16, to the expression measures for variance stabilization. Baseline transformation to median of all samples was applied (for each probe the median of the log summarized values from all the samples is calculated and subtracted from each of the samples). Analysis was limited to the core list of probe sets. The core list comprises 16755 transcript clusters from RefSeq and full-length GenBank mRNAs which are the two sources of input transcript annotations with the highest level of confidence. Two filters were applied before statistical analysis, one on the expression values and one on the fold changes.

The number of genes that remained in the analysis after each step of filtering is given in Table 2. First, genes were retained for further analysis when the expression values for a gene was above the 20th percentile of the overall expression values in at least one condition (i.e. in the three replicates representing that condition). From these genes, only the ones that showed

(**Continuation of legend to Figure 12.)**

are made by a set of putative intron based probe sets from putative housekeeping genes while positive controls is made by a set of putative exon based probe sets from putative housekeeping genes. For this metric, values between 0.8 and 0.9 are typical, while an AUC of 1 reflects perfect separation. For all our chips, this value is over 0.8 suggesting good separation between the positive and the negative controls. In D, the intensity values for the probe sets which hybridize to pre-labeled bacterial spike controls (BioB, BioC, BioD and Cre) are in the expected order and well separated, again suggesting that our data set is of good quality.

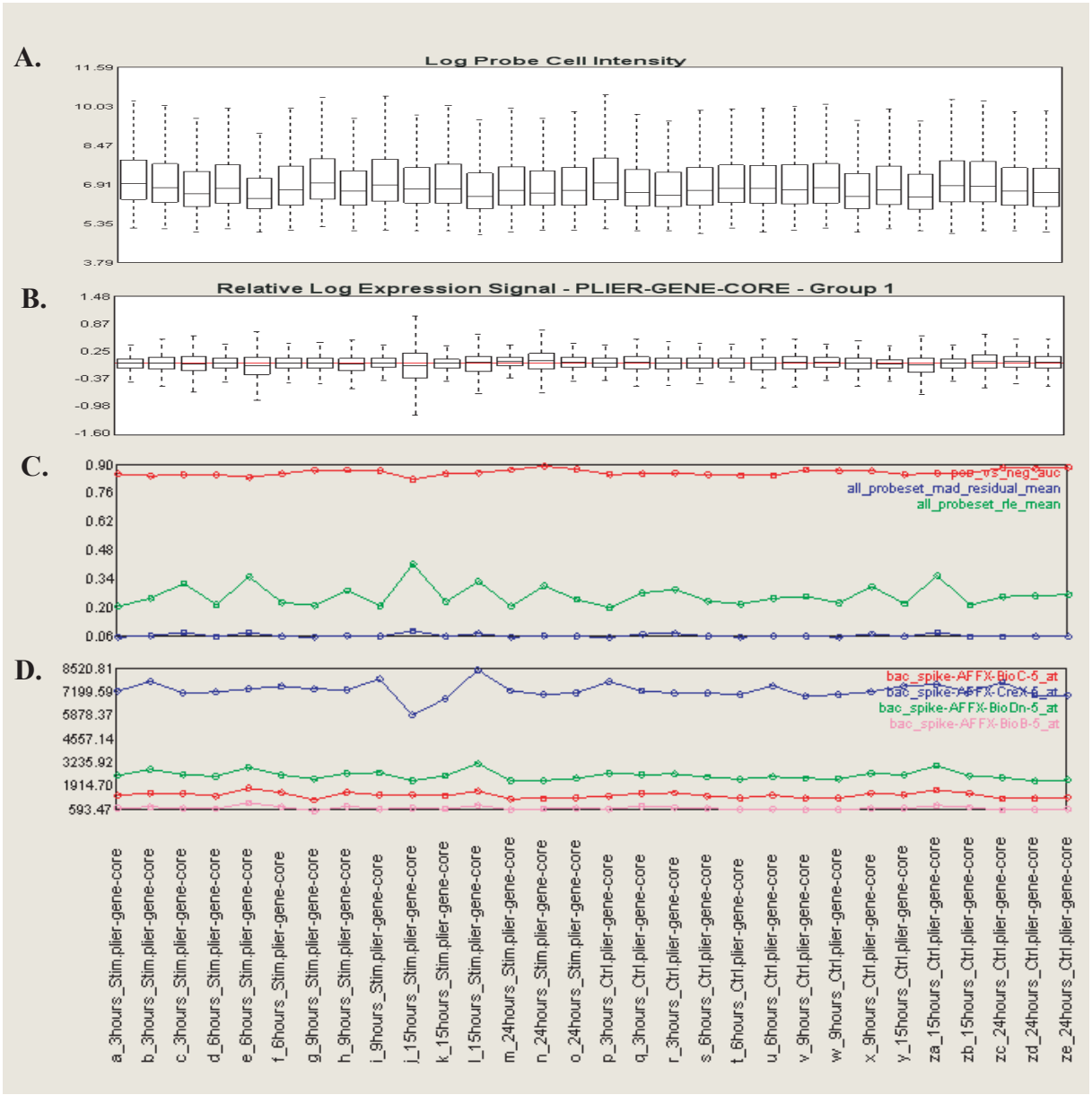

Figure 12. Results of the quality control applied on the chips (identified along the x-axis) used for the time-course. The results shown here are based on metrics calculated by Expression Console according to the Affymetrix white-paper on quality assessment (Santa Clara, USA). In A, log probe cell intensity before summarization of the data and in B, relative log expression signal after summarization using Plier algorithm. In C, the metric all_probeset_mad_residual_mean (in blue) is the mean of the absolute deviation of the residuals from the median. This metric measures how well (or poor) all of the probes on a given chip fit a model for individual feature responses created by Plier. An unusually high mean absolute deviation of the residuals from the median would suggest problematic data. Notice that for our data set, this metric is around 0, assuring that the behavior of the probes in our data set fits with the model created by Plier thus suggesting good quality of our chips; the other metric, all-probeset_rle_mean (in green), is the mean absolute relative log expression. This metric is generated by taking the signal estimated for a given probe set on a given chip and calculating the difference in log base 2 from the median signal value of that probe set over all the chips and then by computing a mean from all the probe sets. This metric is an indicator of the biological variability but if found considerably high could identify a problematic chip. Here, it ranges between 0.21 and 0.42 while it is common in a diverse tissue panel to see values ranging from 0.27 to 0.61. In red, the metrics pos_vs_neg_auc. This metric is the area under the curve (AUC) for a receiver operating characteristic (ROC) plot comparing signal values for the positive controls to the negative controls. On exon arrays, negative controls

←

an absolute fold change of at least 1.25 (plus or minus) between the stimulated and the non-stimulated barrels from the same stimulation period in one or more comparisons were included in further statistical analysis. Welch's ANOVA for unequal variance followed by Tukey HSD as the posthoc test were performed. Raw p-values obtained from statistical tests were adjusted for multiple testing using the Benjamini Hochberg False Discovery Rate (Benjamini and Hochberg, 1995) method to yield an adjusted p value. The Benjamini Hochberg False Discovery Rate controls the proportion of errors among the list of genes identified as significantly regulated by adjusting the raw p value to limit the rate of false positives. Genes that presented an adjusted p value ≤ 0.05 and a fold change ≥ 1.25 (up or down) relative to the control barrels in at least one comparison between the stimulated and the non-stimulated barrels from the same stimulation period were considered to be significantly regulated. Genes that were considered significantly regulated when the analysis was performed with IterPlier or Plier summarization algorithm were pooled together and formed the list of regulated genes which was further considered for studying their possible biological significance. When genes were found regulated by both summarization algorithms (Plier and IterPlier), the values obtained with IterPlier were kept and used for down-stream analysis.

Biological interpretation

Biological interpretation of the data was done using the Gene Ontology Analysis module from Genespring GX 10.0 (Agilent technology, Palo Alto, USA) and the web interface for data mining FatiGO (http://babelomics.bioinfo.cipf.es; Al Shahrour et al., 2007; Al Sharour et al., 2008). In

Table 2. Number of genes analyzed and number of genes remaining after each filter. See text for details on filtering method.

Experiment	Time-course		Restimulation	
Summarization algorithm	Plier	IterPlier	Plier	IterPlier
Total analyzed	16755	16755	16755	16755
Filter on expression	13621	13735	13564	13689
Filter on fold change	760	3192	774	4527
Filter on significance	182	224	187	432
Pass filters in Plier or IterPlier only	37	79	49	294
Pass filters in Plier and IterPlier	145		138	
Pass filters in Plier and/or IterPlier	261		481	

Genespring, genes are automatically mapped to gene ontology terms (GO terms) from the Gene Ontology database (www.geneontology.org; Ashburner et al., 2000) according to their known or putative function or localization. The Gene Ontology Analysis module from Genespring was used to explore the association of gene ontology terms with the list of significantly regulated genes and the raw p value for the association of GO terms within the regulated genes compare to the rest of the genome. FatigGO was used to identify gene ontology terms significantly overrepresented in the list of regulated genes compared to the rest of the genes on the genome and to assess significant enrichment in binding sites for specific transcription factors within the first 5kb of the promoters of the regulated genes. Using FatiGO, significant enrichment was tested using a Fisher's exact test and p-values were adjusted for multiple testing using the Benjamini Hochberg False Discovery Rate (Benjamini and Hochberg, 1995).

Network and functional analyses were generated through the use of Ingenuity Pathways Analysis (Ingenuity® Systems, , Inc., Redwood City, CA, USA; www.ingenuity.com). The Functional Analysis identifies the biological functions and/or diseases that are most significant to the set of regulated genes. Only genes which are associated with biological functions and/or diseases in the Ingenuity Pathways Knowledge Base were considered for the analysis. Fischer's exact test was used to calculate a p-value determining the probability that each biological function and/or disease assigned to that data set is due to chance alone. In addition, using Ingenuity Pathway Analysis, a graphical representation of the molecular relationships between genes/ gene products was generated where genes or gene products are represented as nodes, and the biological relationship between two nodes are represented by a line. All associations are supported by at least one reference from the literature, from a textbook, or from canonical information stored in the Ingenuity Pathways Knowledge Base.

Comparison with published microarray data was performed by importing into Genespring the gene symbols of the genes that were considered regulated in already published studies and visualizing in GeneSpring the overlap between these lists with our data set.

a) Temporal profile of gene expression

Before clustering the genes based on their temporal expression profile, expression values were used and transformed to express expression changes in percent of control values [(expression value Stim minus expression value NonStim) divided by expression value NonStim]. Genes were then grouped together depending on the time point at which they were maximally up or down-regulated. A second method was used to study modified expression as a function of stimulation period. For this, expression changes expressed in percent of control value were normalized to the previous time-points and hierarchical clustering using Ward's minimal distance (Ward,

1963) method was performed to group genes according to gene expression temporal profile. For this, SAS (version 9.1, SS Institute Inc., Cary, NC, USA) as well as Matlab (version R2006b, The MathWorks, Natick, MA, USA) were used.

b) Statistical analysis in the restimulation experiment

Using excel, bilateral Student's t-test was performed between the expression changes (expressed in percent of control value) from 6h stimulated barrels and from restimulated barrels. Using F-test, equality of variance was verified; when necessary Student's t-test for unequal variance was used. Adjustement of the p value for multiple tests using the Benjamini Hochberg False Discovery Rate (Benjamini and Hochberg, 1995) method was performed in SAS (SAS version 9.1, SS Institute Inc., Cary, NC, USA).

II.2. About the microarray analysis

Despite the large amount of information that microarray analysis enables to treat, this technique contains several downsides that needs to be taken into consideration before interpretation of the results. Most important of all is that microarray analyses greatly depend on bioinformatical tools (Ness, 2007). For example signal values is obtained after normalization where the overall fluorescence of each microarray is averaged to the same intensity; hence expression value obtained for a gene after normalization is a relative value that depends on the set of chips that were analyzed together and on the method of normalization chosen. In addition, various criteria can be used to determine whether a gene is considered regulated. Hence the list of genes identified as regulated will depend on the method used to generate it and only subsequent considerations of the biological significance of the results and validation of the results by independent methods will determine whether the choices made were the most appropriate (Seo and Hoffman, 2006).

In the current study, we have hybridized the samples on exon arrays. These arrays have been developed to enable not only gene expression analysis but also to assess exon expression levels. Indeed the probe sets are designed to recognize sequences distributed all along the entire length of the transcripts with approximately four probes per exon and roughly 40 probes per gene. With this design, the analysis can be done at two complementary levels: one on gene expression and one on exon expression. The great advantage of using the exon arrays is that they enable the analysis of alternative splicing, differential promoter usage or differential polyadenylation site usage (Cuperlovic-Culf et al., 2006). Indeed, it is estimated that at least 60% of genes in the human genome exhibit alternative splicing and by changing the structure of the mRNA and their encoded protein, alternative splicing may determine protein abundance, localization and function (reviewed in Stamm et al., 2005). In addition to alternative splicing, many genes have more than one polyadenylation site. Similar to alternative splicing, differential polyadenylation site usage produces more than one transcript from a single gene and is important for the nuclear export, translation and stability of the RNA. These are important events in the process of gene expression and could be altered by neuronal activity. Indeed, it was shown that neuronal activity promotes differential polyadenylation site usage leading to truncated mRNA (Flavell et al., 2008). In addition, BDNF, for example, is encoded by 18 distinct mRNAs (Aid et al., 2007; An et al., 2008) which show differences in their functions (Hong et al., 2008). These findings emphasized the importance of using exon arrays. However we have for the moment limited ourselves to analyze the data at the gene expression level as the bioinformatical tools that are currently available do not optimally enable the treatment of this data set at the exon level.

Analysis at the level of gene expression requires attention as a whole set of probes representing a gene actually represents various exons which may be differentially regulated. A gene may

be considered regulated when actually an alternative splicing or differential promoter usage have occurred or it may be considered not regulated because the removal of certain exons by differential splicing have occurred balancing out the gene value or because exons that are not expressed reduce the gene expression signal (Affymetrix, 2005a). For this reason, in the current study, we have used as the normalization method the Probe Logarithmic Intensity Error (Plier) logarithm and IterPlier (Iterative Probe logarithmic intensity error). Plier is an algorithm designed to increase the sensitivity to changes in expression level for genes with expression value near background without loss of accuracy and was shown to be a good model to reduce the rate of false positive in poorly performing probe sets (Seo and Hoffman, 2006). IterPlier is a variation of Plier that iteratively discard probes that do not correlate well with the overall gene-level signal to only estimate gene signal from the 11 probe sets that are most correlated (Affymetrix, 2005b). Plier by summarizing gene values from all the probe sets might identify genes as not regulated because exons not expressed or differentially spliced might balanced out the gene level. However, IterPlier by excluding probe sets from the analysis might discard important information that could be identified only when combined with an analysis on alternative splicing. For this reason, we have decided to use both algorithms and to group together genes that were identified as regulated by Plier and/or IterPlier.

Also, it is to note that the probes on the chips were designed according to several gene sequence databases with various levels of confidence. We have limited ourselves to the probes that were designed according to the most confident annotations (i.e. the core probe sets that interrogate exons of RefSeq genes and mRNA and ESTs from GenBank) as to limit the risk of altering the gene signal estimation with probes that were designed according to more speculative annotations, although analysis on these probe sets could identify new molecular events.

Before any statistical analysis, we have filtered the list of genes on their expression values as well as on their fold change relative to the control. This was to limit the analysis to only genes that could be reliably considered expressed in the tissue and to a fold change that could also be accurately measured. However, filtering on expression values exclude from the list genes that are expressed only in small subpopulations of cells but could undergo substantial regulation. In addition, filtering on fold change excludes genes that are tightly regulated and undergo only minute change in expression but whose functions are capital. Thus, the various filters used may considerably increase the number of false negatives and thus exclude important molecular players in experience-dependent plasticity. However these criteria were applied in order to limit the number of false positives. Using the same rational, the list of significantly regulated genes was acquired by adjusting the p value for false discovery rate (Benjamini and Hochberg, 1995) a method which limits the rate of false positive while maintaining the rate of false negative

relatively low. These choices were made as considerable efforts and time will be devoted to the confirmation and investigation of the genes that were identified as regulated. It is to note that for confirmation of the results presented here, *in situ* hybridization method would be the method of choice as it may also give information on the histological and cellular localization of the mRNA. Also, changes at the protein level will also have to be examined and this, for the same reason, preferentially by immunohistochemistry.

The overall analysis presented here was established through discussion with Gregory Lefebvre, PhD, from the Bioinformatics and Biostatistics Core Facility at the EPFL.

II.3. Results and characterization of the differentially regulated genes

Twenty-four hours of an increased sensory activity by continuous whisker stimulation alters the functional and structural properties of the neurons in the somatosensory cortex resulting in the reduction of the cortical response to the deflection of the stimulated whisker in layer IV and layer II/III (Quairiaux et al., 2007). As revealed in the first part of this thesis, the structural modifications of the cortical circuitry in layer IV consist of a short-lived increased number of excitatory synapses on dendritic shafts already present after 6 hours and that disappear by 24 hours. The disappearance of these synapses after 24 hours is concomitant with the appearance of inhibitory synapses on dendritic spines. Apart from *bdnf*, the set of genes whose expression is regulated by such passive whisker stimulation and that orchestrate these functional and structural modifications are unknown. Hence, using microarray technologies, large scale gene expression profiling was conducted on transcriptome extracted from laser capture microdissected barrels (Figure 11) whose corresponding whiskers were stimulated for 3, 6, 9, 15 and 24 hours and from the adjacent barrels that served as control. This is the first study to follow the changes in gene transcription in layer IV of the somatosensory cortex that are driven by an increased sensory activity in adult animals. We further assessed the impact of a prior experience on gene expression by analyzing the transcriptome in barrels whose corresponding whiskers were stimulated for a second stimulation period of 6 hours 4 days after 24 hours of stimulation.

II.3a. Transcriptomic changes within 24 hours of whisker stimulation

Genes were considered differentially regulated by increased sensory activity when their level of expression was increased or decreased in the stimulated barrels compared to the adjacent unstimulated ones by ≥1.25 fold and when the adjusted p value was equal or less than 0.05 as identified by Welch's ANOVA followed by Tukey HSD. Out of the 16755 genes analyzed, whisker stimulation differentially regulates significantly the expression of 261 genes. Relative to the internal control i.e. unstimulated barrels, sensory stimulation increases the expression of 133 genes while decreasing the expression of 128 genes. Among the genes identified as regulated are found genes coding for kinases (16 genes), phosphatases (6 genes), peptidases (6 genes) and other enzymes (36 genes), ions channels (15 genes), receptors (19 genes), cytokines (4 genes), growth factors (2 genes), transporters (11 genes) and transcription factors (19 genes). Also out of the 261 genes identified as regulated, 19 are of unknown function. Among these, two of them, AI836003 and 6430550H21Rik, were also regulated by 4 days of visual deprivation performed during the peak of the critical period (Tropea et al., 2006). Both of them are maximally down-regulated after 15 hours of whisker stimulation. The list of all regulated genes with their fold change in expression at the various time-points is given in alphabetical order in the Appendix 2 (page 120). General information about the genes (ex. cellular distribution and function of the

encoded protein) are also given in this list.

a) The 10 most regulated genes

Out of the 10 most regulated genes, 7 are known neuronal activity-dependent genes and three genes that were not previously related to neuronal plasticity, *scn7a*, *pcdh15* and *ccdc3*. For all of them, whisker stimulation increases their expression. Except for *pcdh15*, all of them are already significantly regulated after 3 hours of whisker stimulation although they are not all at their maximal value at that time (Table 3). *Scn7a*, is the most regulated gene and codes for a sodium-sensitive sodium channel (Potts et al., 1993; Hiyama et al., 2002). It is maximally up-regulated by 4.81 fold after 24 hours of stimulation. *Pcdh15* is most regulated after 9 hours with a 2.43 fold change. This gene is a member of the cadherin superfamily which encodes integral membrane proteins that mediate calcium-dependent cell-cell adhesion. Mutations in this gene has been linked to Usher Syndrome, a disorder associated with hearing-loss and degeneration of the retina (Reiners et al., 2006). *Ccdc3* is most regulated after 24 hours with a 2.54 fold change. This gene codes for a recently identified protein which is secreted by adipocytes and endothelial cells and which level of expression is regulated by factors such as insulin and tumor necrosis factor alpha (tnfα) (Kobayashi et al., 2009). Mutation in this gene has been associated with amyotrophic lateral sclerosis as well as in non-insulin-dependent diabetes mellitus (according to Ingenuity Knowledge Base). The top 10 set includes 7 genes for which it is known that neuronal activity regulates their level of expression. These 7 genes are *tnnc1*, *nptx2*, *bdnf*, *sorcs3*, *ptgs2*, *nr4a2* and *npas4*. All of these 7 genes are already up-regulated within 3 hours of whisker

Table 3. List of the 10 genes that were found most differentially expressed in barrels after whisker stimulation relative to the control adjacent non-stimulated barrels and their fold change (FC) at the different periods of stimulation.

Gene	Gene Name	FC 3h	FC 6h	FC 9h	FC 15h	FC 24h
Scn7a	sodium channel, voltage-gated, type VII, alpha	3.61	2.70	2.68	4.14	4.81
Tnnc1	troponin C type 1 (slow)	3.22	3.58	2.63	3.96	4.72
Nptx2	neuronal pentraxin II	2.50	4.03	2.62	1.75	2.07
Sorcs3	sortilin-related VPS10 domain containing receptor 3	1.44	2.57	3.36	1.73	1.50
Bdnf	brain-derived neurotrophic factor	3.75	3.63	3.19	2.44	1.89
Ptgs2	prostaglandin-endoperoxide synthase 2	2.96	2.65	2.56	1.93	1.81
Nr4a2	nuclear receptor subfamily 4, group A, member 2	2.84	2.08	1.31	1.18	1.02
Ccdc3	coiled-coil domain containing 3	1.69	1.88	1.74	2.05	2.54
Npas4	neuronal PAS domain protein 4	2.48	2.54	2.18	1.65	1.69
Pcdh15	protocadherin 15	1.21	1.29	2.43	2.42	1.85

When the corresponding fold change was ≥1.25 and was found significant for the corresponding comparison by Welch's ANOVA followed by Tukey HSD with correction for multiple comparisons (Benjamini Hochberg false discovery rate), the cell was color coded according to the scale bar below (N.S. stands for not significantly regulated and/or do not pass threshold).

Fold change	N.S.	1.25-1.5	1.5-2	2-2.5	2.5-3	≥3
Scale bar						

stimulation although not all of them are at their maximal value at this time-point. Out of these, 3, *nptx2*, *bdnf* and *npas4*, have been shown to be implicated in synaptogenesis (O'Brien et al., 1999; Genoud et al., 2004; Lin et al., 2008). *Bdnf* is maximally expressed at 3 hours by 3.75 fold and is gradually decreased to reach a still significant increase of 1.89 fold by 24 hours. The regulation of *bdnf* by whisker stimulation was already shown by *in situ* hybridization were its up-regulation was maximal after 6 hours and considerably reduced after 24 hours (Rocamora et al., 1996). Among the other, of particular interest is *npas4*, which is significantly up-regulated across the 24 hours of whisker stimulation but is maximally regulated after 6 hours. *Npas4* was recently reported to be transcribed in response to excitatory synaptic activity and to code for a transcription regulator which leads to the formation of inhibitory synapses on excitatory neurons (Lin et al., 2008).

Among the 10 most regulated genes is *nptx2* whose regulation peaks after 6 hours of whisker stimulation. *Nptx2* codes for neuronal pentraxin 2 also known as the neuronal activity-regulated protein (NARP). *Nptx2* is a neuronal immediate early gene whose product is a secreted protein found at excitatory synapses and plays an important role in synaptogenesis as it induces the clustering of AMPA receptors (Tsui et al., 1996; O'Brien et al., 1999; Xu et al., 2003).

Finally, also of interest is *tnnc1*, the second most regulated gene which is found significantly up-regulated at all time-points but reaches its maximum after 24 hours with a 4.72 fold increase. *Tnnc1* codes for cardiac troponin, a calcium binding protein and structural constituent of the cytoskeleton. Troponin c is well known for its role in muscle contraction as it regulates, in a Ca^{2+}-dependent manner, the interaction between actin filaments and the myosin-ATPase in muscle fibers. It was however recently shown by microarray screening to be regulated by neuronal activity as it is highly expressed in the primary visual cortex during the critical period and down-regulated following 2 days or 4 days of monocular deprivation (Tropea et al., 2006; Lyckman et al., 2008). Its specific role in experience-dependent plasticity remains to be elucidated. In this context, also to note, although not part of the 10 most regulated genes, is the gene *mylk3*, coding for Myosin Light Chain Kinase 3. This kinase, specifically expressed in the heart, phosphorylates cardiac myosin and is implicated in muscle contraction. *Mylk3* is significantly over-expressed after 3 hours of whisker stimulation and up to 15 hours with a peak in expression level after 9 hours with a fold change of 1.98 at that time.

b) Comparison with other microarray analyses on activity-dependent gene expresion

A comparison of the genes identified in this study with the genes regulated in cultured hippocampal neurons within 2 to 4 hours after burst of action potentials triggered by the removal of inhibition with the GABAa receptor antagonist bicuculline (Zhang et al., 2007), a protocol that was shown

Table 4. Genes encoding synaptic proteins whose expression were found to be significantly altered by whisker stimulation.

Gene	Gene Name	FC 3h	FC 6h	FC 9h	FC 15h	FC 24h
Arc	activity-regulated cytoskeleton-associated protein	1.21	1.50	1.73	1.40	1.07
Cacng2	calcium channel, voltage-dependent, gamma subunit 2	1.02	1.10	1.27	1.17	1.03
Grasp	GRP1 (general receptor for phosphoinositides 1)-associated scaffold protein	1.36	1.92	1.26	1.27	1.24
Grik1	glutamate receptor, ionotropic, kainate 1	1.28	1.65	1.59	1.28	1.14
Homer1	homer homolog 1 (Drosophila)	1.45	1.37	1.32	1.07	1.03
Nptx2	neuronal pentraxin II	2.50	4.03	2.62	1.75	2.07
Nrn1	neuritin 1	1.27	1.36	1.38	1.27	1.12

When the corresponding fold change was ≥1.25 and was found significant for the corresponding comparison by Welch's ANOVA followed by Tukey HSD with correction for multiple comparisons (Benjamini Hochberg false discovery rate), the cell was color coded according to the scale bar below (N.S. stands for not significantly regulated and/or do not pass threshold).

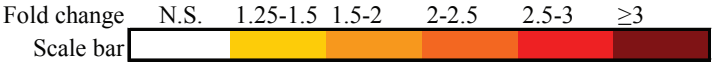

to induces long-lasting synaptic plasticity in the network of cultured neurons, revealed that 36 genes overlap. They are identified as such in the list of the differentially regulated genes given in the Appendix 2 (page 120). Out of these 36 genes, more than two thirds are found up-regulated maximally after 3 or 6 hours of whisker stimulation. Among them are common neuronal activity-dependent genes known to be involved in synapse development, function and plasticity (*npas4*, *nr4a1*, *bdnf*, *homer1a*, *arc*, *nrn1/cpg15* and *crem*; reviewed in Greer and Greenberg, 2008). Also found regulated after whisker stimulation (after 6 hours) and burst of action potential is *grasp*, encoding a protein that binds to scaffolding proteins at the synapse and to AMPA receptors regulating their trafficking (Ye et al., 2000). Related to the synapse but not differentially regulated in the study from Zhang et al. (2007) are *grik1*, coding for ionotropic glutamate receptor kainate1, which is significantly up-regulated after 6 and 9 hours of stimulation, and *cacng2*. This gene is up-regulated precisely after 9 hours and is encoding for an AMPA receptor regulatory protein (TARP gamma 2, also known as stargazin) which controls synaptic strength both by targeting AMPA receptors to the synapses and by modulating their channel activity (Payne, 2008). Genes encoding synaptic proteins and their associated fold changes are given in Table 4.

Out of the genes regulated by whisker stimulation, 79 were previously shown *in vivo* to be altered by 4 days of visual deprivation during the critical period (Tropea et al., 2006). Noteworthy, for 59 of those genes, deprivation has an opposite effect on the sense of regulation compare to stimulation; i.e. 44 genes that are up-regulated by whisker stimulation (including *bdnf*, *ptgs2*, *nptx2*, *tnnc1*) are decreased in their expression level following monocular deprivation induced during the critical period.

Npas4 was shown to be an activity-dependent gene up-regulated in cultured hippocampal neurons after depolarization (Lin et al., 2008). In the same experimental paradigm, the formation of inhibitory synapses was prevented when *npas4* was silenced using RNA interference and a microarray analysis was performed to screen for genes whose expression were altered in this condition (Lin et al., 2008). The comparison between the list of activity-dependent genes that are differentially regulated in the absence of NPAS4 (Lin et al., 2008), with the list of genes that are differentially regulated by whisker stimulation gives an overlap of 9 genes (see Table 5). NPAS4 being a transcription factor necessary to the formation of inhibitory synapses, these genes are prime candidates for being implicated in this process. One of them is *ier5*, coding for an immediate transcription factor which, in contrast to most immediate early genes that are induced within 10 minutes after a stimulation, has a slow kinetic and a delay in its expression by 60 to 90 minutes (Williams et al., 1999). *Ier5* is significantly up-regulated after 6 and 9 hours of whisker stimulation.

Table 5. List of the 9 genes that are found differentially regulated by Npas4 (Lin et al., 2008) and in barrels after whisker stimulation relative to the control adjacent non-stimulated barrels and their fold change (FC) at the different period of stimulation.

Gene	Gene Name	FC 3h	FC 6h	FC 9h	FC 15h	FC 24h
Arc	activity-regulated cytoskeleton-associated protein	1.21	1.50	1.73	1.40	1.07
Bdnf	brain-derived neurotrophic factor	3.75	3.63	3.19	2.44	1.89
Egr2	early growth response 2	1.90	1.72	1.23	1.18	1.18
Egr3	early growth response 3	1.46	1.42	1.37	1.08	1.04
Fxyd6	FXYD domain containing ion transport regulator 6	1.41	1.36	1.25	1.24	1.43
Ier5	immediate early response 5	1.09	1.34	1.32	1.11	1.08
Pcdh17	protocadherin 17	1.39	1.29	1.12	1.07	1.11
Slc24a3	solute carrier family 24 (Na/K/Ca exchanger), member 3	1.13	1.11	1.11	1.34	1.29
Sorcs3	sortilin-related VPS10 domain containing receptor 3	1.44	2.57	3.36	1.73	1.50

When the corresponding fold change was ≥1.25 and was found significant for the corresponding comparison by Welch's ANOVA followed by Tukey HSD with correction for multiple comparisons (Benjamini Hochberg false discovery rate), the cell was color coded according to the scale bar below (N.S. stands for not significantly regulated and/or do not pass threshold).

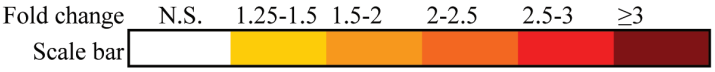

c) Transcription factors

To know whether the regulated genes are under the control of specific transcription factors, the first 5 kb of the promoters of all genes identified as regulated were scanned for the possible presence of transcription factor binding sites using FatiGo (Al Shahrour et al., 2007; Al Shahrour et al., 2007). Binding sites for three transcription factors were detected to be enriched within the promoters of the genes identified regulated by whisker stimulation. These transcription factors are TFII-I (147 genes, adj. p value = 0.002), KROX (36 genes, adj. p value = 0.003) and SREBP-1 (163 genes, adj. p value = 0.02). Genes which contain binding sites for these transcription

factors within their promoters are indicated as such under the columns labeled "transcription factor" in the table given in the Appendix 2 (page 120). Although its role in synaptic plasticity is not known, TFII-I is an ubiquitously expressed transcription factor that is activated in response to various extracellular signal and known to regulate the expression of *c-fos*, an immediate early gene regulated by neuronal activity (Roy, 2007; Kim and Cochran, 2000). TFII-I was reported not only to be involved in transcriptional activation but also repression (Hakimi et al., 2003) and to negatively regulate genes involved in neuroactive ligand-receptor interaction and calcium-signaling pathway (Chimge et al., 2008). Interestingly, TFII-I is associated with William-Beuren syndrome, a rare neurodevelopmental disorder characterized by cardiac, craniofacial, behavioral and cognitive anomalies (Danoff et al., 2004). KROX transcription factors include the plasticity-related transcription factors EGR1 (KROX1/KROX24), EGR2 (KROX20) and EGR3 which are well known for their role in synaptic plasticity and memory formation (Poirier et al., 2008). Interestingly, *egr2* and *egr3* are found significantly up-regulated after whisker stimulation and their level of expression are maximal after 3 hours. SREBP-1, for sterol regulatory element-binding protein 1, can be activated by growth factor through the activation of MAPK pathway and is supposed to mediate lipid uptake and synthesis required for cell growth (Arito et al., 2008). Although not yet investigated for a role in synaptic plasticity, it has been shown to be induced by the excitotoxic activation of NMDA receptors in models of stroke (Taghibiglou et al., 2009).

d) Diseases and biological processes

According to Ingenuity Pathway Analysis, the list of 261 genes that are regulated by whisker stimulation is significantly enriched with genes known to be related to genetic disorder and to neurological disorder (respectively 130 genes, $p=2.57*10^{-6}$ and 96 genes, $p=1.55*10^{-8}$; Ingenuity Pathway Analysis). Among the categories of neurological disorder that are found significantly represented are Alzheimer (28 genes), Schizophrenia (25 genes) and Bipolar Affective Disorder (28 genes). The list of genes associated with the genetic and neurological disorders as well as the name of the various disorders that they comprise is given in the Appendix 3 and 4 (pages 126-127). For example, the gene *mme*, also known as *nep* or neprilysin, is coding for a membrane endopeptidase that is involved in the degradation of endogeneous amyloid-β. *Mme* is precisely down-regulated at 15 hours of whisker stimulation. In Alzheimer's disease, amyloid-β is found in the extracellular space where it aggregates to form the amyloid-β plaque load that is characteristic of the disease pathogenesis (see for review Walsh and Selkoe, 2004).

In addition, the Ingenuity Pathway Analysis shows that the list of regulated genes is significantly associated with a series of biological functions, among which cell morphology represented by 31 genes, cell cycle represented by 12 genes and nervous system development and function

represented by 52 genes. The list of the top biological functions significantly associated with the altered gene expression induced by whisker stimulation is given in Table 6.

To know whether whisker stimulation differentially regulates genes that are part of common biological processes, Gene Ontology Analysis was used. In the Gene Ontology database, genes are grouped into biological processes according to the known or putative function of their products (Ashburner et al., 2000). This analysis performed with Fatigo (Al Shahrour et al., 2008; Al Shahrour et al., 2007) identifies all functional categories (GO terms) which are significantly represented among the list of differentially regulated genes compared to the GO term composition of all genes in the genome. We applied this analysis on the whole set of regulated genes and it revealed that our list is significantly enriched in genes involved in anatomical structure development (GO:0048856, adj. p value = 0.05), in nervous system development (GO:0007399, adj. p value = 0.03) and transmission of nerve impulse (GO:0019226, adj. p value = 0.03). In addition, looking at the Gene Ontology categories associated with the regulated genes, it appears that the genes regulated by whisker stimulation pertain to various biological and molecular processes or cellular compartments that are relevant to synaptic plasticity, including response to stimulus, growth, synapse, nervous system development, neurogenesis, channel activity, gene

Table 6. Listing of the top biological functions and diseases significantly associated with the altered gene expression induced by whisker stimulation according to Ingenuity Pathway Analysis.

Diseases and Disorders

Name	p-value	# Genes
Genetic Disorder	1.17E-08 - 1.32E-02	130
Neurological Disease	1.17E-08 - 1.32E-02	96
Psychological Disorders	1.17E-08 - 1.37E-03	49
Cardiovascular Disease	4.12E-06 - 1.32E-02	60
Endocrine System Disorders	1.35E-04 - 1.32E-02	55

Molecular and Cellular Functions

Name	p-value	# Genes
Cell Morphology	1.95E-06 - 1.32E-02	31
Cell Cycle	8.89E-06 - 1.32E-02	12
Cellular Assembly and Organization	7.55E-05 - 1.32E-02	27
Cellular Movement	1.20E-04 - 1.32E-02	34
Molecular Transport	1.53E-04 - 1.32E-02	24

Physiological System Development and Function

Name	p-value	# Genes
Nervous System Development and Function	1.95E-06 - 1.32E-02	52
Tissue Development	2.04E-06 - 1.32E-02	30
Behavior	2.07E-06 - 1.32E-02	29
Skeletal and Muscular System Development and Function	8.89E-06 - 1.32E-02	9
Reproductive System Development and Function	1.72E-04 - 1.32E-02	5

expression, cell communication, signal transducer activity and cell adhesion. Plotting, for each stimulation period, the number of genes significantly regulated within each category shows that the number of genes pertaining to each category changes over time (Appendix 5, 6 and 7, pages 128-130).

Interesting is one category that includes genes coding for molecules with an histone methyltransferase activity. Out of the 25 genes that belong to this category, 2 are found significantly regulated by whisker stimulation: *dot1l* and *setd7*. *Dot1l* is precisely up-regulated after 9 hours while *set7d* is down-regulated after 15 hours (see Table 7). Histone methylation is known to serve epigenetic gene regulation; it may inhibit or activate transcription depending on the number of methylated groups and the site of methylation on the histones (Berger, 2002). These two genes are the only ones coding for histone methyltransferases in the list of regulated genes. However, also known to play a role in post-translational modifications of histones and found down-regulated after 15 hours, is *rps6ka5*. This gene encodes the mitogen- and stress-activated kinase 1 (MSK1), a kinase activated by ERK and p38 MAP kinases. In addition to phosphorylate CREB, MSK1 is known to elicit histone phosphorylation.

Fifteen hours of whisker stimulation show strong tendency to increase the number of genes associated with the biological process “rhythmic process”, i.e. genes that are associated with any processes pertinent to the generation and maintenance of rhythms in the physiology of an organism (raw p value 0.0002). Regulated genes pertaining to this category are *egr2*, *hlf*, *nfil3*,

Table 7. List of differentially regulated genes that belong to the Gene Ontology Categories "histone methyltransferase" and "Rhythmic process".

Gene	Gene Name	FC 3h	FC 6h	FC 9h	FC 15h	FC 24h
Histone methyltransferase (GO:0042054)						
Dot1l	DOT1-like, histone H3 methyltransferase (S. cerevisiae)	1.17	1.24	1.29	1.20	1.09
Setd7	SET domain containing (lysine methyltransferase) 7	-1.11	-1.05	-1.08	-1.31	-1.11
Rhythmic process (GO:0048511)						
Dbp	D site of albumin promoter (albumin D-box) binding protein	-1.37	-1.34	-1.39	-1.60	-1.22
Egr2	early growth response 2	1.90	1.72	1.23	1.18	1.18
Hlf	hepatic leukemia factor	-1.31	-1.23	-1.17	-1.39	-1.27
Nfil3|LOC	nuclear factor, interleukin 3 regulated	1.23	1.40	1.33	1.38	1.15
Per3	period homolog 3 (Drosophila)	-1.13	-1.11	-1.19	-1.42	1.03
Tef	thyrotrophic embryonic factor	-1.16	-1.14	-1.20	-1.32	-1.06

When the corresponding fold change was ≥1.25 and was found significant for the corresponding comparison by Welch's ANOVA followed by Tukey HSD with correction for multiple comparisons (Benjamini Hochberg false discovery rate), the cell was color coded according to the scale bar below (N.S. stands for not significantly regulated and/or do not pass threshold). The minus sign indicates down-regulation.

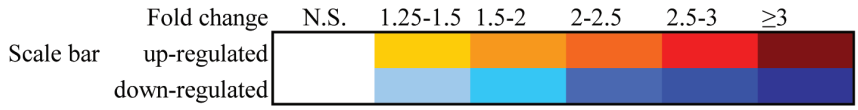

tee, *per3* and *dip* (see Table 7). All these gene code for transcription factors except *per3* which codes for a signal transducer. Also to note in this context as a modulator of the circadian rhythm (Harmer, 2003; Harmar et al., 2002; Hannibal et al., 1998) is the up-regulation of *adcyap1*, coding for the pituitary adenylate cyclase activating peptide (PACAP). Its regulation is maximal at 9h with a fold change of 2.15 at that time.

Table 8. List of differentially regulated genes that belong to the Gene Ontology Categories "Cell adhesion" and "Nervous System Development".

Gene	Gene Name	FC 3h	FC 6h	FC 9h	FC 15h	FC 24h
Cell adhesion (GO term: 0007155)						
C230078I	contactin associated protein-like 5B	-1.06	-1.22	-1.25	-1.73	-1.33
Cd34	CD34 molecule	1.12	-1.02	-1.13	-1.47	-1.29
Chl1	cell adhesion molecule with homology to L1CAM	1.40	1.86	1.52	1.42	1.45
Cntn2	contactin 2 (axonal)	-1.17	-1.20	-1.17	-1.37	-1.14
Ctnna1	catenin (cadherin-associated protein), alpha 1, 102kDa	-1.21	-1.22	-1.23	-1.46	-1.17
Dcbld2	discoidin, CUB and LCCL domain containing 2	-1.08	-1.23	-1.11	-1.33	-1.19
Fzd3	frizzled homolog 3 (Drosophila)	1.19	1.15	1.32	1.32	1.20
Mag	myelin associated glycoprotein	-1.01	1.01	-1.13	-1.31	-1.06
Pcdh15	protocadherin 15	1.21	1.29	2.43	2.42	1.85
Pcdh17	protocadherin 17	1.39	1.29	1.12	1.07	1.11
Rnd3	Rho family GTPase 3	1.85	1.94	1.74	1.60	1.26
Spon1	spondin 1, extracellular matrix protein	1.33	1.36	1.17	1.22	1.49
Nervous System Development (GO term: 0007399)						
Bdnf	brain-derived neurotrophic factor	3.75	3.63	3.19	2.44	1.89
Chl1	cell adhesion molecule with homology to L1CAM	1.40	1.86	1.52	1.42	1.45
Cntn2	contactin 2 (axonal)	-1.17	-1.20	-1.17	-1.37	-1.14
Ctnna1	catenin (cadherin-associated protein), alpha 1, 102kDa	-1.21	-1.22	-1.23	-1.46	-1.17
Egr2	early growth response 2	1.90	1.72	1.23	1.18	1.18
Egr3	early growth response 3	1.46	1.42	1.37	1.08	1.04
Fzd3	frizzled homolog 3 (Drosophila)	1.19	1.15	1.32	1.32	1.20
Gap43	growth associated protein 43	1.28	1.35	1.27	1.31	1.64
Gfra2	GDNF family receptor alpha 2	1.05	1.29	1.50	1.44	1.27
Nefl	neurofilament, light polypeptide	1.15	1.36	1.26	1.16	1.16
Neurod1	neurogenic differentiation 1	-1.13	-1.38	-1.19	-1.30	-1.15
Nr4a2	nuclear receptor subfamily 4, group A, member 2	2.84	2.08	1.31	1.18	1.02
Nrn1	neuritin 1	1.27	1.36	1.38	1.27	1.12
Nrxn3	neurexin 3	1.05	1.25	1.39	1.34	1.15
Prkg1	protein kinase, cGMP-dependent, type I	-1.14	-1.16	-1.25	-1.33	-1.23
Rtn4	reticulon 4	-1.04	-1.09	-1.01	-1.29	-1.14
Ttl	tubulin tyrosine ligase	1.28	1.17	1.09	1.07	1.02

When the corresponding fold change was ≥1.25 and was found significant for the corresponding comparison by Welch's ANOVA followed by Tukey HSD with correction for multiple comparisons (Benjamini Hochberg false discovery rate), the cell was color coded according to the scale bar below (N.S. stands for not significantly regulated and/or do not pass threshold). The minus sign indicates down-regulation.

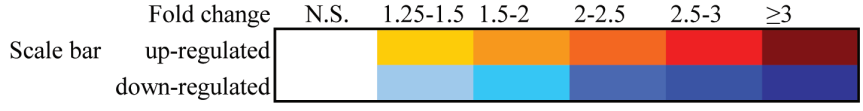

Finally, of particular interest are the biological processes of cell adhesion and nervous system development (genes are listed in Table 8). The maximal number of genes that pertain to these two categories is found at 15 hours (Figure 13) (raw p value 0.005 and 0.006). At that time, it appears that most of the genes pertaining to cell adhesion are down-regulated, among which *mag*, coding for myelin-associated glycoprotein and *cntn2* coding for contacting 2, an axonal glycoprotein. Among the genes that pertain to nervous system development and that are found significantly up-regulated after 15 hours are the genes known to be implicated in synaptogenesis *bdnf* and *nrn1/cpg15* (Genoa et al., 2004; Javaherian and Cline, 2005) as well as the gene coding for the growth-associated protein 43 (*gap43*) a marker of neuronal outgrowth and regeneration also implicated in LTP (reviewed in Benefits and Rotenberg, 1997). Among the down-regulated genes is *rtn4* for reticulum 4. *Rtn4* codes for NOGO, a growth inhibitor (Huber and Schwab, 2000; Montani et al., 2009) which has also been shown to play a role in synaptogenesis as over expression of NOGO destabilizes inhibitory synapses in mouse cerebella Purkinje terminals (Alloy et al., 2006).

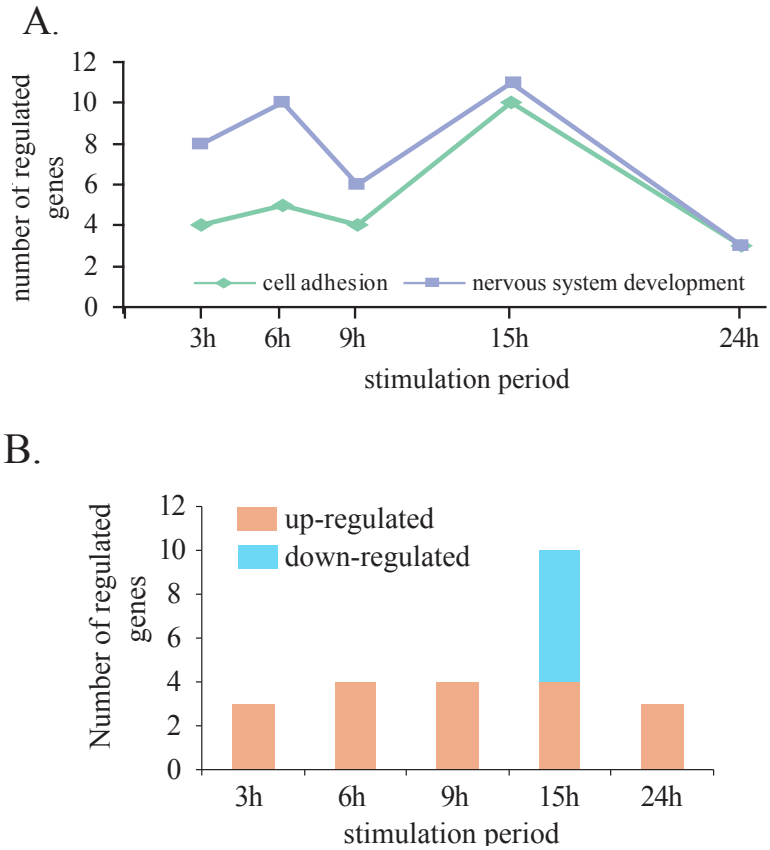

Figure 13. Cell adhesion and nervous system development. A. Number of significantly regulated genes per stimulation period for two Gene Ontology categories «cell adhesion» and «nervous system development». B. Number of genes in the gene ontology category «cell adhesion» that were found up-regulated (orange) and down-regulated (blue) at each stimulation period.

e) Temporal profile of gene expression

Out of the 261 regulated genes, only 17 are significantly regulated across the entire period of 24 hours of whisker stimulation while 162 are considered significantly regulated exclusively at one time-point. In addition, grouping genes according to their peak of expression shows that gene expression is tightly regulated over time. Figure 14A shows the mean temporal expression profile for each cluster (the expression profile of all the genes per group is given in Appendix 8 page 131). This observation is further emphasized by hierarchical clustering. Mean expression profiles of the various clusters formed by hierarchical clustering using Ward's distance show that, in general, genes that pertain to the same cluster are maximally expressed at one specific time-point (except for one cluster of 14 down-regulated genes which show two peaks of expression) and that the clusters differs from one another mainly by the time at which the genes are maximally expressed. Hierarchical clustering also identifies a few genes that differ considerably from the rest in their expression profile. These genes are *gpr115* (for G protein-coupled receptor 115), *mylk3*, *pcdh15* that form one cluster and *tnnc1*, *scn7a*, *sorcs3* and *nptx2* whose expression profile differed considerably from the rest and could not be grouped with other genes into clusters. These last 4 genes are among the 10 most regulated genes. Mean temporal profile for the clusters identified by hierarchical clustering is given in Appendix 9 (page 132). Also worth to note is that, within 24 hours of whisker stimulation, there are no genes that are found significantly up-regulated at one stimulation period and significantly down-regulated at another time point.

Grouping genes into temporal profile reveals that 9 hours is the time at which the greatest number of up-regulated genes are at their maximal level of activation (32% of the genes) while 15 hours correspond to the time at which the greatest number of down-regulated genes are at their maximal level of regulation; i.e. 61% of the down-regulated genes are maximally down-regulated at 15 hours (Figure 14B). This suggests that between 9 and 15 hours of stimulation, there is a massive repression of transcription where the induction of previously up-regulated genes is shut down while a great number of genes which were not previously differentially regulated are down-regulated. At these time-points, in addition to the genes *dot1l*, *setd7*, *ier5* and *adcyap1* which were mentioned above, found up-regulated after 9 hours is *hnrpll* (for heterogeneous nuclear ribonucleoprotein L-like) encoding a protein shown to play a role in mRNA splicing event (Wu et al., 2008).

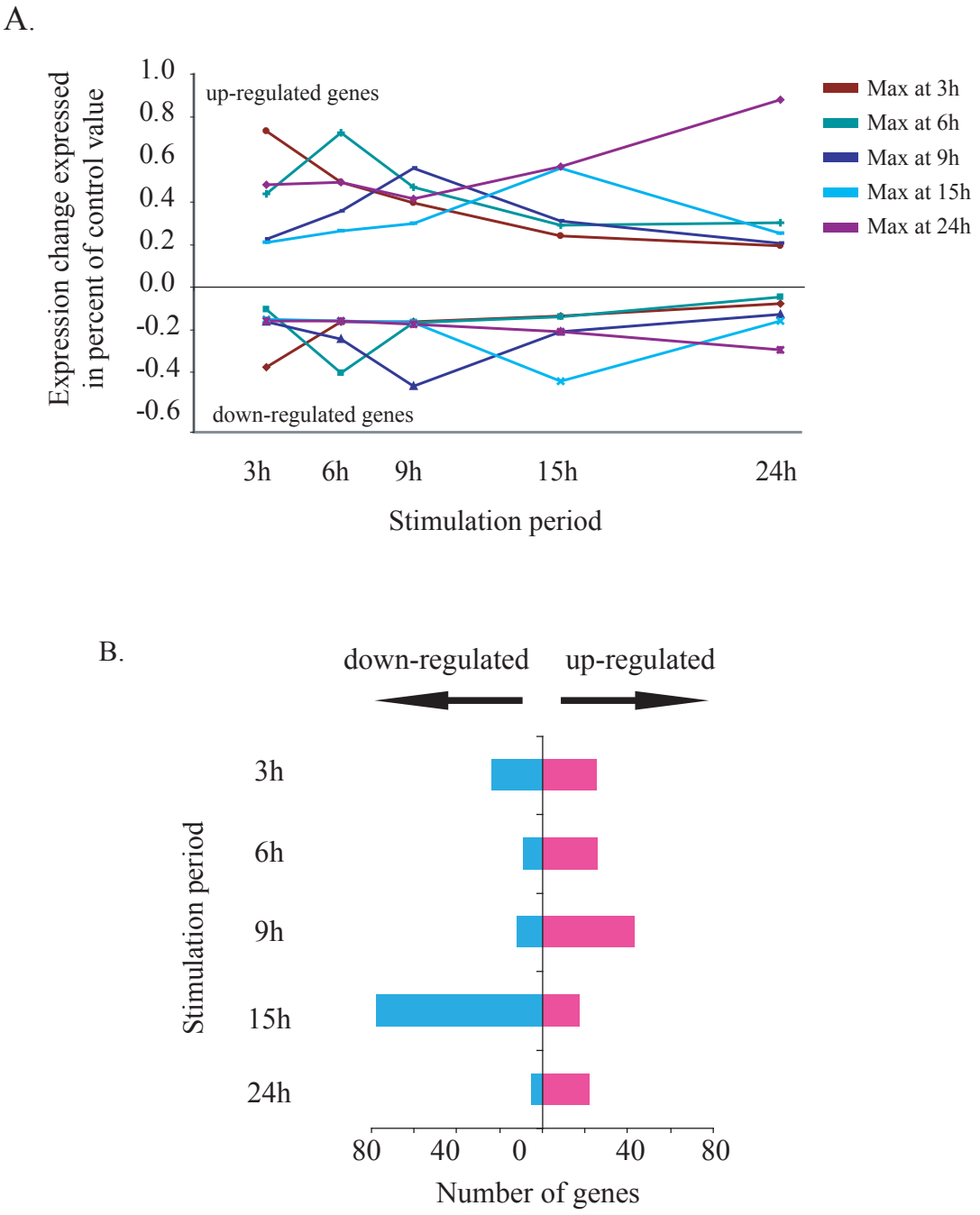

Figure 14. Temporal profile of gene regulation. A. Mean temporal profiles of gene expresion changes expressed in percent of control values across 24 hours of stimulation for clusters of genes that were grouped according to the time at which they showed maximal expression change relative to control for the list of up- and down-regulated genes. B. Number of down-regulated and up-regulated genes that are at their maximal level of regulation at the specified stimulation period.

f) Molecular network induced by whisker stimulation: identifying key molecular players in synaptic plasticity

In order to explore how the genes identified as regulated by whisker stimulation or their products are associated with one another and in the hope of identifying new molecular player in synaptic plasticity, we treated them as if they were all expressed within one hypothetical cell in layer IV of the barrel cortex and used Ingenuity Pathway Analysis to found and visualize known direct and indirect relationships between the genes and their products and allocate them to their cellular compartment. From the 261 regulated genes, 45 genes could be connected into a molecular network. Molecules on the schema were further color-coded according to the period of stimulation at which they showed maximal regulation (Figure 15).

From this network, two genes, *bdnf* and *egr2*, show a relatively important number of connections with the rest of the genes. In addition, they are both already maximally regulated at 3 hours and are connected to genes encoding proteins found at the plasma membrane and cytoplasm. For example, both *bdnf* and *egr2* are connected to *homer1* which is itself connected to *grik1* encoding the glutamate receptor kainate 1. These features underline that *bdnf* and *egr2* are most likely key players in experience-dependent plasticity. Both of them are known neuronal-activity induced genes and although *bdnf* has already been shown to play a crucial role in the ultrastructural modifications induced by whisker stimulation (Genoa et al., 2004) nothing is known about *egr2* in this context. Intriguing are the connections of *egr2* with proteins encoded by genes that are down-regulated after 15 hours (*mme*, *mag* and *s100a1*, encoding a calcium binding protein).

Noteworthy in Figure 15 is the regulation of *adcyap1* encoding the neuropeptides PACAP which is secreted in the extracellular space and connected by Ingenuity Pathway Analysis to the gene *pcsk1* encoding the prohormone convertase 1 (PCSK1 for proprotein convertase subtilisin/kexin type 1). PCSK1 is an enzyme implicated in the conversion of proPACAP into its two mature,

Figure 15 (on the right). Molecular network induced by whisker stimulation. The genes significantly regulated by whisker stimulation were connected into a network according to their known relationship using Ingenuity Pathway Analysis according to their database In this display all regulated genes were placed to be active within one hypothetical layer IV cortical cell. In addition they are represented into the cellular compartment where their encoded proteins are localized. Note that the color coding here pertains to the period of stimulation at which they were found maximally regulated and not to their level of expression. Out of the 261 genes, 45 could be interconnected. Of interest are BDNF and EGR2, respectively in the extracellular space and in the nucleus, which connect directly or indirectly with the highest number of genes and in the extracellular space are the neuropeptide adcyap1, connected to EGR2 and EGR3 and regulated by PCSK1, and INHBA, a growth factor which appears to activate a network independent from BDNF and ADCYAP1. Also to note are the genes down-regulated after 15 hours found in the nucleus, cytoplasm and plasma membrane. No genes maximally regulated after 24 hours are found in the nucleus. See text for a more detailed description on these points of interest.

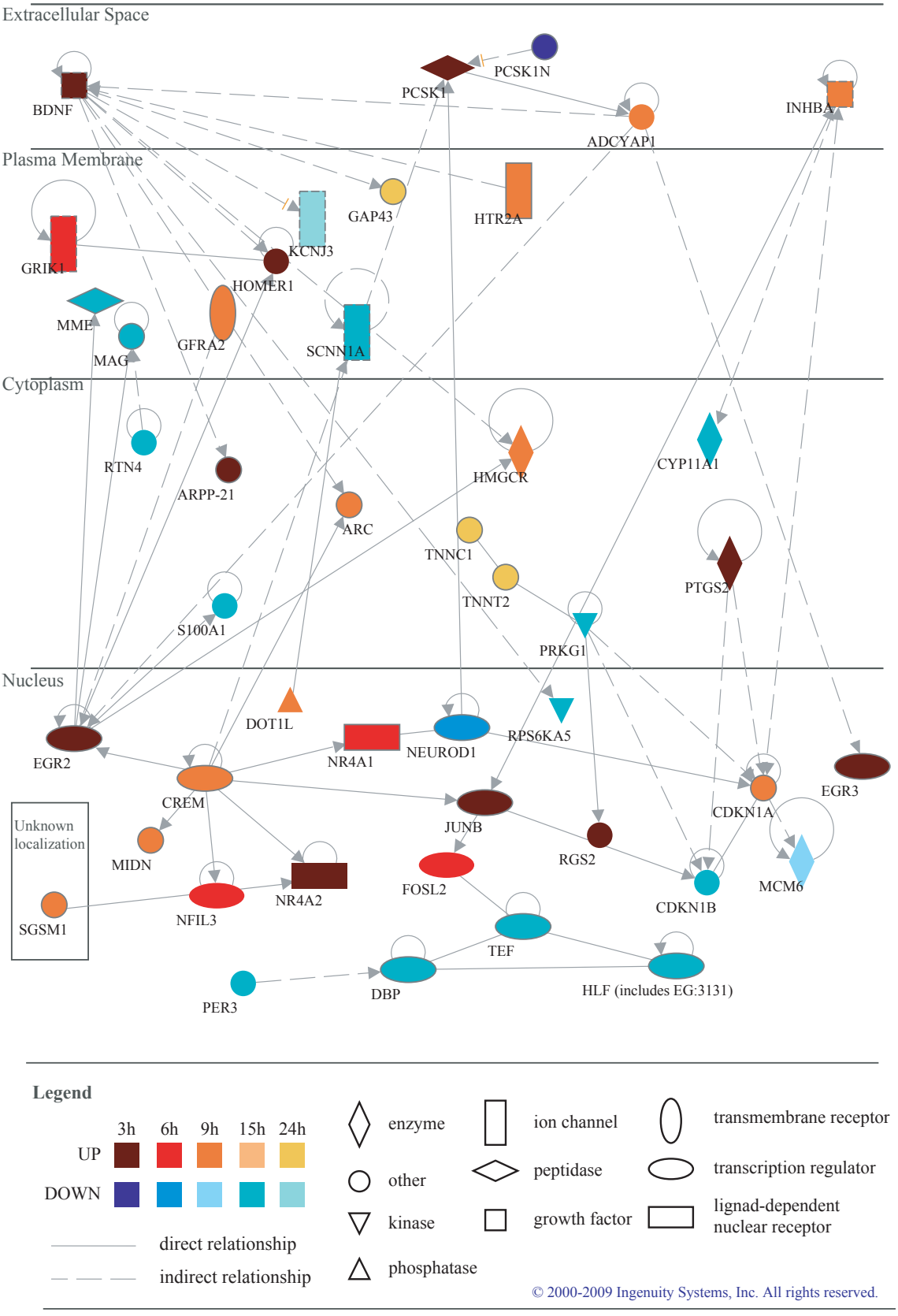

bioactive forms PACAP 27 and PACAP38, (Li et al., 1999). *Pcsk1* is up-regulated maximally at 3 hours and up to 6 hours of stimulation while the gene coding for its inhibitor, *pcsk1n*, is significantly down-regulated precisely after 3 hours. According to Ingenuity Knowledge Base, PACAP indirectly interacts with *egr2* and *egr3*, genes encoding transcription factors from the KROX transcription factor family. The up-regulation of *adcyp1* and *pcsk1* and the down-regulation of *pcskin1*, strongly suggest that the end-product of *adcyap1* would be expressed and active following whisker stimulation and play an important role in synaptic plasticity by activating the adenylate cyclase and thus the formation of cAMP, a key molecular player in long-term memory.

Another gene whose end-product is located in the extracellular space is *inhba*, encoding the growth factor activin, which is regulated as quickly as 3 hours after whisker stimulation and up to 9 hours. Activin was shown to be regulated by neuronal activity (Andreasson and Worley, 1995) and to increase the number of synapses and the length of dendritic spines in cultured hippocampal neurons (Shoji-Kasai et al., 2007).

Furthermore, to note in Figure 15 is the group of genes that are found down-regulated maximally after 15 hours; some in the nucleus, *per3*, *dbp*, *tef*, *hlf* which are mostly genes implicated in rhythmic processes and others found in the cytoplasm or at the plasma membrane such as *rnt4*, *mme*, *mag*, *scnn1a* and *prkg1*.

Finally, Figure 15 also points out that genes maximally regulated after 24 hours are located at the plasma membrane and in the cytoplasm and absent from the nucleus or from the extracellular space. This is further emphasized by comparing the known cellular distribution (according to Ingenuity Knowledge Base) of the proteins encoded by the genes found maximally regulated after 3 hours or after 24 hours (Figure 16). While 3 hours of whisker stimulation alter the expression of genes that encode mostly proteins localized in the cytoplasm or in the nucleus, most of the genes maximally regulated by 24 hours of whisker stimulation encode proteins located in the cytoplasm or at the plasma membrane.

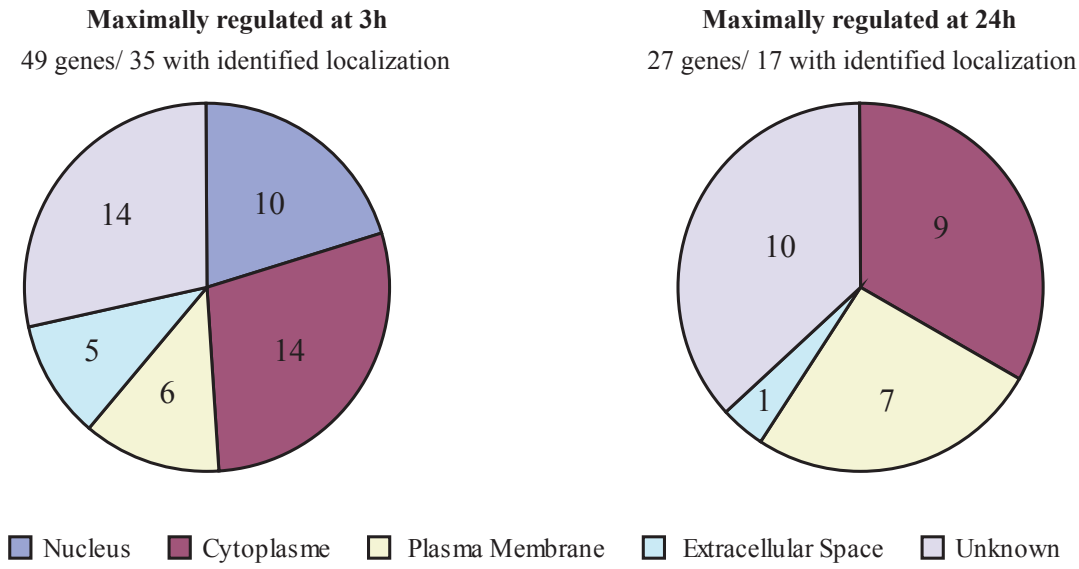

Figure 16. Comparison of cellular localization of the proteins encoded by the genes that were maximally regulated at 3 hours and maximally regulated at 24 hours. The number of genes per cellular compartment (written within the pie charts) is depicted as a fraction of the total number of genes per cluster. Cellular localization was attributed according to Ingenuity Knowledge Database. Note at 24 hours, the proportional decrease in «nuclear proteins» and the proportional increase in genes coding for cytoplasmic and plasma membrane proteins compared to 3 hours.

II.3b. Effect of a second exposure to whisker stimulation

To assess the effect of a second period of whisker stimulation on gene expression, a second set of analysis was done where some animals were kept after a period of 24 hours of whiskers stimulation and 4 days later, were restimulated for 6 hours.

In naïve mice, 6 hours of stimulation significantly regulates 111 genes, 84 are up-regulated and 27 down-regulated (Figure 17). In mice that underwent 24 hours of whisker stimulation, 4 days earlier, 6h of whisker stimulation induces a significant regulation of 410 genes, among which 77 are up-regulated and 333 down-regulated (Figure). Only 40 genes are found regulated after both events, among which *npas4*, *bdnf*, *crem*, *gap43* and *grasp*. Table 9 gives a selection of genes that were regulated in one or the other condition or in both and in the Appendix 10 is given the list of all the genes (page 133).

Among the top 10 genes that had shown the most alteration in their expression value in the time-course experiment and to be significantly expressed after 6 hours, 2 genes are no-longer significantly regulated after a second trial, *pcdh15* and *nr4a2*. *Nr4a2*, coding for a ligand-dependent nuclear receptor, shows a mark decrease in its expression change; being significantly regulated after 6 hours by 1.83 fold, its expression change after the second exposure is of 1.14

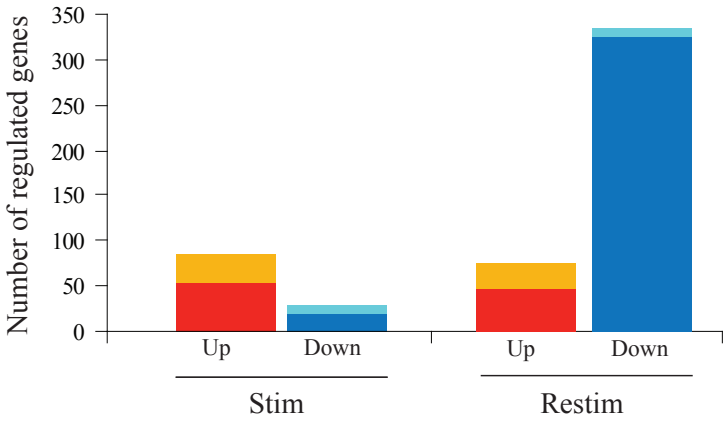

Figure 17. Number of genes significantly up- or down-regulated after 6 hours of whisker stimulation in naïve mice (Stim) and after 6 hours of whisker stimulation in mice that were exposed to 24 hours of stimulation 4 days earlier (Restim). Lighter color indicates the number of genes that are found regulated in both conditions (31 in the up-regulated genes and 9 in the down-regulated genes).

fold. Puzzling is *nptx2* which was shown to be up-regulated by 4.03 fold by 6 hours of whisker stimulation in the time-course analysis and which presents here a non-significant 1.9 fold change in the same condition. It is however found significantly up-regulated by 1.95 fold after restimulation. As the expression of this gene in the time-course experiment was found regulated only by the analysis that used IterPlier as the summarization algorithm, these differences in the fold changes may be due to a differential selection of the probe sets on which the gene value was based and may indicate that this gene undergoes substantial alternative splicing. For the other genes, the fold change values obtained after 6 hours of stimulation in the time-course analysis and in the restimulation analysis were similar.

Only induced in the first exposure to the stimulus are 71 genes, among which *adcyap1*, *egr3*, *nrn1*/*cpg15*, *homer1*, *pcsk1* and *grik*. Finally, 370 genes are induced by 6 hours of sensory stimulation only in animals that were already exposed to 24 hours of this sensory experience. Among these genes, 324 are down-regulated among which *grid1* encoding for the subunit delta 1 of the ionotropic glutamate channels, *sumo1* encoding the small ubiquitin-related modifier 1 which plays a role in postranslational modification and regulates many cellular processes among which gene transcription and spinogenesis (Muraoka et al., 2008; Chao et al., 2008), *gad1*, coding for GAD a limiting enzyme for the synthesis of GABA, and *rcor3*, coding for REST co-repressor 3. REST co-repressors are known to interact with the transcription factor REST (RE1 silencing transcription factor) and inhibit specifically neuronal gene expression in non-neuronal cells (Andres et al., 1999; Ballas et al., 2001; Abrajano et al., 2009). Among

Table 9. A selection of genes that were found significantly regulated in the restimulation paradigm.

Gene	Gene Name	FC 6h	FC Restim6h	raw p value	adj. p value
Only significant in naïve mice					
Abcb6	ATP-binding cassette, sub-family B (MDR/TAP), member 6	-1.33	1.05	0.00	0.02
Adcyap1	adenylate cyclase activating polypeptide 1	1.60	1.08	0.03	0.16
Egr3	early growth response 3	1.42	-1.04	0.04	0.17
Grik1	glutamate receptor, ionotropic, kainate 1	1.73	-1.06	0.00	0.10
Homer1	homer homolog 1 (Drosophila)	1.31	1.09	0.09	0.19
Nr4a2 *	nuclear receptor subfamily 4, group A, member 2	1.83	1.14	0.03	0.15
Nrn1	neuritin 1	1.33	-1.01	0.05	0.17
Pcdh15 *	protocadherin 15	1.34	1.19	0.24	0.29
Pcsk1	proprotein convertase subtilisin/kexin type 1	1.65	1.03	0.01	0.13
Only significant in mice that were already exposed to the stimulus 4 days earlier					
Dmp1	dentin matrix protein 1	1.07	-1.26	0.00	0.02
Gad1	glutamic acid decarboxylase 1	-1.05	-1.34	0.11	0.20
Grid1	glutamate receptor, ionotropic, delta 1	-1.05	-1.47	0.05	0.17
Hdac8	histone deacetylase 8	1.01	-1.38	0.04	0.17
Hebp1	heme binding protein 1	-1.16	1.32	0.00	0.03
Mag	myelin-associated glycoprotein	1.04	-1.51	0.00	0.03
Myt1l	myelin transcription factor 1-like	-1.11	-1.33	0.22	0.28
Nos2	nitric oxide synthase 2, inducible, macrophage	-1.06	1.37	0.05	0.17
Nptx2 *	neuronal pentraxin 2	1.90	1.95	0.61	0.63
Rcor3	REST corepressor 3	-1.01	-1.47	0.02	0.14
Sumo1	SMT3 suppressor of mif two 3 homolog 1 (yeast)	1.11	-1.83	0.03	0.16
Significant in both conditions					
Bdnf *	brain derived neurotrophic factor	3.42	1.98	0.02	0.14
Ccdc3 *	coiled-coil domain containing 3	1.86	1.66	0.27	0.32
Crem	cAMP responsive element modulator	1.41	1.38	0.89	0.89
Inhba	inhibin beta-A	1.60	1.59	0.70	0.72
Npas4 *	neuronal PAS domain protein 4	2.60	1.98	0.15	0.24
Ptgs2 *	prostaglandin-endoperoxide synthase 2	2.64	1.65	0.01	0.14
Scn7a *	sodium channel, voltage-gated, type VII, alpha	2.91	3.57	0.20	0.27
Sorcs3 *	sortilin-related VPS10 domain containing receptor 3	2.39	1.76	0.05	0.17
Tnnc1 *	troponin C, cardiac/slow skeletal	3.40	3.00	0.16	0.24

Statistical difference between expression changes after 6 hours of whisker stimulation in naïve mice and after 6 hours in mice that were 4 days earlier exposed to 24 hours of whisker stimulation was tested using Student's t-test (raw p value) and adjusted for false discovery rate using the Benjamini Hochberg method (adj. p value). In grey are the 4 genes for which adj. p value is ≤ 0.05. The star behind the gene names identifies genes that were part of the 10 most regulated genes in the time-course experiment.

the genes that appear up-regulated after the second exposure to 6 hours of stimulation (n=46) is *nos2* encoding for the inducible nitric oxide synthase 2. Nitric oxide is well known for its role in synaptic plasticity (reviewed in Garthwaite and Boulton, 1995). It was for example shown to play a role in spine innervations (Nikonenko et al., 2003; Nikonenko et al., 2008) and in the homeostatic control of the excitation-inhibition balance in the visual cortex (Le Roux et al., 2009). Interestingly, among the genes that could be identified to encode transcription regulators according to Ingenuity Knowledge Base, 8 are differentially regulated after 6 hours of stimulation in the naïve mice while 24 are differentially regulated after the second trial and only 4 genes overlap. Among the genes encoding transcription regulators that are differentially regulated only after the second trial, 18 are found down-regulated among which *hdac8*, coding for an histone deacetylase and *myt1l* encoding the myelin transcription factor 1 like. Among the genes encoding transcription regulators which are no longer regulated after the second trial is *egr3*.

Statistical differences in fold changes between the first exposure and the second exposure was calculated for the 481 genes that came out as regulated in one condition only or in both conditions (associated p value is given in the list of regulated genes). One hundred and thirty-five genes have a raw p value under 0.05. For 36 of them, their expression change relative to control was higher after a second exposure to stimulation while for 109 of them, their expression change relative to control was lower after the second exposition. However, once adjusted for multiple testing, only 4 remain statistically significant (*abcb6*, *hebp1*, *mag* and *dmp1*). For examples, both *mag*, encoding for myelin associated glycoprotein, and *dmp1*, for dentin matrix protein 1, are found significantly down-regulated after 6 hours in mice which were exposed to 24 hours of whisker stimulation 4 days earlier but not regulated after a single exposure to the stimulation. The list of all the genes that were identified as significantly regulated in at least one condition is given in the Appendix 10 (page 133) with their associated fold change values relative to control as well as the raw and adjusted p values associated with the Student t-test for comparison between a first and a second exposure to the stimulus.

II.4. Remarque and conclusion

The microarray analysis was performed on transcriptome that was extracted from laser microdissected barrels which are well delineated cortical structures in layer IV of the somatosensory cortex. This is to our knowledge the first time that a study on large-scale gene expression changes in response to sensory experience is restricted to this cortical layer and, as demonstrated by deoxyglucose study (Melzer et al., 1985), is restricted to the cortical columns that is activated by the altered sensory activity. Indeed, previous studies showed that the molecular, metabolic, structural and physiological changes induced by whisker stimulation are restricted to the barrels whose related whiskers are stimulated (Welker et al., 1989a; Welker et al., 1992; Rocamora et al., 1996; Knott et al., 2002; Quairiaux et al., 2007). This particularity of the barrelfield enabled the use of the adjacent barrel as control material and genes were considered regulated depending on the change in gene expression level relative to these internal controls who received normal sensory input. Out of precaution, the barrels used as controls were always at least one arc away from the stimulated barrels; i.e. the direct neighbors of the stimulated barrels were not taken. It is to note that, although previous studies failed to see any changes in the adjacent barrels, we cannot rule out that for some of the genes found to be altered in their expression by whisker stimulation, changes could actually be occurring within the barrels that received normal sensory input in response to the increased sensory activity occurring in the neighboring receptive fields. Only further experiments by in situ hybridization or immunohistochemistry will make this distinction possible.

By using microdissection technology in this well characterized sensory area, we have been able to compare samples who had received an increased sensory input with the ones that were driven by normal sensory input. Such effort enabled the identification of changes that are tightly coupled to the sensory activity at the periphery and, in addition, by favoring the internal control, we have limited the impact of other unforeseen variables such as the hormonal state of the animals, the general effect of exposure to magnetic field bursts, anesthesia and circadian rhythms. In this context, this study differs from others that used large scale gene expression screening. For example, transcriptomic analyses after monocular deprivation were performed on samples taken within the whole primary visual cortex containing all cortical layers and not only the deprived monocular zone but also the binocular zone which still receives visual input from the ipsilateral open eye and samples were compared to samples from control mice, or monkeys of the same age or to adjacent non-visual cortex (Lyckman et al., 2008; Tropea et al., 2006; Lachance and Chaudhuri, 2004; Majdan and Shatz, 2006).

Restricting the analysis to cortical layer IV has its importance as cortical plasticity is layer-specific; layer IV being generally recognized as less plastic than layer II/III (Diamond et al.,

1994; Glazewski and Fox, 1996) though this might depend on the type of sensory alteration that the animal experiences (Rema et al., 2006). However, the current study was not cell-specific and the molecular alterations observed arise from a mixture of cell types including various classes of neurons and glial cells which differ in their plasticity and their signaling cascade. *In situ* hybridization or immunohistochemistry will be necessary now not only to validate the regulation of the identified genes but also to determine their specific localization and cell-specificity. In addition, cells from layer IV are not only interconnected between each others but receive synaptic contacts from cells in the thalamus and from other cortical layers and make synaptic contacts with cells from layers II/III, thus, as mRNA can be translocated to the synapses, it is possible that some molecular changes identified here might be initiated or serve other cortical layers or subcortical stations.

It is also to note that this work is limited to changes at the transcriptional level and does not take into account all the modifications that occur at the post-translational level nor at the splicing level although these events are main components of the signaling cascades and play important role in synaptic plasticity. Phosphorlyation, for example, mediates the trafficking and the channel activity of the AMPA and GABA receptors (Song and Huganir, 2002; Luscher and Keller, 2004). The proteases, also, by cleaving specific synaptic proteins such as adhesion molecules, receptors, cytoskeleton components or signaling molecules into their mature active forms such as for proPACAP and proBDNF, have been shown to play a crucial role in synaptic plasticity (reviewed in Lee et al., 2008). Differential splicing or polyadenylation site usage also determines the localization, the stability of the mRNA and thus the function of the encoded protein. Finally, most recently, microRNAs (small non-coding RNAs) have emerged as new modulators in synaptic plasticity by regulating the translation of synaptic proteins (reviewed in Schratt, 2009). Hence, although, this study by using microarray technology gives a large overview of the transcriptional changes that are induced by sensory experience, it does not, by far, take into consideration all the molecular events that determine where and when the end-product of gene expression becomes functional; a matter crucial in understatnding how synaptic plasticity is taking place.

Despite its limitation, this study enabled the identification of a number of genes regulated in experience-dependent plasticity in the adult cerebral cortex. These genes were found to encode transcription factors (*egr2*, *npas4*, *ier5*, *crem*), growth factors (*bdnf*, *inhba*) and neuropeptides (*adcyap1*) that would be the main inducers of the transcriptional changes but also the identification of genes encoding effectors such as ion channels (*grik1*, *cacng2*, *scn7a*), cytoskeleton constituents or interacting molecules (*tnnc1*, *mylk3*) and adhesion molecules (*pcdh15*, *mag*). Intriguing are the up- regulation after 9 hours of *hnrpll* encoding for a molecule

which was shown to play an important role in mRNA splicing event (Wu et al., 2008), or of *dot1l* coding for an histone methyltransferase. Further investigation would be required to first know whether these genes are truly regulated by whisker stimulation and if so, to reveal their implications in synaptic plasticity.

Altogether, this study enabled the identification of unanticipated molecular players in experience-dependent plasticity induced in adult animals (e.g. *scn7a*, *rnt4*, *mag*, *dot1l*, *cacng2*, *mme*) as well as the striking down-regulation of genes after 15 hours which could not have been identified without large scale screening the transcriptional changes that are occurring across 24 hours of whisker stimulation. These points will be further developed in the following discussion.

Finally, by comparing the transcriptomic response to 6 hours of whisker stimulation occurring in naïve animals or in animals that were exposed to 24 hours of such sensory stimulation 4 days earlier, this study shows that 24 hours of whisker stimulation leave long-lasting traces in the cortical network that alter the transcriptomic response to subsequent similar sensory experience.

General Discussion

Twenty-four hours of increased sensory experience by whisker stimulation induces synaptic and physiological changes in the somatosensory cortex of adult animals and some of these modifications remain for at least 4 days after the stimulation period (Knott et al., 2002; Quairiaux et al., 2007). This study add to these observations by showing that the cortical network in layer IV of the somatosensory cortex in adult mice adapt to an increased sensory activity through successive step of structural and molecular changes that lead by 24 hours to long-lasting modifications of the circuitry (Figure 18). The long-lasting changes take place structurally by the addition of inhibitory synapses on dendritic spines. Prior to these changes, the excitatory synapses undergo substantial but transient reorganization which is observed through the temporary addition of excitatory synapses on dendritic shafts. At the molecular level these changes are orchestrated by a vast transcriptomic program composed of several phases of transcription with known neuronal activity-dependent transcriptional regulators and synaptic proteins being regulated within the first phases. These waves of transcription are followed by the striking down-regulation of a substantial number of genes among which cell adhesion molecules and known growth inhibitors (Figure 18). Finally, this study also shows that the modifications that have taken place within 24 hours leave long lasting traces that ultimately alter the transcriptomic response of the cortical network to a subsequent similar sensory stimulation when experienced 4 days later.

I. Discussion

I.1. About the experimental design

Plasticity was investigated by passively and continuously stimulating one or several whiskers by gluing a piece of metal on the whisker(s) and exposing the animals to bursts of magnetic field after recovery from anesthesia. In these respects, this experimental paradigm is of course far from representing a naturally occurring sensory stimulation. However, it does passively increase the sensory stimulation at the periphery and this in a manner that is incoherent with sensory activity of the neighboring whiskers and incoherent with the muscular control of the whisker follicles that is under the influence of the primary motor system. Electrophysiological recordings after 24 hours of whisker stimulation have shown that in addition to generally lower neuronal activity in the corresponding barrel, it also sharpens the receptive field of the neurons in the stimulated barrels (Quairiaux et al., 2007). Thus the cortical changes observed after 24 hours can be considered to serve two aspects of adaptation: one as an attempt to decrease neuronal activity and the other to refine the cortical network to maintain coherence in the neuronal activity. It is possible that the decrease in neuronal activity could be associated to desensitization (or habituation) to the stimulus while the refinement of the cortical network could be associated to increased discriminatory skills. However, no behavioral test has been performed after such passive stimulation and should be done in order to fully grasp the behavioral impact of the cortical modifications observed.

Although synaptic plasticity is known to be triggered by an altered neuronal activity and to depend on the coincidence in spike-timing between two neuronal partners (Bliss and Lomo, 1970; Bliss and Lomo, 1973; Artola and Singer, 1987; Bindman et al., 1988; Markram et al., 1997), it is for the moment not known, in our paradigm, which are the neuronal partners implicated in cortical plasticity. Plasticity could be driven by the thalamocortical afferents alone or may also involve afferents coming from layer VI which receive inputs from the thalamus and send axons to layer IV (Welker et al., 1996; Gheorghita et al., 2006; Pichon et al., 2008). Further experiment should be done to identify the neuronal partners implicated in the plastic modifications characterized in the current study.

It is to note that this study was designed to obtain an overview of the transcriptomic and structural modifications that are induced by an increased sensory activity in a well defined cortical area and for this reason, the electron microscopy study and the microarray analysis were both based on the identifications of the transcriptomic and structural modifications that are taking place within volumes of tissue. To this respect both techniques have the merit to gather many of the changes that are taking place within the volume of tissue sampled; i.e. it is not biased for specific

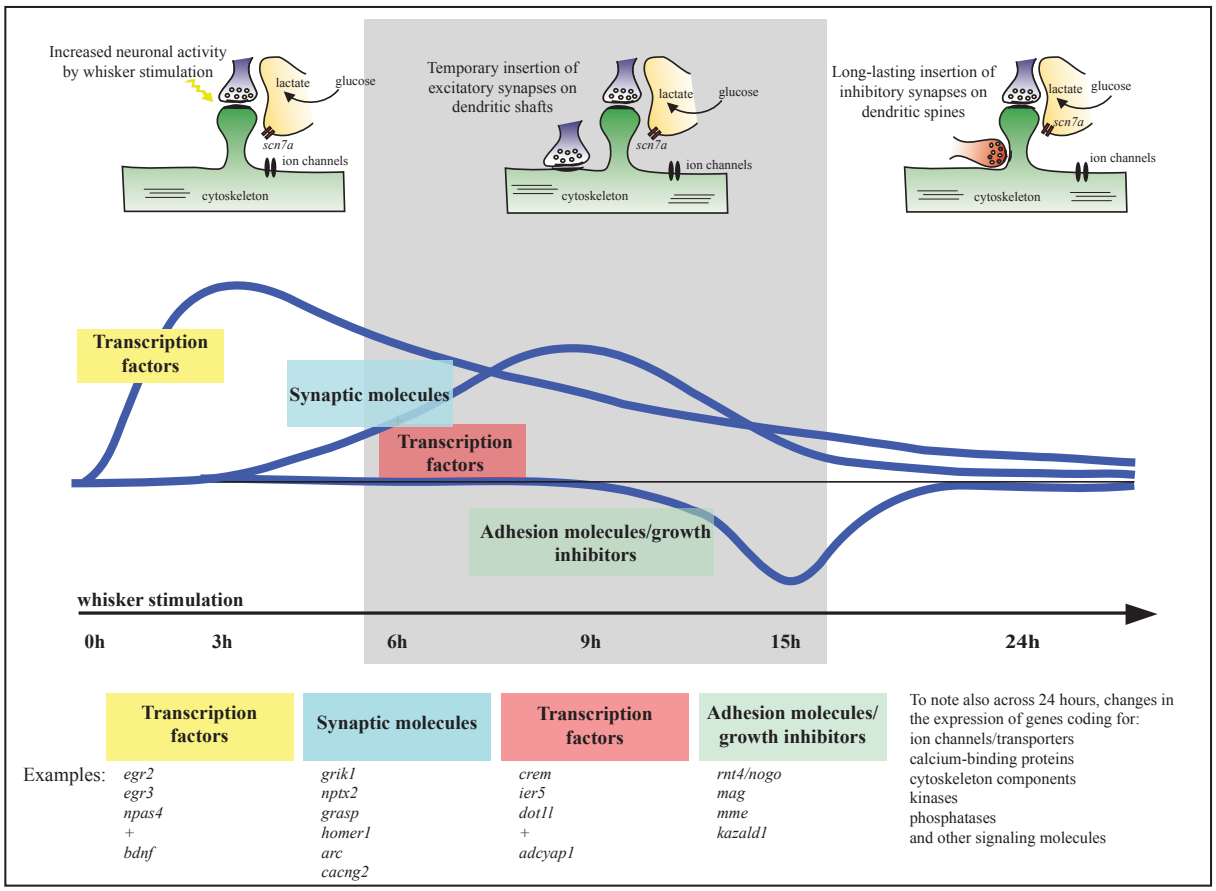

Figure 18. Temporal profile of experience-dependent changes in layer IV of the somatosensory cortex following whisker stimulation: a synthesis. Whisker stimulation induces a transient insertion of excitatory synapses (in blue) on dendritic shafts followed by the insertion of inhibitory synapses on dendritic spines after 24 hours of stimulation. This ultrastructural changes are paralleled by a vast transcriptomic program composed by several phases of transcription (for simplification only 2 are represented here) and a striking down-regulation of transcription after 15 hours. Each phase is characterized by the regulation of a particular set of genes which are believed to be important molecular players in experience-dependent plasticity.

subpopulation of synaptic contacts within the neuropil for the electron microscopy study or for specific key molecular player for the microarray analysis. However, this study does not enable to know whether these structural and molecular changes occur within particular subpopulation of cells, i.e. how they are taking place within the cortical network. It is for example not possible to know whether the temporary excitatory synapses are formed selectively on dendrites of excitatory or inhibitory neurons or on both cell types as it is not possible to know whether the molecular changes induced by the regulation of gene transcription would by targeted to specific synaptic contacts and if so in which ones. We also cannot rule out that some changes occurring in one cell population counterbalance modifications occurring in another cell population and, for this reason, remain unidentified. We also do not know whether the changes identified here also occur in other cortical layers or other cortical or subcortical areas.

In addition, we designed this experiment in order to describe the temporal profile of the molecular and structural changes triggered by sensory stimulation by characterizing the modifications that were induced after various stimulation periods. However, they remain snap-shots which were not successively taken from the same individuals and thus the correlation between the observed modifications is lost. It is for this reason not possible to know whether the inhibitory synapses are formed on previously existing or newly formed spines or whether the localization of the excitatory synapses inserted on the dendritic shafts is locally related to the insertion of the inhibitory synapses on the spines.

Despite its limitations, using this experimental paradigm we were able to identify new molecular players in experience-dependent plasticity and to point out several mechanisms underlying the formation of long-lasting traces in the cortical network. These could not have been identified without studying the temporal, structural and molecular aspects of experience-dependent plasticity and without doing so in a well characterized model of experience-dependent plasticity which is the whisker-to-barrel pathway.

I.2. Identification of new molecular players in experience-dependent plasticity: example of *scn7a*

One of the newly identified genes, in the context of experience-dependent plasticity, is the most regulated gene *scn7a* encoding for a glial sodium-sensitive sodium channel ($Na_{(x)}$). Interestingly, the supply of energy to the excitatory synapses through production of lactate occurs through a tight neuro-glia metabolic coupling initiated by the clearance of glutamate by the glial glutamate transporters GLAST and GLT1 and the sodium-dependent activation of the Na^+-K^+ ATPases which initiate glycolysis (for review see (Magistretti, 2009). GLAST and GLT1 have both been shown to be up-regulated at the protein level after 24 hours of whisker stimulation (Genoud et al., 2006b) and silencing *glast* by intracortical injection of RNA interference disrupt the increase in glucose utilization brought about by whisker stimulation (Cholet et al., 2001). SCN7A could be a new player in this neuro-glia metabolic coupling as it could be activated by the extracellular release of Na^+ triggered by the activation of the Na^+-K^+ ATPases from the excitatory synapse following activation. Its up-regulation after whisker stimulation may be necessary for re-establishing sodium homeostasis in the extracellular space and also to provide the required amount of energy to the neurons. Interestingly, in the subfornical organ, SCN7A was seen to be an activator of the glycolysis localized in astrocytic processes surrounding inhibitory neurons (Shimizu et al., 2007). Thus its precise localization within the somatosensory cortex should be investigated. If located in astrocytic processes surrounding inhibitory neurons, SCN7A could specifically provide to the inhibitory neurons the amount of energy that is required for their

increased level of activity brought about by continuous whiskers stimulation and be a limiting factor in their capacity to decrease the level of excitation brought about by such stimulation.

I.3. Plasticity of excitatory and inhibitory synapses

Genes directly related to excitatory synapses such as glutamate receptor (*grik*) or scaffolding proteins localized at the excitatory synapse (*homer*, *grasp*, *nrn1*/*cpg15*, *nptx2*) were found regulated within the first 3 or 6 hours of the sensory stimulation which is concomitant with the early modifications of the excitatory synapses seen at the ultrastructural level. Among these genes, the expression of one of them, *nrn1*/*cpg1*, was already shown in 4 weeks old mice to be maximally increased in the spared barrel and decreased in the deprived barrels 12 hours after clipping all whiskers from one whisker pad except one (Harwell et al., 2005). As in our results, 24 hours later its expression had returned to control level. Neuritin was shown in the developing Xenopus tectum to increase axonal growth rate and synapse maturation by recruiting AMPA receptors at the synapse (Cantallops et al., 2000). Similarly, protein encoded by *nptx2*, was shown to induce the clustering of AMPA receptors (Tsui et al., 1996; O'Brien et al., 1999; Xu et al., 2003). Also implicated in the trafficking of AMPA receptors is CACNG2, also known as TARP gamma-2 or stargazin, a glutamate receptor interacting protein which stabilizes AMPA receptors at the postsynaptic membrane by interacting with the scaffolding protein PSD-95 (postsynaptic density protein-95; (Bats et al., 2007). Thus, it appears that the proteins encoded by genes found up-regulated by whisker stimulation in the early phase of whisker stimulation have been shown to be implicated in the internalization (*homer*, *arc*) or the insertion (*nptx2*, *nrn1*/*cpg15*, *cacng2*) of glutamatergic receptors at the synapse concomitant with the finding that these synapses undergo structural reorganization quickly after the onset of the stimulation. In addition, it was shown that CACNG2 modifies the channel properties of the AMPA receptors (Osten and Stern-Bach, 2006; Morimoto-Tomita et al., 2009; Sager et al., 2009). Hence, the synaptic proteins encoded by the genes differentially regulated by sensory stimulation may not only be necessary for the structural reorganization of the excitatory synapses but, by altering the molecular composition of the synapse, may also directly alter its efficiency.

In contrast to excitatory system, no genes with a direct relation to inhibitory synapses (genes coding for GAD, GABA receptors, gephyrin). were found regulated across 24 hours of whisker stimulation At the protein level, the expression of the enzyme GAD (glutamic acid decarboxylase, a limiting enzyme for the synthesis of GABA) was shown to be increased after whisker stimulation but in this experiment the whiskers were stimulated for 4 days (Welker et al., 1989a) suggesting that a longer stimulation period might be required for considerably altering the expression of these genes. Also, the activity of GAD and of the GABA receptors are themselves tightly regulated by neuronal activity (Monnerie and Le Roux, 2008; Luscher

and Keller, 2004) and thus it is possible that for this reason no change at the transcriptional level would be required. Interestingly, we found, and show for the first time, that sensory stimulation induce the expression of *npas4*, and maximally so within 6 hours. NPAS4, was shown to be a transcriptional factor regulated in cultured hippocampal neurons by depolarization and required for the development of inhibitory but not excitatory synapses (Lin et al., 2008). In addition Lin et al., combining microarray screening and RNA interference strategy to knock down the expression of *npas4* in depolarized 7 days old cultured cortical neurons, found that the majority of the activity-dependent genes were up-regulated in the absence of NPAS4 suggesting that NPAS4 may not only be a transcriptional activator but also a transcriptional repressor (Lin et al., 2008). This suggests that NPAS4 and thus the formation of inhibitory synapses may be linked to the transcriptional shut-off observed after 15 hours of sensory stimulation. Identifying which cell population expresses the gene *npas4* and the genes for other transcriptional factors following the increased sensory stimulation would help clarify how plasticity of the inhibitory synapses is related to the plasticity of the excitatory ones. Interesting is that NPAS4 was found predominantly in excitatory neurons (Lin et al., 2008) suggesting that the plasticity of these two neuronal populations are intrinsically interconnected.

I.4. Down-regulation of transcription: a common mechanism mediating memory formation in adult CNS?

Fifteen hours of sensory stimulation was characterized by the down-regulation of a vast number of genes. A general down-regulation of transcription has already been reported in microarray studies also oriented in determining the temporal profile of gene expression following learning tasks where it was observed in the dentate gyrus of adult rats 12 hours after a passive avoidance learning task and in the hippocampus of adult mice 6 hours after trace fear conditioning (O'Sullivan et al., 2007; Sirri et al., 2010). These considerations suggest that down-regulation of transcription is a common mechanism and could be a necessary event in the formation of mnesic traces in adult animals.

Among the genes that were found down-regulated at this time were genes coding for adhesion molecules. These molecules mediate cell-cell interactions or cell interactions with the extracellular matrix and are also important in mediating intracellular signaling cascades (for review see Dalva et al., 2007). When located at the synapse, these molecules play an important role in synapse consolidation and their down-regulation observed precisely at 15 hours may be associated with the destabilization of synaptic contacts. In addition, among the other genes that were found down-regulated precisely at that time were genes encoding the myelin-associated growth inhibitors MAG and NOGO. Both of them are ligands for NOGO receptors. The activation of these receptors is known to limit axonal regeneration in adults (Huber and Schwab, 2000).

The transcript for NOGO receptors was shown to be down-regulated in adult rats after exposure to kainic acid or to running wheels (Josephson et al., 2003). In addition, electrophysiological recordings show that mutant mice for this receptor undergo ocular dominance plasticity even at 4 months of age while this form of plasticity is limited to the critical period in wild-type mice (McGee et al., 2005). Interesting is that the formation of myelin is developmentally regulated: in the mouse somatosensory cortex, the first myelinated axons appears in layer VI at P11 while by P32, their abundance and the thickness of the myelin sheaths have reached adult values throughout all cortical layers (De Felipe et al., 1997).

Coincident with the down-regulation of gene expression at 15 hours is the significant higher level of expression for genes whose end-products are implicated in the development of the nervous system. All of them are seen up-regulated at earlier time-points among which *bdnf*, *gap43* and *nrn1*/*cpg15* which are known to induce neurites outgrowth. Hence 15 hours may represent an important temporal event in the process of experience-dependent plasticity in the adult brain where specific circuitry-stabilizing molecules are lowered at a time when growth inducing factors are expressed. Importantly, by 24 hours most genes that were down-regulated at 15 hours have returned to control level suggesting that this event is limited to a specific temporal window. This may preserve the integrity of the circuitry and result in the formation and stabilization of the newly formed synapses as suggested by the maintenance of the inhibitory synapses on spines 4 days post whisker stimulation (Knott et al., 2002).

The precise timing of the transcription shut-off may provide a permissive molecular and structural environment for circuitry reorganization, which may be especially favorable to the plasticity of inhibitory neurons. Indeed, neurons, but especially the inhibitory ones, during development become progressively surrounded by a perineuronal net formed by the condensation of chondroitin sulphate proteoglycans, a component of the extracellular matrix. This event coincides with the closure of the critical period in the visual cortex while the removal of this perineuronal net by intracortical injection of chondroitinase in adult rats (P>100) is sufficient to reactivate ocular dominance plasticity (Pizzorusso et al., 2002). This suggests that inhibitory neurons might be particularly sensitive to the specific pattern of gene expression that characterize 15 hours of stimulation and that these modifications might be a prerequisite for the insertion of the inhibitory synapses on spines seen to take place between 18 and 24 hours of whisker stimulation.

Down-regulation of genes coding for protein mediating cell-cell adhesion would most likely also affect the excitatory circuitry and such phenomena might be associated with the increased spine turn-over that is reported to occur when neuronal activity is altered by trimming whiskers

in a chessboard pattern (Trachtenberg et al., 2002). Also spine motility is highest when cortical receptive fields are most plastic and decreases with age (Lendvai et al., 2000; Grutzendler et al., 2002; Holtmaat et al., 2005). To this respect, excitatory synapses on shafts have been associated to the appearance and disappearance of spines (Fiala et al., 1998; Marrs et al., 2001; Hasbani et al., 2001; Ovtscharoff Jr. et al., 2008). Thus it is possible that the transient excitatory synapses seen to occur on dendritic shafts after 6 and 18 hours of whisker stimulation might be the structural landmark of the pruning of old spines and the formation of new spines that would be facilitated by altering cell-cell adhesion properties. The regulation of genes coding for Ca^{2+}-dependent cytoskeleton associated proteins such as *tnnc1* and *mylk3*, most known for their role in cardiac contraction, and the regulation of *arc* coding for an activity-regulated cytoskeleton-associated protein might sustain such structural reorganization. Their specific localization within the cortical network should be investigated.

Interestingly, we show that 79 genes that are differentially regulated by whisker stimulation were also found regulated in the visual system following monocular deprivation during the critical period (Tropea et al., 2006; Lyckman et al., 2008; Majdan and Shatz, 2006; Lyckman et al., 2008) but the sense of regulation of 59 of them (among which *bdnf*, *adcyap1*, *dot1l*, *grasp*, *homer*, *egr2*, *egr3*, *tnnc1*, *mme*) was found to be reversed. The critical period in the visual cortex is a developmental period during which the neuronal network is highly plastic and becomes stabilized with normal sensory experience. This phase is associated with transcriptomic changes and monocular deprivation during this critical period reverse the expression pattern of the genes associated with this developmental period (Lyckman et al., 2008).

Altogether, these considerations suggests that the elevated neuronal activity induced by passive whisker stimulation differentially regulates certain genes that are normally associated with the maturation of the cortical network and that in adult animals, plasticity is not solely mediated by the up-regulation of growth-mediating factors but also by the down-regulation of genes that are important for the structural stabilization of the neuronal network that comes with the maturation of the brain.

Finally, these considerations also point to the importance of cell-cell adhesion and of the cellular matrix in the structural stabilization of the neuronal network and in mediating cell-cell interactions, a critical issue in cortical plasticity (Matsumoto-Miyai et al., 2009; Dalva et al., 2007; Berardi et al., 2004).

I.5. Rhythm in synaptic plasticity

Studying the temporal profile of the molecular and structural changes induced by sensory stimulation revealed that changes occur in a series of successive events that are temporally regulated. This is particularly striking for gene expression. Indeed, in addition to reveal molecular candidates underlying synaptic plasticity, looking at the transcriptional changes across 24 hours of whisker stimulation revealed that transcription is tightly controlled and that neuronal activity induces several waves of transcription with each stimulation period analyzed being characterized by a set of genes that are maximally regulated at that time. For simplification, this can be summarized into 4 main phases (see Figure 18). The first one is characterized by a set of genes that are maximally expressed by 3 hours of stimulation and which contains known neuronal activity-dependent genes (*egr2*, *egr3*, *npas4*, *bdnf*, *homer1*). This is followed by another wave of transcription which may peak after 6 or 9 hours and is associated with the regulation of genes encoding synaptic proteins relevant to the excitatory synapses (*grik1*, *cacng2*, *grasp*) and the regulation of genes that regulate gene expression either directly or indirectly (*ier5*, *crem*/*icer*, *dot1l*, *adcyap1*). This second phase is followed by the striking down-regulation of genes after 15 hours. Finally, by 24 hours, most genes that were down-regulated in the previous phase have returned to control values.

Genes related to the control of the circadian rhythms were found regulated in response to whisker stimulation. As we have designed the experiment so that all animals were sacrificed at the same time in their day/night cycle and have used an internal control to identify the genes regulated by the sensory stimulation, it is unlikely that this simply reflects the oscillating regulation of transcription that is associated with the daily (circadian) rhythm but instead suggests that the temporal regulation of transcription initiated by the increased sensory stimulation shares common mechanisms with the control of the circadian rhythms. This is not surprising as light, a major regulator of the circadian rhythm, is in itself a sensory stimulus to which all living organisms have to adapt.

Interesting in this context is that circadian rhythms depend on the rhythmic synthesis of genes which is controlled by a transcriptional negative feedback loop where transcription activated by transcription activators induces their own repression by increasing the expression of transcription repressors. One of the many molecular players in this negative auto-regulatory loop is cAMP and the gene *crem* (Foulkes et al., 1997). Increase in the cAMP intracellular level, which peaks during the second part of the night in the pineal gland, activates the cAMP-dependent protein kinase (PKA) which phosphorylates the constitutively expressed transcriptional factor CRE-binding protein (CREB) increasing its transcriptional activity. Phosphorylated CREB binds to an alternative cAMP-inducible promoter within the crem gene which generates the inducible

cAMP early repressor (ICER). By competing with CREB for the CRE-binding site, ICER represses the transcription of CREB-activated genes in a concentration-dependent manner thus generating a negative auto-regulatory loop. *Crem* is found differentially regulated after whisker stimulation as well as the gene *adcyap1* coding for the pituitary adenylate cyclase activating peptide (PACAP). This suggests that this negative auto-regulatory loop could contribute to the down-regulation of gene transcription which is striking 15 hours after whisker stimulation. Icer was shown by immunohistochemistry to be up-regulated in the barrel cortex in an experiment where rats could explore overnight an enriched environment with all whiskers from the right side of the snout clipped except one (Staiger et al., 2000). However, within 24 hours of whisker stimulation, at least 19 transcription regulators are differentially regulated and all of them show very distinct temporal expression profile suggesting that crem and cAMP are probably not the only molecular players in this tight temporal regulation of transcription but that it is orchestrated by the subtle regulation of a series of transcription activators and transcription repressors that is initiated by the increased sensory activity.

The activation of a negative auto-regulatory loop to stop the transcription of the neuronal activity-dependent genes would probably also result in the down-regulation of constitutively transcribed genes which in the mature cortex would be important in the maintenance and stabilization of the cortical network. This is suggested by the down-regulation of adhesion molecules and growth inhibitors after 15 hours and maybe a prerequisite to the formation of the inhibitory synapses on spines as mentioned above. Altogether, these considerations suggest that a tight balance between transcriptional activators and repressors are necessary for the formation of long-lasting traces in the network.

I.6. Effect of prior experiences on gene expression

The great difference between the gene expression pattern after 6 hours of whisker stimulation in naïve mice or in mice exposed to such stimulus 4 days earlier shows that the changes that have occurred within the first 24 hours have left long-lasting traces that alter the transcriptomic response of the neuronal network to subsequent similar sensory experiences. After a second exposure, some plasticity-related genes are up-regulated such as *bdnf*, *nos2*, *inhba* while genes coding for known myelin-associated growth inhibitors are down-regulated (*mag*, *mobp*) while other genes are no longer regulated by the stimulus (*homer*, *grik*, *egr3*, *adcyap1*). This suggests that a second exposure to a stimulus might elicit substantial reorganization of the network but which might differ from the reorganization triggered by the first exposition to the stimulus. Concomitant with this idea, it was shown that prior monocular deprivation during adulthood makes the visual cortex more susceptible to subsequent monocular deprivation as the ocular shift induced by a second period of deprivation was faster and more persistent than after the

first exposure (Hofer et al., 2006a). In addition it was shown that although the first exposure to monocular deprivation increased spine dynamics, this was no more the case after the second (Hofer et al., 2009). Also, whisker and monocular deprivation performed early during the development were shown to alter the response to subsequent similar sensory experience when experienced during adulthood (Akhtar and Land, 1991; Hofer et al., 2006a). This suggests that the modifications induced by whisker stimulation may persist well beyond 4 days as investigated here. The importance of the identified transcriptomic differences between a first and a second exposure to an increased sensory stimulation should now be further investigated and this also at the ultrastructural level or at the electrophysiological level. Reversely, characterizing the structural changes that occur after a second exposure would give clues on the function of the genes found regulated in one or the other condition.

One remaining question is the nature of the transcriptomic difference between the first and the second exposure to the stimulus. It was already shown that 24 hours of whisker stimulation leaves long lasting traces in the circuitry as inhibitory synapses on spines are found increased 4 days after the end of 24 hours of whisker stimulation (Knott et al., 2002) and the neuronal activity remains altered as shown by electrophysiological recordings (Quairiaux et al., 2007). Also 4 days after 24 hours of whisker stimulation, the gene expression is already altered relative to control barrels (data not shown). These considerations alone could explain the differential expression pattern between 6 hours of stimulation in naïve mice and subsequent stimulations. However, the identification of the regulation of genes coding for histone methyltransferases (*dot1l* and *setd7*) or kinase (*rps6ka5*) suggests that epigenetic mechanisms could be involved in these long-term effects. Indeed, the regulation of chromatin structure through post-translational modifications of histone by phosphorylation or methylation is part of epigenetic mechanisms known to produce long-lasting changes in pattern of gene expression and to be implicated in memory formation (Levenson and Sweatt, 2006). The possibility and the importance of such mechanism and its link to the plasticity of the synapse should be further investigated.

I.7. Plasticity of excitatory synapses: a prerequisite for plasticity of inhibitory synapses and long-term plasticity?

Electrophysiological recordings in cultured hippocampal neurons had previously shown that 12 hours of pharmacological treatments (using bicuculline or flunitrazepam to respectively block or potentiate GABAa receptors or NBQX to block AMPA receptors) were required to modify synaptic efficiency but stabilization of the functional balance between inhibition and excitation was reached only after 24 hours (Liu, 2004). In addition, clinical and experimental observations on memory showed that memory is formed in at least two stages and that it first persists in a fragile state and consolidate over time (reviewed in McGaugh, 2000). Concomitant with these

observations, our results at the structural level show that following a new sensory stimulation, cortical circuitry undergoes successive phases of reorganization with a first phase of transient modifications through the addition of excitatory synapses on dendritic shafts and a second phase with the addition of inhibitory synapses on spines. This particular type of synapses were shown to remain 4 days after the cessation of the stimulus (Knott et al., 2002). This suggests that the addition of excitatory synapses on dendritic shafts may be a transient phase in memory formation and underlie short-term memory while the addition of inhibitory synapses may be the substrate for long-term memory. Concomitant with this idea, the synthesis of BDNF which was shown to be necessary for the formation of the inhibitory synapses on spines following whisker stimulation (Genoud et al., 2004) was shown to be required 12 hours after an inhibitory avoidance task for the persistence of memory (Bekinschtein et al., 2008).

From the molecular and structural observations, it appears that an increased sensory activity rapidly modifies the excitatory synapses at both the structural and molecular level, while the plasticity of the inhibitory synapses is delayed. Such delay in the maturation of the inhibitory synapses compared to the development of the excitatory synapses was observed at the structural level during development of the somatosensory cortex between postnatal day 15 and 20, a period characterized by an increased sensory activity when the animals start to actively use their whiskers (Micheva and Beaulieu, 1996). Also, electrophysiological recordings of the binocular response of excitatory and inhibitory neurons in mice after monocular deprivation during the critical period showed that while excitatory neurons had already shifted their response towards the non-deprived eye after 2 days of monocular deprivation, 4 days were necessary for the inhibitory cells to shift their response (Gandhi et al., 2008). In accordance with our findings, these observations show that plasticity of the inhibitory circuitry is generally preceded by plasticity of the excitatory synapses.

Interesting is that the level of neuronal activity is an important factor in determining plasticity and this also for the plasticity of the neurons in cortical layer IV. Indeed, removing all whiskers but one past a critical period induces no clear sign of plasticity in layer IV even after 60 days of deprivation (Glazewski and Fox, 1996) while plasticity of layer IV cortical neurons is observed in adult rats 3 days after whisker-pairing, an experimental paradigm in which all whiskers are clipped except two adjacent whiskers (Diamond et al., 1993) and 15 hours of whisker pairing is sufficient to induce plasticity if the animals can explore an enriched environment (Rema et al., 2006).

II. Conclusions and Perspectives

Twenty-four hours of continuous whisker stimulation was shown to induce synaptic and physiological changes in the somatosensory cortex of adult animals (Knott et al., 2002; Quairiaux et al., 2007). Here, by studying the temporal, molecular and structural aspects of experience-dependent plasticity in layer IV of the somatosensory cortex, we were able to show that whisker stimulation triggers a series of successive cellular processes that lead within 24 hours to long-lasting changes in the cortical network. First part of this thesis showed that structural modification of the circuitry occurs in two phases, first a temporary increase in excitatory synapses on dendritic shafts between 6 and 18 hours of stimulation which is followed by the insertion of inhibitory synapses on spines that shifts the balance between excitation and inhibition by 24 hours. In the second part of this thesis, we show that whisker stimulation regulates a vast transcriptional program in layer IV of the somatosensory cortex and that this change in gene expression is precisely temporally regulated. Particularly striking is at 15 hours the down-regulation of a vast number of genes among which genes coding for cell adhesion molecules and growth inhibitors. Finally, we show that exposure to 6 hours of whisker stimulation 4 days after 24 hours of such stimulation considerably alter the transcriptomic response in comparison to 6 hours of whisker stimulation in a naïve animal, showing that 24 hours of whisker stimulation leave long lasting changes in the cortical network that modify the response to subsequent stimulation.

From these results and taken into considerations all the various observations discussed above, it appears that an increased neuronal activity would first initiate plasticity of the excitatory synapses. Plasticity of the excitatory synapses then, through the vast and tightly regulated transcriptomic program that they initiate and their transient insertion on dendritic shafts, would give the appropriate conditions for plasticity of the inhibitory neurons to be induced. This in turn would lead to the insertion of inhibitory synapses on spines. Plasticity of the inhibitory neurons, which are known for their crucial role in shaping the receptive fields (Dykes, 1997), would in this way leave long lasting traces in the cortical network to fine tune the properties of the neurons in accordance to past sensory experiences.

This hypothesis leads to several points and questions that could initiate new experiments. First of all, the genes found to be regulated in the microarray analysis should be confirmed and their distribution within the cellular population identified. Particularly interesting would be the localization of the transcription factors in order to determine whether plasticity of the excitatory and inhibitory neurons are truly interconnected or instead function as two independent processes. Also, the gene found most regulated by whisker stimulation code for a sodium-sensitive sodium channel expressed specifically in glial cells. Determining whether whisker stimulation differentially alter the expression of other genes within this cell population and

through which transcriptomic program would give further insight on the importance of these cells in experience-dependent plasticity. Also, the cellular distribution of synaptic proteins and cytoskeleton constituents encoded by the regulated genes should be investigated. As they might be located to the "active" synapses as the activity-regulated cytoskeleton-associated protein ARC, they might help locate within the network the site of synaptic plasticity.

One main point for the moment unanswered is whether the insertion of the excitatory synapses on dendritic shafts is the landmark of increased spine turn-over. Also unknown is whether the inhibitory synapses on spines are formed on new spines or on already existing spines and whether these synapses replace the excitatory synapses that are transiently formed on the dendritic shafts. Answering these questions would give a better insight on the link between the plasticity of excitatory synapses and inhibitory synapses and also on the link between short-term memory and long-term memory. For this, spine dynamic should be investigated. However, for the moment the investigation of the dynamic of spines *in vivo* using time-lapse two-photon microscopy has been restricted to the upper layers of the cortex due to technical limitations (Lendvai et al., 2000; Trachtenberg et al., 2002; Holtmaat et al., 2005; Zuo et al., 2005). Considering this point, plasticity following whisker stimulation should also be investigated in cortical layers I and II/III so to be combined with *in vivo* imaging. This would also enable comparisons with other studies on experience-dependent plasticity which are mainly performed in these supragranular layers. Spine dynamic could also be assessed by measuring morphometric properties of the spines; for example the ratio surface to volume was shown to be higher for newly formed spines (Knott et al., 2006). However, a direct link between excitatory synapses on shaft, spine formation and inhibitory synapses would still be missing. Considering the importance of the inhibitory synapses on spine in experience-dependent plasticity, their physiological function as well as their role in spine dynamic and their link to memory consolidation should be further investigated. However, considering their small prevalence, forming only 6% of the total number of synapses present in the neuropil, this would represent another challenge.

Our study showed that a vast transcriptomic program is initiated by whisker stimulation and that long-lasting modification of the circuitry may depend on a tight balance between transcriptional activators and repressors. So one question would be whether altering this balance would alter the formation of long-lasting changes in the network and more precisely alter the formation of the inhibitory synapses on spines. Also, it is known that the memory of newly learned information is disrupted by the learning of other information shortly after the original learning (McGaugh, 2000). The following question would be whether this tight regulation of transcription and the formation of inhibitory synapses is altered by the presentation of a new sensory stimulation. Answering these questions would give stronger arguments for proposing the inhibitory synapses

on spines as the structural substrate of mnesic traces. It would also give further insight on the importance of sleep (or a phase of low sensory stimulation) in memory.

For the moment we have investigated experience-dependent plasticity through the application of a continuous sensory stimulus but we do not know what would be the minimal duration of whisker stimulation required to induce long-lasting modifications of the cortical network. Is the initiation of the transcriptomic program seen after 3 hours or the insertion of the excitatory synapses on the shaft sufficient to induce long-lasting traces or does the stimulus need to be continued until 15 hours? Also, it is probable that the minimal amount of time required to leave long-lasting changes would depend on the strength of the sensory stimulus or its association with a noxious stimulus as in fear conditioning experiment. Testing how this parameter influences the transcriptomic and structural programs initiated by whisker stimulation would give further insight on the mechanisms leading to experience-dependent plasticity.

Changes induced by 24 hours of whisker stimulation alter the transcriptomic response when the animals are stimulated for a second time. Investigating the structural changes that are induced after a second exposure would now be required to understand the significance of this transcriptomic differences. We have shown that genes coding for histone methyltransferase were regulated by whisker stimulation, a strong indication for the implication of epigenetic phenomena in experience-dependent plasticity. These lead to several questions: “Are the inhibitory synapses on spines sufficient to alter the response to a second period of stimulation or does it require long-term modification of the chromatin structure? How are these two components linked to one another to leave in the cortical network long lasting traces of past sensory experiences? Can one persist without the other?”

Finally, one major finding in this study is that an increased sensory stimulation, although passive, rapidly induces plastic changes in the adult cortex which is associated with the up-regulation of growths factors and the down-regulation of myelin-associated growth inhibitors known to inhibit axonal regeneration in the adult central nervous system. This strongly underlines that a new sensory stimulation, even passive, could be of a great therapeutically tool in neuro-rehabilitation. The whisker-to-barrel pathway could be of a great advantage in testing the impact of sensory stimulation in rehabilitation after neuronal damage. In addition, considering the vast amount of genes differentially regulated by whisker stimulation that are linked to neurological disorders, elucidating their role in our model of experience-dependent plasticity should considerably increase the current understanding of the diseases. It may also help evaluate the impact of sensory stimulation, deprivation or overstimulation in the induction and prevention of these diseases.

References

Abrajano JJ, Qureshi IA, Gokhan S, Zheng D, Bergman A, Mehler MF (2009) REST and CoREST modulate neuronal subtype specification, maturation and maintenance. PLoS One 4: e7936.

Affymetrix (2005a) Gene Signal Estimates from Exon Arrays. Affymetrix Whitepaper.

Affymetrix (2005b) Technical Note: Guide to Probe Logarithmic Intensitiy Error (PLIER) Estimation. Affymetrix Whitepaper.

Agmon A, Yang LT, O'Dowd DK, Jones EG (1993) Organized growth of thalamocortical axons from the deep tier of terminations into layer IV of developing mouse barrel cortex. J Neurosci 13: 5365-5382.

Aid T, Kazantseva A, Piirsoo M, Palm K, Timmusk T (2007) Mouse and rat BDNF gene structure and expression revisited. J Neurosci Res 85: 525-535.

Akhtar ND, Land PW (1991) Activity-dependent regulation of glutamic acid decarboxylase in the rat barrel cortex: effects of neonatal versus adult sensory deprivation. J Comp Neurol 307: 200-213.

Al Shahrour F, Carbonell J, Minguez P, Goetz S, Conesa A, Tarraga J, Medina I, Alloza E, Montaner D, Dopazo J (2008) Babelomics: advanced functional profiling of transcriptomics, proteomics and genomics experiments. Nucleic Acids Res 36: W341-W346.

Al Shahrour F, Minguez P, Tarraga J, Medina I, Alloza E, Montaner D, Dopazo J (2007) FatiGO +: a functional profiling tool for genomic data. Integration of functional annotation, regulatory motifs and interaction data with microarray experiments. Nucleic Acids Res 35: W91-W96.

Alberini CM (2009) Transcription factors in long-term memory and synaptic plasticity. Physiol Rev 89: 121-145.

Allard T, Clark SA, Jenkins WM, Merzenich MM (1991) Reorganization of somatosensory area 3b representations in adult owl monkeys after digital syndactyly. J Neurophysiol 66: 1048-1058.

Aloy EM, Weinmann O, Pot C, Kasper H, Dodd DA, Rulicke T, Rossi F, Schwab ME (2006) Synaptic destabilization by neuronal Nogo-A. Brain Cell Biol 35: 137-156.

An JJ, Gharami K, Liao GY, Woo NH, Lau AG, Vanevski F, Torre ER, Jones KR, Feng Y, Lu B, Xu B (2008) Distinct role of long 3' UTR BDNF mRNA in spine morphology and synaptic plasticity in hippocampal neurons. Cell 134: 175-187.

Anderson JC, Martin KA (2001) Does bouton morphology optimize axon length? Nat Neurosci 4: 1166-1167.

Andreasson K, Worley PF (1995) Induction of [beta]-A activin expression by synaptic activity and during neocortical development. Neuroscience 69: 781-796.

Andres ME, Burger C, Peral-Rubio MJ, Battaglioli E, Anderson ME, Grimes J, Dallman J, Ballas N, Mandel G (1999) CoREST: a functional corepressor required for regulation of neural-specific gene expression. Proc Natl Acad Sci U S A 96: 9873-9878.

Araya R, Eisenthal KB, Yuste R (2006) Dendritic spines linearize the summation of excitatory potentials. Proc Natl Acad Sci U S A 103: 18799-18804.

Arito M, Horiba T, Hachimura S, Inoue J, Sato R (2008) Growth factor-induced

phosphorylation of sterol regulatory element-binding proteins inhibits sumoylation, thereby stimulating the expression of their target genes, low density lipoprotein uptake, and lipid synthesis. J Biol Chem 283: 15224-15231.
Armstrong-James M, Diamond ME, Ebner FF (1994) An innocuous bias in whisker use in adult rats modifies receptive fields of barrel cortex neurons. J Neurosci 14: 6978-6991.
Armstrong-James M, Fox K (1987) Spatiotemporal convergence and divergence in the rat S1 "barrel" cortex. J Comp Neurol 263: 265-281.
Artola A, Singer W (1987) Long-term potentiation and NMDA receptors in rat visual cortex. Nature 330: 649-652.
Ashburner M, Ball CA, Blake JA, Botstein D, Butler H, Cherry JM, Davis AP, Dolinski K, Dwight SS, Eppig JT, Harris MA, Hill DP, Issel-Tarver L, Kasarskis A, Lewis S, Matese JC, Richardson JE, Ringwald M, Rubin GM, Sherlock G (2000) Gene ontology: tool for the unification of biology. The Gene Ontology Consortium. Nat Genet 25: 25-29.
Ballas N, Battaglioli E, Atouf F, Andres ME, Chenoweth J, Anderson ME, Burger C, Moniwa M, Davie JR, Bowers WJ, Federoff HJ, Rose DW, Rosenfeld MG, Brehm P, Mandel G (2001) Regulation of neuronal traits by a novel transcriptional complex. Neuron 31: 353-365.
Bara-Jimenez W, Catalan MJ, Hallett M, Gerloff C (1998) Abnormal somatosensory homunculus in dystonia of the hand. Ann Neurol 44: 828-831.
Barrionuevo G, Schottler F, Lynch G (1980) The effects of repetitive low frequency stimulation on control and "potentiated" synaptic responses in the hippocampus. Life Sci 27: 2385-2391.
Barth AL, McKenna M, Glazewski S, Hill P, Impey S, Storm D, Fox K (2000) Upregulation of cAMP response element-mediated gene expression during experience-dependent plasticity in adult neocortex. J Neurosci 20: 4206-4216.
Bats C, Groc L, Choquet D (2007) The interaction between Stargazin and PSD-95 regulates AMPA receptor surface trafficking. Neuron 53: 719-734.
Beaulieu C, Colonnier M (1985) A laminar analysis of the number of round-asymmetrical and flat-symmetrical synapses on spines, dendritic trunks, and cell bodies in area 17 of the cat. J Comp Neurol 231: 180-189.
Bekinschtein P, Cammarota M, Katche C, Slipczuk L, Rossato JI, Goldin A, Izquierdo I, Medina JH (2008) BDNF is essential to promote persistence of long-term memory storage. Proc Natl Acad Sci U S A 105: 2711-2716.
Belford GR, Killackey HP (1979) Vibrissae representation in subcortical trigeminal centers of the neonatal rat. J Comp Neurol 183: 305-321.
Benjamini Y, Hochberg Y (1995) Controlling the False Discovery Rate: A Practical and Powerful Approach to Multiple Testing. Journal of the Royal Statistical Society Series B (Methodological) 57: 289-300.
Benowitz LI, Routtenberg A (1997) GAP-43: an intrinsic determinant of neuronal development and plasticity. Trends Neurosci 20: 84-91.
Benshalom G, White EL (1986) Quantification of thalamocortical synapses with spiny stellate neurons in layer IV of mouse somatosensory cortex. J Comp Neurol 253: 303-314.
Berardi N, Pizzorusso T, Maffei L (2004) Extracellular matrix and visual cortical plasticity: freeing the synapse. Neuron 44: 905-908.
Berger SL (2002) Histone modifications in transcriptional regulation. Curr Opin Genet Dev 12: 142-148.

Bernardo KL, Woolsey TA (1987) Axonal trajectories between mouse somatosensory thalamus and cortex. J Comp Neurol 258: 542-564.
Bindman LJ, Murphy KP, Pockett S (1988) Postsynaptic control of the induction of long-term changes in efficacy of transmission at neocortical synapses in slices of rat brain. J Neurophysiol 60: 1053-1065.
Bliss TV, Lomo T (1970) Plasticity in a monosynaptic cortical pathway. J Physiol 207: 61P.
Bliss TV, Lomo T (1973) Long-lasting potentiation of synaptic transmission in the dentate area of the anaesthetized rabbit following stimulation of the perforant path. J Physiol 232: 331-356.
Bloodgood BL, Sabatini BL (2005) Neuronal activity regulates diffusion across the neck of dendritic spines. Science 310: 866-869.
Bourne J, Harris KM (2007) Do thin spines learn to be mushroom spines that remember? Curr Opin Neurobiol 17: 381-386.
Bourne JN, Harris KM (2008) Balancing structure and function at hippocampal dendritic spines. Annu Rev Neurosci 31: 47-67.
Brecht M (2007) Barrel cortex and whisker-mediated behaviors. Curr Opin Neurobiol 17: 408-416.
Brodmann K (1909) Vergleichende lokalisationslehre der grosshirnrinde in ihren prinzipien dargestellt auf grund des zellenbaues. Leipzig: JA Barth.
Bruno RM, Sakmann B (2006) Cortex is driven by weak but synchronously active thalamocortical synapses. Science 312: 1622-1627.
Buonomano DV, Merzenich MM (1998) Cortical plasticity: from synapses to maps. Annu Rev Neurosci 21: 149-186.
Byl NN, Merzenich MM, Jenkins WM (1996) A primate genesis model of focal dystonia and repetitive strain injury: I. Learning-induced dedifferentiation of the representation of the hand in the primary somatosensory cortex in adult monkeys. Neurology 47: 508-520.
Cantallops I, Haas K, Cline HT (2000) Postsynaptic CPG15 promotes synaptic maturation and presynaptic axon arbor elaboration in vivo. Nat Neurosci 3: 1004-1011.
Cauli B, Audinat E, Lambolez B, Angulo MC, Ropert N, Tsuzuki K, Hestrin S, Rossier J (1997) Molecular and physiological diversity of cortical nonpyramidal cells. J Neurosci 17: 3894-3906.
Chang FL, Greenough WT (1982) Lateralized effects of monocular training on dendritic branching in adult split-brain rats. Brain Res 232: 283-292.
Chang FL, Greenough WT (1984) Transient and enduring morphological correlates of synaptic activity and efficacy change in the rat hippocampal slice. Brain Res 309: 35-46.
Chao HW, Hong CJ, Huang TN, Lin YL, Hsueh YP (2008) SUMOylation of the MAGUK protein CASK regulates dendritic spinogenesis. J Cell Biol 182: 141-155.
Chen BE, Lendvai B, Nimchinsky EA, Burbach B, Fox K, Svoboda K (2000) Imaging high-resolution structure of GFP-expressing neurons in neocortex in vivo. Learn Mem 7: 433-441.
Chetkovich DM, Sweatt JD (1993) nMDA receptor activation increases cyclic AMP in area CA1 of the hippocampus via calcium/calmodulin stimulation of adenylyl cyclase. J Neurochem 61: 1933-1942.
Chiaia NL, Rhoades RW, Bennett-Clarke CA, Fish SE, Killackey HP (1991) Thalamic processing of vibrissal information in the rat. I. Afferent input to the medial ventral

posterior and posterior nuclei. J Comp Neurol 314: 201-216.
Chimge NO, Makeyev AV, Ruddle FH, Bayarsaihan D (2008) Identification of the TFII-I family target genes in the vertebrate genome. Proc Natl Acad Sci U S A 105: 9006-9010.
Cholet N, Pellerin L, Welker E, Lacombe P, Seylaz J, Magistretti P, Bonvento G (2001) Local injection of antisense oligonucleotides targeted to the glial glutamate transporter GLAST decreases the metabolic response to somatosensory activation. J Cereb Blood Flow Metab 21: 404-412.
Connor JR, Diamond MC (1982) A comparison of dendritic spine number and type on pyramidal neurons of the visual cortex of old adult rats from social or isolated environments. J Comp Neurol 210: 99-106.
Crair MC, Malenka RC (1995) A critical period for long-term potentiation at thalamocortical synapses. Nature 375: 325-328.
Cruikshank SJ, Lewis TJ, Connors BW (2007) Synaptic basis for intense thalamocortical activation of feedforward inhibitory cells in neocortex. Nat Neurosci 10: 462-468.
Cuperlovic-Culf M, Belacel N, Culf AS, Ouellette RJ (2006) Microarray analysis of alternative splicing. OMICS 10: 344-357.
Dalva MB, McClelland AC, Kayser MS (2007) Cell adhesion molecules: signalling functions at the synapse. Nat Rev Neurosci 8: 206-220.
Danoff SK, Taylor HE, Blackshaw S, Desiderio S (2004) TFII-I, a candidate gene for Williams syndrome cognitive profile: parallels between regional expression in mouse brain and human phenotype. Neuroscience 123: 931-938.
De Felipe J, Marco P, Fairen A, Jones EG (1997) Inhibitory synaptogenesis in mouse somatosensory cortex. Cereb Cortex 7: 619-634.
De Paola V, Holtmaat A, Knott G, Song S, Wilbrecht L, Caroni P, Svoboda K (2006) Cell type-specific structural plasticity of axonal branches and boutons in the adult neocortex. Neuron 49: 861-875.
Dehay C, Douglas RJ, Martin KA, Nelson C (1991) Excitation by geniculocortical synapses is not ‘vetoed’ at the level of dendritic spines in cat visual cortex. J Physiol 440: 723-734.
Demeulemeester H, Arckens L, Vandesande F, Orban GA, Heizmann CW, Pochet R (1991) Calcium binding proteins and neuropeptides as molecular markers of GABAergic interneurons in the cat visual cortex. Exp Brain Res 84: 538-544.
Diamond J., Gray E.G., Yasargil G.M. (1970) The function of the dendritic spine: an hypothesis. In: Excitatory synaptic mechanisms (P.Andersen, J.K.S Jansen, eds), pp 175-187. Oslo: Universitetsforlag.
Diamond MC, Krech D, Rosenzweig MR (1964) The effects of an enriched environment on the histology of the rat cerebral cortex. J Comp Neurol 123: 111-120.
Diamond MC, Lindner B, Johnson R, Bennett EL, Rosenzweig MR (1975) Differences in occipital cortical synapses from environmentally enriched, impoverished, and standard colony rats. J Neurosci Res 1: 109-119.
Diamond ME, Armstrong-James M, Ebner FF (1992) Somatic sensory responses in the rostral sector of the posterior group (POm) and in the ventral posterior medial nucleus (VPM) of the rat thalamus. J Comp Neurol 318: 462-476.
Diamond ME, Armstrong-James M, Ebner FF (1993) Experience-dependent plasticity in adult rat barrel cortex. Proc Natl Acad Sci U S A 90: 2082-2086.
Diamond ME, Huang W, Ebner FF (1994) Laminar comparison of somatosensory cortical

plasticity. Science 265: 1885-1888.
Diamond ME, von Heimendahl M, Knutsen PM, Kleinfeld D, Ahissar E (2008) 'Where' and 'what' in the whisker sensorimotor system. Nat Rev Neurosci 9: 601-612.
Douglas R., Markram H., Martin K. (2004) Neocortex. In: The Synaptic Organization of the Brain (Shepherd G.M., ed), pp 499-558. Oxford: Oxford University Press.
Douglas RM, Goddard GV (1975) Long-term potentiation of the perforant path-granule cell synapse in the rat hippocampus. Brain Res 86: 205-215.
Dykes RW (1997) Mechanisms controlling neuronal plasticity in somatosensory cortex. Can J Physiol Pharmacol 75: 535-545.
Engert F, Bonhoeffer T (1999) Dendritic spine changes associated with hippocampal long-term synaptic plasticity. Nature 399: 66-70.
Erzurumlu RS, Jhaveri S (1990) Thalamic axons confer a blueprint of the sensory periphery onto the developing rat somatosensory cortex. Brain Res Dev Brain Res 56: 229-234.
Fairént A, Regidort J, Kruger L (1992) The Cerebral Cortex of the Mouse (A First Contribution - The Acoustic Cortex). Somatosensory and Motor Research 9: 3-36.
Feldman DE, Brecht M (2005) Map plasticity in somatosensory cortex. Science 310: 810-815.
Feldman DE, Nicoll RA, Malenka RC, Isaac JT (1998) Long-term depression at thalamocortical synapses in developing rat somatosensory cortex. Neuron 21: 347-357.
Feldman ML, Peters A (1978) The forms of non-pyramidal neurons in the visual cortex of the rat. J Comp Neurol 179: 761-793.
Feldmeyer D, Lubke J, Sakmann B (2006) Efficacy and connectivity of intracolumnar pairs of layer 2/3 pyramidal cells in the barrel cortex of juvenile rats. J Physiol 575: 583-602.
Fiala JC, Feinberg M, Popov V, Harris KM (1998) Synaptogenesis via dendritic filopodia in developing hippocampal area CA1. J Neurosci 18: 8900-8911.
Fiala JC, Spacek J, Harris KM (2002) Dendritic spine pathology: cause or consequence of neurological disorders? Brain Res Brain Res Rev 39: 29-54.
Flavell SW, Kim TK, Gray JM, Harmin DA, Hemberg M, Hong EJ, Markenscoff-Papadimitriou E, Bear DM, Greenberg ME (2008) Genome-wide analysis of MEF2 transcriptional program reveals synaptic target genes and neuronal activity-dependent polyadenylation site selection. Neuron 60: 1022-1038.
Foulkes NS, Borjigin J, Snyder SH, Sassone-Corsi P (1997) Rhythmic transcription: the molecular basis of circadian melatonin synthesis. Trends Neurosci 20: 487-492.
Fox K (1992) A critical period for experience-dependent synaptic plasticity in rat barrel cortex. J Neurosci 12: 1826-1838.
Froemke RC, Merzenich MM, Schreiner CE (2007) A synaptic memory trace for cortical receptive field plasticity. Nature 450: 425-429.
Frost DO, Caviness VS, Jr. (1980) Radial organization of thalamic projections to the neocortex in the mouse. J Comp Neurol 194: 369-393.
Fukunaga K (1993) [The role of Ca2+/calmodulin-dependent protein kinase II in the cellular signal transduction]. Nippon Yakurigaku Zasshi 102: 355-369.
Gabbott PL, Somogyi P (1986) Quantitative distribution of GABA-immunoreactive neurons in the visual cortex (area 17) of the cat. Exp Brain Res 61: 323-331.
Gandhi SP, Yanagawa Y, Stryker MP (2008) Delayed plasticity of inhibitory neurons in developing visual cortex. Proc Natl Acad Sci U S A 105: 16797-16802.
Garthwaite J, Boulton CL (1995) Nitric oxide signaling in the central nervous system. Annu Rev Physiol 57: 683-706.

Genoud, C., Knott, G., and Welker, E. Ultrastructural analysis of neuronal plasticity in the adult mouse. 2006a.
Ref Type: Thesis/Dissertation
Genoud C, Knott GW, Sakata K, Lu B, Welker E (2004) Altered synapse formation in the adult somatosensory cortex of brain-derived neurotrophic factor heterozygote mice. J Neurosci 24: 2394-2400.
Genoud C, Quairiaux C, Steiner P, Hirling H, Welker E, Knott GW (2006b) Plasticity of astrocytic coverage and glutamate transporter expression in adult mouse cortex. PLoS Biol 4: e343.
Gheorghita F, Kraftsik R, Dubois R, Welker E (2006) Structural basis for map formation in the thalamocortical pathway of the barrelless mouse. J Neurosci 26: 10057-10067.
Gierdalski M, Jablonska B, Siucinska E, Lech M, Skibinska A, Kossut M (2001) Rapid regulation of GAD67 mRNA and protein level in cortical neurons after sensory learning. Cereb Cortex 11: 806-815.
Giese KP, Fedorov NB, Filipkowski RK, Silva AJ (1998) Autophosphorylation at Thr286 of the alpha calcium-calmodulin kinase II in LTP and learning. Science 279: 870-873.
Glazewski S, Barth AL, Wallace H, McKenna M, Silva A, Fox K (1999) Impaired experience-dependent plasticity in barrel cortex of mice lacking the alpha and delta isoforms of CREB. Cereb Cortex 9: 249-256.
Glazewski S, Chen CM, Silva A, Fox K (1996) Requirement for alpha-CaMKII in experience-dependent plasticity of the barrel cortex. Science 272: 421-423.
Glazewski S, Fox K (1996) Time course of experience-dependent synaptic potentiation and depression in barrel cortex of adolescent rats. J Neurophysiol 75: 1714-1729.
Glazewski S, Giese KP, Silva A, Fox K (2000) The role of alpha-CaMKII autophosphorylation in neocortical experience-dependent plasticity. Nat Neurosci 3: 911-918.
Globus A, Rosenzweig MR, Bennett EL, Diamond MC (1973) Effects of differential experience on dendritic spine counts in rat cerebral cortex. J Comp Physiol Psychol 82: 175-181.
Gogolla N, Galimberti I, Caroni P (2007) Structural plasticity of axon terminals in the adult. Curr Opin Neurobiol 17: 516-524.
Golgi C (1873) Sulla struttura della sostanza grigia del cervello. Gazzetta Medica Italiana: Lombardia 244-246.
Gottlieb JP, Keller A (1997) Intrinsic circuitry and physiological properties of pyramidal neurons in rat barrel cortex. Exp Brain Res 115: 47-60.
Gray EG (1959a) Axo-somatic and axo-dendritic synapses of the cerebral cortex: an electron microscope study. J Anat 93: 420-433.
Gray EG (1959b) Electron microscopy of synaptic contacts on dendrite spines of the cerebral cortex. Nature 183: 1592-1593.
Greenough WT, Hwang HM, Gorman C (1985) Evidence for active synapse formation or altered postsynaptic metabolism in visual cortex of rats reared in complex environments. Proc Natl Acad Sci U S A 82: 4549-4552.
Greer PL, Greenberg ME (2008) From synapse to nucleus: calcium-dependent gene transcription in the control of synapse development and function. Neuron 59: 846-860.
Grunditz A, Holbro N, Tian L, Zuo Y, Oertner TG (2008) Spine neck plasticity controls postsynaptic calcium signals through electrical compartmentalization. J Neurosci 28: 13457-13466.

Grutzendler J, Kasthuri N, Gan WB (2002) Long-term dendritic spine stability in the adult cortex. Nature 420: 812-816.

Gupta A, Wang Y, Markram H (2000) Organizing principles for a diversity of GABAergic interneurons and synapses in the neocortex. Science 287: 273-278.

Hakimi MA, Dong Y, Lane WS, Speicher DW, Shiekhattar R (2003) A candidate X-linked mental retardation gene is a component of a new family of histone deacetylase-containing complexes. J Biol Chem 278: 7234-7239.

Hannibal J, Ding JM, Chen D, Fahrenkrug J, Larsen PJ, Gillette MU, Mikkelsen JD (1998) Pituitary adenylate cyclase activating peptide (PACAP) in the retinohypothalamic tract: a daytime regulator of the biological clock. Ann N Y Acad Sci 865: 197-206.

Harmar AJ (2003) An essential role for peptidergic signalling in the control of circadian rhythms in the suprachiasmatic nuclei. J Neuroendocrinol 15: 335-338.

Harmar AJ, Marston HM, Shen S, Spratt C, West KM, Sheward WJ, Morrison CF, Dorin JR, Piggins HD, Reubi JC, Kelly JS, Maywood ES, Hastings MH (2002) The VPAC(2) receptor is essential for circadian function in the mouse suprachiasmatic nuclei. Cell 109: 497-508.

Harris KM, Jensen FE, Tsao B (1989) Ultrastructure, development, and plasticity of dendritic spine synapses in area CA1 of the rat hippocampus: Extending our vision with serial electron microscopy and three-dimensional analyses. In: The Hippocampus-New Vistas, Neurology and Neurobiology Volume 52 (Chan-Palay V, Kohler C, eds), pp 33-52. New York: Alan R. Liss.

Harris JA, Iguchi F, Seidl AH, Lurie DI, Rubel EW (2008) Afferent deprivation elicits a transcriptional response associated with neuronal survival after a critical period in the mouse cochlear nucleus. J Neurosci 28: 10990-11002.

Harris KM (1999) Structure, development, and plasticity of dendritic spines. Curr Opin Neurobiol 9: 343-348.

Harris KM, Jensen FE, Tsao B (1992) Three-dimensional structure of dendritic spines and synapses in rat hippocampus (CA1) at postnatal day 15 and adult ages: implications for the maturation of synaptic physiology and long-term potentiation. J Neurosci 12: 2685-2705.

Harris KM, Stevens JK (1989) Dendritic spines of CA 1 pyramidal cells in the rat hippocampus: serial electron microscopy with reference to their biophysical characteristics. J Neurosci 9: 2982-2997.

Harwell C, Burbach B, Svoboda K, Nedivi E (2005) Regulation of cpg15 expression during single whisker experience in the barrel cortex of adult mice. J Neurobiol 65: 85-96.

Hasbani MJ, Schlief ML, Fisher DA, Goldberg MP (2001) Dendritic spines lost during glutamate receptor activation reemerge at original sites of synaptic contact. J Neurosci 21: 2393-2403.

Hiyama TY, Watanabe E, Ono K, Inenaga K, Tamkun MM, Yoshida S, Noda M (2002) Na(x) channel involved in CNS sodium-level sensing. Nat Neurosci 5: 511-512.

Hofer SB, Mrsic-Flogel TD, Bonhoeffer T, Hubener M (2006a) Prior experience enhances plasticity in adult visual cortex. Nat Neurosci 9: 127-132.

Hofer SB, Mrsic-Flogel TD, Bonhoeffer T, Hubener M (2009) Experience leaves a lasting structural trace in cortical circuits. Nature 457: 313-317.

Hofer SB, Mrsic-Flogel TD, Bonhoeffer T, H³bener M (2006b) Lifelong learning: ocular dominance plasticity in mouse visual cortex. Current Opinion in Neurobiology 16: 451-459.

Holtmaat AJ, Trachtenberg JT, Wilbrecht L, Shepherd GM, Zhang X, Knott GW, Svoboda K (2005) Transient and persistent dendritic spines in the neocortex in vivo. Neuron 45: 279-291.

Hong EJ, McCord AE, Greenberg ME (2008) A biological function for the neuronal activity-dependent component of Bdnf transcription in the development of cortical inhibition. Neuron 60: 610-624.

Huang EP (1998) Synaptic plasticity: going through phases with LTP. Curr Biol 8: R350-R352.

Hubel DH, Wiesel TN (1970) The period of susceptibility to the physiological effects of unilateral eye closure in kittens. J Physiol 206: 419-436.

Huber AB, Schwab ME (2000) Nogo-A, a potent inhibitor of neurite outgrowth and regeneration. Biol Chem 381: 407-419.

Igaz LM, Vianna MRM, Medina JH, Izquierdo I (2002) Two Time Periods of Hippocampal mRNA Synthesis Are Required for Memory Consolidation of Fear-Motivated Learning. J Neurosci 22: 6781-6789.

Isaacson JS, Solis JM, Nicoll RA (1993) Local and diffuse synaptic actions of GABA in the hippocampus. Neuron 10: 165-175.

Javaherian A, Cline HT (2005) Coordinated motor neuron axon growth and neuromuscular synaptogenesis are promoted by CPG15 in vivo. Neuron 45: 505-512.

Jeanmonod D, Rice FL, Van der LH (1981) Mouse somatosensory cortex: alterations in the barrelfield following receptor injury at different early postnatal ages. Neuroscience 6: 1503-1535.

Jenkins WM, Merzenich MM, Ochs MT, Allard T, Guic-Robles E (1990) Functional reorganization of primary somatosensory cortex in adult owl monkeys after behaviorally controlled tactile stimulation. J Neurophysiol 63: 82-104.

Jones EG, Powell TP (1969) Morphological variations in the dendritic spines of the neocortex. J Cell Sci 5: 509-529.

Jones TA, Klintsova AY, Kilman VL, Sirevaag AM, Greenough WT (1997) Induction of multiple synapses by experience in the visual cortex of adult rats. Neurobiol Learn Mem 68: 13-20.

Josephson A, Trifunovski A, Scheele C, Widenfalk J, Wahlestedt C, Brene S, Olson L, Spenger C (2003) Activity-induced and developmental downregulation of the Nogo receptor. Cell Tissue Res 311: 333-342.

Jourdain P, Bergersen LH, Bhaukaurally K, Bezzi P, Santello M, Domercq M, Matute C, Tonello F, Gundersen V, Volterra A (2007) Glutamate exocytosis from astrocytes controls synaptic strength. Nat Neurosci 10: 331-339.

Kawaguchi Y (1993) Groupings of nonpyramidal and pyramidal cells with specific physiological and morphological characteristics in rat frontal cortex. J Neurophysiol 69: 416-431.

Kawaguchi Y, Karube F, Kubota Y (2006a) Dendritic branch typing and spine expression patterns in cortical nonpyramidal cells. Cereb Cortex 16: 696-711.

Keller A, White EL (1987) Synaptic organization of GABAergic neurons in the mouse SmI cortex. J Comp Neurol 262: 1-12.

Killackey HP (1973) Anatomical evidence for cortical subdivisions based on vertically discrete thalamic projections from the ventral posterior nucleus to cortical barrels in the rat. Brain Res 51: 326-331.

Kilman V, van Rossum MC, Turrigiano GG (2002) Activity deprivation reduces miniature

IPSC amplitude by decreasing the number of postsynaptic GABA(A) receptors clustered at neocortical synapses. J Neurosci 22: 1328-1337.
Kim DW, Cochran BH (2000) Extracellular Signal-Regulated Kinase Binds to TFII-I and Regulates Its Activation of the c-fos Promoter. Mol Cell Biol 20: 1140-1148.
Knott GW, Holtmaat A, Wilbrecht L, Welker E, Svoboda K (2006) Spine growth precedes synapse formation in the adult neocortex in vivo. Nat Neurosci 9: 1117-1124.
Knott GW, Quairiaux C, Genoud C, Welker E (2002) Formation of dendritic spines with GABAergic synapses induced by whisker stimulation in adult mice. Neuron 34: 265-273.
Kobayashi S, Fukuhara A, Taguchi T, Matsuda M, Tochino Y, Otsuki M, Shimomura I (2009) Identification of a new secretory factor, CCDC3, in adipocytes and endothelial cells. Biochem Biophys Res Commun.
Koch C, Zador A (1993) The function of dendritic spines: devices subserving biochemical rather than electrical compartmentalization. J Neurosci 13: 413-422.
Koralek KA, Jensen KF, Killackey HP (1988) Evidence for two complementary patterns of thalamic input to the rat somatosensory cortex. Brain Res 463: 346-351.
Kornhauser JM, Cowan CW, Shaywitz AJ, Dolmetsch RE, Griffith EC, Hu LS, Haddad C, Xia Z, Greenberg ME (2002) CREB transcriptional activity in neurons is regulated by multiple, calcium-specific phosphorylation events. Neuron 34: 221-233.
Lachance PE, Chaudhuri A (2004) Microarray analysis of developmental plasticity in monkey primary visual cortex. J Neurochem 88: 1455-1469.
Larkman AU (1991) Dendritic morphology of pyramidal neurones of the visual cortex of the rat: III. Spine distributions. J Comp Neurol 306: 332-343.
Le Roux N, Amar M, Moreau AW, Fossier P (2009) Roles of nitric oxide in the homeostatic control of the excitation-inhibition balance in rat visual cortical networks. Neuroscience 163: 942-951.
Lee KJ, Woolsey TA (1975) A proportional relationship between peripheral innervation density and cortical neuron number in the somatosensory system of the mouse. Brain Res 99: 349-353.
Lee KS, Schottler F, Oliver M, Lynch G (1980) Brief bursts of high-frequency stimulation produce two types of structural change in rat hippocampus. J Neurophysiol 44: 247-258.
Lee TW, Tsang VW, Birch NP (2008) Synaptic plasticity-associated proteases and protease inhibitors in the brain linked to the processing of extracellular matrix and cell adhesion molecules. Neuron Glia Biol 4: 223-234.
Lendvai B, Stern EA, Chen B, Svoboda K (2000) Experience-dependent plasticity of dendritic spines in the developing rat barrel cortex in vivo. Nature 404: 876-881.
Levenson JM, Sweatt JD (2006) Epigenetic mechanisms: a common theme in vertebrate and invertebrate memory formation. Cell Mol Life Sci 63: 1009-1016.
Levin BE, Dunn-Meynell A (1991) Adult rat barrel cortex plasticity occurs at 1 week but not at 1 day after vibrissectomy as demonstrated by the 2-deoxyglucose method. Exp Neurol 113: 237-248.
Li M, Shuto Y, Somogyvari-Vigh A, Arimura A (1999) Prohormone convertases 1 and 2 process ProPACAP and generate matured, bioactive PACAP38 and PACAP27 in transfected rat pituitary GH4C1 cells. Neuroendocrinology 69: 217-226.
Lin Y, Bloodgood BL, Hauser JL, Lapan AD, Koon AC, Kim TK, Hu LS, Malik AN, Greenberg ME (2008) Activity-dependent regulation of inhibitory synapse

development by Npas4. Nature 455: 1198-1204.
Lisman J (2003) Long-term potentiation: outstanding questions and attempted synthesis. Philos Trans R Soc Lond B Biol Sci 358: 829-842.
Liu G (2004) Local structural balance and functional interaction of excitatory and inhibitory synapses in hippocampal dendrites. Nat Neurosci 7: 373-379.
Luscher B, Keller CA (2004) Regulation of GABAA receptor trafficking, channel activity, and functional plasticity of inhibitory synapses. Pharmacol Ther 102: 195-221.
Lyckman AW, Horng S, Leamey CA, Tropea D, Watakabe A, Van Wart A, McCurry C, Yamamori T, Sur M (2008) Gene expression patterns in visual cortex during the critical period: synaptic stabilization and reversal by visual deprivation. Proc Natl Acad Sci U S A 105: 9409-9414.
Ma PM (1991) The barrelettes--architectonic vibrissal representations in the brainstem trigeminal complex of the mouse. I. Normal structural organization. J Comp Neurol 309: 161-199.
Magistretti PJ, Pellerin L (1999) Cellular mechanisms of brain energy metabolism and their relevance to functional brain imaging. Philos Trans R Soc Lond B Biol Sci 354: 1155-1163.
Magistretti PJ (2009) Role of glutamate in neuron-glia metabolic coupling. Am J Clin Nutr ajcn.
Majdan M, Shatz CJ (2006) Effects of visual experience on activity-dependent gene regulation in cortex. Nat Neurosci 9: 650-659.
Markram H, Lubke J, Frotscher M, Sakmann B (1997) Regulation of synaptic efficacy by coincidence of postsynaptic APs and EPSPs. Science 275: 213-215.
Markram H, Toledo-Rodriguez M, Wang Y, Gupta A, Silberberg G, Wu C (2004) Interneurons of the neocortical inhibitory system. Nat Rev Neurosci 5: 793-807.
Marrs GS, Green SH, Dailey ME (2001) Rapid formation and remodeling of postsynaptic densities in developing dendrites. Nat Neurosci 4: 1006-1013.
Matsumoto-Miyai K, Sokolowska E, Zurlinden A, Gee CE, Luscher D, Hettwer S, Wolfel J, Ladner AP, Ster J, Gerber U, Rulicke T, Kunz B, Sonderegger P (2009) Coincident pre- and postsynaptic activation induces dendritic filopodia via neurotrypsin-dependent agrin cleavage. Cell 136: 1161-1171.
Mayr B, Montminy M (2001) Transcriptional regulation by the phosphorylation-dependent factor CREB. Nat Rev Mol Cell Biol 2: 599-609.
McGaugh JL (2000) Memory--a century of consolidation. Science 287: 248-251.
McGuire BA, Hornung JP, Gilbert CD, Wiesel TN (1984) Patterns of synaptic input to layer 4 of cat striate cortex. J Neurosci 4: 3021-3033.
Melzer P, Van der LH, Dorfl J, Welker E, Robert P, Emery D, Berrini JC (1985) A magnetic device to stimulate selected whiskers of freely moving or restrained small rodents: its application in a deoxyglucose study. Brain Res 348: 229-240.
Merzenich MM, Jenkins WM (1993) Reorganization of cortical representations of the hand following alterations of skin inputs induced by nerve injury, skin island transfers, and experience. J Hand Ther 6: 89-104.
Merzenich MM, Kaas JH, Wall J, Nelson RJ, Sur M, Felleman D (1983) Topographic reorganization of somatosensory cortical areas 3b and 1 in adult monkeys following restricted deafferentation. Neuroscience 8: 33-55.
Merzenich MM, Nelson RJ, Stryker MP, Cynader MS, Schoppmann A, Zook JM (1984) Somatosensory cortical map changes following digit amputation in adult monkeys. J

Comp Neurol 224: 591-605.
Micheva KD, Beaulieu C (1995a) An anatomical substrate for experience-dependent plasticity of the rat barrel field cortex. Proc Natl Acad Sci U S A 92: 11834-11838.
Micheva KD, Beaulieu C (1995b) Postnatal development of GABA neurons in the rat somatosensory barrel cortex: a quantitative study. Eur J Neurosci 7: 419-430.
Micheva KD, Beaulieu C (1996) Quantitative aspects of synaptogenesis in the rat barrel field cortex with special reference to GABA circuitry. J Comp Neurol 373: 340-354.
Miller KD, Pinto DJ, Simons DJ (2001) Processing in layer 4 of the neocortical circuit: new insights from visual and somatosensory cortex. Curr Opin Neurobiol 11: 488-497.
Mollgaard K, Diamond MC, BENNETT EL, ROSENZWEIG MR, Lindner B (1971) Quantitative synaptic changes with differential experience in rat brain. Int J Neurosci 2: 113-127.
Monnerie H, Le Roux PD (2008) Glutamate alteration of glutamic acid decarboxylase (GAD) in GABAergic neurons: the role of cysteine proteases. Exp Neurol 213: 145-153.
Montani L, Gerrits B, Gehrig P, Kempf A, Dimou L, Wollscheid B, Schwab ME (2009) Neuronal Nogo-A modulates growth cone motility via Rho-GTP/LIMK1/cofilin in the unlesioned adult nervous system. J Biol Chem 284: 10793-10807.
Moore CI, Nelson SB (1998) Spatio-temporal subthreshold receptive fields in the vibrissa representation of rat primary somatosensory cortex. J Neurophysiol 80: 2882-2892.
Morimoto-Tomita M, Zhang W, Straub C, Cho CH, Kim KS, Howe JR, Tomita S (2009) Autoinactivation of neuronal AMPA receptors via glutamate-regulated TARP interaction. Neuron 61: 101-112.
Mountcastle VB (1957) Modality and topographic properties of single neurons of cat's somatic sensory cortex. J Neurophysiol 20: 408-434.
Muir DW, Mitchell DE (1973) Visual resolution and experience: acuity deficits in cats following early selective visual deprivation. Science 180: 420-422.
Muller W, Connor JA (1991) Dendritic spines as individual neuronal compartments for synaptic Ca2+ responses. Nature 354: 73-76.
Muraoka A, Maeda A, Nakahara N, Yokota M, Nishida T, Maruyama T, Ohshima T (2008) Sumoylation of CoREST modulates its function as a transcriptional repressor. Biochem Biophys Res Commun 377: 1031-1035.
Nagerl UV, Kostinger G, Anderson JC, Martin KA, Bonhoeffer T (2007) Protracted synaptogenesis after activity-dependent spinogenesis in hippocampal neurons. J Neurosci 27: 8149-8156.
Ness SA (2007) Microarray analysis: basic strategies for successful experiments. Mol Biotechnol 36: 205-219.
Nikonenko I, Boda B, Steen S, Knott G, Welker E, Muller D (2008) PSD-95 promotes synaptogenesis and multiinnervated spine formation through nitric oxide signaling. J Cell Biol 183: 1115-1127.
Nikonenko I, Jourdain P, Muller D (2003) Presynaptic remodeling contributes to activity-dependent synaptogenesis. J Neurosci 23: 8498-8505.
Nusser Z, Lujan R, Laube G, Roberts JD, Molnar E, Somogyi P (1998) Cell type and pathway dependence of synaptic AMPA receptor number and variability in the hippocampus. Neuron 21: 545-559.
O'Brien RJ, Xu D, Petralia RS, Steward O, Huganir RL, Worley P (1999) Synaptic clustering of AMPA receptors by the extracellular immediate-early gene product Narp. Neuron 23: 309-323.

O'Sullivan NC, McGettigan PA, Sheridan GK, Pickering M, Conboy L, O'Connor JJ, Moynagh PN, Higgins DG, Regan CM, Murphy KJ (2007) Temporal change in gene expression in the rat dentate gyrus following passive avoidance learning. J Neurochem 101: 1085-1098.

Oh SH, Kim CS, Song JJ (2007) Gene expression and plasticity in the rat auditory cortex after bilateral cochlear ablation. Acta Otolaryngol 127: 341-350.

Osten P, Stern-Bach Y (2006) Learning from stargazin: the mouse, the phenotype and the unexpected. Curr Opin Neurobiol 16: 275-280.

Otmakhov N, Griffith LC, Lisman JE (1997) Postsynaptic inhibitors of calcium/calmodulin-dependent protein kinase type II block induction but not maintenance of pairing-induced long-term potentiation. J Neurosci 17: 5357-5365.

Otmakhov N, Tao-Cheng JH, Carpenter S, Asrican B, Dosemeci A, Reese TS, Lisman J (2004) Persistent accumulation of calcium/calmodulin-dependent protein kinase II in dendritic spines after induction of NMDA receptor-dependent chemical long-term potentiation. J Neurosci 24: 9324-9331.

Ovtscharoff W, Jr., Segal M, Goldin M, Helmeke C, Kreher U, Greenberger V, Herzog A, Michaelis B, Braun K (2008) Electron microscopic 3D-reconstruction of dendritic spines in cultured hippocampal neurons undergoing synaptic plasticity. Dev Neurobiol 68: 870-876.

Palay SL (1956) Synapses in the central nervous system. J Biophys Biochem Cytol 2: 193-202.

Pascual-Leone A, Amedi A, Fregni F, Merabet LB (2005) The plastic human brain cortex. Annu Rev Neurosci 28: 377-401.

Passingham R (1982) The Human Primate. Oxford: W.H. Freeman.

Pasternak JR, Woolsey TA (1975) The number, size and spatial distribution of neurons in lamina IV of the mouse SmI neocortex. J Comp Neurol 160: 291-306.

Payne HL (2008) The role of transmembrane AMPA receptor regulatory proteins (TARPs) in neurotransmission and receptor trafficking (Review). Mol Membr Biol 25: 353-362.

Peters A, Palay SL, Webster HD (1991) The fine structure of the nervous system: the neurons and supporting cells. Philadelphia: Saunders.

Petersen CC, Sakmann B (2001) Functionally independent columns of rat somatosensory barrel cortex revealed with voltage-sensitive dye imaging. J Neurosci 21: 8435-8446.

Petrak LJ, Harris KM, Kirov SA (2005) Synaptogenesis on mature hippocampal dendrites occurs via filopodia and immature spines during blocked synaptic transmission. J Comp Neurol 484: 183-190.

Pichon, F., Kraftsik, R., and Welker, E. Intracortical connectivity of layer VI pyramidal cells in the barrel cortex of mice. 2008.
Ref Type: Thesis/Dissertation

Pizzorusso T, Medini P, Berardi N, Chierzi S, Fawcett JW, Maffei L (2002) Reactivation of ocular dominance plasticity in the adult visual cortex. Science 298: 1248-1251.

Poirier R, Cheval H, Mailhes C, Garel S, Charnay P, Davis S, Laroche S (2008) Distinct functions of egr gene family members in cognitive processes. Front Neurosci 2: 47-55.

Polley DB, Kvasnak E, Frostig RD (2004) Naturalistic experience transforms sensory maps in the adult cortex of caged animals. Nature 429: 67-71.

Potts JF, Regan MR, Rochelle JM, Seldin MF, Agnew WS (1993) A glial-specific voltage-sensitive Na channel gene maps close to clustered genes for neuronal isoforms on mouse chromosome 2. Biochem Biophys Res Commun 197: 100-104.

Quairiaux C, Armstrong-James M, Welker E (2007) Modified sensory processing in the barrel cortex of the adult mouse after chronic whisker stimulation. J Neurophysiol 97: 2130-2147.

Rall W (1970) Cable properties of dendrites and effects of synaptic location. In: Excitatory synaptic mechanisms (P.Andersen, J.K.S Jansen, eds), pp 175-187. Oslo: Universitetsforlag.

Ramon y Cajal (1904) Textura del sistema nervioso del hombre y de los vertebrados. Madrid: N.Moya.

Recanzone GH, Merzenich MM, Jenkins WM, Grajski KA, Dinse HR (1992) Topographic reorganization of the hand representation in cortical area 3b owl monkeys trained in a frequency-discrimination task. J Neurophysiol 67: 1031-1056.

Reiners J, Nagel-Wolfrum K, Jurgens K, Marker T, Wolfrum U (2006) Molecular basis of human Usher syndrome: deciphering the meshes of the Usher protein network provides insights into the pathomechanisms of the Usher disease. Exp Eye Res 83: 97-119.

Rema V, Armstrong-James M, Jenkinson N, Ebner FF (2006) Short exposure to an enriched environment accelerates plasticity in the barrel cortex of adult rats. Neuroscience 140: 659-672.

Rice FL, Mance A, Munger BL (1986) A comparative light microscopic analysis of the sensory innervation of the mystacial pad. I. Innervation of vibrissal follicle-sinus complexes. J Comp Neurol 252: 154-174.

Rocamora N, Welker E, Pascual M, Soriano E (1996) Upregulation of BDNF mRNA expression in the barrel cortex of adult mice after sensory stimulation. J Neurosci 16: 4411-4419.

Roy AL (2007) Signal-induced functions of the transcription factor TFII-I. Biochim Biophys Acta 1769: 613-621.

Rusakov DA, Harrison E, Stewart MG (1998) Synapses in hippocampus occupy only 1-2% of cell membranes and are spaced less than half-micron apart: a quantitative ultrastructural analysis with discussion of physiological implications. Neuropharmacology 37: 513-521.

Sager C, Tapken D, Kott S, Hollmann M (2009) Functional modulation of AMPA receptors by transmembrane AMPA receptor regulatory proteins. Neuroscience 158: 45-54.

Schratt G (2009) microRNAs at the synapse. Nat Rev Neurosci 10: 842-849.

Schroeder A, Mueller O, Stocker S, Salowsky R, Leiber M, Gassmann M, Lightfoot S, Menzel W, Granzow M, Ragg T (2006) The RIN: an RNA integrity number for assigning integrity values to RNA measurements. BMC Mol Biol 7: 3.

Senft SL, Woolsey TA (1991) Growth of thalamic afferents into mouse barrel cortex. Cereb Cortex 1: 308-335.

Seo J, Hoffman EP (2006) Probe set algorithms: is there a rational best bet? BMC Bioinformatics 7: 395.

Shimegi S, Ichikawa T, Akasaki T, Sato H (1999) Temporal characteristics of response integration evoked by multiple whisker stimulations in the barrel cortex of rats. J Neurosci 19: 10164-10175.

Shimizu H, Watanabe E, Hiyama TY, Nagakura A, Fujikawa A, Okado H, Yanagawa Y, Obata K, Noda M (2007) Glial Nax channels control lactate signaling to neurons for brain [Na+] sensing. Neuron 54: 59-72.

Shoji-Kasai Y, Ageta H, Hasegawa Y, Tsuchida K, Sugino H, Inokuchi K (2007) Activin

increases the number of synaptic contacts and the length of dendritic spine necks by modulating spinal actin dynamics. J Cell Sci 120: 3830-3837.
Simons DJ (1978) Response properties of vibrissa units in rat SI somatosensory neocortex. J Neurophysiol 41: 798-820.
Simons DJ (1985) Temporal and spatial integration in the rat SI vibrissa cortex. J Neurophysiol 54: 615-635.
Sirevaag AM, Greenough WT (1985) Differential rearing effects on rat visual cortex synapses. II. Synaptic morphometry. Brain Res 351: 215-226.
Sirri A, Bianchi V, Pelizzola M, Mayhaus M, Ricciardi-Castagnoli P, Toniolo D, D'Adamo P (2010) Temporal gene expression profile of the hippocampus following trace fear conditioning. Brain Res 1308: 14-23.
Siucinska E, Kossut M (2006) Short-term sensory learning does not alter parvalbumin neurons in the barrel cortex of adult mice: a double-labeling study. Neuroscience 138: 715-724.
Song I, Huganir RL (2002) Regulation of AMPA receptors during synaptic plasticity. Trends Neurosci 25: 578-588.
Spacek J, Harris KM (1997) Three-dimensional organization of smooth endoplasmic reticulum in hippocampal CA1 dendrites and dendritic spines of the immature and mature rat. J Neurosci 17: 190-203.
Spolidoro M, Sale A, Berardi N, Maffei L (2009) Plasticity in the adult brain: lessons from the visual system. Exp Brain Res 192: 335-341.
Staiger JF, Bisler S, Schleicher A, Gass P, Stehle JH, Zilles K (2000) Exploration of a novel environment leads to the expression of inducible transcription factors in barrel-related columns. Neuroscience 99: 7-16.
Staiger JF, Zilles K, Freund TF (1996) Distribution of GABAergic elements postsynaptic to ventroposteromedial thalamic projections in layer IV of rat barrel cortex. Eur J Neurosci 8: 2273-2285.
Stamm S, Ben Ari S, Rafalska I, Tang Y, Zhang Z, Toiber D, Thanaraj TA, Soreq H (2005) Function of alternative splicing. Gene 344: 1-20.
Sterio DC (1984) The unbiased estimation of number and sizes of arbitrary particles using the disector. J Microsc 134: 127-136.
Stettler DD, Yamahachi H, Li W, Denk W, Gilbert CD (2006) Axons and synaptic boutons are highly dynamic in adult visual cortex. Neuron 49: 877-887.
Szentagothai J (1978) The Ferrier Lecture, 1977. The neuron network of the cerebral cortex: a functional interpretation. Proc R Soc Lond B Biol Sci 201: 219-248.
Taghibiglou C, Martin HG, Lai TW, Cho T, Prasad S, Kojic L, Lu J, Liu Y, Lo E, Zhang S, Wu JZ, Li YP, Wen YH, Imm JH, Cynader MS, Wang YT (2009) Role of NMDA receptor-dependent activation of SREBP1 in excitotoxic and ischemic neuronal injuries. Nat Med 15: 1399-1406.
Taha S, Hanover JL, Silva AJ, Stryker MP (2002) Autophosphorylation of alphaCaMKII is required for ocular dominance plasticity. Neuron 36: 483-491.
Trachtenberg JT, Chen BE, Knott GW, Feng G, Sanes JR, Welker E, Svoboda K (2002) Long-term in vivo imaging of experience-dependent synaptic plasticity in adult cortex. Nature 420: 788-794.
Trommald M, Hulleberg G, Andersen P (1996) Long-term potentiation is associated with new excitatory spine synapses on rat dentate granule cells. Learn Mem 3: 218-228.
Tropea D, Kreiman G, Lyckman A, Mukherjee S, Yu H, Horng S, Sur M (2006) Gene

expression changes and molecular pathways mediating activity-dependent plasticity in visual cortex. Nat Neurosci 9: 660-668.
Tropea D, Van Wart A, Sur M (2009) Molecular mechanisms of experience-dependent plasticity in visual cortex. Philos Trans R Soc Lond B Biol Sci 364: 341-355.
Tsui CC, Copeland NG, Gilbert DJ, Jenkins NA, Barnes C, Worley PF (1996) Narp, a novel member of the pentraxin family, promotes neurite outgrowth and is dynamically regulated by neuronal activity. J Neurosci 16: 2463-2478.
Turner AM, Greenough WT (1985) Differential rearing effects on rat visual cortex synapses. I. Synaptic and neuronal density and synapses per neuron. Brain Res 329: 195-203.
Turrigiano GG, Nelson SB (2000) Hebb and homeostasis in neuronal plasticity. Curr Opin Neurobiol 10: 358-364.
Uylings HB, Kuypers K, Diamond MC, Veltman WA (1978) Effects of differential environments on plasticity of dendrites of cortical pyramidal neurons in adult rats. Exp Neurol 62: 658-677.
Van der Loos H. (1976) Neuronal circuitry and its development. Prog Brain Res 45: 259-278.
Van der Loos H., Dorfl J, Welker E (1984) Variation in pattern of mystacial vibrissae in mice. A quantitative study of ICR stock and several inbred strains. J Hered 75: 326-336.
Van der Loos H., Woolsey TA (1973) Somatosensory cortex: structural alterations following early injury to sense organs. Science 179: 395-398.
Veinante P, Jacquin MF, Deschenes M (2000) Thalamic projections from the whisker-sensitive regions of the spinal trigeminal complex in the rat. J Comp Neurol 420: 233-243.
Wallace H, Fox K (1999) The effect of vibrissa deprivation pattern on the form of plasticity induced in rat barrel cortex. Somatosens Mot Res 16: 122-138.
Walsh DM, Selkoe DJ (2004) Deciphering the molecular basis of memory failure in Alzheimer's disease. Neuron 44: 181-193.
Ward JH. (1963). Hierarchical Grouping to optimize an objective function. Journal of American Statistical Association, 58(301), 236-244.
Waterston RH, Lindblad-Toh K, Birney E, Rogers J, Abril JF, Agarwal P, et al. (2002) Initial sequencing and comparative analysis of the mouse genome. Nature 420: 520-562.
Welker C (1976) Receptive fields of barrels in the somatosensory neocortex of the rat. J Comp Neurol 166: 173-189.
Welker E, Armstrong-James M, Bronchti G, Ourednik W, Gheorghita-Baechler F, Dubois R, Guernsey DL, Van der LH, Neumann PE (1996) Altered sensory processing in the somatosensory cortex of the mouse mutant barrelless. Science 271: 1864-1867.
Welker E, Armstrong-James M, Van der LH, Kraftsik R (1993) The mode of activation of a barrel column: response properties of single units in the somatosensory cortex of the mouse upon whisker deflection. Eur J Neurosci 5: 691-712.
Welker E, Rao SB, Dorfl J, Melzer P, Van der LH (1992) Plasticity in the barrel cortex of the adult mouse: effects of chronic stimulation upon deoxyglucose uptake in the behaving animal. J Neurosci 12: 153-170.
Welker E, Soriano E, Dorfl J, Van der LH (1989a) Plasticity in the barrel cortex of the adult mouse: transient increase of GAD-immunoreactivity following sensory stimulation. Exp Brain Res 78: 659-664.
Welker E, Soriano E, Van der LH (1989b) Plasticity in the barrel cortex of the adult mouse: effects of peripheral deprivation on GAD-immunoreactivity. Exp Brain Res 74: 441-452.
Welker E, Van der LH (1986) Quantitative correlation between barrel-field size and the

sensory innervation of the whiskerpad: a comparative study in six strains of mice bred for different patterns of mystacial vibrissae. J Neurosci 6: 3355-3373.
White EL (1978) Identified neurons in mouse Sml cortex which are postsynaptic to thalamocortical axon terminals: a combined Golgi-electron microscopic and degeneration study. J Comp Neurol 181: 627-661.
White EL, Keller A, Cipolloni PB (1985) The identification of thalamocortical axon terminals in barrels of mouse Sml cortex using immunohistochemistry of anterogradely transported lectin (Phaseolus vulgaris-leucoagglutinin). Brain Res 343: 159-165.
White EL, Weinfeld E, Lev DL (2004) Quantitative analysis of synaptic distribution along thalamocortical axons in adult mouse barrels. J Comp Neurol 479: 56-69.
Wiesel TN, Hubel DH (1963) single-cell responses in striate cortex of kittens deprived of vision in one eye. J Neurophysiol 26: 1003-1017.
Wilent WB, Contreras D (2005) Dynamics of excitation and inhibition underlying stimulus selectivity in rat somatosensory cortex. Nat Neurosci 8: 1364-1370.
Williams M, Lyu MS, Yang YL, Lin EP, Dunbrack R, Birren B, Cunningham J, Hunter K (1999) Ier5, a novel member of the slow-kinetics immediate-early genes. Genomics 55: 327-334.
Woolsey TA, Dierker ML, Wann DF (1975) Mouse SmI cortex: qualitative and quantitative classification of golgi-impregnated barrel neurons. Proc Natl Acad Sci U S A 72: 2165-2169.
Woolsey TA, Van der Loos H. (1970) The structural organization of layer IV in the somatosensory region (SI) of mouse cerebral cortex. The description of a cortical field composed of discrete cytoarchitectonic units. Brain Res 17: 205-242.
Woolsey TA, Wann JR (1976) Areal changes in mouse cortical barrels following vibrissal damage at different postnatal ages. J Comp Neurol 170: 53-66.
Wu Z, Jia X, de la CL, Su XC, Marzolf B, Troisch P, Zak D, Hamilton A, Whittle B, Yu D, Sheahan D, Bertram E, Aderem A, Otting G, Goodnow CC, Hoyne GF (2008) Memory T cell RNA rearrangement programmed by heterogeneous nuclear ribonucleoprotein hnRNPLL. Immunity 29: 863-875.
Xu D, Hopf C, Reddy R, Cho RW, Guo L, Lanahan A, Petralia RS, Wenthold RJ, O'Brien RJ, Worley P (2003) Narp and NP1 form heterocomplexes that function in developmental and activity-dependent synaptic plasticity. Neuron 39: 513-528.
Ye B, Liao D, Zhang X, Zhang P, Dong H, Huganir RL (2000) GRASP-1: a neuronal RasGEF associated with the AMPA receptor/GRIP complex. Neuron 26: 603-617.
Zhang SJ, Steijaert MN, Lau D, Schutz G, Delucinge-Vivier C, Descombes P, Bading H (2007) Decoding NMDA receptor signaling: identification of genomic programs specifying neuronal survival and death. Neuron 53: 549-562.
Zhang ZW, Deschenes M (1997) Intracortical axonal projections of lamina VI cells of the primary somatosensory cortex in the rat: a single-cell labeling study. J Neurosci 17: 6365-6379.
Zito K, Scheuss V, Knott G, Hill T, Svoboda K (2009) Rapid functional maturation of nascent dendritic spines. Neuron 61: 247-258.
Zuo Y, Yang G, Kwon E, Gan WB (2005) Long-term sensory deprivation prevents dendritic spine loss in primary somatosensory cortex. Nature 436: 261-265.

Appendix

Appendix 1. Comparison of published synaptic densities for the neuropil of the somatosensory cortex with values obtained in our ultrastructural analysis.

			De Felipe et al., 1997 C57Bl mice		Micheva and Beaulieu, 1996 Long-Evans rats						Knott et al., 2002 NOR mice 8 weeks			Present results NOR P42-P49					Genoud et al., 2004 C57Bl6 mice 8 weeks				Landers et al., in process C57Bl6 /P100	
			P32 layer IV	P100 layer IV	P5	P10	P15	P20	P30	P60	Ctrl Layer IV	24h Layer IV	Layer IV	Ctrl Layer IV	6h Layer IV	12h Layer IV	18h Layer IV	24h Layer IV	wild-type Ctrl LIV	wild-type 24h LIV	BDNF +/- Ctrl LIV	BDNF +/- 24h LIV	control layer IV	Enriched layer IV
					Total, total exc and total inh: layer IV on spine, on shafts: all layers																			
Density of excitatory	all	mean	1.90	1.03	0.11	0.22	0.50	0.60	0.57	0.51	0.45	0.55	0.44	1.30	1.36	1.38	1.28	1.13	*0.79*	*0.83*	*0.80*	*0.74*	1.26	1.66*
		SD	0.47	0.31	0.03	0.05	0.07	0.06	0.04	0.05	0.03	0.01	0.03	0.05	0.14	0.14	0.10	0.16					0.08 (SE)	0.07 (SE)
	spine	mean	-	-	0.04	0.07	0.33	0.47	0.45	0.41	0.41	0.48	0.41	1.25	1.24	1.22	1.14	1.07	0.55	0.73	0.66	0.62	1.11	1.34
		SD			0.01	0.01	0.06	0.05	0.03	0.02	0.04	0.01	0.05	0.07	0.13	0.06	0.12	0.15	0.13	0.01	0.17	0.12	0.06 (SE)	0.07 (SE)
	shaft	mean	-	-	0.05	0.06	0.07	0.07	0.07	0.07	*0.04*	*0.07*	*0.03*	0.05	0.12	0.16	0.14	0.07	*0.24*	*0.10*	*0.14*	*0.12*	0.15	0.32*
		SD			0.01	0.01	0.01	0.00	0.00	0.01				0.03	0.03	0.11	0.06	0.02					0.03 (SE)	0.05 (SE)
ratio shaft/spine					*1.34*	*0.91*	*0.21*	*0.15*	*0.15*	*0.17*	*0.10*	*0.15*	*0.07*	*0.04*	*0.10*	*0.13*	*0.12*	*0.07*	*0.44*	*0.14*	*0.21*	*0.19*	*0.14*	*0.24*
Density of inhibitory	all	mean	0.26	0.36	0.03	0.02	0.10	0.10	0.12	0.13	0.10	0.19	0.13	0.24	0.29	0.29	0.27	0.32	0.13	0.24	0.17	0.20	0.23	0.34*
		SD	0.18	0.21	0.01	0.01	0.01	0.03	0.03	0.01	0.02	0.01	0.03	0.03	0.02	0.05	0.06	0.02	0.03	0.04	0.07	0.06	0.02 (SE)	0.04 (SE)
	spine	mean	-	-	0.01	0.00	0.03	0.03	0.03	0.03	0.02	0.07	0.06	0.08	0.11	0.08	0.09	0.12	0.03	0.08	0.05	0.06	0.07	0.112*
		SD			0.00	0.00	0.00	0.01	0.01	0.01	0.01	0.03	0.01	0.01	0.03	0.01	0.01	0.01	0.01	0.01	0.03	0.03	0.01 (SE)	0.01 (SE)
	shaft	mean	-	-	0.01	0.02	0.04	0.04	0.05	0.05	*0.08*	*0.12*	*0.07*	0.16	0.18	0.21	0.18	0.20	*0.10*	*0.16*	*0.12*	*0.14*	0.17	0.22
		SD			0.00	0.00	0.01	0.00	0.00	0.01				0.02	0.03	0.05	0.06	0.02					0.02 (SE)	0.03 (SE)
ratio shaft/spine					*1.63*	*4.25*	*1.41*	*1.38*	*1.61*	*1.96*	*4.16*	*1.60*	*1.17*	*2.00*	*1.64*	*2.63*	*2.00*	*1.67*	*3.33*	*2.00*	*2.40*	*2.33*	*2.43*	*1.96*
ratio inh/exc on spine		mean	-	-	*0.23*	*0.06*	*0.08*	*0.06*	*0.06*	*0.06*	*0.05*	*0.15*	*0.15*	0.06	0.09	0.07	0.08	0.11	*0.05*	*0.11*	*0.08*	*0.10*	0.06	0.08
ratio inh/exc on shaft		mean			*0.28*	*0.28*	*0.55*	*0.52*	*0.69*	*0.70*	*1.98*	*1.67*	*2.33*	3.20	1.50	1.31	1.29	2.86	*0.42*	*1.60*	*0.86*	*1.17*	1.10	0.69
Total synaptic density	all	mean	2.15	1.38	*0.15*	*0.23*	*0.60*	*0.70*	*0.69*	*0.64*	*0.55*	*0.74*	*0.57*	1.54	1.65	1.67	1.55	1.45	0.92	1.07	0.97	0.94	1.42	1.89*
		SD												0.05	0.16	0.14	0.09	0.16	0.06	0.03	0.20	0.21	0.09 (SE)	0.065 (SE)
percentage exc.		mean	*88*	*74*	*77*	*93*	*83*	*86*	*83*	*80*	*82*	*74*	*77*	84	82	83	83	78	*86*	*78*	*82*	*79*	*0.89*	*0.88*
percentage inh.		mean	*12*	*26*	*23*	*7*	*17*	*14*	*17*	*20*	*18*	*26*	*23*	16	18	17	17	22	15		17		*0.16*	*0.18*
																			5		4.90			
ratio inh/exc		mean	*0.14*	*0.35*	*0.29*	*0.07*	*0.21*	*0.17*	*0.21*	*0.25*	*0.22*	*0.35*	*0.30*	*0.18*	*0.21*	*0.21*	*0.21*	*0.28*	*0.16*	*0.29*	*0.21*	*0.27*	*0.19*	*0.20*
stimulation-dependent shift in ratio inh/exc												*1.59*	*1.36*					*1.53*		*1.76*		*1.27*		

In italic are numbers that were calculated from the above mean densities as they were not given in the published studies and for this reason do not take into account the standard deviation. For comparison, ratio from the present results were also calculated directly from the mean densities. Yellow indicates mean values calculated for all cortical layers.

Appendix 2. List of genes identified as regulated in at least one stimulation period across 24 hours of whisker stimulation (in alphabetical order)

Scale bar FC: N.S. | 1.25-1.5 | 1.5-2 | 2-2.5 | 2.5-3 | ≥3 (up / down)

genesymbol	Gene Name	adj. p-value	p-value	sens of regulation	FC 3h	FC 6h	FC 9h	FC 15h	FC 24h	IterPlier (224 genes)	Plier (182 genes)	Protein information: Location	Protein information: Type(s)	Comparison with others: AP bursting (Zhang et al, 2007)	Comparison with others: 4 days MD (Tropea et al., 2006)	Comparison with others: Npas4 (Lin et al., 2008)	Transcription factor: TFII-I	Transcription factor: KROX	Transcription factor: SREBP-1	Clustering: Max at	Clustering: Ward's distance
1200009F10Rik	IKK interacting protein	0.05	0.03	down	-1.01	1.00	1.00	-1.31	1.02		*	Cytoplasm	other					y	y	Max 15h	Down Cluster 1
1700019N12Rik	chromosome 11 open reading frame 20	0.03	0.01	down	-1.33	-1.14	-1.18	-1.19	-1.11	*	*	Unknown	other				y			Max 03h	Down Cluster 2
1700028P14Rik	chromosome 9 open reading frame 135	0.01	0.00	up	-1.01	1.09	1.54	-1.06	1.01	*	*	Unknown	other				y			Max 09h	UP Cluster 1
3110035E14Rik	chromosome 8 open reading frame 46	0.00	0.00	up	1.09	1.14	1.20	1.20	1.37	*	*	Unknown	other						y	Max 24h	UP Cluster 2
4922501L14Rik|BC0(	chromosome 1 open reading frame 173	0.01	0.00	down	-1.10	-1.25	-1.52	-1.14	-1.09	*	*	Unknown	other							Max 09h	Down Cluster 5
4930431L04Rik	RIKEN cDNA 4930431L04 gene	0.01	0.00	up	1.29	1.45	1.17	1.63	1.52	*	*	Unknown	enzyme				y		y	Max 15h	UP Cluster 2
4930471G03Rik	RIKEN cDNA 4930471G03 gene	0.04	0.02	down	1.12	-1.30	-1.01	1.06	1.02	*	*	Unknown	other							max 06h	Down Cluster 5
5830403L16Rik	RIKEN cDNA 5830403L16 gene	0.00	0.00	down	1.00	-1.37	-1.14	1.04	-1.15		*	Unknown	other				y		y	max 06h	Down Cluster 5
6030405A18Rik	chromosome 13 open reading frame 36	0.00	0.00	up	1.55	1.36	1.10	1.17	1.19	*	*	Unknown	other				y	y	y	Max 03h	UP Cluster 5
6430550H21Rik	family with sequence similarity 70, member A	0.02	0.01	down	-1.23	-1.49	-1.19	-1.82	-1.43	*	*	Unknown	other		up		y			Max 15h	Down Cluster 3
9130213B05Rik	prostatic androgen-repressed message-1	0.00	0.00	down	-1.30	-1.07	-1.21	-1.28	-1.11	*		Extracellular S	other		up		y		y	Max 03h	Down Cluster 2
A630033E08Rik	RIKEN cDNA A630033E08 gene	0.01	0.00	down	1.01	-1.08	1.02	-1.43	-1.19	*	*	Unknown	other							Max 15h	Down Cluster 4
A830006F12Rik	von Willebrand factor C domain-containing protein 2-like	0.04	0.02	down	-1.22	-1.20	-1.34	-1.10	1.05		*	Unknown	other		up				y	Max 09h	Down Cluster 2
A830019P07Rik	RIKEN cDNA A830019P07 gene	0.02	0.01	down	-1.01	-1.10	-1.54	-1.31	-1.04	*		Unknown	other							Max 09h	Down Cluster 5
A930016P21Rik	family with sequence similarity 173, member B	0.01	0.00	down	1.00	-1.44	-1.10	-1.09	1.20	*	*	Unknown	other				y		y	max 06h	Down Cluster 4
Aard	chromosome 8 open reading frame 85	0.01	0.00	down	-1.65	-1.49	-1.24	-1.23	-1.09	*	**	Unknown	other				y			Max 03h	Down Cluster 2
Abhd11	abhydrolase domain containing 11	0.01	0.00	down	-1.30	-1.28	-1.23	-1.45	-1.07	*		Unknown	enzyme				y		y	Max 15h	Down Cluster 1
Acot5	acyl-CoA thioesterase 5	0.00	0.00	down	-1.39	-1.32	-1.39	-1.31	-1.13	*	*	Cytoplasm	enzyme						y	Max 09h	Down Cluster 2
Acyp1	acylphosphatase 1, erythrocyte (common) type	0.01	0.00	down	-1.11	-1.03	-1.13	-1.35	-1.08	*	*	Unknown	enzyme				y		y	Max 15h	Down Cluster 1
Adam19|LOC1000457	ADAM metallopeptidase domain 19 (meltrin beta)	0.01	0.00	up	1.23	1.25	1.51	1.18	1.24	*		Plasma Memb	peptidase		down					Max 09h	UP Cluster 1
Adcyap1	adenylate cyclase activating polypeptide 1 (pituitary)	0.00	0.00	up	1.48	1.88	2.15	1.65	1.48	*	**	Extracellular S	other		down				y	Max 09h	UP Cluster 1
AI836003	chromosome 12 open reading frame 68	0.00	0.00	down	-1.09	-1.11	-1.17	-1.31	-1.12	*		Unknown	other		down		y		y	Max 15h	Down Cluster 1
Aifm3	apoptosis-inducing factor, mitochondrion-associated, 3	0.00	0.00	down	-1.08	-1.22	-1.11	-1.45	-1.29	*		Cytoplasm	enzyme				y		y	Max 15h	Down Cluster 4
Alg12	asparagine-linked glycosylation 12, alpha-1,6-mannosyltransfera	0.03	0.01	down	-1.04	-1.39	-1.05	-1.14	1.03	*		Cytoplasm	enzyme						y	max 06h	Down Cluster 4
Alkbh7	alkB, alkylation repair homolog 7 (E. coli)	0.01	0.00	down	-1.50	-1.03	1.01	-1.04	1.01	*	*	Unknown	other						y	Max 03h	Down Cluster 2
Ankzf1	ankyrin repeat and zinc finger domain containing 1	0.01	0.00	down	-1.03	-1.07	-1.03	-1.56	-1.22	*		Nucleus	transcription regulator							Max 15h	Down Cluster 3
Antxr1	anthrax toxin receptor 1	0.02	0.01	down	-1.42	-1.47	-1.17	-1.63	-1.27	*	*	Plasma Memb	other				y		y	Max 15h	Down Cluster 3
Ap1g2|EG667952	adaptor-related protein complex 1, gamma 2 subunit	0.01	0.00	down	-1.31	-1.27	-1.19	-1.14	-1.05	*		Cytoplasm	transporter							Max 03h	Down Cluster 2
Apip|LOC100044135	APAF1 interacting protein	0.03	0.02	down	-1.05	-1.12	-1.09	-1.29	-1.10		*	Unknown	other							Max 15h	Down Cluster 1
Apod	apolipoprotein D	0.00	0.00	down	-1.30	-1.24	-1.34	-1.42	-1.17	*	*	Extracellular S	transporter				y		y	Max 15h	Down Cluster 1
Arc	activity-regulated cytoskeleton-associated protein	0.00	0.00	up	1.21	1.50	1.73	1.40	1.07	*	*	Cytoplasm	other	*		*	y		y	Max 09h	UP Cluster 1
Arg2	arginase, type II	0.02	0.01	up	-1.01	1.10	1.01	1.40	1.03	*	*	Cytoplasm	enzyme							Max 15h	UP Cluster 4
Arhgap26	Rho GTPase activating protein 26	0.00	0.00	up	1.19	1.37	1.17	1.46	1.49	*	*	Cytoplasm	other	*	up		y		y	Max 24h	UP Cluster 2
Arpp21	cyclic AMP-regulated phosphoprotein, 21 kD	0.00	0.00	up	1.28	1.23	1.24	1.13	1.11	*		Cytoplasm	other	*			y		y	Max 03h	UP Cluster 1
Asb13	ankyrin repeat and SOCS box-containing 13	0.01	0.00	down	-1.14	-1.18	-1.31	-1.14	-1.09	*		Unknown	other		down		y			Max 09h	Down Cluster 2
Atpbd1c	GPN-loop GTPase 3	0.00	0.00	down	-1.13	-1.13	-1.10	-1.53	-1.12	*	*	Unknown	other				y			Max 15h	Down Cluster 3

AU040320	KIAA0319-like	0.00	0.00	down	-1.30	1.08	-1.04	-1.50	-1.07	*		Unknown	other		down	y		y	Max 15h	Down Cluster 1
B830045N13Rik	family with sequence similarity 5, member C	0.00	0.00	up	1.25	1.19	1.28	1.12	1.12		*	Cytoplasm	other					y	Max 09h	UP Cluster 1
BC145678	RIKEN cDNA 4930441O14 gene	0.02	0.00	down	-1.12	-1.10	-1.06	-1.43	-1.07	*	*	Unknown	other						Max 15h	Down Cluster 1
Bdnf	brain-derived neurotrophic factor	0.00	0.00	up	3.75	3.63	3.19	2.44	1.89	*	**	Extracellular S	growth factor	*	down	*			Max 03h	UP Cluster 5
Bgn	biglycan	0.01	0.00	down	-1.11	-1.15	-1.26	-1.10	-1.03	*		Extracellular S	other			y		y	Max 09h	Down Cluster 2
Bhlhb3	basic helix-loop-helix family, member e41	0.01	0.00	down	-1.37	-1.29	-1.21	-1.87	-1.08	*	*	Nucleus	transcription regulator			y	y		Max 15h	Down Cluster 3
Brd9	bromodomain containing 9	0.00	0.00	down	-1.28	-1.31	-1.41	-1.44	-1.24	*	*	Unknown	other						Max 15h	Down Cluster 2
C230078M14Rik|Cntn	contactin associated protein-like 5B	0.00	0.00	down	-1.06	-1.22	-1.25	-1.73	-1.33	*	*	Unknown	other						Max 15h	Down Cluster 3
C630007B19Rik	family with sequence similarity 19 (chemokine (C-C motif)-like)	0.00	0.00	up	1.33	1.56	1.67	1.49	1.38	*	*	Extracellular S	other			y			Max 09h	UP Cluster 1
C730025P13Rik	transmembrane protein 203	0.02	0.01	down	-1.01	1.06	1.08	-1.46	-1.06	*	*	Unknown	other		down				Max 15h	Down Cluster 3
Cabyr	calcium binding tyrosine-(Y)-phosphorylation regulated	0.01	0.00	down	-1.15	-1.25	-1.30	-1.33	-1.13	*	*	Cytoplasm	other			y		y	Max 15h	Down Cluster 2
Cacng2	calcium channel, voltage-dependent, gamma subunit 2	0.00	0.00	up	1.02	1.10	1.27	1.17	1.03	*	*	Plasma Memb	ion channel						Max 09h	UP Cluster 1
Camk1g	calcium/calmodulin-dependent protein kinase IG	0.00	0.00	up	1.85	1.41	1.40	1.36	1.33	*	*	Cytoplasm	kinase		down	y		y	Max 03h	UP Cluster 5
Cap1	CAP, adenylate cyclase-associated protein 1 (yeast)	0.01	0.00	up	1.08	1.20	1.36	1.22	1.18	*	*	Plasma Memb	other		down			y	Max 09h	UP Cluster 1
Car4	carbonic anhydrase IV	0.01	0.00	up	1.18	1.32	1.37	1.38	1.20	*	*	Plasma Memb	enzyme			y		y	Max 15h	UP Cluster 2
Cbln2	cerebellin 2 precursor	0.00	0.00	up	1.64	1.57	1.79	1.33	1.12	*	*	Extracellular S	other		down	y		y	Max 09h	UP Cluster 1
Ccdc3	coiled-coil domain containing 3	0.00	0.00	up	1.69	1.88	1.74	2.05	2.54	*	**	Cytoplasm	other			y		y	Max 24h	UP Cluster 2
Cd34	CD34 molecule	0.02	0.01	down	1.12	-1.02	-1.13	-1.47	-1.29	*	*	Plasma Memb	other			y	y		Max 15h	Down Cluster 1
Cdkn1a	cyclin-dependent kinase inhibitor 1A (p21, Cip1)	0.00	0.00	up	1.31	1.70	1.77	1.61	1.42	*	*	Nucleus	other	*	down	y		y	Max 09h	UP Cluster 3
Cdkn1b	cyclin-dependent kinase inhibitor 1B (p27, Kip1)	0.03	0.02	down	1.01	1.03	-1.06	-1.34	-1.11		*	Nucleus	other					y	Max 15h	Down Cluster 1
Cenpk	centromere protein K	0.01	0.00	down	-1.29	1.01	-1.48	-1.77	-1.11	*	*	Nucleus	other			y			Max 15h	Down Cluster 1
Chl1	cell adhesion molecule with homology to L1CAM (close homol	0.00	0.00	up	1.40	1.86	1.52	1.42	1.45	*	*	Plasma Memb	other		up	y		y	Max 06h	UP Cluster 3
Chml	choroideremia-like (Rab escort protein 2)	0.01	0.00	up	1.63	1.08	1.35	1.40	1.18	*	*	Cytoplasm	enzyme						Max 03h	UP Cluster 5
Cntn2	contactin 2 (axonal)	0.01	0.00	down	-1.17	-1.20	-1.17	-1.37	-1.14	*		Plasma Memb	other			y		y	Max 15h	Down Cluster 1
Coch	coagulation factor C homolog, cochlin (Limulus polyphemus)	0.00	0.00	down	1.02	-1.26	-1.18	-1.38	-1.17	*	*	Extracellular S	other				y	y	Max 15h	Down Cluster 4
Cplx1	complexin 1	0.02	0.01	down	-1.25	-1.12	-1.12	-1.15	-1.08	*		Unknown	transporter		down			y	Max 03h	Down Cluster 2
Cpne4	copine IV	0.01	0.00	up	1.57	1.58	1.52	-1.02	1.52	*	*	Cytoplasm	other		up				Max 06h	UP Cluster 6
Cpne5	copine V	0.00	0.00	up	1.51	1.32	1.39	1.27	1.33	*		Unknown	other		down			y	Max 03h	UP Cluster 5
Crem	cAMP responsive element modulator	0.00	0.00	up	1.49	1.42	1.50	1.34	1.33	*	*	Nucleus	transcription r	*		y		y	Max 09h	UP Cluster 1
Ctnna1	catenin (cadherin-associated protein), alpha 1, 102kDa	0.00	0.00	down	-1.21	-1.22	-1.23	-1.46	-1.17	*		Plasma Memb	other		up	y	y	y	Max 15h	Down Cluster 1
Cyp11a1	cytochrome P450, family 11, subfamily A, polypeptide 1	0.00	0.00	down	-1.32	-1.40	-1.39	-1.54	-1.45	*	*	Cytoplasm	enzyme			y			Max 15h	Down Cluster 1
Cyp39a1	cytochrome P450, family 39, subfamily A, polypeptide 1	0.00	0.00	down	-1.28	-1.25	-1.19	-1.34	-1.23		*	Cytoplasm	enzyme				y	y	Max 15h	Down Cluster 1
D12Ertd647e	interferon, alpha-inducible protein 27	0.00	0.00	down	-1.38	-1.26	-1.31	-1.18	-1.23	*	*	Cytoplasm	other						Max 03h	Down Cluster 2
Dapk2	death-associated protein kinase 2	0.04	0.02	up	-1.02	1.07	1.35	1.01	-1.04	*		Cytoplasm	kinase					y	Max 09h	UP Cluster 1
Dbp	D site of albumin promoter (albumin D-box) binding protein	0.00	0.00	down	-1.37	-1.34	-1.39	-1.60	-1.22	*	*	Nucleus	transcription regulator			y	y	y	Max 15h	Down Cluster 1
Dcbld2	discoidin, CUB and LCCL domain containing 2	0.00	0.00	down	-1.08	-1.23	-1.11	-1.33	-1.19		*	Plasma Memb	other		up	y		y	Max 15h	Down Cluster 4
Dhtkd1|Sec61a2	dehydrogenase E1 and transketolase domain containing 1	0.00	0.00	up	1.01	1.30	1.11	1.14	1.07	*		Unknown	enzyme		down				Max 06h	UP Cluster 3
Disp1	dispatched homolog 1 (Drosophila)	0.03	0.01	up	-1.01	-1.11	-1.09	1.28	-1.02		*	Unknown	transporter			y		y	Max 15h	UP Cluster 4
Dmgdh	dimethylglycine dehydrogenase	0.00	0.00	down	-1.10	-1.43	-1.47	-1.66	-1.40	*		Cytoplasm	enzyme			y		y	Max 15h	Down Cluster 4
Dnajb5	DnaJ (Hsp40) homolog, subfamily B, member 5	0.00	0.00	up	1.14	1.57	1.39	1.29	1.18	*	*	Unknown	other	*	down	y	y	y	Max 06h	UP Cluster 3
Doc2g	double C2, gamma pseudogene	0.02	0.01	down	1.06	-1.02	1.06	-1.30	-1.08	*		Nucleus	other			y		y	Max 15h	Down Cluster 4
Dot1l	DOT1-like, histone H3 methyltransferase (S. cerevisiae)	0.01	0.00	up	1.17	1.24	1.29	1.20	1.09	*		Nucleus	phosphatase		down	y		y	Max 09h	UP Cluster 1
Dusp6	dual specificity phosphatase 6	0.00	0.00	up	1.48	1.55	1.51	1.45	1.31	*	*	Cytoplasm	phosphatase	*	down		y	y	Max 06h	UP Cluster 1
Edg3	sphingosine-1-phosphate receptor 3	0.00	0.00	up	1.29	1.03	1.17	1.25	1.10		*	Plasma Memb	G-protein coupled re		up			y	Max 03h	UP Cluster 5
Egr2	early growth response 2	0.03	0.02	up	1.90	1.72	1.23	1.18	1.18		*	Nucleus	transcription r	*	*	y	y	y	Max 03h	UP Cluster 5
Egr3	early growth response 3	0.02	0.01	up	1.46	1.42	1.37	1.08	1.04	*	*	Nucleus	transcription r	*	down	*	y		y	Max 03h	UP Cluster 1
Ehf	ets homologous factor	0.00	0.00	down	-1.30	-1.48	-1.61	-1.00	-1.42	*		Nucleus	transcription regulator				y		Max 09h	Down Cluster 5
Enc1	ectodermal-neural cortex (with BTB-like domain)	0.00	0.00	up	1.12	1.25	1.34	1.27	1.20	*	*	Nucleus	peptidase			y		y	Max 09h	UP Cluster 1
Enpp2	ectonucleotide pyrophosphatase/phosphodiesterase 2	0.02	0.01	down	-1.14	-1.17	-1.09	-1.51	-1.20	*	*	Plasma Memb	enzyme					y	Max 15h	Down Cluster 3
Ext1	exostoses (multiple) 1	0.02	0.01	up	1.36	1.07	1.20	1.03	-1.07	*		Cytoplasm	enzyme	*		y		y	Max 03h	UP Cluster 5
Fbxw5	F-box and WD repeat domain containing 5	0.01	0.00	down	-1.37	-1.22	1.01	-1.00	1.12	*		Cytoplasm	other		down				Max 03h	Down Cluster 2

Fndc5	fibronectin type III domain containing 5	0.01	0.00	down	-1.27	-1.28	-1.22	-1.33	-1.19	*		Unknown	other		down		y		y	Max 15h	Down Cluster 1
Fosl2	FOS-like antigen 2	0.00	0.00	up	1.68	1.78	1.49	1.12	1.06	*	*	Nucleus	transcription r	*				y	y	Max 06h	UP Cluster 5
Fstl5	follistatin-like 5	0.00	0.00	up	1.03	1.19	1.33	1.12	1.17		*	Extracellular S	other				y	y		Max 09h	UP Cluster 1
Fxyd6	FXYD domain containing ion transport regulator 6	0.01	0.00	up	1.41	1.36	1.25	1.24	1.43	*	*	Plasma Memb	ion channel			*	y		y	Max 24h	UP Cluster 2
Fzd3	frizzled homolog 3 (Drosophila)	0.00	0.00	up	1.19	1.15	1.32	1.32	1.20	*	*	Plasma Memb	G-protein cou	*			y		y	Max 15h	UP Cluster 1
Galnt13	UDP-N-acetyl-alpha-D-galactosamine:polypeptide N-acetylgala	0.01	0.00	down	-1.13	-1.10	-1.15	-1.30	-1.22		*	Cytoplasm	enzyme		up					Max 15h	Down Cluster 1
Gap43	growth associated protein 43	0.00	0.00	up	1.28	1.35	1.27	1.31	1.64	*	*	Plasma Memb	other				y		y	Max 24h	UP Cluster 2
Garnl3	GTPase activating Rap/RanGAP domain-like 3	0.01	0.00	down	-1.27	-1.29	-1.26	-1.39	-1.15	*	*	Unknown	other							Max 15h	Down Cluster 1
Gcnt2	glucosaminyl (N-acetyl) transferase 2, I-branching enzyme (I bl	0.00	0.00	up	1.14	1.19	1.21	1.27	1.28		*	Cytoplasm	enzyme		down		y		y	Max 24h	UP Cluster 2
Gfra2	GDNF family receptor alpha 2	0.00	0.00	up	1.05	1.29	1.50	1.44	1.27	*	*	Plasma Memb	transmembrane rece		down		y	y	y	Max 09h	UP Cluster 1
Glrx	glutaredoxin (thioltransferase)	0.01	0.00	down	-1.30	-1.33	-1.24	-1.18	-1.14	*	*	Cytoplasm	enzyme				y		y	max 06h	Down Cluster 2
Gng4	guanine nucleotide binding protein (G protein), gamma 4	0.00	0.00	up	1.22	1.47	1.49	1.40	1.34	*	*	Plasma Memb	enzyme		down		y		y	Max 09h	UP Cluster 3
Gpr108	G protein-coupled receptor 108	0.02	0.01	down	-1.22	-1.02	-1.04	-1.37	-1.02	*		Plasma Memb	G-protein coupled receptor				y		y	Max 15h	Down Cluster 1
Gpr115	G protein-coupled receptor 115	0.01	0.00	up	-1.03	-1.05	1.42	1.35	1.09	*	*	Plasma Memb	G-protein coupled receptor						y	Max 09h	UP Cluster 7
Gpr126	G protein-coupled receptor 126	0.00	0.00	down	-1.01	-1.37	-1.34	-1.64	-1.35	*		Plasma Memb	G-protein coupled receptor					y	y	Max 15h	Down Cluster 4
Gpr171	G protein-coupled receptor 171	0.01	0.00	down	-1.31	-1.13	-1.05	1.00	-1.06	*		Plasma Memb	G-protein coupled receptor				y		y	Max 03h	Down Cluster 2
Gpr21	G protein-coupled receptor 21	0.00	0.00	up	1.24	1.31	1.57	1.98	1.31	*	*	Plasma Memb	G-protein coupled receptor				y		y	Max 15h	UP Cluster 4
Gpr3	G protein-coupled receptor 3	0.03	0.01	up	1.47	1.19	1.22	1.20	1.10	*	**	Plasma Memb	G-protein cou	*			y		y	Max 03h	UP Cluster 5
Gpr39	G protein-coupled receptor 39	0.00	0.00	up	1.69	1.78	1.58	1.55	1.76	*	*	Plasma Memb	G-protein cou	*			y		y	Max 06h	UP Cluster 2
Gpr83	G protein-coupled receptor 83	0.01	0.00	up	1.15	1.20	1.30	1.19	1.27		*	Plasma Memb	G-protein coupled receptor				y			Max 09h	UP Cluster 1
Grasp	GRP1 (general receptor for phosphoinositides 1)-associated scaf	0.00	0.00	up	1.36	1.92	1.26	1.27	1.24	*	*	Plasma Memb	other	*	down				y	Max 06h	UP Cluster 3
Grik1	glutamate receptor, ionotropic, kainate 1	0.00	0.00	up	1.28	1.65	1.59	1.28	1.14	*	*	Plasma Memb	ion channel				y			Max 06h	UP Cluster 3
Hgsnat	heparan-alpha-glucosaminide N-acetyltransferase	0.00	0.00	down	-1.26	-1.03	-1.10	-1.05	-1.04	*		Unknown	other							Max 03h	Down Cluster 2
Hkdc1	hexokinase domain containing 1	0.02	0.01	up	1.44	1.74	1.38	1.37	1.57	*		Unknown	kinase		down		y			Max 06h	UP Cluster 3
Hlf	hepatic leukemia factor	0.00	0.00	down	-1.31	-1.23	-1.17	-1.39	-1.27	*		Nucleus	transcription regulat		up		y		y	Max 15h	Down Cluster 1
Hmgcr	3-hydroxy-3-methylglutaryl-Coenzyme A reductase	0.00	0.00	up	1.20	1.26	1.30	1.17	1.12		*	Cytoplasm	enzyme							Max 09h	UP Cluster 1
Hnrpll	heterogeneous nuclear ribonucleoprotein L-like	0.00	0.00	up	1.04	1.22	1.45	1.03	1.04	*	*	Unknown	other	*					y	Max 09h	UP Cluster 1
Homer1	homer homolog 1 (Drosophila)	0.00	0.00	up	1.45	1.37	1.32	1.07	1.03	*	*	Plasma Memb	other	*	down		y	y	y	Max 03h	UP Cluster 1
Hpcal4	hippocalcin like 4	0.00	0.00	up	1.14	1.26	1.24	1.28	1.44	*	**	Unknown	other				y		y	Max 24h	UP Cluster 2
Hrh3	histamine receptor H3	0.00	0.00	down	-1.39	-1.22	-1.37	-1.42	-1.10	*	*	Plasma Memb	G-protein coupled receptor				y		y	Max 15h	Down Cluster 1
Hsph1	heat shock 105kDa/110kDa protein 1	0.01	0.00	up	1.08	1.16	1.29	-1.01	-1.01	*		Cytoplasm	other							Max 09h	UP Cluster 1
Htr2a	5-hydroxytryptamine (serotonin) receptor 2A	0.00	0.00	up	1.21	1.30	1.43	1.41	1.38	*	*	Plasma Memb	G-protein coupled receptor						y	Max 09h	UP Cluster 1
Ier5	immediate early response 5	0.02	0.01	up	1.09	1.34	1.32	1.11	1.08	*	*	Unknown	other	*	down	*	y		y	Max 06h	UP Cluster 3
Ifrd1	interferon-related developmental regulator 1	0.02	0.01	up	1.37	1.37	1.27	1.08	1.04	*	*	Nucleus	other	*					y	Max 03h	UP Cluster 1
Igfn1	immunoglobulin-like and fibronectin type III domain containing	0.00	0.00	up	1.74	1.82	1.72	2.38	1.92	*	**	Unknown	other							Max 15h	UP Cluster 4
Il12a	interleukin 12A (natural killer cell stimulatory factor 1, cytotoxi	0.00	0.00	up	1.18	1.34	1.24	-1.03	1.06	*		Extracellular S	cytokine							Max 06h	UP Cluster 1
Il1rapl2	interleukin 1 receptor accessory protein-like 2	0.00	0.00	up	1.68	1.32	1.39	1.32	1.68	*	*	Plasma Memb	transmembrane receptor				y			Max 03h	UP Cluster 2
Inhba	inhibin, beta A	0.00	0.00	up	1.73	1.58	1.80	1.34	1.25	*	**	Extracellular S	growth factor	*						Max 09h	UP Cluster 1
Jmjd4	jumonji domain containing 4	0.03	0.02	up	1.10	-1.07	-1.05	1.38	-1.05	*		Unknown	other				y		y	Max 15h	UP Cluster 4
Junb	jun B proto-oncogene	0.04	0.03	up	1.98	1.59	1.38	1.18	1.21		*	Nucleus	transcription r	*				y	y	Max 03h	UP Cluster 5
Kazald1	Kazal-type serine peptidase inhibitor domain 1	0.01	0.00	down	-1.40	-1.32	-1.46	-1.67	-1.39	*	*	Extracellular S	other				y		y	Max 15h	Down Cluster 1
Kcnab3	potassium voltage-gated channel, shaker-related subfamily, beta	0.00	0.00	down	-1.22	-1.22	-1.27	-1.30	-1.32	*	*	Plasma Memb	ion channel				y		y	Max 24h	Down Cluster 2
Kcnf1	potassium voltage-gated channel, subfamily F, member 1	0.00	0.00	up	1.86	1.85	1.94	1.84	1.89	*	*	Plasma Memb	ion channel		down		y		y	Max 09h	UP Cluster 1
Kcnj3	potassium inwardly-rectifying channel, subfamily J, member 3	0.00	0.00	down	-1.10	-1.17	-1.16	-1.22	-1.26	*		Plasma Memb	ion channel						y	Max 24h	Down Cluster 2
Kcnv1	potassium channel, subfamily V, member 1	0.00	0.00	up	1.32	1.31	1.29	1.36	1.21	*	*	Unknown	ion channel	*	down					Max 15h	UP Cluster 2
Krt9	keratin 9	0.00	0.00	down	-1.19	-1.17	-1.29	-1.34	-1.18		*	Cytoplasm	other							Max 15h	Down Cluster 2
Lhfp	lipoma HMGIC fusion partner	0.01	0.00	down	-1.29	-1.04	1.07	1.14	1.01	*		Unknown	other				y			Max 03h	Down Cluster 2
Lphn2|ENSMUSG000	latrophilin 2	0.02	0.01	down	-1.28	-1.23	-1.22	-1.37	-1.19	*	*	Plasma Memb	G-protein coupled receptor							Max 15h	Down Cluster 1
Lrfn2	leucine rich repeat and fibronectin type III domain containing 2	0.01	0.00	up	1.10	1.20	1.24	1.11	1.35	*	*	Unknown	other				y		y	Max 24h	UP Cluster 1
Lrrc57	leucine rich repeat containing 57	0.00	0.00	down	-1.46	-1.22	-1.20	-1.20	-1.13	*	*	Unknown	other							Max 03h	Down Cluster 2
Lrrtm1	leucine rich repeat transmembrane neuronal 1	0.00	0.00	up	1.12	1.13	1.13	1.25	1.28		*	Unknown	other	*	up		y			Max 24h	UP Cluster 2

Lrrtm3	leucine rich repeat transmembrane neuronal 3	0.01	0.00	up	1.25	1.29	1.11	1.24	1.22	*		Unknown	other		up-down	y			Max 06h	UP Cluster 2
Lrrtm4	leucine rich repeat transmembrane neuronal 4	0.01	0.00	up	1.16	1.19	1.34	1.05	1.52	*	*	Unknown	other					y	Max 24h	UP Cluster 6
Lrtm1	leucine-rich repeats and transmembrane domains 1	0.00	0.00	down	-1.11	-1.07	-1.06	-1.23	-1.27	*		Unknown	other			y		y	Max 24h	Down Cluster 2
Lsr	lipolysis stimulated lipoprotein receptor	0.01	0.00	down	1.10	1.03	-1.16	-1.32	-1.04	*		Nucleus	transcription regulator			y	y		Max 15h	Down Cluster 1
Lyz2|Lyz1	lysozyme (renal amyloidosis)	0.01	0.00	down	-1.02	1.00	1.06	-1.35	1.10		*	Extracellular S	enzyme						Max 15h	Down Cluster 3
Mab21l1	mab-21-like 1 (C. elegans)	0.02	0.01	down	1.05	1.14	-1.22	-1.39	-1.15		*	Unknown	other					y	Max 15h	Down Cluster 1
Mag	myelin associated glycoprotein	0.03	0.01	down	-1.01	1.01	-1.13	-1.31	-1.06	*		Plasma Memb	other			y		y	Max 15h	Down Cluster 1
Mapk4	mitogen-activated protein kinase 4	0.05	0.02	up	1.15	1.38	1.15	1.14	1.01	*	*	Cytoplasm	kinase		down	y			Max 06h	UP Cluster 3
March1	membrane-associated ring finger (C3HC4) 1	0.01	0.00	down	-1.29	-1.22	-1.36	-1.49	-1.22	*	*	Unknown	other			y	y		Max 15h	Down Cluster 1
Mcm6	minichromosome maintenance complex component 6	0.02	0.00	down	-1.22	-1.29	-1.54	-1.19	-1.10	*		Nucleus	enzyme			y		y	Max 09h	Down Cluster 5
Mical2	microtubule associated monoxygenase, calponin and LIM domai	0.01	0.00	up	1.05	1.20	1.32	1.10	1.12	*		Cytoplasm	other			y			Max 09h	UP Cluster 1
Midn	midnolin	0.00	0.00	up	-1.04	1.08	1.34	1.20	1.09	*		Nucleus	other			y		y	Max 09h	UP Cluster 1
Mme	membrane metallo-endopeptidase	0.01	0.00	down	1.03	-1.10	-1.16	-1.39	-1.29		*	Plasma Memb	peptidase		up		y	y	Max 15h	Down Cluster 1
Mrpl14	mitochondrial ribosomal protein L14	0.01	0.00	down	-1.45	-1.11	-1.21	-1.05	1.04	*	*	Unknown	other			y	y		Max 03h	Down Cluster 2
Mtus1	mitochondrial tumor suppressor 1	0.04	0.02	down	-1.23	-1.43	-1.24	-1.31	-1.15	*		Unknown	other		up	y		y	max 06h	Down Cluster 4
Mylk3	myosin light chain kinase 3	0.00	0.00	up	1.78	1.58	1.98	1.68	1.06	*	*	Unknown	kinase						Max 09h	UP Cluster 7
Ncald	neurocalcin delta	0.02	0.01	up	1.15	1.37	1.26	1.12	1.36	*	*	Cytoplasm	other		down	y	y		Max 06h	UP Cluster 1
Necab1	N-terminal EF-hand calcium binding protein 1	0.00	0.00	up	1.36	1.47	1.51	1.36	1.91	*	*	Cytoplasm	other						Max 24h	UP Cluster 6
Necab3	N-terminal EF-hand calcium binding protein 3	0.02	0.01	down	-1.25	-1.21	-1.26	-1.21	-1.33	*		Cytoplasm	other						Max 24h	Down Cluster 2
Nefh	neurofilament, heavy polypeptide	0.01	0.00	down	-1.41	-1.20	-1.20	-1.16	-1.08	*	*	Cytoplasm	other			y		y	Max 03h	Down Cluster 2
Nefl	neurofilament, light polypeptide	0.01	0.00	up	1.15	1.36	1.26	1.16	1.16	*	*	Cytoplasm	other					y	Max 06h	UP Cluster 3
Neurod1	neurogenic differentiation 1	0.01	0.00	down	-1.13	-1.38	-1.19	-1.30	-1.15		*	Nucleus	transcription regulat		up			y	max 06h	Down Cluster 4
Nfic	nuclear factor I/C (CCAAT-binding transcription factor)	0.03	0.01	down	-1.29	-1.24	-1.13	-1.19	-1.12	*	*	Nucleus	transcription regulator			y	y	y	Max 03h	Down Cluster 1
Nfic	nuclear factor I/C (CCAAT-binding transcription factor)	0.00	0.00	down	-1.32	-1.06	-1.21	-1.02	-1.20	*		Nucleus	transcription regulator						Max 03h	Down Cluster 2
Nfil3|LOC100046232	nuclear factor, interleukin 3 regulated	0.00	0.00	up	1.23	1.40	1.33	1.38	1.15	*	*	Nucleus	transcription r	*					Max 06h	UP Cluster 2
Npas4	neuronal PAS domain protein 4	0.00	0.00	up	2.48	2.54	2.18	1.65	1.69	*	*	Nucleus	transcription r	*		y	y	y	Max 06h	UP Cluster 5
Nptx2	neuronal pentraxin II	0.00	0.00	up	2.50	4.03	2.62	1.75	2.07	*		Extracellular S	other	*	down			y	Max 06h	UP Cluster 11
Nr1d2	nuclear receptor subfamily 1, group D, member 2	0.00	0.00	down	-1.12	-1.23	-1.23	-1.27	-1.14	*		Nucleus	ligand-dependent nu		up	y		y	Max 15h	Down Cluster 2
Nr4a1	nuclear receptor subfamily 4, group A, member 1	0.00	0.00	up	1.69	2.02	1.59	1.39	1.08	*	*	Nucleus	ligand-depend.	*		y	y	y	Max 06h	UP Cluster 3
Nr4a2	nuclear receptor subfamily 4, group A, member 2	0.01	0.00	up	2.84	2.08	1.31	1.18	1.02	*	*	Nucleus	ligand-depend.	*	down	y		y	Max 03h	UP Cluster 5
Nrd1	nardilysin (N-arginine dibasic convertase)	0.00	0.00	up	1.04	1.15	1.34	-1.04	1.05	*		Unknown	peptidase		down			y	Max 09h	UP Cluster 1
Nrn1	neuritin 1	0.01	0.00	up	1.27	1.36	1.38	1.27	1.12	*	*	Cytoplasm	other	*	down			y	Max 09h	UP Cluster 1
Nrxn3	neurexin 3	0.00	0.00	up	1.05	1.25	1.39	1.34	1.15	*		Plasma Memb	transporter		down				Max 09h	UP Cluster 1
Nt5c3l	5'-nucleotidase, cytosolic III-like	0.04	0.02	down	-1.04	-1.17	-1.18	-1.62	-1.10	*	*	Unknown	other			y		y	Max 15h	Down Cluster 3
Ocm|LOC100048547	oncomodulin 2	0.00	0.00	up	1.13	1.08	1.16	1.45	1.16	*	*	Unknown	other						Max 15h	UP Cluster 4
Osbpl1a	oxysterol binding protein-like 1A	0.01	0.00	down	-1.07	-1.07	-1.09	-1.41	-1.08	*		Cytoplasm	other						Max 15h	Down Cluster 1
Palm2|Akap2|Palm2-a	paralemmin 2	0.01	0.00	down	-1.05	-1.29	-1.19	-1.49	-1.09	*	*	Plasma Memb	other						Max 15h	Down Cluster 4
Pcdh15	protocadherin 15	0.00	0.00	up	1.21	1.29	2.43	2.42	1.85	*	*	Plasma Memb	other			y			Max 09h	UP Cluster 7
Pcdh17	protocadherin 17	0.02	0.00	up	1.39	1.29	1.12	1.07	1.11	*	*	Unknown	other		up *	y		y	Max 03h	UP Cluster 5
Pck2	phosphoenolpyruvate carboxykinase 2 (mitochondrial)	0.00	0.00	down	-1.45	-1.28	-1.21	-1.42	1.03	*		Cytoplasm	kinase			y		y	Max 03h	Down Cluster 1
Pcp4	Purkinje cell protein 4	0.00	0.00	up	1.22	1.31	1.10	1.46	1.47	*	*	Cytoplasm	other						Max 24h	UP Cluster 2
Pcsk1	proprotein convertase subtilisin/kexin type 1	0.00	0.00	up	2.27	1.42	1.31	1.14	-1.01	*	*	Extracellular S	peptidase	*	down	y	y		Max 03h	UP Cluster 5
Pcsk1n	proprotein convertase subtilisin/kexin type 1 inhibitor	0.02	0.01	down	-1.37	-1.10	-1.20	-1.18	-1.08	*	*	Extracellular S	other		down	y		y	Max 03h	Down Cluster 2
Pde1a	phosphodiesterase 1A, calmodulin-dependent	0.00	0.00	up	1.41	1.71	1.51	1.17	1.93	*	*	Cytoplasm	enzyme				y		Max 24h	UP Cluster 6
Pdgfrl	platelet-derived growth factor receptor-like	0.01	0.00	up	1.00	1.05	1.21	1.66	-1.09	*	*	Plasma Memb	kinase			y			Max 15h	UP Cluster 4
Per3	period homolog 3 (Drosophila)	0.01	0.00	down	-1.13	-1.11	-1.19	-1.42	1.03	*		Nucleus	other			y		y	Max 15h	Down Cluster 1
Pi4ka	phosphatidylinositol 4-kinase, catalytic, alpha	0.00	0.00	up	1.05	1.20	1.34	1.11	1.07	*		Cytoplasm	kinase						Max 09h	UP Cluster 1
Pigl	phosphatidylinositol glycan anchor biosynthesis, class L	0.02	0.01	up	-1.12	-1.11	1.00	1.38	1.14	*		Cytoplasm	enzyme						Max 15h	UP Cluster 4
Pik3ip1	phosphoinositide-3-kinase interacting protein 1	0.02	0.01	down	-1.25	-1.63	-1.27	-1.41	-1.04	*	*	Unknown	other						max 06h	Down Cluster 4
Pip5k1b	phosphatidylinositol-4-phosphate 5-kinase, type I, beta	0.00	0.00	up	1.29	1.42	1.68	1.17	1.07	*		Cytoplasm	kinase			y		y	Max 09h	UP Cluster 1
Pkmyt1	protein kinase, membrane associated tyrosine/threonine 1	0.00	0.00	down	-1.09	-1.18	-1.14	-1.26	-1.05	*		Cytoplasm	kinase					y	Max 15h	Down Cluster 1

Polr3g	polymerase (RNA) III (DNA directed) polypeptide G (32kD)	0.01	0.00	down	1.00	-1.20	-1.56	-1.24	-1.06	*		Nucleus	enzyme			y		y	Max 09h	Down Cluster 5
Pp11r	26 serine protease	0.01	0.00	up	1.29	1.35	1.31	1.39	1.58	*	*	Unknown	peptidase			y		y	Max 24h	UP Cluster 2
Ppm1h	protein phosphatase 1H (PP2C domain containing)	0.00	0.00	up	1.29	1.38	1.35	1.11	1.23	*		Unknown	phosphatase			y		y	Max 06h	UP Cluster 1
Ppme1	protein phosphatase methylesterase 1	0.02	0.01	up	1.32	1.34	1.34	1.16	1.01	*	*	Unknown	enzyme			y	y	y	Max 09h	UP Cluster 1
Praf2	PRA1 domain family, member 2	0.02	0.01	down	-1.30	1.06	-1.03	-1.11	-1.08	*	*	Unknown	other			y			Max 03h	Down Cluster 2
Prim1	primase, DNA, polypeptide 1 (49kDa)	0.01	0.00	down	-1.26	-1.20	-1.20	-1.43	-1.10	*	*	Nucleus	enzyme		up				Max 15h	Down Cluster 1
Prkg1	protein kinase, cGMP-dependent, type I	0.00	0.00	down	-1.14	-1.16	-1.25	-1.33	-1.23		*	Cytoplasm	kinase		up	y		y	Max 15h	Down Cluster 1
Prkg2	protein kinase, cGMP-dependent, type II	0.02	0.01	up	1.32	1.27	1.29	1.08	-1.02		*	Cytoplasm	kinase		down	y		y	Max 03h	UP Cluster 1
Ptgs2	prostaglandin-endoperoxide synthase 2 (prostaglandin G/H syntl	0.00	0.00	up	2.96	2.65	2.56	1.93	1.81	*	*	Cytoplasm	enzyme	*	down	y		y	Max 03h	UP Cluster 1
Pth2r	parathyroid hormone 2 receptor	0.00	0.00	down	-1.16	-1.51	-1.75	-1.52	-1.42	*	*	Plasma Memb	G-protein coupled receptor						Max 09h	Down Cluster 5
Ptprk	protein tyrosine phosphatase, receptor type, K	0.00	0.00	up	1.14	1.29	1.38	1.26	1.28	*	*	Plasma Memb	phosphatase		up	y		y	Max 09h	UP Cluster 1
Ptprn	protein tyrosine phosphatase, receptor type, N	0.05	0.03	up	1.11	1.26	1.31	1.25	1.15		*	Plasma Memb	phosphatase		down			y	Max 09h	UP Cluster 1
Rab30	RAB30, member RAS oncogene family	0.00	0.00	down	-1.41	-1.21	-1.23	-1.50	-1.17	*		Cytoplasm	enzyme						Max 15h	Down Cluster 1
Rasl11b	RAS-like, family 11, member B	0.00	0.00	up	1.11	1.35	1.27	1.18	1.04		*	Unknown	enzyme			y		y	Max 06h	UP Cluster 3
Rassf3	Ras association (RalGDS/AF-6) domain family member 3	0.00	0.00	down	-1.11	-1.11	-1.13	-1.09	-1.29	*		Unknown	other		down	y		y	Max 24h	Down Cluster 2
Rbp4	retinol binding protein 4, plasma	0.00	0.00	up	1.27	1.89	2.06	2.13	1.57	*	*	Extracellular S	transporter		down			y	Max 15h	UP Cluster 3
Rgs2	regulator of G-protein signaling 2, 24kDa	0.00	0.00	up	1.56	1.54	1.30	-1.06	1.12	*	*	Nucleus	other	*		y		y	Max 03h	UP Cluster 5
Rgs8	regulator of G-protein signaling 8	0.00	0.00	up	1.16	1.33	1.53	1.21	1.38	*		Unknown	other			y		y	Max 09h	UP Cluster 1
Rnd3	Rho family GTPase 3	0.00	0.00	up	1.85	1.94	1.74	1.60	1.26	*	*	Cytoplasm	enzyme	*	down	y		y	Max 06h	UP Cluster 3
Rnf152	ring finger protein 152	0.04	0.02	down	-1.16	-1.29	-1.40	-1.51	-1.16	*	**	Unknown	other			y	y	y	Max 15h	Down Cluster 1
Rnf2	ring finger protein 2	0.02	0.01	down	-1.12	-1.11	-1.05	-1.37	-1.07		*	Nucleus	transcription regulat		up			y	Max 15h	Down Cluster 1
Rprm	reprimo, TP53 dependent G2 arrest mediator candidate	0.01	0.00	up	1.27	1.22	1.15	1.23	1.23	*		Cytoplasm	other			y		y	Max 03h	UP Cluster 2
Rps6ka5	ribosomal protein S6 kinase, 90kDa, polypeptide 5	0.01	0.00	down	-1.15	-1.29	-1.28	-1.49	-1.30		*	Nucleus	kinase	*	up	y		y	Max 15h	Down Cluster 1
Rtn4	reticulon 4	0.01	0.00	down	-1.04	-1.09	-1.01	-1.29	-1.14	*		Cytoplasm	other			y		y	Max 15h	Down Cluster 4
Rtp4	receptor (chemosensory) transporter protein 4	0.01	0.00	down	-1.26	-1.11	-1.17	1.02	1.00		*	Plasma Memb	other					y	Max 03h	Down Cluster 2
Rwdd2a	RWD domain containing 2A	0.00	0.00	down	-1.20	-1.22	-1.06	-1.46	-1.05	*	*	Unknown	other						Max 15h	Down Cluster 3
S100a1	S100 calcium binding protein A1	0.01	0.00	down	-1.23	-1.10	-1.03	-1.55	-1.05	*	*	Cytoplasm	other			y			Max 15h	Down Cluster 3
Scg2	secretogranin II (chromogranin C)	0.00	0.00	up	1.64	1.61	1.62	1.72	1.44	*	*	Extracellular S	cytokine	*	down				Max 15h	UP Cluster 2
Scn2b	sodium channel, voltage-gated, type II, beta	0.01	0.00	down	-1.12	-1.18	-1.25	-1.16	-1.08		*	Plasma Memb	ion channel			y			Max 09h	Down Cluster 2
Scn3b	sodium channel, voltage-gated, type III, beta	0.01	0.00	up	1.90	1.76	1.86	1.99	2.22	*	*	Plasma Memb	ion channel		up				Max 24h	UP Cluster 2
Scn7a	sodium channel, voltage-gated, type VII, alpha	0.00	0.00	up	3.61	2.70	2.68	4.14	4.81	*	*	Plasma Memb	ion channel			y		y	Max 24h	UP Cluster 9
Scnn1a	sodium channel, nonvoltage-gated 1 alpha	0.01	0.00	down	-1.29	-1.23	-1.25	-1.42	-1.27		*	Plasma Memb	ion channel					y	Max 15h	Down Cluster 1
Sertad4	SERTA domain containing 4	0.00	0.00	down	-1.28	-1.22	-1.06	-1.32	-1.13		*	Unknown	other			y	y	y	Max 15h	Down Cluster 1
Setd7	SET domain containing (lysine methyltransferase) 7	0.02	0.01	down	-1.11	-1.05	-1.08	-1.31	-1.11	*	*	Nucleus	enzyme			y		y	Max 15h	Down Cluster 1
Sgsm1	small G protein signaling modulator 1	0.02	0.00	up	1.32	1.49	1.63	1.54	1.26	*	*	Unknown	other						Max 09h	UP Cluster 1
Slc24a3	solute carrier family 24 (sodium/potassium/calcium exchanger),	0.01	0.00	up	1.13	1.11	1.11	1.34	1.29		*	Plasma Memb	transporter		down *	y	y		Max 15h	UP Cluster 2
Slc44a2	solute carrier family 44, member 2	0.04	0.02	down	-1.08	-1.19	-1.02	-1.62	-1.19	*		Extracellular S	transporter			y		y	Max 15h	Down Cluster 3
Slc6a17	solute carrier family 6, member 17	0.01	0.00	up	1.13	1.32	1.35	1.22	1.14	*	*	Unknown	transporter		down	y		y	Max 09h	UP Cluster 3
Smoc2	SPARC related modular calcium binding 2	0.00	0.00	down	-1.02	-1.23	-1.08	-1.61	-1.14	*		Extracellular S	other			y		y	Max 15h	Down Cluster 3
Snf1lk2	salt-inducible kinase 2	0.01	0.00	up	1.51	1.22	1.22	1.07	1.06	*	*	Cytoplasm	kinase	*	down	y	y		Max 03h	UP Cluster 5
Sorcs3	sortilin-related VPS10 domain containing receptor 3	0.00	0.00	up	1.44	2.57	3.36	1.73	1.50	*	*	Nucleus	transporter		down *	y	y	y	Max 09h	UP Cluster 10
Spon1	spondin 1, extracellular matrix protein	0.00	0.00	up	1.33	1.36	1.17	1.22	1.49	*	*	Extracellular S	other		up	y	y	y	Max 24h	UP Cluster 2
Spred2	sprouty-related, EVH1 domain containing 2	0.01	0.00	up	1.35	1.35	1.31	1.15	1.21	*		Extracellular S	cytokine			y		y	Max 03h	UP Cluster 1
Spred2	sprouty-related, EVH1 domain containing 2	0.00	0.00	up	1.27	1.26	1.28	1.29	1.25	*	*	Extracellular S	cytokine			y			Max 15h	UP Cluster 2
St6galnac6	ST6 (alpha-N-acetyl-neuraminyl-2,3-beta-galactosyl-1,3)-N-ace	0.01	0.00	down	-1.02	-1.04	-1.15	-1.48	-1.20	*	*	Cytoplasm	enzyme			y		y	Max 15h	Down Cluster 1
Stard8	StAR-related lipid transfer (START) domain containing 8	0.00	0.00	up	1.40	1.54	1.65	1.39	1.13	*	*	Unknown	other					y	Max 09h	UP Cluster 1
Stk32c	serine/threonine kinase 32C	0.00	0.00	up	1.16	1.07	1.13	1.29	1.36	*		Unknown	kinase			y		y	Max 24h	UP Cluster 2
Sycp3	synaptonemal complex protein 3	0.01	0.00	down	-1.19	1.03	1.05	-1.39	-1.08		*	Nucleus	other			y	y		Max 15h	Down Cluster 3
Synj2	synaptojanin 2	0.01	0.00	up	1.20	1.30	1.30	1.38	1.22	*	*	Cytoplasm	phosphatase		down	y		y	Max 15h	UP Cluster 2
Tagln2|Ccdc19	transgelin 2	0.03	0.01	down	-1.12	1.05	-1.18	-1.51	-1.33	*	*	Cytoplasm	other						Max 15h	Down Cluster 1
Tef	thyrotrophic embryonic factor	0.01	0.00	down	-1.16	-1.14	-1.20	-1.32	-1.06	*		Nucleus	transcription regulator					y	Max 15h	Down Cluster 1

Tgm3	transglutaminase 3 (E polypeptide, protein-glutamine-gamma-gl	0.00	0.00	down	-1.17	-1.06	-1.48	-1.29	-1.11	*		Cytoplasm	enzyme			y	Max 09h	Down Cluster 5
Tle6	transducin-like enhancer of split 6 (E(sp1) homolog, Drosophila	0.00	0.00	down	-1.56	-1.22	-1.31	-1.22	-1.11	*		Nucleus	other			y	Max 03h	Down Cluster 2
Tmprss7	transmembrane protease, serine 7	0.00	0.00	down	-1.57	-1.27	-1.49	-1.36	-1.30	*		Unknown	other			y	Max 03h	Down Cluster 2
Tnnc1	troponin C type 1 (slow)	0.00	0.00	up	3.22	3.58	2.63	3.96	4.72	*	*	Cytoplasm	other	down	y	y	Max 24h	UP Cluster 8
Tnnt2	troponin T type 2 (cardiac)	0.03	0.01	up	1.21	1.16	1.08	1.18	1.37	*	*	Cytoplasm	other		y	y	Max 24h	UP Cluster 2
Trpc3	transient receptor potential cation channel, subfamily C, membe	0.00	0.00	up	1.42	1.42	1.36	1.33	1.25	*	*	Plasma Memb	ion channel		y	y	Max 06h	UP Cluster 2
Trpc5|Mageb16|24100	transient receptor potential cation channel, subfamily C, membe	0.01	0.00	up	1.14	1.13	1.21	-1.05	1.57	*	*	Plasma Memb	ion channel				Max 24h	UP Cluster 6
Trpc6	transient receptor potential cation channel, subfamily C, membe	0.00	0.00	up	1.52	2.32	1.93	1.47	1.77	*	*	Plasma Memb	ion channel				Max 06h	UP Cluster 3
Trpv6	transient receptor potential cation channel, subfamily V, membe	0.01	0.00	down	-1.13	-1.34	-1.23	1.07	-1.04	*		Plasma Memb	ion channel		y	y	max 06h	Down Cluster 5
Ttc9c	tetratricopeptide repeat domain 9C	0.00	0.00	down	-1.26	-1.04	-1.15	-1.15	-1.04		*	Unknown	other		y	y	Max 03h	Down Cluster 2
Ttl	tubulin tyrosine ligase	0.00	0.00	up	1.28	1.17	1.09	1.07	1.02	*		Cytoplasm	enzyme	down			Max 03h	UP Cluster 2
Txnl4b	thioredoxin-like 4B	0.01	0.00	down	-1.22	-1.11	1.03	-1.37	-1.02	*	*	Nucleus	enzyme		y	y	Max 15h	Down Cluster 3
Tyw1	tRNA-yW synthesizing protein 1 homolog (S. cerevisiae)	0.01	0.00	down	-1.21	-1.18	-1.24	-1.45	-1.12	*		Unknown	other			y	Max 15h	Down Cluster 1
Uck2	uridine-cytidine kinase 2	0.02	0.01	up	1.11	1.28	1.43	1.13	1.02	*	*	Cytoplasm	kinase	down		y	Max 09h	UP Cluster 1
Vamp1|E130112N10R	vesicle-associated membrane protein 1 (synaptobrevin 1)	0.04	0.02	down	-1.32	-1.09	-1.16	-1.49	-1.28	*		Plasma Memb	transporter	down			Max 15h	Down Cluster 1
Wrb	tryptophan rich basic protein	0.00	0.00	down	1.13	1.07	1.02	-1.35	-1.04	*		Extracellular S	other			y	Max 15h	Down Cluster 1
Zbtb1	zinc finger and BTB domain containing 1	0.02	0.01	up	1.29	1.62	1.17	1.09	1.11	*	*	Nucleus	other		y	y	Max 06h	UP Cluster 3
Zbtb20	zinc finger and BTB domain containing 20	0.03	0.01	down	-1.17	-1.13	-1.15	-1.32	-1.14	*		Nucleus	other				Max 15h	Down Cluster 1
Zdhhc23	zinc finger, DHHC-type containing 23	0.00	0.00	up	1.41	1.18	1.12	1.16	1.57	*	**	Unknown	other			y	Max 24h	UP Cluster 2
Zfp758|1300003B13R	RIKEN cDNA 1300003B13 gene	0.03	0.01	down	-1.10	1.02	-1.02	-1.35	-1.10		*	Unknown	other				Max 15h	Down Cluster 1
327987	mediator complex subunit 13	0.01	0.00	down	-1.34	-1.32	-1.10	-1.14	-1.16	*	*	Nucleus	transcription regulator				Max 03h	Down Cluster 2

When the corresponding fold change was ≥1.25 and was found significant for the corresponding comparison by Welch's ANOVA followed by Tukey HSD with correction for multiple comparisons (Benjamini Hochberg false discovery rate), the cell was color coded according to the scale bar below (N.S. stands for not significantly regulated and/or do not pass threshold). The minus sign indicates down-regulation.

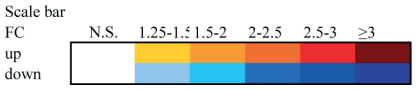

Appendix 3. List of genetic disorders and neurological disorders associated with the list of genes differentially regulated by whisker stimulation according to Ingenuity Pathway Analysis.

Genetic Disorder	p-value	# Genes
schizophrenia	1.17E-08	25
schizophrenia of humans	5.04E-05	11
genetic disorder	2.57E-06	130
genetic disorder of humans	6.38E-05	16
coronary artery disease	2.97E-05	35
amyotrophic lateral sclerosis	5.49E-05	21
amyotrophic lateral sclerosis of mice	7.23E-03	2
Alzheimer's disease	6.86E-05	28
obsessive-compulsive disorder	1.21E-04	6
non-insulin-dependent diabetes mellitus	1.35E-04	37
Huntington's disease	3.15E-04	21
Crohn's disease	4.06E-04	31
inflammatory bowel disease	6.12E-04	32
progressive supranuclear palsy	1.23E-03	4
bipolar affective disorder	1.37E-03	28
multiple sclerosis	1.54E-03	9
postmenopausal osteoporosis	4.58E-03	2
migraines	9.10E-03	5
familial amyotrophic lateral sclerosis	1.04E-02	2
Parkinson's disease	1.18E-02	16
Usher Syndrome, type 1F	1.32E-02	1
hypogonadotropic hypogonadism of humans	1.32E-02	1

Neurological Disease	p-value	# Genes
schizophrenia	1.17E-08	25
schizophrenia of humans	5.04E-05	11
neurological disorder	1.55E-08	96
neurological disorder of mammalia	3.21E-05	25
neurological disorder of humans	8.33E-05	14
neurological disorder of rodents	1.09E-02	14
neuropathy	7.54E-07	40
progressive motor neuropathy	1.73E-06	38
neurodegenerative disorder	4.41E-06	32
amyotrophic lateral sclerosis	5.49E-05	21
amyotrophic lateral sclerosis of mice	7.23E-03	2
Alzheimer's disease	6.86E-05	28
obsessive-compulsive disorder	1.21E-04	6
Huntington's disease	3.15E-04	21
progressive supranuclear palsy	1.23E-03	4
bipolar affective disorder	1.37E-03	28
multiple sclerosis	1.54E-03	9
cerebral hemorrhage	1.86E-03	3
tremor of mice	3.27E-03	3
subarachnoid hemorrhage	3.46E-03	2
polyneuropathy	4.17E-03	3
loss of axons	8.76E-03	2
neurodegeneration of hippocampus	8.76E-03	2
migraines	9.10E-03	5
deafness of mice	1.04E-02	2
familial amyotrophic lateral sclerosis	1.04E-02	2
Parkinson's disease	1.18E-02	16
Usher Syndrome, type 1F	1.32E-02	1
atrophy of motor axons	1.32E-02	1
peripheral neuropathy of humans	1.32E-02	1

Appendix 4. List of genes that are found regulated after whisker stimulation and are related to neurological diseases or to genetic diseases according to Ingenuity Pathway Analysis

Category	Neurological Disease	Genetic Disorder
p-value	1.55E-08	2.57E-06
# Genes	96	130
# Genes	ADCYAP1, APOD, ARHGAP26, ARPP-21, BDNF, BGN, C8ORF46, CA4, CACNG2, CCDC3, CDKN1B, CHL1, COCH, CPNE4, CPNE5, CREM, CTNNA1, DBP, DUSP6, EGR2, EGR3, ENPP2, EXT1, FAM19A1, FAM5C, FAM70A, FSTL5, FXYD6, FZD3, GALNT13, GAP43, GARNL3, GCNT2, GFRA2, GLRX, GNG4, GPR83, GRIK1, HMGCR, HOMER1, HRH3, HSPH1, HTR2A, IER5, IGFN1, IL12A, IL1RAPL2, JUNB, LPHN2, LRFN2, MAG, MICAL2, MME, NEFH, NEFL, NEUROD1, NR4A1, NR4A2, NRXN3, OSBPL1A, P11, PCDH15, PCP4, PCSK1, PDE1A, PER3, PI4KA, PIK3IP1, PIP5K1B, PPM1H, PRKG1, PTGS2, RBP4, RGS8, RTN4, S100A1, SCG2, SCN2B, SCN3B, SCN7A, SGSM1, SLC24A3, SORCS3, SPON1, SPRED2, STARD8, STK32C, SYNJ2, TNNT2, TRPC5, TRPC6, TYW1, UCK2, VAMP1, ZBTB20, ZDHHC23	ADAM19, ALG12, ANTXR1, APOD, ARHGAP26, ARPP-21, ASB13, BDNF, BGN, C8ORF46, C8ORF85, CA4, CACNG2, CCDC3, CDKN1A, CDKN1B, CHL1, COCH, CPNE4, CPNE5, CREM, CYP11A1, CYP39A1, DAPK2 (includes EG:23604), DBP, DISP1, DMGDH, DUSP6, EGR2, EGR3, ENC1, ENPP2, EXT1, FAM19A1, FAM5C, FAM70A, FOSL2, FSTL5, FXYD6, FZD3, GALNT13, GAP43, GARNL3, GCNT2, GFRA2, GLRX, GNG4, GPR39, GPR83, GPR115, GRIK1, HGSNAT, HMGCR, HOMER1, HPCAL4, HRH3, HSPH1, HTR2A, IER5, IGFN1, IKIP, IL12A, IL1RAPL2, JUNB, KIAA0319L, LHFP, LPHN2, LRFN2, LRRTM3, LYZ, MAG, MCM6, MICAL2, MME, MTUS1, NCALD, NEFH, NEFL, NEUROD1, NFIC, NR4A1, NR4A2, NRXN3, OSBPL1A, P11, PCDH15, PCP4, PCSK1, PDE1A, PDGFRL, PER3, PI4KA, PIGL, PIK3IP1, PIP5K1B, PPM1H, PRKG1, PRKG2, PTGS2, PTH2R, RASSF3, RBP4, RNF152, RPS6KA5, RTN4, S100A1, SCG2, SCN2B, SCN3B, SCN7A, SCNN1A, SGSM1, SIK2, SLC24A3, SORCS3, SPON1, SPRED2, ST6GALNAC6, STARD8, STK32C, SYNJ2, TNNT2, TRPC5, TRPC6, TYW1, UCK2, VAMP1, VWC2L, ZBTB20, ZDHHC23

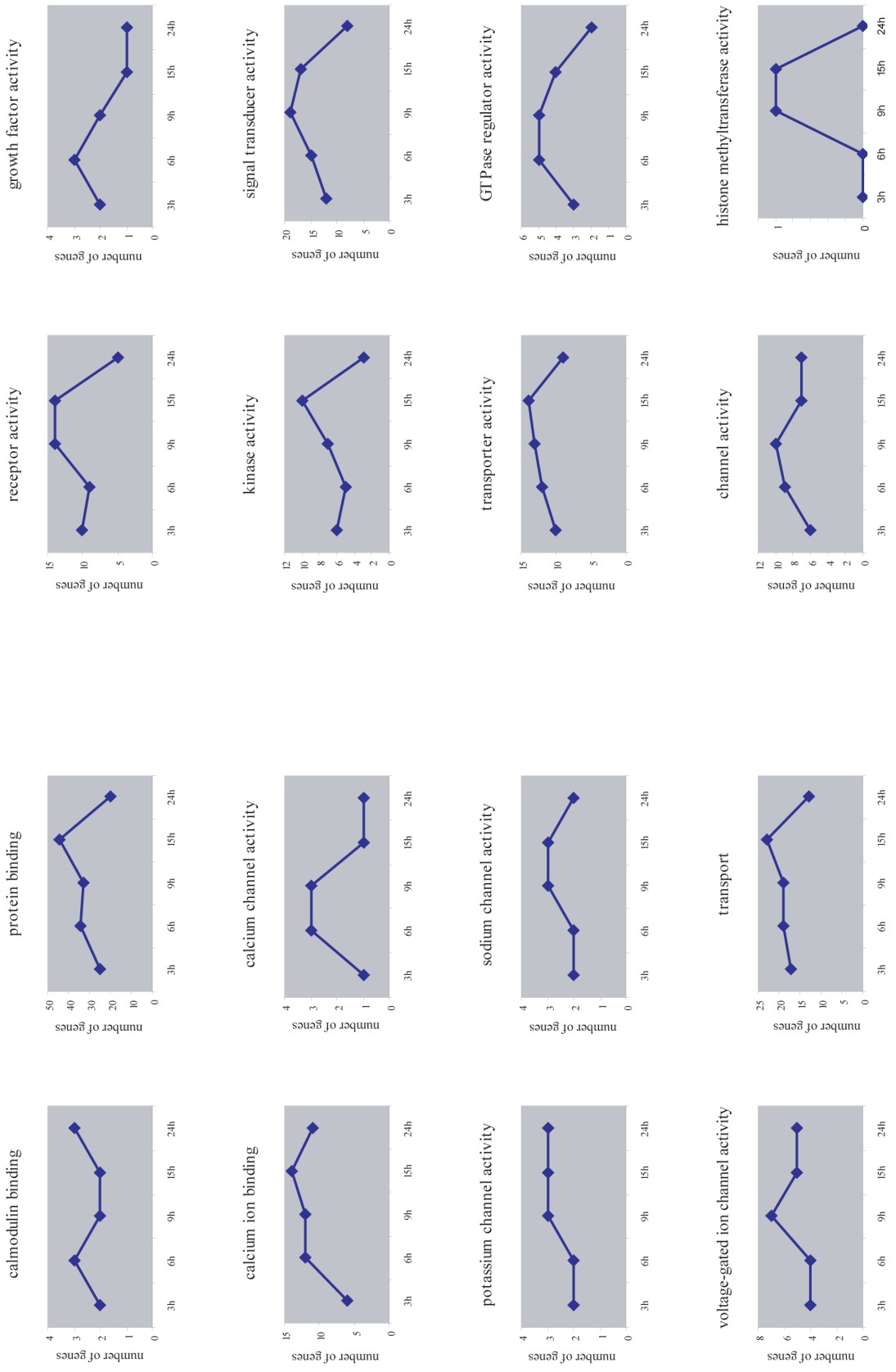

Appendix 5. Temporal profile of the number of regulated genes for a selection of Gene Ontology categories related to molecular activity.

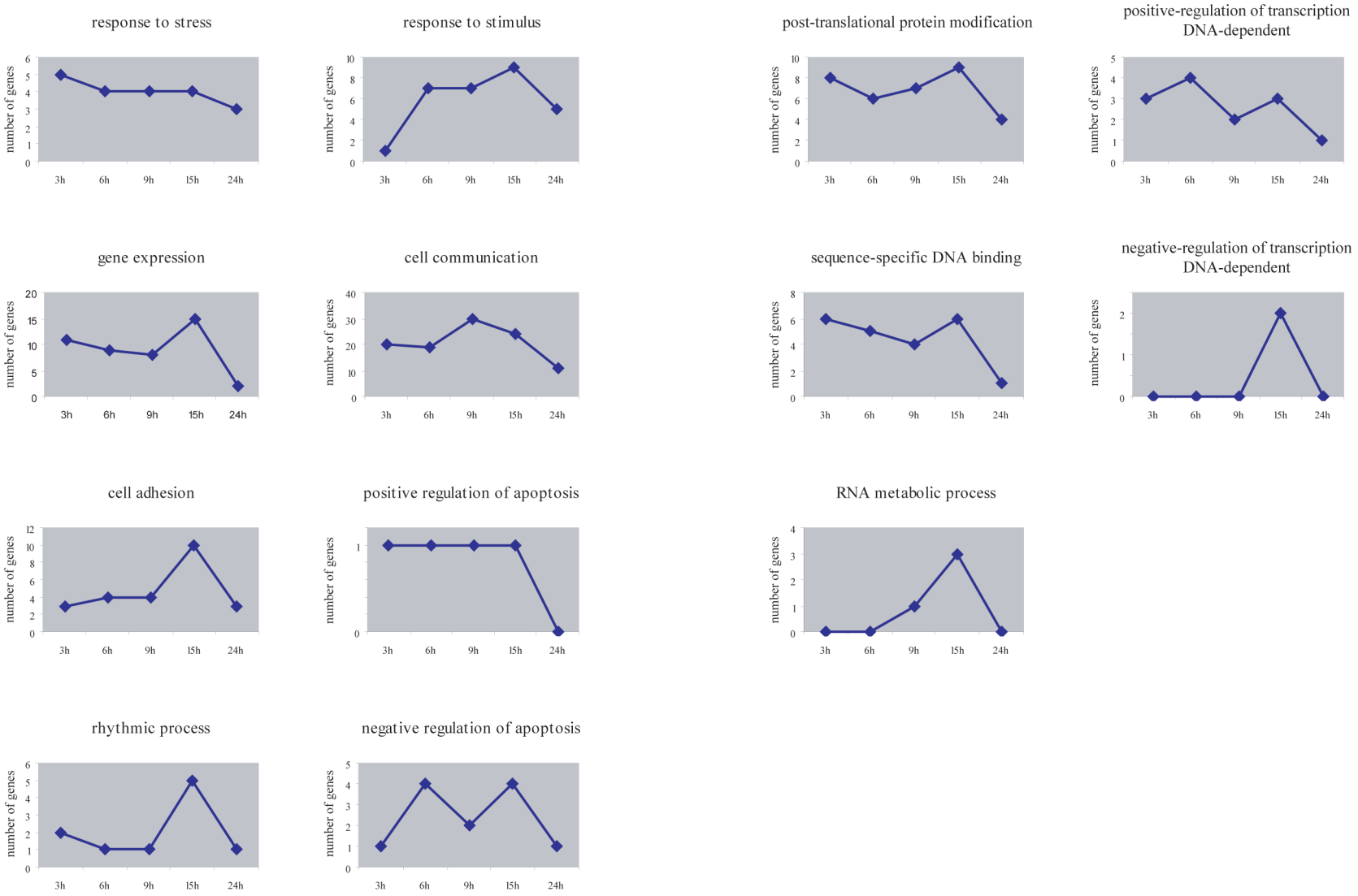

Appendix 6. Temporal profile of the number of regulated genes for a selection of gene ontology terms related to cellular processes

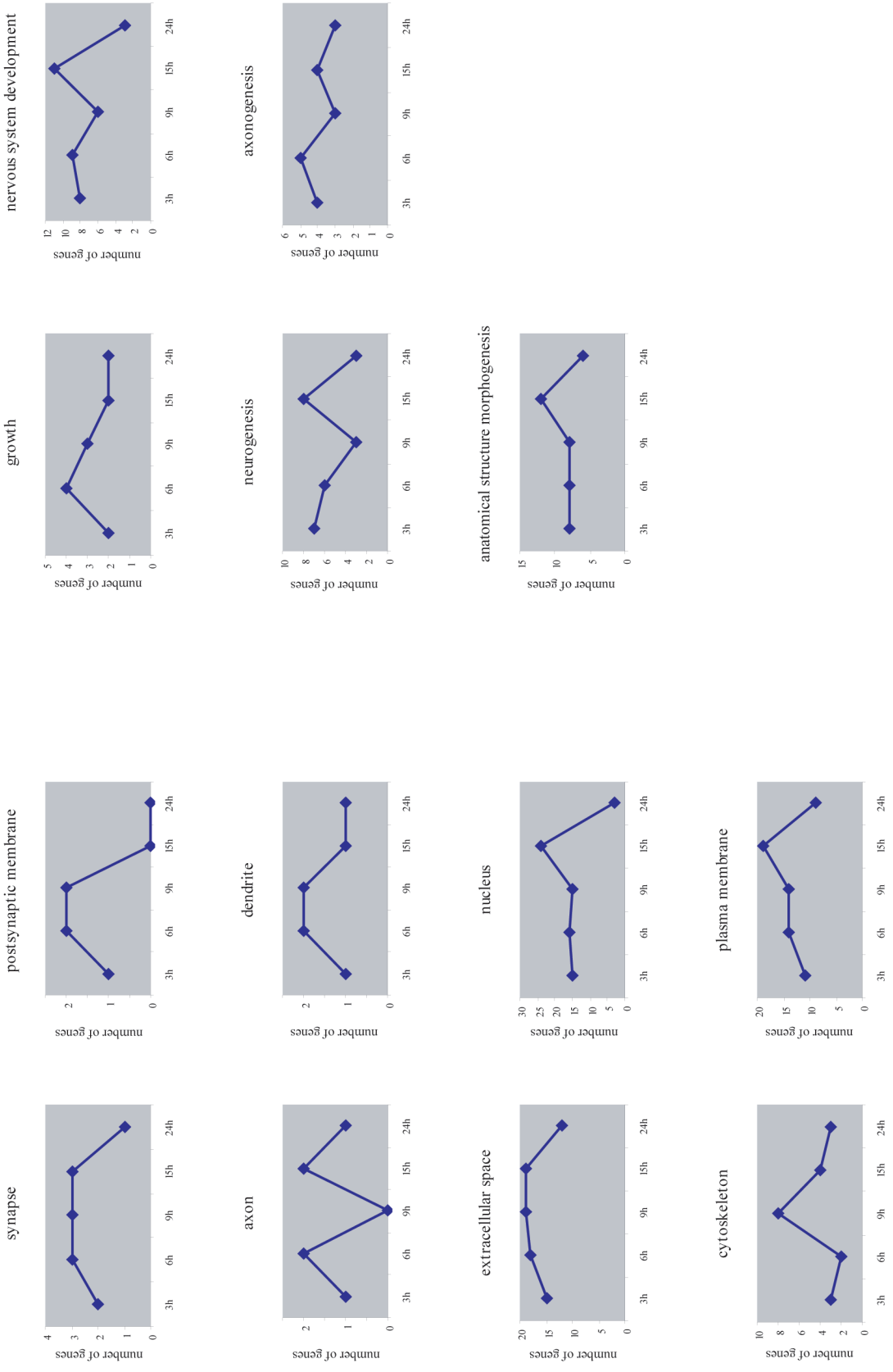

Appendix 7. Temporal profile of the number of regulated genes for a selection of gene ontology terms related to cellular compartment as well as development

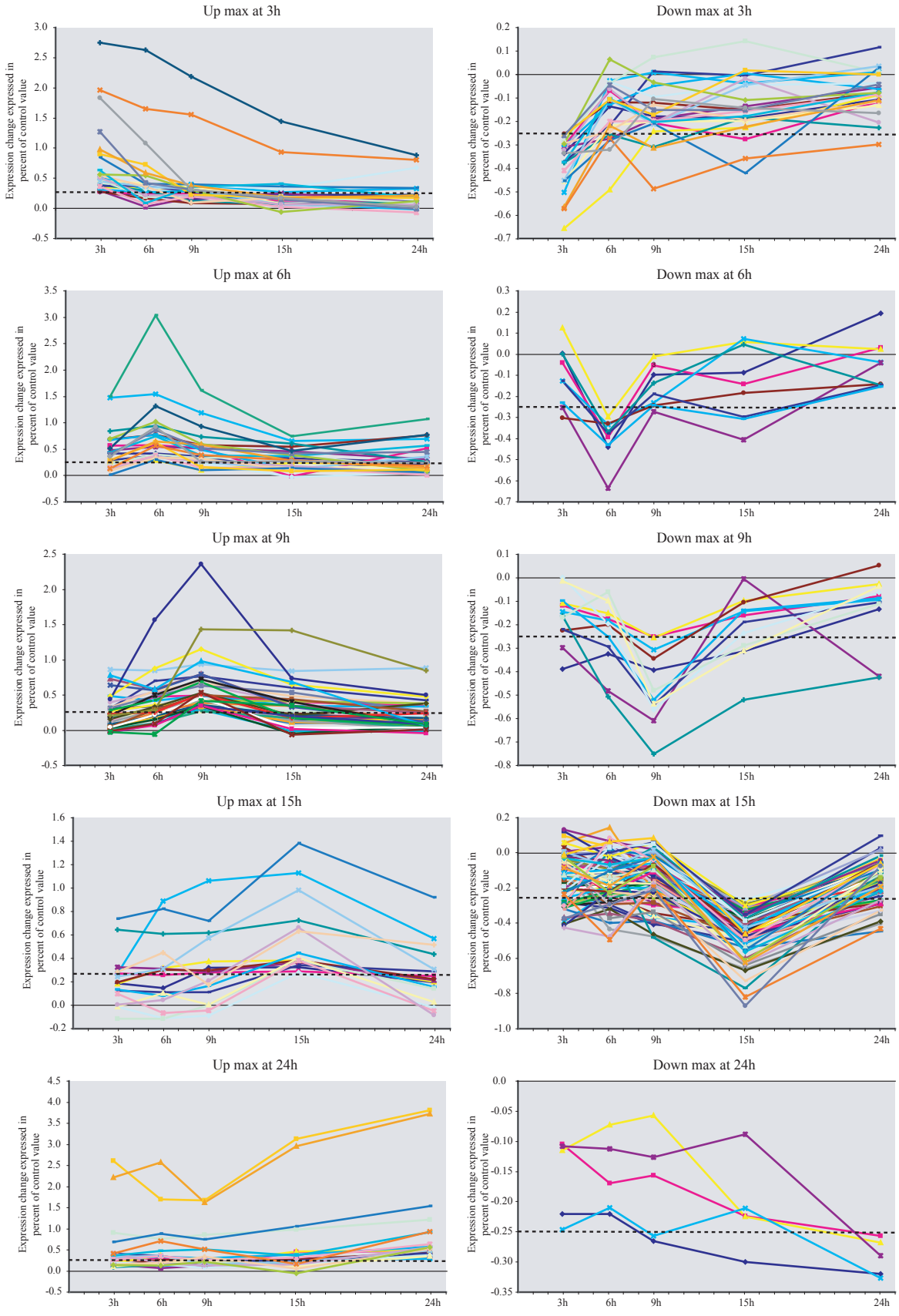

Appendix 8. Temporal profile of expression changes expressed in percent of control values across 24 hours of whisker stimulation for genes grouped by the time at which they show maximal level of regulation. Dashed lines represent the threshold set for considering a gene regulated.

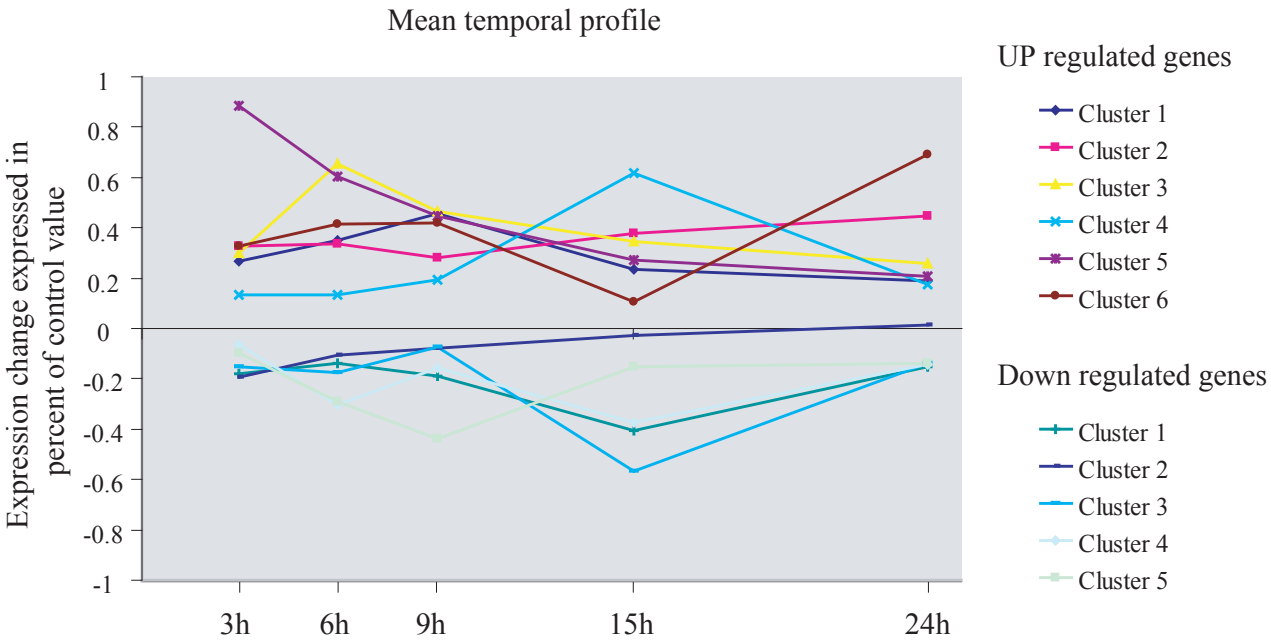

Appendix 9. Mean temporal profile of expression changes expressed in percent of control values across 24 hours of whisker stimulation for the 11 clusters of genes (each formed by ≥ 3 genes) identified using Ward's distance in the hierarchical cluster analysis.

Appendix 10. List of genes identified as regulated after 6 hours of stimulation in naïve mice (6h) or in mice that were exposed to 24 hours of whisker stimulation 24 hours earlier (restim). Genes are listed in alphabetical order.

genesymbol	Significant Comparison	FD 6h	FD restim	raw p value (6h VS Restim)	adj. p value (6h VS Restim)	IterPlier	Plier	Localization	Molecular function
0610031J06Rik	restim	1.06	-1.33	0.002	0.100	*		Extracellular	other
1100001G20Rik	restim	-1.09	1.31	0.006	0.132	*	*	Unknown	other
1110032A04Rik	both	-1.38	-1.86	0.102	0.195	*	*	Unknown	other
1200009I06Rik	restim	1.05	1.26	0.077	0.182	*			
1200013P24Rik	restim	-1.14	-1.45	0.142	0.228	*		Unknown	enzyme
1500031L02Rik	restim	1.01	-1.29	0.046	0.173	*		Unknown	other
1700028K03Rik|A	restim	-1.17	-1.28	0.359	0.395		*		
1700081L11Rik	restim	-1.05	-1.28	0.159	0.237	*			
2610024E20Rik	restim	-1.10	-1.38	0.194	0.260	*			
2610507B11Rik	restim	-1.06	-1.42	0.137	0.223	*		Extracellular	other
2810407C02Rik	restim	-1.13	-1.31	0.299	0.340	*		Unknown	other
2810439F02Rik	restim	-1.19	-1.40	0.002	0.100	*		Unknown	other
3110050N22Rik	restim	-1.14	-1.42	0.189	0.257	*	*	Unknown	other
4833436C18Rik	restim	-1.24	-1.65	0.071	0.179	*	*	Unknown	other
4921515J06Rik	restim	-1.16	1.26	0.011	0.136	*		Unknown	other
4930431L04Rik	6h	1.44	1.38	0.574	0.599	*	*	Unknown	enzyme
4931406C07Rik	6h	-1.33	-1.15	0.033	0.162	*		Nucleus	other
5730437N04Rik	restim	1.01	-1.45	0.058	0.176	*		Unknown	other
5830403L16Rik	6h	-1.47	-1.14	0.134	0.222	*	*	Unknown	other
6430550H21Rik	6h	-1.48	-1.15	0.172	0.245	*	*		
6430706D22Rik|A	restim	-1.15	-1.43	0.084	0.187	*	*		
6620401K05Rik|T	restim	-1.11	1.29	0.034	0.162	*			
9130213B05Rik	restim	-1.10	-1.45	0.143	0.229	*		Extracellular	other
A230083H22Rik|I	restim	-1.21	-1.35	0.431	0.463		*	Unknown	other
A2bp1	restim	-1.11	-1.27	0.132	0.220	*		Cytoplasm	other
A630047E20Rik	restim	-1.03	-1.29	0.061	0.177	*		Unknown	kinase
A730017C20Rik	restim	1.20	1.31	0.344	0.380	*		Unknown	other
A930016P21Rik	6h	-1.40	1.04	0.068	0.177	*	*	Unknown	other
Aard	both	-1.42	-1.37	0.671	0.691	*		Unknown	other
Abca2	restim	-1.05	-1.38	0.004	0.112	*		Membrane	transporter
Abca5	restim	1.02	-1.56	0.096	0.191	*		Membrane	transporter
Abcb6*	6h	-1.33	1.05	0.000	0.025	*		Cytoplasm	transporter
Abcd2	restim	-1.17	-1.34	0.219	0.281		*	Cytoplasm	transporter
Abhd2	restim	1.16	-1.35	0.023	0.150	*		Unknown	enzyme
Abhd3	restim	-1.15	-1.42	0.174	0.246	*	*	Unknown	enzyme
Ablim1	restim	-1.09	-1.41	0.033	0.162	*		Cytoplasm	other
Acbd5	restim	-1.09	-1.31	0.253	0.307		*	Unknown	other
Acot10|Acot9	restim	-1.09	-1.36	0.059	0.176	*	*		
Acot5	6h	-1.43	-1.13	0.054	0.173	*	*	Cytoplasm	enzyme

Acox3	restim	-1.13	-1.54	0.033	0.162	*		
Adam23	restim	-1.19	-1.37	0.280	0.327	*	Membrane	peptidase
Adcyap1	6h	1.60	1.08	0.033	0.162	*	*	Extracellular	other
Adcyap1r1	restim	-1.07	-1.36	0.048	0.173	*	Membrane	receptor
Aebp2	restim	1.03	-1.50	0.093	0.188	*	Nucleus	transcription
Aftph	restim	-1.02	-1.58	0.051	0.173	*	Cytoplasm	other
Agxt	restim	-1.10	1.35	0.010	0.132	*	Cytoplasm	enzyme
AI427515	restim	1.02	1.39	0.008	0.132	*	Unknown	enzyme
Aifm3	restim	-1.27	-1.37	0.240	0.296	*	Cytoplasm	enzyme
Ak3|LOC672214	restim	1.10	-1.36	0.019	0.137	*		
Akap2|Palm2|Paln	restim	-1.25	-1.38	0.058	0.176	*	*	Cytoplasm	other
Aldh3a2	restim	-1.06	-1.26	0.103	0.195	*	Cytoplasm	enzyme
Ank1	restim	-1.24	-1.51	0.111	0.199	*	Membrane	other
Ank3	restim	-1.06	-1.43	0.074	0.181	*	Membrane	other
Antxr1	6h	-1.49	-1.34	0.326	0.365	*	*	Membrane	other
Ap1gbp1	restim	-1.02	-1.27	0.018	0.137	*	Cytoplasm	other
Ap3m2	restim	-1.10	-1.45	0.166	0.239	*	Cytoplasm	transporter
Apoa4	restim	1.10	1.27	0.081	0.186	*	Extracellular	transporter
Apod	restim	-1.23	-1.45	0.258	0.312	*	*	Extracellular	transporter
Arhgap26	6h	1.33	1.15	0.281	0.327	*		
Arhgap29	restim	-1.18	-1.65	0.074	0.181	*	*	Cytoplasm	other
Arhgef2	restim	-1.09	-1.28	0.007	0.132		*	Cytoplasm	other
Arhgef3	restim	1.03	-1.40	0.066	0.177	*	Cytoplasm	other
Arhgef6	restim	-1.03	-1.42	0.055	0.173	*	Cytoplasm	other
Asah2	restim	-1.23	-1.63	0.229	0.286	*	*	Cytoplasm	enzyme
Asb7	restim	1.10	-1.38	0.009	0.132	*	Unknown	other
Astn2	restim	-1.17	-1.38	0.146	0.230	*	Unknown	other
Atg16l1	restim	-1.08	-1.50	0.102	0.195	*		
Atg4c|ENSMUSG	restim	-1.11	-1.33	0.205	0.268		*		
Atic|LOC100046	restim	-1.13	-1.61	0.202	0.266	*	Unknown	enzyme
Atp6v1b2	restim	1.05	-1.37	0.039	0.168	*	Cytoplasm	transporter
Atpaf1	restim	-1.11	-1.46	0.183	0.253	*	*	Unknown	other
B230209C24Rik	restim	-1.12	-1.35	0.179	0.250	*	Unknown	other
B230220N19Rik	restim	1.08	-1.48	0.045	0.173	*	*	Unknown	other
B4galnt3	restim	-1.05	1.53	0.027	0.157	*	Unknown	enzyme
B930006L02Rik	restim	-1.18	-1.43	0.187	0.257	*	Unknown	other
BC005764	restim	1.16	1.38	0.205	0.268	*	Unknown	other
BC026682	restim	-1.00	1.28	0.010	0.132	*		
BC048546	restim	-1.37	-1.61	0.341	0.379	*	*	Unknown	other
Bcas1	restim	-1.08	-1.49	0.051	0.173	*	Unknown	other
Bdnf	both	3.42	1.98	0.019	0.137	*	*	Extracellular	growth factor
Blm	restim	-1.30	-1.62	0.327	0.365	*	Nucleus	enzyme
Bmp2k	restim	-1.09	-1.41	0.027	0.157	*		
Brd9	both	-1.27	-1.39	0.186	0.256	*	Unknown	other
Brms1l	restim	-1.01	-1.42	0.157	0.236	*	Unknown	other
C230078M14Rik|	restim	-1.32	-1.60	0.287	0.332	*		
C630007B19Rik	both	1.60	1.37	0.107	0.196	*	*	Extracellular	other
Cacna1e	restim	-1.02	-1.48	0.128	0.217	*	Membrane	ion channel
Cacna2d2	restim	-1.10	-1.40	0.029	0.158	*	Membrane	ion channel
Cadps2	restim	-1.13	-1.41	0.133	0.221	*	*	Membrane	other
Cage1	restim	1.09	1.31	0.050	0.173	*	Unknown	other
Camk2g|Usp54	restim	-1.09	-1.48	0.082	0.187	*	*		
Car4	6h	1.30	1.21	0.077	0.183	*	*	Membrane	enzyme
Cbln2	6h	1.58	1.18	0.218	0.281	*	Extracellular	other
Cc2d2a	restim	-1.16	-1.59	0.192	0.259	*	Unknown	other
Ccdc100	restim	-1.19	-1.38	0.271	0.323	*	Unknown	other

Ccdc3	both	1.86	1.66	0.274	0.323	*	*	Cytoplasm	other
Ccdc91	restim	-1.14	-1.26	0.250	0.304		*	Unknown	other
Ccnb1	restim	1.09	1.56	0.003	0.100		*		
Cdh6	restim	-1.06	-1.28	0.118	0.204	*		Membrane	other
Cdkn1a	both	1.62	1.68	0.680	0.699	*	*	Nucleus	other
Cdkn1b	restim	1.07	-1.38	0.063	0.177	*		Nucleus	other
Cds1	restim	-1.07	-1.49	0.049	0.173	*		Cytoplasm	enzyme
Chd4	restim	-1.10	-1.37	0.108	0.196	*		Nucleus	enzyme
Chl1	both	1.70	1.37	0.154	0.236	*	*	Membrane	other
Chn1	restim	-1.07	-1.26	0.131	0.220	*		Membrane	other
Chpt1	restim	-1.07	-1.26	0.116	0.202		*	Unknown	enzyme
Chrdl1	restim	-1.14	-1.95	0.053	0.173	*	*	Extracellular	other
Clasp2	restim	-1.07	-1.51	0.143	0.229	*		Cytoplasm	other
Clcn3	restim	-1.04	-1.53	0.103	0.195	*		Membrane	ion channel
Clcn5	restim	1.07	-1.43	0.088	0.187	*		Membrane	ion channel
Clgn	restim	-1.27	-1.53	0.280	0.327	*		Cytoplasm	peptidase
Clic4	restim	-1.04	-1.65	0.009	0.132	*		Cytoplasm	ion channel
Clip4	restim	-1.27	-1.42	0.506	0.534	*		Unknown	other
Clk3	restim	-1.08	-1.37	0.153	0.236	*		Nucleus	kinase
Coch	6h	-1.26	-1.06	0.063	0.177	*		Extracellular	other
Cog6	restim	-1.15	-1.43	0.163	0.239	*		Cytoplasm	transporter
Cpeb1	restim	-1.13	-1.44	0.087	0.187	*			
Cplx1	restim	-1.10	-1.28	0.027	0.157	*		Unknown	transporter
Cpne4	both	1.58	1.61	0.866	0.875	*	*	Cytoplasm	other
Cpsf1	restim	1.04	1.38	0.024	0.152	*			
Crb1	restim	-1.06	1.41	0.013	0.137	*		Membrane	other
Creb1	restim	-1.05	-1.42	0.109	0.196	*		Nucleus	transcription
Crem	both	1.41	1.38	0.889	0.893	*	*	Nucleus	transcription
Cs	restim	1.08	-1.26	0.048	0.173		*		
Csnrp3	restim	-1.05	-1.33	0.129	0.217	*		Nucleus	other
Ctnnd1	restim	1.16	-1.48	0.042	0.171	*			
Ctps	restim	1.06	-1.46	0.049	0.173	*		Nucleus	enzyme
Cux1	restim	-1.13	-1.27	0.075	0.181		*	Nucleus	transcription
Cyfip2|OTTMUS(	restim	-1.08	-1.27	0.165	0.239	*		Cytoplasm	other
Cyp11a1	both	-1.44	-1.32	0.149	0.235	*	*	Cytoplasm	enzyme
Cyp20a1	restim	-1.28	-1.57	0.102	0.195	*		Unknown	enzyme
Cyp39a1	restim	-1.37	-1.57	0.491	0.521	*	*	Cytoplasm	enzyme
D15Ertd621e	restim	1.09	-1.45	0.063	0.177	*		Unknown	other
D430015B01Rik	restim	-1.18	-1.27	0.379	0.415		*	Unknown	other
Dbp	both	-1.39	-1.38	0.905	0.907	*	*	Nucleus	transcription
Dcbld2	restim	-1.22	-1.35	0.248	0.304		*	Membrane	other
Dcc	restim	-1.06	-1.46	0.056	0.174	*	*	Membrane	receptor
Dck	restim	-1.15	-1.26	0.393	0.428		*	Nucleus	kinase
Dctd	restim	-1.07	-1.56	0.088	0.187	*		Unknown	enzyme
Ddc	restim	-1.21	-1.49	0.055	0.173	*		Cytoplasm	enzyme
Ddx24	restim	-1.04	-1.26	0.067	0.177	*		Nucleus	enzyme
Depdc5	restim	-1.05	-1.47	0.161	0.239	*		Unknown	other
Diap1	restim	-1.11	-1.44	0.169	0.241	*		Cytoplasm	other
Disp2	restim	-1.06	-1.34	0.104	0.196	*	*	Unknown	other
Dixdc1	restim	-1.14	-1.29	0.110	0.198	*		Unknown	other
Dlg3	restim	1.02	-1.56	0.080	0.186	*		Membrane	kinase
Dmc1	restim	1.12	-1.33	0.009	0.132	*		Nucleus	enzyme
Dmgdh	6h	-1.45	-1.18	0.034	0.162	*		Cytoplasm	enzyme
Dmp1*	restim	1.07	-1.26	0.000	0.025	*		Extracellular	other
Dnajb5	6h	1.55	1.18	0.045	0.173	*	*	Unknown	other
Dnm3	restim	-1.04	-1.44	0.136	0.223	*	*		

Dock3	restim	-1.01	-1.42	0.089	0.187	*		Cytoplasm	other
Dopey1	restim	-1.08	-1.27	0.204	0.268		*		
Dpagt1	restim	-1.07	-1.53	0.049	0.173	*		Cytoplasm	enzyme
Dpp8	restim	-1.10	-1.34	0.233	0.291	*		Cytoplasm	peptidase
Dst	restim	-1.05	-1.36	0.151	0.236	*			
Dtd1	restim	1.00	-1.26	0.190	0.257	*		Cytoplasm	enzyme
Dtnbp1	restim	-1.06	1.29	0.019	0.137	*		Membrane	other
Dusp14	6h	1.28	1.07	0.015	0.137	*		Unknown	phosphatase
Dusp6	6h	1.55	1.36	0.076	0.182	*	*	Cytoplasm	phosphatase
Dync1h1	restim	-1.03	-1.39	0.092	0.188	*		Cytoplasm	peptidase
Dysf	restim	1.05	1.49	0.018	0.137	*		Membrane	other
E130009J12Rik	6h	-1.29	1.21	0.003	0.100	*		Unknown	other
EG207157	restim	-1.00	1.57	0.026	0.154	*		Unknown	other
EG432987|Krt6b	restim	-1.11	1.32	0.019	0.137	*			
Egr3	6h	1.42	-1.04	0.041	0.170	*	*	Nucleus	transcription
Elmo3	restim	-1.01	1.34	0.044	0.173	*		Cytoplasm	other
Endod1	restim	-1.11	-1.53	0.043	0.173	*	*	Extracellular	enzyme
Enpp2	restim	-1.17	-1.48	0.219	0.281	*	*	Membrane	enzyme
Epb4.1	restim	-1.09	-1.43	0.141	0.227	*	*	Membrane	other
Epb4.1l3	restim	-1.17	-1.49	0.299	0.340	*		Membrane	other
Ermn	restim	-1.10	-1.33	0.291	0.336		*	Extracellular	other
Etl4|EG667723|Pt	restim	-1.02	-1.29	0.083	0.187	*			
Exph5	both	-1.33	-1.33	0.998	0.998	*	*	Unknown	other
Eya4	restim	-1.10	-1.27	0.161	0.239		*	Cytoplasm	phosphatase
Farp2	restim	-1.15	-1.79	0.096	0.191	*			
Fbxo32	restim	-1.11	-1.38	0.125	0.213	*		Cytoplasm	enzyme
Fcgr2b|Fcgr3	restim	1.01	1.41	0.001	0.100	*			
Fchsd2	restim	-1.04	-1.40	0.056	0.173	*			
Fjx1	6h	1.32	1.12	0.166	0.239	*	*	Extracellular	other
Fktn	restim	-1.12	-1.27	0.222	0.282		*	Extracellular	other
Fnbp1l	6h	1.26	1.06	0.220	0.282	*		Unknown	other
Fosl2	6h	1.78	1.24	0.018	0.137	*	*	Nucleus	transcription
Foxn3	restim	-1.01	-1.26	0.043	0.172	*	*	Nucleus	transcription
Fxyd6	both	1.36	1.77	0.011	0.136	*	*	Membrane	ion channel
G6pdx|G6pd2	restim	-1.16	-1.38	0.149	0.235	*			
Gad1	restim	-1.05	-1.34	0.108	0.196	*		Cytoplasm	enzyme
Gap43	both	1.33	1.26	0.583	0.607	*	*	Membrane	other
Garnl3	restim	-1.19	-1.62	0.087	0.187	*	*	Unknown	other
Gas2	restim	-1.27	-1.59	0.145	0.230	*		Cytoplasm	other
Gats	restim	-1.07	-1.60	0.038	0.167	*		Unknown	other
Gbe1	restim	1.11	-1.29	0.036	0.163		*	Cytoplasm	enzyme
Gcn5l2	restim	-1.01	-1.33	0.072	0.179	*		Cytoplasm	enzyme
Gcnt2	6h	1.27	1.23	0.751	0.765	*		Cytoplasm	enzyme
Gfra2	6h	1.33	1.04	0.061	0.177		*	Membrane	receptor
Gins3	restim	-1.20	-1.50	0.106	0.196	*		Unknown	other
Gng4	6h	1.55	1.18	0.025	0.152	*	*	Membrane	enzyme
Gpr39	both	1.77	1.79	0.884	0.890	*	*		
Grasp	both	1.89	1.38	0.016	0.137	*	*	Membrane	other
Grid1	restim	-1.05	-1.47	0.045	0.173	*		Membrane	ion channel
Grik1	6h	1.73	-1.06	0.003	0.100	*	*	Membrane	ion channel
Gsta3	restim	-1.31	-1.44	0.324	0.363	*	*	Cytoplasm	enzyme
Gucy1a3	restim	1.26	1.32	0.462	0.494	*		Cytoplasm	enzyme
Gucy2g	restim	1.05	-1.39	0.021	0.143	*		Cytoplasm	enzyme
Hapln4	restim	-1.17	-1.40	0.092	0.188	*	*	Extracellular	other
Hcn2	restim	-1.00	-1.36	0.041	0.170	*		Membrane	ion channel
Hdac8	restim	1.01	-1.38	0.040	0.168	*		Nucleus	transcription

Hebp1*	restim	-1.16	1.32	0.000	0.033	*		Cytoplasm	other
Hebp2	6h	-1.27	-1.08	0.019	0.137	*		Cytoplasm	other
Hkdc1	6h	1.66	1.25	0.017	0.137	*		Unknown	kinase
Hlf	restim	-1.19	-1.44	0.091	0.188	*		Nucleus	transcription
Hmgcr	6h	1.26	1.01	0.108	0.196		*	Cytoplasm	enzyme
Homer1	6h	1.31	1.09	0.089	0.187	*			
Hpca	restim	1.05	-1.35	0.035	0.162		*	Cytoplasm	other
Hpcal4	6h	1.25	1.18	0.476	0.507	*		Unknown	other
Hrh3	restim	-1.22	-1.38	0.068	0.177	*		Membrane	receptor
Hsd17b4	restim	-1.04	-1.41	0.136	0.223	*		Cytoplasm	enzyme
Hspa12a	restim	-1.24	-1.47	0.156	0.236	*	*	Unknown	other
Ier5	6h	1.32	1.18	0.242	0.298	*		Unknown	other
Ifrd2	restim	1.09	1.32	0.097	0.191	*		Unknown	other
Ifrg15|Tor1aip2	restim	1.11	-1.28	0.014	0.137	*			
Igf2	6h	1.34	1.07	0.054	0.173	*		Extracellular	growth factor
Igfn1	6h	1.69	1.34	0.029	0.158	*	*	Unknown	other
Ikzf5	restim	-1.06	-1.43	0.115	0.201	*		Nucleus	other
Il12a	6h	1.36	-1.11	0.010	0.132	*		Extracellular	cytokine
Il1r1	restim	-1.10	-1.34	0.067	0.177		*	Membrane	receptor
Il1rapl2	restim	1.37	1.57	0.280	0.327	*	*	Membrane	receptor
Inhba	both	1.60	1.59	0.700	0.718	*	*	Extracellular	growth factor
Itsn1	restim	-1.15	-1.49	0.163	0.239	*		Cytoplasm	other
Jag1	6h	-1.33	-1.08	0.069	0.177	*		Extracellular	growth factor
Kcna2	restim	-1.06	-1.35	0.028	0.157	*	*	Membrane	ion channel
Kcnab3	restim	-1.20	-1.42	0.176	0.247	*	*	Membrane	ion channel
Kcnf1	both	1.82	1.91	0.658	0.680	*	*	Membrane	ion channel
Kcnv1	both	1.31	1.31	0.883	0.890	*	*	Unknown	ion channel
Klhl23	restim	1.05	-1.40	0.033	0.162	*		Unknown	other
Krt222	restim	-1.18	-1.38	0.023	0.149		*	Unknown	other
Krt9	restim	-1.19	-1.27	0.274	0.323		*	Cytoplasm	other
Lactb2	restim	-1.02	-1.37	0.038	0.167	*	*	Cytoplasm	other
Lcmt1	restim	-1.15	-1.28	0.259	0.312	*		Unknown	enzyme
Lgi2	restim	-1.09	-1.70	0.158	0.237	*	*	Extracellular	other
Lgi3	restim	-1.09	-1.26	0.061	0.177		*	Extracellular	other
Lgmn	restim	-1.06	-1.47	0.077	0.182	*		Cytoplasm	peptidase
Limk2	restim	-1.08	-1.28	0.180	0.250	*		Cytoplasm	kinase
Lingo2	restim	-1.10	-1.38	0.197	0.264	*		Unknown	other
Lmo3	restim	-1.17	-1.39	0.106	0.196	*	*	Nucleus	other
Lnp	restim	-1.10	-1.38	0.189	0.257		*	Unknown	other
Lphn2|ENSMUSC	restim	-1.24	-1.45	0.222	0.282	*	*		
Lrfn2	restim	1.17	1.37	0.098	0.192	*		Unknown	other
Lrp11	restim	-1.02	-1.37	0.064	0.177	*		Unknown	other
Lrrc33	restim	-1.31	-1.38	0.456	0.488	*		Unknown	other
Lrrc4	restim	-1.05	-1.28	0.091	0.188	*	*	Membrane	other
Lrrc57	restim	-1.22	-1.33	0.064	0.177	*		Unknown	other
Lrrtm3	6h	1.26	1.03	0.099	0.194	*		Unknown	other
Lrtm1	restim	-1.05	-1.30	0.032	0.162	*	*	Unknown	other
Lsm11	6h	1.30	1.21	0.249	0.304	*		Nucleus	other
Lsm14a	restim	1.03	-1.45	0.048	0.173	*		Unknown	other
Lypd1	both	1.24	1.30	0.545	0.571	*	*		
Lypla3	restim	1.05	1.29	0.108	0.196	*		Cytoplasm	enzyme
Mag*	restim	1.04	-1.51	0.000	0.033	*	*	Membrane	other
Magi3	restim	-1.07	-1.75	0.066	0.177	*	*	Cytoplasm	kinase
Map2k4	restim	-1.14	-1.39	0.283	0.328	*		Cytoplasm	kinase
Map2k6	restim	-1.16	-1.29	0.199	0.264	*	*	Cytoplasm	kinase
Map3k9	restim	-1.07	-1.34	0.091	0.188	*		Cytoplasm	kinase

Mapk9	restim	1.00	-1.34	0.081	0.186	*		Cytoplasm	kinase
Mapre3	restim	-1.09	-1.26	0.187	0.257		*	Cytoplasm	enzyme
March1	restim	-1.20	-1.40	0.278	0.327	*	*	Unknown	other
Mbtps2|Yy2|LOC	restim	-1.00	-1.41	0.018	0.137	*			
Mcf2	restim	-1.14	-1.39	0.262	0.315	*		Cytoplasm	other
Mcm6	6h	-1.36	-1.06	0.018	0.137	*		Nucleus	enzyme
Mcoln1	restim	-1.07	-1.36	0.035	0.162	*		Cytoplasm	ion channel
Mgll	restim	-1.09	-1.28	0.176	0.247	*		Membrane	enzyme
Mitd1|Lipt1	restim	1.02	-1.46	0.066	0.177	*			
Mitf	restim	-1.22	-1.66	0.175	0.247	*	*	Nucleus	transcription
Mkx|2410129H14	restim	-1.16	-1.31	0.199	0.264		*		
Mobp	restim	-1.15	-1.39	0.013	0.137	*		Cytoplasm	other
Ms4a10	6h	-1.31	1.07	0.012	0.136	*		Unknown	other
Mtmr15	restim	-1.17	-1.38	0.196	0.263	*		Unknown	other
Mtus1	both	-1.37	-1.44	0.664	0.685	*		Unknown	other
Myh9	6h	1.28	1.08	0.039	0.168	*		Cytoplasm	enzyme
Mylk3	6h	1.66	1.25	0.227	0.285	*		Unknown	kinase
Myo16	restim	-1.05	-1.42	0.115	0.201	*		Cytoplasm	other
Myt1l	restim	-1.11	-1.33	0.224	0.282	*		Nucleus	transcription
Napg	restim	1.01	-1.29	0.040	0.168	*		Cytoplasm	transporter
Nbn	restim	-1.13	-1.34	0.307	0.346	*		Nucleus	other
Nbr1	restim	-1.01	-1.50	0.113	0.200	*		Unknown	other
Ncald	both	1.35	1.31	0.705	0.721	*		Cytoplasm	other
Ncapd2	restim	-1.43	-1.71	0.234	0.291	*		Nucleus	other
Ncoa2	restim	1.02	-1.35	0.006	0.132	*		Nucleus	transcription
Necab1	both	1.47	1.52	0.747	0.762	*	*	Cytoplasm	other
Nedd9	restim	1.09	1.34	0.065	0.177	*		Nucleus	other
Nefh	restim	-1.27	-1.47	0.222	0.282	*	*	Cytoplasm	other
Nefl	6h	1.35	1.07	0.080	0.186	*	*		
Neurod1	6h	-1.39	-1.28	0.497	0.527	*	*	Nucleus	transcription
Nfat5	restim	-1.03	-1.37	0.121	0.207	*		Nucleus	transcription
Nfil3|LOC100046	both	1.39	1.30	0.273	0.323	*	*	Nucleus	transcription
Nlrp9a	restim	1.10	1.29	0.066	0.177	*			
Nmi	restim	1.06	1.34	0.012	0.136	*		Cytoplasm	transcription
Nope	restim	-1.08	-1.55	0.098	0.192	*		Unknown	other
Nos2	restim	-1.06	1.37	0.053	0.173	*		Cytoplasm	enzyme
Npas4	both	2.60	1.98	0.153	0.236	*	*	Nucleus	transcription
Nptx2	restim	1.90	1.95	0.611	0.633	*	*	Extracellular	other
Nr1d2	6h	-1.25	-1.22	0.797	0.807	*		Nucleus	nucl.receptor
Nr4a1	6h	2.03	1.30	0.029	0.158	*		Nucleus	nucl.receptor
Nr4a2	6h	1.83	1.14	0.025	0.152		*	Nucleus	nucl.receptor
Nrn1	6h	1.33	-1.01	0.053	0.173	*	*	Cytoplasm	other
Nudt16|LOC1000	restim	1.06	1.28	0.049	0.173	*		Unknown	other
Nup188	restim	1.13	-1.57	0.050	0.173	*		Nucleus	other
Nxf7	6h	1.53	1.13	0.089	0.187	*	*	Nucleus	transporter
Ocm|LOC100048	restim	1.07	1.34	0.009	0.132	*	*	Unknown	other
Ogt	restim	-1.10	-1.49	0.211	0.275	*		Cytoplasm	enzyme
Olfr1508|Olfr150	restim	-1.12	1.39	0.012	0.136	*	*		
Olfr645	restim	1.15	1.98	0.086	0.187		*	Membrane	receptor
Oprs1	6h	1.35	1.17	0.121	0.207		*		
ORF34	restim	1.20	-1.36	0.006	0.132	*			
Osbpl1a	restim	-1.04	-1.35	0.075	0.181	*		Cytoplasm	other
Osbpl6	restim	-1.16	-1.53	0.156	0.236	*	*	Cytoplasm	other
Osbpl9	restim	-1.02	-1.59	0.189	0.257	*			
Pafah1b1	restim	-1.02	-1.26	0.132	0.220	*		Cytoplasm	enzyme
Pafah1b2	restim	1.06	-1.29	0.040	0.168	*			

Palm2|Akap2|Palr	restim	-1.28	-1.44	0.306	0.346	*	*		
Parva	restim	-1.16	-1.46	0.150	0.235	*	*	Cytoplasm	other
Pcdh15	6h	1.34	1.19	0.237	0.293	*		Membrane	other
Pcdh7	restim	1.07	-1.45	0.022	0.149	*	*	Membrane	other
Pcdhb16	restim	-1.16	-1.33	0.265	0.317	*		Membrane	other
Pcnx	restim	1.02	-1.52	0.055	0.173	*		Membrane	other
Pcp4	both	1.31	1.26	0.155	0.236	*	*	Cytoplasm	other
Pcp4l1	restim	-1.16	-1.35	0.207	0.270	*		Unknown	other
Pcsk1	6h	1.65	1.03	0.009	0.132	*	*	Extracellular	peptidase
Pde1a	both	1.67	2.12	0.221	0.282	*	*	Cytoplasm	enzyme
Pde6c	6h	1.65	1.49	0.505	0.534	*		Cytoplasm	enzyme
Pdha1	restim	1.04	-1.45	0.088	0.187	*			
Pex5l	restim	-1.02	-1.31	0.087	0.187	*		Cytoplasm	other
Pftk1	restim	-1.06	-1.29	0.154	0.236	*		Nucleus	kinase
Phf12	restim	1.00	-1.38	0.009	0.132	*		Nucleus	transcription
Pik3r3	restim	-1.08	-1.26	0.273	0.323		*	Cytoplasm	kinase
Pir	restim	-1.19	-1.56	0.139	0.226	*	*	Nucleus	transcription
Pknox2	restim	-1.14	-1.52	0.064	0.177	*		Nucleus	other
Pla2g7	restim	-1.03	-1.27	0.089	0.187		*	Extracellular	enzyme
Plxdc1	restim	-1.21	-1.65	0.163	0.239	*	*	Membrane	other
Pml	restim	-1.09	-1.49	0.096	0.191	*		Nucleus	transcription
Polr3gl	restim	-1.02	-1.30	0.044	0.173	*		Unknown	other
Ppif	restim	1.07	1.26	0.199	0.264	*		Cytoplasm	enzyme
Ppil2	restim	1.04	-1.40	0.035	0.162	*		Nucleus	enzyme
Ppm1h	6h	1.37	1.09	0.030	0.158	*		Unknown	phosphatase
Ppm1l	restim	-1.03	-1.54	0.086	0.187	*	*	Unknown	phosphatase
Ppm1m	restim	-1.13	1.26	0.003	0.100	*		Nucleus	phosphatase
Ppme1	6h	1.37	1.05	0.052	0.173	*	*	Unknown	enzyme
Ppp1r3f	restim	1.05	-1.25	0.022	0.149		*	Unknown	other
Prcp	restim	-1.07	-1.61	0.019	0.137	*	*	Cytoplasm	peptidase
Prkd1	restim	-1.22	-1.44	0.166	0.239	*			
Prkg1	restim	-1.17	-1.25	0.479	0.510		*	Cytoplasm	kinase
Prkg2	6h	1.26	1.08	0.135	0.222		*		
Prmt7	restim	-1.07	-1.30	0.108	0.196	*		Cytoplasm	enzyme
Pscd3	restim	-1.22	-1.40	0.384	0.419	*		Cytoplasm	other
Psd	restim	1.05	-1.47	0.076	0.182	*		Unknown	other
Ptgs2	both	2.64	1.65	0.011	0.136	*	*	Cytoplasm	enzyme
Pth2r	restim	-1.21	-1.33	0.396	0.430		*	Membrane	receptor
Ptk2b	restim	-1.04	-1.38	0.096	0.191	*		Cytoplasm	kinase
Ptprk	6h	1.28	1.24	0.585	0.608	*		Membrane	phosphatase
Ptprt	restim	-1.23	-1.52	0.259	0.312	*	*	Membrane	phosphatase
Qdpr	restim	-1.07	-1.33	0.093	0.188	*		Cytoplasm	enzyme
Qrich1	restim	-1.13	-1.25	0.315	0.354		*	Unknown	other
Rab30	restim	-1.23	-1.45	0.294	0.337	*	*	Cytoplasm	enzyme
Rab31	restim	1.01	-1.29	0.020	0.139	*			
Rab6ip1	restim	-1.06	-1.29	0.167	0.239	*		Unknown	other
Rap1gds1	restim	-1.09	-1.30	0.176	0.247	*		Unknown	other
Rasl11b	6h	1.49	-1.06	0.007	0.132	*	*	Unknown	enzyme
Rassf3	restim	-1.10	-1.29	0.015	0.137	*		Unknown	other
Raver2	restim	-1.18	-1.46	0.238	0.295	*		Nucleus	other
Rbl2	restim	-1.05	-1.48	0.118	0.204	*			
Rbp4	6h	1.84	1.40	0.083	0.187	*	*	Extracellular	transporter
Rcan2	restim	-1.13	-1.26	0.100	0.194	*		Unknown	other
Rcor3	restim	-1.01	-1.47	0.015	0.137	*		Nucleus	other
Rgl1	restim	1.01	-1.45	0.053	0.173	*		Cytoplasm	other
Rgs2	6h	1.58	1.14	0.060	0.177	*	*	Nucleus	other

Rgs8	both	1.34	1.36	0.753	0.766 *		Unknown	other
Rit2	restim	1.01	-1.37	0.067	0.177 *		Membrane	enzyme
Rmnd5a|LOC100(	restim	-1.05	-1.57	0.094	0.190 *	*		
Rnd3	both	1.88	1.30	0.002	0.100 *	*	Cytoplasm	enzyme
Rom1	restim	-1.06	-1.36	0.046	0.173 *		Membrane	other
Rorb	restim	-1.31	-1.37	0.776	0.788 *	*	Nucleus	nucl.receptor
RP23-136K12.4	restim	-1.17	-1.38	0.264	0.316 *		Cytoplasm	phosphatase
Rpgrip1l	restim	-1.07	-1.65	0.134	0.222 *	*	Unknown	other
Rprm	restim	1.16	1.35	0.087	0.187 *		Cytoplasm	other
Rps6ka5	both	-1.34	-1.65	0.220	0.282 *	*	Nucleus	kinase
Rufy3	restim	-1.02	-1.50	0.124	0.212 *		Unknown	other
Sacm1l	restim	-1.04	-1.27	0.168	0.239	*	Cytoplasm	phosphatase
Samhd1	restim	-1.37	-1.54	0.525	0.552 *		Nucleus	enzyme
Scg2	both	1.59	1.48	0.411	0.444 *	*	Extracellular	cytokine
Scn1a	restim	-1.16	-1.26	0.342	0.379 *			
Scn3b	both	1.71	2.00	0.299	0.340 *	*	Membrane	ion channel
Scn7a	both	2.91	3.57	0.205	0.268 *	*	Membrane	ion channel
Scnn1a	both	-1.44	-1.99	0.069	0.177 *	*	Membrane	ion channel
Scp2	restim	-1.13	-1.43	0.098	0.193 *		Cytoplasm	transporter
Sema7a	restim	-1.13	-1.32	0.260	0.313 *	*	Membrane	other
Sergef	restim	1.14	1.40	0.108	0.196 *		Cytoplasm	other
Sertad1	restim	1.37	1.50	0.335	0.373 *	*	Nucleus	transcription
Sgpp2	restim	-1.26	-1.41	0.373	0.409 *	*	Cytoplasm	phosphatase
Sgsm1	6h	1.49	1.27	0.108	0.196 *		Unknown	other
Sgtb	restim	-1.01	-1.40	0.052	0.173 *	*	Unknown	other
Slc12a2	restim	-1.05	-1.29	0.062	0.177	*	Membrane	transporter
Slc13a5	restim	-1.21	-1.47	0.300	0.341 *		Membrane	transporter
Slc22a13	restim	1.01	1.40	0.052	0.173 *			
Slc25a37	restim	-1.06	-1.28	0.071	0.179	*	Cytoplasm	transporter
Slc30a9	restim	1.02	-1.53	0.071	0.179 *	*	Nucleus	transporter
Slc35c1	6h	1.28	1.00	0.002	0.100	*	Cytoplasm	transporter
Slc44a1	restim	-1.20	-1.34	0.423	0.457 *		Membrane	transporter
Slc4a4	restim	1.02	-1.53	0.026	0.156 *	*	Membrane	transporter
Slc6a17	6h	1.29	-1.05	0.019	0.137 *		Unknown	transporter
Slmap	restim	1.02	-1.42	0.088	0.187 *		Membrane	other
Sntb2	restim	-1.04	-1.37	0.009	0.132 *		Membrane	other
Sorcs3	both	2.39	1.76	0.055	0.173 *	*	Nucleus	transporter
Sox1	restim	1.14	-1.34	0.003	0.100 *		Nucleus	transcription
Sox6	restim	1.05	-1.56	0.019	0.137 *		Nucleus	transcription
Spg7	restim	-1.09	-1.46	0.015	0.137 *		Cytoplasm	peptidase
Spock2	restim	-1.02	-1.48	0.113	0.200 *		Extracellular	other
Spon1	both	1.33	1.38	0.429	0.461 *	*	Extracellular	other
Spred2	6h	1.25	1.31	0.518	0.546 *	*		
Spred2	both	1.32	1.14	0.072	0.179 *	*	Extracellular	cytokine
Stard8	6h	1.51	1.24	0.225	0.283 *	*	Unknown	other
Stk3	restim	-1.19	-1.43	0.317	0.357 *		Cytoplasm	kinase
Stx17	restim	-1.11	-1.37	0.069	0.177	*	Membrane	other
Sumo1	restim	1.11	-1.83	0.029	0.158 *	*	Nucleus	enzyme
Syt2	restim	-1.15	-1.49	0.080	0.186 *	*	Cytoplasm	transporter
Tars	restim	-1.06	-1.48	0.040	0.168 *		Nucleus	enzyme
Tbc1d23	restim	-1.05	-1.25	0.155	0.236	*	Unknown	other
Tbccd1	restim	-1.17	-1.34	0.155	0.236 *		Unknown	other
Tcf20	restim	-1.09	-1.26	0.140	0.226 *		Nucleus	transcription
Tcp11l2	restim	-1.31	-1.42	0.549	0.574 *		Unknown	other
Tfdp2	restim	-1.02	-1.37	0.068	0.177 *			
Tln2	restim	-1.03	-1.35	0.165	0.239 *		Nucleus	other

Tmed9	restim	1.11	-1.26	0.025	0.152 *		Cytoplasm	transporter
Tmem127	restim	-1.01	-1.32	0.017	0.137 *		Unknown	other
Tmem131	restim	-1.14	-1.60	0.156	0.236 *		Unknown	other
Tmem63b	restim	-1.06	-1.26	0.055	0.173 *		Unknown	other
Tmem65	restim	-1.22	-1.55	0.167	0.239 *	*	Unknown	other
Tmod1	restim	-1.01	-1.42	0.033	0.162 *		Cytoplasm	enzyme
Tnfrsf4	restim	-1.07	1.38	0.003	0.100 *		Membrane	receptor
Tnip1	restim	-1.01	-1.32	0.003	0.100 *		Nucleus	other
Tnnc1	both	3.40	3.00	0.163	0.239 *	*	Cytoplasm	other
Tnr	restim	-1.01	-1.39	0.069	0.177 *		Membrane	other
Tnrc6a	restim	-1.06	-1.46	0.009	0.132 *		Nucleus	other
Tollip	restim	-1.00	-1.33	0.004	0.100 *	*	Cytoplasm	other
Tor1aip1	restim	1.01	-1.33	0.015	0.137 *			
Trap1	restim	1.01	-1.47	0.034	0.162 *		Cytoplasm	enzyme
Treml4	restim	1.07	1.29	0.030	0.158 *		Unknown	other
Trerf1	restim	-1.02	-1.33	0.084	0.187 *		Nucleus	transcription
Trf	restim	-1.12	-1.26	0.071	0.179 *		Extracellular	transporter
Trib2	6h	1.28	1.23	0.295	0.338 *		Membrane	kinase
Trim59|LOC6305	restim	-1.09	-1.89	0.023	0.150 *	*	Unknown	other
Trim8	restim	1.12	-1.37	0.030	0.158 *		Nucleus	other
Trpc3	6h	1.41	1.27	0.405	0.439 *	*	Membrane	ion channel
Trpc4	restim	-1.20	-1.35	0.353	0.389 *		Membrane	ion channel
Trpc6	6h	2.23	1.54	0.291	0.336 *		Membrane	ion channel
Tshz2	restim	-1.05	1.34	0.037	0.165 *		Unknown	other
Tspan2	restim	-1.06	-1.33	0.160	0.238 *		Unknown	other
Ttc22	restim	-1.06	1.34	0.013	0.137 *		Unknown	other
Ttll5	restim	-1.04	-1.47	0.064	0.177 *		Unknown	enzyme
Twf1	restim	-1.02	-1.32	0.013	0.137 *	*	Cytoplasm	kinase
Ubac1	restim	-1.05	-1.33	0.085	0.187 *		Unknown	other
Ubash3b	restim	-1.07	-1.25	0.112	0.199	*	Unknown	enzyme
Usp28	restim	-1.03	-1.46	0.103	0.195 *		Unknown	peptidase
Usp46	restim	-1.09	-1.48	0.075	0.181 *	*	Unknown	peptidase
Usp6nl	restim	-1.05	-1.34	0.085	0.187	*	Membrane	other
Vamp1|E130112N	restim	-1.09	-1.36	0.053	0.173 *		Membrane	transporter
Vps36	restim	-1.07	-1.36	0.181	0.251 *	*	Cytoplasm	other
Vps8	restim	-1.18	-1.53	0.189	0.257 *		Unknown	other
Vstm2b	restim	-1.22	-1.33	0.250	0.304 *		Unknown	other
Vta1	restim	-1.00	-1.58	0.102	0.195 *		Unknown	other
Wdfy3	restim	-1.01	-1.60	0.114	0.201 *		Cytoplasm	enzyme
Wdr37	restim	-1.13	-1.56	0.153	0.236 *		Unknown	other
Wdsub1	restim	-1.27	-1.40	0.293	0.337 *		Unknown	other
Wnt2b	restim	-1.20	-1.57	0.144	0.230 *		Extracellular	other
Xiap	restim	-1.01	-1.33	0.064	0.177	*	Cytoplasm	other
Zbtb20	restim	-1.13	-1.44	0.058	0.176 *	*	Nucleus	other
Zc3h6	restim	-1.13	-1.47	0.215	0.279 *	*	Unknown	other
Zfp192	restim	-1.12	-1.35	0.225	0.283 *		Nucleus	transcription
Zfp385b|LOC100	restim	-1.09	-1.26	0.126	0.213	*	Nucleus	other
Zfp52|Zfp760	6h	-1.29	-1.17	0.346	0.382 *			
Zfpm1|Gm22	6h	1.31	-1.03	0.006	0.132 *			
-----	6h	-1.32	-1.07	0.052	0.173 *		Nucleus	transcription

Statistical difference between expression change after 6 hours of whisker stimulation in naïve mice and after 6 hours in mice that were 4 days earlier exposed to 24 hours of whisker stimulation was tested using Student's t-test (raw p value) and adjusted for false discovery rate using the Benjamini Hochberg method adj. p value). In grey are the genes for which raw p value is ≤ 0.05 (adj. p value is ≤ 0.05 for Abcn6, Dmp1, Hebp1 and Mag; indicated with a star behind their name). The minus sign in front of the fold change indicates that the expression of the gene was decreased by the respective fold change. Also note that in the last column, «transcription» stands for transcription regulator and «nucl.rec» for nuclear receptor.